

**WestminsterResearch**

<http://www.westminster.ac.uk/westminsterresearch>

**The study of highly pathogenic emerging zoonotic virus envelope proteins through pseudotyped virus generation**

**Bentley, E.**

This is an electronic version of a PhD thesis awarded by the University of Westminster.  
© Miss Emma Bentley, 2017.

---

The WestminsterResearch online digital archive at the University of Westminster aims to make the research output of the University available to a wider audience. Copyright and Moral Rights remain with the authors and/or copyright owners.

---

Whilst further distribution of specific materials from within this archive is forbidden, you may freely distribute the URL of WestminsterResearch: (<http://westminsterresearch.wmin.ac.uk/>).

In case of abuse or copyright appearing without permission e-mail [repository@westminster.ac.uk](mailto:repository@westminster.ac.uk)

THE STUDY OF HIGHLY PATHOGENIC EMERGING  
ZOO NOTIC VIRUS ENVELOPE PROTEINS THROUGH  
PSEUDOTYPED VIRUS GENERATION

Emma May Bentley

A thesis submitted in partial fulfilment of the requirements of the University  
of Westminster for the degree of Doctor of Philosophy

September 2017

## Abstract

Emerging zoonotic viruses pose an increasing threat, causing outbreaks with high rates of morbidity and mortality and frequently significant economic implications. Often, there is a lack or shortfall of effective prophylaxis and diagnostic capabilities. Research towards their development, together with improved surveillance activities are high priority activities to prepare and respond to outbreak threats. Yet handling these viruses commonly requires high containment levels. This can be circumvented by the use of replication defective pseudotyped viruses (PVs), incorporating the viral envelope protein of interest which constitutes the primary surface antigen. This permits the serological detection of neutralising antibodies without the need to handle live virus, as well as other viral entry studies. Hence, PVs are increasingly proving to be a valuable tool for emerging virus research. The aim of this study was to exploit novelties in the unique flexibility of the PV platform to allow the serological assessment of emerging viruses and evaluate technical aspects towards standardisation.

Current prophylaxis provides robust protection against rabies virus, yet only confers limited protection against other lyssavirus species, which have a near 100% fatality rate. It is thought protection is afforded against isolates of phylogroup I rabies virus, yet there is limited biological data for the Arctic-like rabies virus (AL RABV) lineage which is endemic across the Middle East and Asia. Although other lyssaviruses pseudotype efficiently, titres of AL RABV PV were low. Within this study, high titre PV was produced by constructing chimeric envelope proteins, splicing the AL RABV ecto-transmembrane domain with the cytoplasmic domain of vesicular stomatitis virus. Comparisons showed this did not alter the serological profile of the AL RABV and they were effectively neutralised by vaccines and antivirals. It could therefore be concluded that they do not pose a significant public health risk. However it is recognised broadly neutralising prophylaxis needs to be developed to protect against more divergent lyssaviruses. In a further study, again utilising the flexibility to manipulate the envelope protein, PV was produced switching the five known antigenic sites of the envelope protein between a phylogroup I (rabies virus) and III (West Caucasian bat virus) isolate. Screening polyclonal sera via a neutralisation assay, the immunologically dominant sites for phylogroup I and III were identified as III and I respectively. This can act to inform future development of more broadly neutralising vaccines.

The 2013-16 outbreak of Ebola virus focused global efforts towards the urgent need for effective vaccines and antivirals. To permit low containment level serology studies to assist their development, a panel of filovirus PVs were rapidly produced. Work was carried out to optimise their method of production; determining lentiviral core PV produced by transfecting HEK 293T/17 cells was most efficient. Efforts to repeat the use of chimeric envelope proteins to increase titre

proved unsuccessful. The evaluation of target cell lines permissive to infection and appropriate for neutralisation assays identified that the CHO-K1 cell line produced the clearest data. The PV neutralisation assay was subsequently applied to a range of projects to assess candidate prophylaxis and demonstrated the value of the platform to respond to emerging virus outbreaks.

Given the increasing prominence in the use of PV, work was undertaken to expand their utility and methods for standardisation. An assessment of new reporter genes found a red fluorescent protein, with a nuclear localisation signal, improved the clarity of data collection and output in additional spectrum to the current repertoire. To be able to correlate the disparate readout units of fluorescent and luminescent reporters, recorded as infectious units (IFU) and relative light units (RLU) respectively, a new construct was produced to integrate and equally express two reporters from cells transduced with PV. It was determined that approximately 1260 RLU equates to 1 IFU, although future work to determine how this fluctuates between cell lines is required. Finally, alternative methods to quantify PV were evaluated, measuring the number of particles, genome copies and reverse transcriptase (RT) activity, in addition to the currently used biological titre. It was found that measures of genome copies and RT activity, in combination with biological titre provides information on the quality of PV preparations and could be used to standardise assay input.

# Table of Contents

<b>ABSTRACT .....</b>	<b>I</b>
<b>TABLE OF CONTENTS .....</b>	<b>III</b>
<b>LIST OF FIGURES.....</b>	<b>VII</b>
<b>LIST OF TABLES .....</b>	<b>X</b>
<b>ACKNOWLEDGEMENTS.....</b>	<b>XII</b>
<b>AUTHOR'S DECLARATION.....</b>	<b>XIII</b>
<b>LIST OF ABBREVIATIONS.....</b>	<b>XIV</b>
<b>CHAPTER 1. INTRODUCTION .....</b>	<b>1</b>
<b>1.1. EMERGING ZOOONOTIC VIRUSES .....</b>	<b>1</b>
1.1.1. History and Processes of Zoonotic Virus Emergence.....	1
1.1.2. Significance and Future Direction of the Emerging Virus Field .....	6
1.1.3. Lyssaviruses .....	9
1.1.4. Filoviruses .....	13
<b>1.2. THE VIRAL ENVELOPE PROTEIN .....</b>	<b>16</b>
1.2.1. Importance and Structure of the Viral Envelope Protein.....	16
1.2.2. The Viral Envelope Protein as a Target.....	20
<b>1.3. SEROLOGY .....</b>	<b>21</b>
1.3.1. Serological Investigations.....	21
1.3.2. Serological Assays.....	23
<b>1.4. PSEUDOTYPED VIRUS .....</b>	<b>25</b>
1.4.1. Pseudotyped Virus Definition .....	25
1.4.2. History of Pseudotyped Virus.....	26
1.4.3. Pseudotyped Virus Production .....	32
1.4.4. Pseudotyped Virus Applications .....	37
<b>1.5. AIMS AND OBJECTIVES .....</b>	<b>42</b>
<b>CHAPTER 2. MATERIALS AND METHODS .....</b>	<b>44</b>
<b>2.1. MATERIALS .....</b>	<b>44</b>
2.1.1. Bacterial Strains and General Media .....	44
2.1.2. Virus Envelope Protein and Reporter Protein Sequences .....	44
2.1.3. Plasmids and Primers .....	44
<b>2.2. METHODS .....</b>	<b>52</b>
2.2.1. Chemically Competent TOP10 <i>E. coli</i> Cell Preparation .....	52
2.2.2. Agarose Gel Electrophoresis .....	52
2.2.3. cDNA PCR Amplification.....	53

2.2.4. Splicing by Overlap Extension (SOE) PCR Amplification .....	55
2.2.5. Restriction Enzyme Digestion and Cloning into Plasmid Vector .....	57
2.2.6. Transformation of Chemically Competent Cells .....	57
2.2.7. Plasmid Propagation .....	57
2.2.8. Confirmation of Cloned Gene Sequences .....	58
2.2.9. Cell Culture .....	58
2.2.10. Transfection for Pseudotyped Virus Production .....	60
2.2.11. Pseudotyped Virus Titration .....	61
2.2.11.1. Infection Assay .....	61
2.2.11.2. Titre Designation Assay .....	61
2.2.12. Titration Readout .....	62
2.2.12.1. Luminescence .....	62
2.2.12.2. Colourimetric .....	63
2.2.12.2.1. $\beta$ -Galactosidase Assay .....	63
2.2.12.2.2. Alkaline Phosphatase Enzymatic Assay .....	63
2.2.12.3. Fluorescence .....	64
2.2.12.3.1. Microscopy .....	64
2.2.12.3.2. Flow Cytometry .....	64
2.2.13. Neutralisation Assay .....	65
2.2.14. Sucrose Purification .....	65
2.2.15. Pseudotyped Virus Genome Analysis .....	66
2.2.15.1. RNA Extraction .....	66
2.2.15.2. Quantitative Reverse Transcription PCR (RT-qPCR) .....	66
2.2.16. SYBR Green Product-Enhanced Reverse Transcriptase (SG-PERT) Assay .....	69
2.2.17. Nanoparticle Tracking Analysis .....	71
<b>CHAPTER 3. PRODUCTION OF CHIMERIC ARCTIC-LIKE RABIES VIRUS GLYCOPROTEINS TO IMPROVE PSEUDOTYPED VIRUS TITRES AND PERMIT SEROLOGICAL STUDIES .....</b>	<b>72</b>
<b>3.1. INTRODUCTION .....</b>	<b>72</b>
<b>3.2. RESULTS .....</b>	<b>75</b>
3.2.1. Chimeric AL RABV Envelope Glycoprotein Construction .....	75
3.2.2. Production of Arctic-like Rabies Virus Pseudotyped Virus .....	76
3.2.3. Neutralisation Assays to Evaluate the Efficacy of Existing Prophylaxis against the Arctic-like Rabies Virus Lineage .....	81
<b>3.3. DISCUSSION .....</b>	<b>89</b>
<b>CHAPTER 4. USING PSEUDOTYPED VIRUS TO STUDY THE ANTIGENICITY OF PHYLOGROUP I AND III LYSSAVIRUSES BY SWITCHING ANTIGENIC SITES OF THE ENVELOPE GLYCOPROTEIN .....</b>	<b>94</b>

<b>4.1. INTRODUCTION.....</b>	<b>94</b>
<b>4.2. RESULTS .....</b>	<b>96</b>
4.2.1. Antigenic Site Swapping and Pseudotyped Virus Production .....	96
4.2.2. Characterising Neutralisation of RABV and WCBV Antigenic Variants by Serum Samples .....	100
<b>4.3. DISCUSSION .....</b>	<b>105</b>
<b>CHAPTER 5. OPTIMISING THE PRODUCTION OF FILOVIRUS PSEUDOTYPES FOR USE IN SEROLOGICAL STUDIES.....</b>	<b>110</b>
<b>5.1. INTRODUCTION.....</b>	<b>110</b>
<b>5.2. RESULTS .....</b>	<b>112</b>
5.2.1. Optimal Producer and Target Cell Lines .....	112
5.2.2. Chimeric and Truncated <i>Ebolavirus</i> Envelope Glycoprotein Construction .....	121
5.2.3. Influence of Target Cell Line on <i>Ebolavirus</i> Pseudotyped Virus Serology Studies .....	126
<b>5.3. DISCUSSION .....</b>	<b>134</b>
<b>CHAPTER 6. PSEUDOTYPED VIRUS QUANTIFICATION AND REPORTER GENE CHARACTERISATION .....</b>	<b>141</b>
<b>6.1. INTRODUCTION.....</b>	<b>141</b>
<b>6.2. RESULTS .....</b>	<b>147</b>
6.2.1. Incorporating New Reporters into the Pseudotyped Virus Platform .....	147
6.2.2. Comparison and Correlation of the Disparate Readout Units of Pseudotyped Virus Reporters.....	159
6.2.3. Quantification of Pseudotyped Virus.....	168
<b>6.3. DISCUSSION .....</b>	<b>175</b>
<b>CHAPTER 7. CONCLUSIONS AND FUTURE WORK .....</b>	<b>183</b>
<b>APPENDIX I.....</b>	<b>188</b>
<b>I.1. VIRUS ENVELOPE PROTEIN.....</b>	<b>188</b>
<b>I.2. REPORTER PROTEIN SEQUENCES .....</b>	<b>197</b>
<b>I.3. PLASMID MAPS .....</b>	<b>202</b>
<b>APPENDIX II .....</b>	<b>205</b>
<b>II.1. ARCTIC-LIKE RABIES VIRUS PHYLOGENY.....</b>	<b>205</b>
<b>II.2. SERUM SAMPLES FROM RABIES VIRUS VACCINATED HUMANS AND DOMESTIC ANIMALS .....</b>	<b>206</b>
<b>APPENDIX III.....</b>	<b>207</b>
<b>III.1. ASSESSMENT OF EXPRESSION PLASMID FOR <i>EBOLAVIRUS</i> ENVELOPE PROTEIN.....</b>	<b>207</b>
<b>III.2. MORPHOLOGY OF <i>ZAIRE EBOLAVIRUS</i> PSEUDOTYPED VIRUS .....</b>	<b>208</b>
<b>APPENDIX IV .....</b>	<b>209</b>

<b>IV.1. QUANTIFICATION OF PV GENOME COPIES VIA RT-QPCR.....</b>	<b>209</b>
<b>IV.2. QUANTIFICATION OF PV CORE RT ACTIVITY VIA SG-PERT ASSAY .....</b>	<b>210</b>
<b>REFERENCES .....</b>	<b>211</b>

# List of Figures

FIGURE 1.1	TIMELINE MAPPING THE EMERGENCE OF VIRUSES CONSIDERED A RESEARCH AND DEVELOPMENT PRIORITY BY THE WHO.....	3
FIGURE 1.2	DIVERSITY WITH THE <i>LYSSAVIRUS</i> GENUS.....	11
FIGURE 1.3	SCHEMATIC REPRESENTATION OF CONFORMATIONAL REARRANGEMENTS FOR DIFFERENT CLASSES OF VIRAL FUSION PROTEIN DURING VIRAL AND CELL MEMBRANE FUSION .....	19
FIGURE 1.4	SCHEMATIC REPRESENTATION OF THE LENTIVIRAL GENOME AND VECTOR SYSTEM.....	30
FIGURE 1.5	SCHEMATIC REPRESENTATION OF THE THREE PLASMID TRANSFECTION SYSTEM FOR RETROVIRAL PSEUDOTYPED VIRUS PRODUCTION AND USE IN A NEUTRALISATION ASSAY .....	33
FIGURE 1.6	REPRESENTATION OF COST AND TIME CONSTRAINTS OF REPORTER GENES INCORPORATED WITH THE RETROVIRAL PSEUDOTYPED VIRUS PLATFORM.....	35
FIGURE 2.1	PRIMER DESIGN FOR SPLICING BY OVERLAP EXTENSION (SOE) PCR.....	56
FIGURE 3.1	SCHEMATIC REPRESENTATION OF CHIMERIC ENVELOPE GLYCOPROTEIN CONSTRUCTS .....	76
FIGURE 3.2	COMPARISON OF PSEUDOTYPED VIRUS TITRES USING WILDTYPE AND CHIMERIC ENVELOPE GLYCOPROTEINS.....	77
FIGURE 3.3	COMPARISON OF CELL INFECTION BY PSEUDOTYPED VIRUS BEARING WILDTYPE VERSUS CHIMERIC ENVELOPE GLYCOPROTEIN .....	79
FIGURE 3.4	GATING OF CELLS FOR FLOW CYTOMETRY ANALYSIS .....	80
FIGURE 3.5	DEGREE OF NUCLEOTIDE AND AMINO ACID SEQUENCE IDENTITY BETWEEN ARCTIC-LIKE RABIES VIRUS AND CVS-11 ENVELOPE GLYCOPROTEIN ECTO-TRANSMEMBRANE DOMAIN .....	82
FIGURE 3.6	NEUTRALISATION OF PSEUDOTYPED VIRUS BY OIE AND WHO SERUM STANDARDS .....	83
FIGURE 3.7	PSEUDOTYPED VIRUS NEUTRALISATION IC <sub>100</sub> ENDPOINT DILUTIONS FOR HUMAN AND ANIMAL SERUM SAMPLES .....	85
FIGURE 3.8	PSEUDOTYPED VIRUS NEUTRALISATION IC <sub>100</sub> ENDPOINT DILUTIONS FOR HRIG AND MAB SAMPLES .....	87
FIGURE 3.9	COMPARISON OF THE NEUTRALISATION IC <sub>100</sub> ENDPOINT TITRES FOR WILDTYPE CVS-11 G PV COMPARED TO CHIMERIC CVS-11 ETMVSVC G PSEUDOTYPED VIRUS .....	88
FIGURE 4.1	SCHEMATIC REPRESENTATION OF THE ANTIGENIC SITE SWAPPED ENVELOPE GLYCOPROTEINS PRODUCED.....	98
FIGURE 4.2	COMPARISON OF TITRES OF PSEUDOTYPED VIRUS PRODUCED COMPRISING WILD TYPE AND ANTIGENIC SITE SWAPPED ENVELOPE GLYCOPROTEINS .....	99
FIGURE 4.3	COMPARISON OF SERUM IC <sub>100</sub> ENDPOINT NEUTRALISATION OF RABV AND WCBV ANTIGENIC SITE SWAP GLYCOPROTEIN PSEUDOTYPED VIRUS .....	104
FIGURE 5.1	SEQUENCE HOMOLOGY BETWEEN FILOVIRUS ENVELOPE GLYCOPROTEINS .....	113
FIGURE 5.2	CELL LINES PERMISSIVE TO INFECTION BY FILOVIRUS ENVELOPE GLYCOPROTEIN PSEUDOTYPED VIRUS .....	115
FIGURE 5.3	COMPARATIVE TITRATION OF LENTIVIRAL PSEUDOTYPED VIRUS PRODUCED WITH AND WITHOUT ENVELOPE GLYCOPROTEIN ON THREE CELL LINES PERMISSIVE TO FILOVIRUS INFECTION...	117
FIGURE 5.4	COMPARISON OF CELL LINES FOR PRODUCTION OF FILOVIRUS PSEUDOTYPED VIRUS .....	118

FIGURE 5.5	PRODUCTION OF PSEUDOTYPED VIRUS AFTER TRANSFECTING WITH DIFFERENT QUANTITIES OF ENVELOPE PLASMID DNA .....	120
FIGURE 5.6	SCHEMATIC REPRESENTATION OF CHIMERIC AND TRUNCATED <i>EBOLAVIRUS</i> ENVELOPE GLYCOPROTEIN CONSTRUCTS.....	122
FIGURE 5.7	PERCENTAGE CHANGE IN <i>EBOLAVIRUS</i> PSEUDOTYPED VIRUS TITRE USING A CHIMERIC OR TRUNCATED ENVELOPE GLYCOPROTEIN .....	123
FIGURE 5.8	SCHEMATIC REPRESENTATION OF CHIMERIC <i>EBOLAVIRUS</i> ENVELOPE GLYCOPROTEIN CONSTRUCTS WITH A HA OR HIV CYTOPLASMIC DOMAIN .....	124
FIGURE 5.9	PERCENTAGE CHANGE IN <i>EBOLAVIRUS</i> PSEUDOTYPED VIRUS TITRE USING A CHIMERIC ENVELOPE GLYCOPROTEIN WITH A HA OR HIV CYTOPLASMIC DOMAIN .....	125
FIGURE 5.10	ASSESSMENT OF THE NEUTRALISATION OF LENTIVIRAL PSEUDOTYPED VIRUS WITH AND WITHOUT ENVELOPE GLYCOPROTEIN .....	127
FIGURE 5.11	COMPARISON OF <i>EBOLAVIRUS</i> PSEUDOTYPED VIRUS NEUTRALISATION BY MONOCLONAL ANTIBODY SAMPLES ON THREE TARGET CELL LINES .....	129
FIGURE 5.12	COMPARISON OF <i>EBOLAVIRUS</i> PSEUDOTYPED VIRUS NEUTRALISATION BY SERUM SAMPLES ON THREE TARGET CELL LINES .....	132
FIGURE 6.1	SCHEMATIC REPRESENTATION OF THE PCS[REPORTER]W AND pDUAL REPORTER GENE EXPRESSION PLASMIDS.....	145
FIGURE 6.2	COMPARATIVE TITRATION OF PSEUDOTYPED VIRUS INCORPORATING EXISTING AND NEW LUCIFERASE REPORTER GENES.....	149
FIGURE 6.3	TITRATION OF PSEUDOTYPED VIRUS INCORPORATING A SECRETED ALKALINE PHOSPHATASE REPORTER GENE.....	151
FIGURE 6.4	TITRES OF PSEUDOTYPED VIRUS INCORPORATING A SECRETED ALKALINE PHOSPHATASE OR FIREFLY LUCIFERASE REPORTER GENE AFTER CHANGING THE MEDIA DURING INCUBATION .....	153
FIGURE 6.5	CELL INFECTION BY PSEUDOTYPED VIRUS INCORPORATING NEW FLUORESCENT REPORTER PROTEIN GENES IN COMPARISON TO STANDARD GFP .....	155
FIGURE 6.6	GATING OF CELLS FOR FLOW CYTOMETRY ANALYSIS VIA THE FITC OR PE-TEXAS RED CHANNEL 157	
FIGURE 6.7	COMPARISON OF INFECTIVE TITRES MEASURED FOR PSEUDOTYPED VIRUS INCORPORATING NEW AND EXISTING FLUORESCENT REPORTER GENES .....	158
FIGURE 6.8	SCHEMATIC REPRESENTATION OF THE ORIENTATION OF REPORTER GENES INCORPORATED WITHIN THE pDUAL EXPRESSION PLASMID.....	159
FIGURE 6.9	INFECTIVE TITRES TO EVALUATE INCORPORATING TWO REPORTER GENES WITHIN THE PSEUDOTYPED VIRUS CORE VIA A pDUAL EXPRESSION PLASMID.....	161
FIGURE 6.10	SCHEMATIC REPRESENTATION OF THE T2A PEPTIDE SEQUENCE AND ORIENTATION OF REPORTER GENES INCORPORATED WITHIN THE PCS-T2A-W EXPRESSION PLASMID .....	163
FIGURE 6.11	INFECTIVE TITRES TO EVALUATE INCORPORATING TWO REPORTER GENES WITHIN THE CORE OF PSEUDOTYPED VIRUS WITH A VSV, RABV OR EBOV ENVELOPE GLYCOPROTEIN VIA THE PCS-T2A-W EXPRESSION PLASMID .....	165

FIGURE 6.12	RATIO BETWEEN LUMINESCENT (RLU) AND FLUORESCENT (IFU) READOUT UNITS USING REPORTER GENES LINKED BY A T2A PEPTIDE.....	167
FIGURE 6.13	QUANTIFICATION OF FIREFLY LUCIFERASE REPORTER GENE PSEUDOTYPED VIRUS COMPRISING A VSV, RABV OR EBOV ENVELOPE GLYCOPROTEIN .....	170
FIGURE 6.14	QUANTIFICATION OF GREEN FLUORESCENT PROTEIN REPORTER GENE PSEUDOTYPED VIRUS COMPRISING A VSV, RABV OR EBOV ENVELOPE GLYCOPROTEIN .....	171
FIGURE 6.15	QUANTIFICATION OF <i>LacZ</i> REPORTER GENE PSEUDOTYPED VIRUS COMPRISING A VSV, RABV OR EBOV ENVELOPE GLYCOPROTEIN .....	172
FIGURE XVI	pI.18 EXPRESSION PLASMID .....	202
FIGURE XVII	pCAGGS EXPRESSION PLASMID .....	203
FIGURE XVIII	pCS[REPORTER]W EXPRESSION PLASMID.....	204
FIGURE XIX	MAXIMUM LIKELIHOOD PHYLOGENETIC TREE OF 96 RABV GLYCOPROTEIN CODING SEQUENCES.....	205
FIGURE XX	COMPARISON OF EBOLAVIRUS PV TITRES USING DIFFERENT ENVELOPE GP EXPRESSION PLASMIDS	207
FIGURE XXI	ELECTRON MICROSCOPY OF <i>ZAIRE EBOLAVIRUS</i> PV.....	208
FIGURE XXII	STANDARD CURVE FOR RT-QPCR GENOME QUANTIFICATION OF PV .....	209
FIGURE XXIII	STANDARD CURVE FOR SG-PERT ASSAY CORE RT ACTIVITY QUANTIFICATION OF PV	210

## List of Tables

TABLE 2.1	<i>ESCHERICHIA COLI</i> STRAIN AND ASSOCIATED GENOTYPE.....	44
TABLE 2.2	BACTERIAL CULTURE MEDIA .....	44
TABLE 2.3	PRIMERS AND CLONING SITES FOR ENVELOPE PROTEIN GENES INSERTED INTO THE pI.18 EXPRESSION PLASMID .....	46
TABLE 2.4	PRIMERS AND CLONING SITES FOR ENVELOPE PROTEIN GENES INSERTED INTO THE pCAGGS EXPRESSION PLASMID .....	48
TABLE 2.5	PRIMERS AND CLONING SITES FOR REPORTER PROTEIN SEQUENCES INSERTED INTO THE PCS[INSERT]W EXPRESSION PLASMID.....	50
TABLE 2.6	PRIMERS AND CLONING SITES FOR REPORTER PROTEIN SEQUENCES INSERTED INTO THE pDUAL EXPRESSION PLASMID .....	51
TABLE 2.7	SEQUENCING PRIMERS.....	51
TABLE 2.8	PCR CYCLING CONDITIONS FOR ACCUPRIME PFX SUPERMIX .....	54
TABLE 2.9	PCR CYCLING CONDITIONS FOR Q5 HOT START HIGH-FIDELITY 2X MASTER MIX .....	54
TABLE 2.10	CELL LINES .....	59
TABLE 2.11	PLASMID DNA MIX FOR TRANSFECTION .....	60
TABLE 2.12	TRANSFECTION REAGENT.....	60
TABLE 2.13	FLOW CYTOMETRY FLUROCHROME CHANNEL PARAMETERS.....	65
TABLE 2.14	HIV-LTR PRIMER AND PROBE SEQUENCE FOR RT-QPCR.....	68
TABLE 2.15	RT-QPCR CYCLING CONDITIONS FOR RNA ULTRASENSE™ MASTER MIX .....	68
TABLE 2.16	MS2 cDNA PRIMER SEQUENCE FOR SG-PERT ASSAY .....	70
TABLE 2.17	SG-PERT ASSAY CYCLING CONDITIONS.....	70
TABLE 3.1	ARCTIC-LIKE RABIES VIRUS ISOLATES .....	75
TABLE 3.2	FOLD INCREASE IN PSEUDOTYPED VIRUS TITRE USING A CHIMERIC VSV CYTOPLASMIC DOMAIN ENVELOPE GLYCOPROTEIN.....	77
TABLE 3.3	FOLD INCREASE IN TITRE OF PSEUDOTYPED VIRUS WITH A CHIMERIC VSV CYTOPLASMIC DOMAIN GLYCOPROTEIN MEASURED USING FLOW CYTOMETRY ANALYSIS.....	80
TABLE 4.1	SEQUENCE ALIGNMENT OF RABIES VIRUS AND WEST CAUCASIAN BAT VIRUS ENVELOPE GLYCOPROTEIN ANTIGENIC SITES .....	97
TABLE 4.2	RABIES VIRUS ANTIGENIC SITE SWAP PSEUDOTYPED VIRUS NEUTRALISATION BY SERUM SAMPLES.....	101
TABLE 4.3	WEST CAUCASIAN BAT VIRUS ANTIGENIC SITE SWAP PSEUDOTYPED VIRUS NEUTRALISATION BY SERUM SAMPLES .....	103
TABLE 5.1	<i>FILOVIRIDAE</i> ISOLATES.....	112
TABLE 5.2	NEUTRALISATION IC <sub>50</sub> ENDPOINT TITRES OF MONOCLONAL ANTIBODY SAMPLES MEASURED BY PSEUDOTYPED VIRUS NEUTRALISATION ASSAY ON THREE TARGET CELL LINES .....	130
TABLE 5.3	NEUTRALISATION IC <sub>50</sub> ENDPOINT TITRES OF SERUM SAMPLES MEASURED BY PSEUDOTYPED VIRUS NEUTRALISATION ASSAY ON THREE TARGET CELL LINES .....	133
TABLE 6.1	PRIMERS FOR CLONING NEW REPORTER GENES .....	147

TABLE 6.2	RATIO OF PSEUDOTYPED VIRUS QUANTIFIED BY COUNTING PARTICLES, GENOME COPIES AND RT ACTIVITY TO BIOLOGICAL TITRE .....	174
TABLE III	FAVN TITRE ASSIGNED TO VACCINATED HUMAN SERUM SAMPLES .....	206
TABLE IV	FAVN TITRE ASSIGNED TO VACCINATED DOMESTIC ANIMAL SERUM SAMPLES .....	206

# Acknowledgements

I am enormously thankful for the great support of my supervisor Dr Edward Wright. Working within his lab has been a wonderful experience. Ed constantly goes out of his way to make things happen and he has provided me with so many opportunities. It has further been a privilege to be a part of the VPU.

Thank you to the University of Westminster for providing me with a scholarship to undertake this work. Additionally, to the many members of staff who have supported me throughout my studies.

I would like to thank Dr Giada Mattiuzzo and James Ashall for their hard work and generosity in supporting me to undertake the RT-qPCR and Nanoparticle Tracking Analysis elements of my work at NIBSC.

I have been lucky to share a lab with some brilliant people. I'd like to thank Karima for her endless support and encouragement, George for his big song voice, chats and many enjoyable hours in the micro-room, Haddy for her laughter and Pamela for her wise words and enthusiasm. Lastly, thanks to Kavita, for the great advice and sharing of equipment during our time working together. His GBB tip-racking extravaganzas made the extra work he gave me worthwhile!

All my peers have contributed towards such an enjoyable working environment. I'd particularly like to acknowledge some great friends I've made during this time. Faye, Katie, Lorenza, Artun and Brad for guiding the way while sharing many a good time - with plenty more to come! Louise, Moyin, Olga and Rachith, thank you for, in turn, being there all the way, threatening to overtake me, our lunchtime chinwags and for always asking to see my results.

I'd like to especially thank Rima for living with me for the past 5 years, moving 3 times and not once threatening to run away! I'm lucky to have such a good friend who has inspired and taught me a lot during this time.

Most importantly, I have an amazing family to thank. Mum, Dad, thank you for always going above and beyond to support me, no matter what mad ventures I choose to pursue! Lana, I might be older but it seems that you are wiser (almost!) and you may not realise how much I look up to you – thanks for being my big little sister. Here is another book for the bookshelf, no pressure to read this one, but it is dedicated to you!

## **Author's Declaration**

I declare that the present work was carried out in accordance with the Guidelines and Regulations of the University of Westminster. The work is original except where indicated by special reference in the text.

The submission as a whole or part is not substantially the same as any that I previously or am currently making, whether in published or unpublished form, for a degree, diploma or similar qualification at any university or similar institution.

Until the outcome of the current application to the University of Westminster is known, the work will not be submitted for any such qualification at another university or similar institution.

Any views expressed in this work are those of the author and in no way represent those of the University of Westminster.

## List of Abbreviations

Ψ	Packaging signal
AL RABV	Arctic-like rabies virus
BSL	Biosafety level
cDNA	Complementary DNA
cPPT	Central polypurine tract
CVS	Challenge virus standard
DALYs	Disability Adjusted Life Years
DNA	Deoxyribonucleic acid
dNG	Dual-nuclear localised GFP
dNT	Dual-nuclear localised tomato fluorescent protein
DUVV	Duvenhage lyssavirus
EBLV	European bat lyssavirus
EBOV	Ebola virus (sp. <i>Zaire ebolavirus</i> )
EIDs	Emerging infectious diseases
ELISA	Enzyme-linked immunosorbent assay
emGFP	Emerald green fluorescent protein
EVD	Ebola virus disease
FAVN	Fluorescent antibody virus neutralisation test
FDA	US Food and Drugs Administration
FLuc	Firefly luciferase
G	Lyssavirus envelope glycoprotein
GFP	Green fluorescent protein
GP	Ebolavirus envelope glycoprotein
HA	Haemagglutinin
HI	Haemagglutination-inhibition assay
HIV	Human immunodeficiency virus
HRIG	Human rabies immunoglobulin
IC <sub>100</sub> /IC <sub>50</sub>	Full/half maximum inhibitory concentration
IFA	Immunofluorescent antibody assay
IFU	Infectious units
Ig	Immunoglobulin
IHR	International Health Regulations
IKOV	Ikoma virus
LB	Luria broth

LBV	Lagos bat virus
LTR	Long terminal repeat
mAb	Monoclonal antibody
MERS-CoV	Middle East respiratory syndrome coronavirus
MeV	Measles virus
MLV	Murine leukaemia virus
MOKV	Mokola virus
mRNA	Messenger RNA
MVD	Marburg virus disease
NA	Neuraminidase
NAb	Neutralising antibody
NAI	Neuraminidase inhibitors
NHPs	Non-human primates
NIBSC	National Institute for Biological Standards and Control
NPC1	Niemann-Pick C1
OIE	World Organisation for Animal Health
PCR	Polymerase chain reaction
PEP	Post-exposure prophylaxis
PHEIC	Public health emergency of international concern
PV	Pseudotyped virus
PVNA	Pseudotyped virus neutralisation assay
RABV	Rabies virus
RAVV	Ravn virus (sp. <i>Marburg marburgvirus</i> )
RFFIT	Rapid fluorescent focus inhibition test
RIG	Rabies immunoglobulin
RLU	Relative light units
RNA	Ribonucleic acid
RRE	Rev-response element
RT-qPCR	Quantitative reverse transcription PCR
SARS-CoV	Sever acute respiratory syndrome coronavirus
SEAP	Secreted alkaline phosphatase
SIN	Self-inactivating
SFFV	Spleen focus forming virus
SG-PERT	SYBR Green product-enhanced reverse transcriptase assay
SOE PCR	Splicing by overlap extension PCR
SUDV	Sudan virus (sp. <i>Sudan ebolavirus</i> )
sGP	Secreted GP

TCID <sub>50</sub>	50% tissue culture infective dose
USAID	United States Agency for International Development
VNA	Virus neutralisation assay
VSV	Vesicular stomatitis virus
WAHID	World Animal Health Information Database
WCBV	West Caucasian bat virus
WHO	World Health Organisation
WPRE	Woodchuck hepatitis virus post-transcriptional regulatory element

# Chapter 1. Introduction

## 1.1. Emerging Zoonotic Viruses

### 1.1.1. History and Processes of Zoonotic Virus Emergence

Emerging infectious diseases (EIDs) present a continuing threat to human, animal and crop health, constituting a source of great global burden and economic demand (Jones *et al.*, 2008; Weiss & McMichael, 2004). Little over half a century ago there was widespread belief among the medical community that EIDs were moving towards eradication, a view which was rumoured to be shared by the US Surgeon General of the time, Dr. William Stuart (1965-1969), with the largely cited quote “It is time to close the book on infectious diseases”, although this has more recently been reported as inaccurate (Spellberg & Taylor-Blake, 2013). Advances in sanitation and disease surveillance along with increased vaccine availability and use of antibiotics had given rise to a decline in infectious disease occurrence in the developed world, yet this phenomenon was short lived. Within the last 40 years there has been a marked, steady increase in the incidence of EIDs which is reflected in the current and continuing demand for research advances coupled with ever heightening media attention (Jones *et al.*, 2008; Meslin *et al.*, 2000; Reperant & Osterhaus, 2017; Smith *et al.*, 2014).

Zoonotic pathogens, causing infections in animals which are capable of transmission to humans, are accountable for around 65% of EIDs, with zoonosis caused by viral pathogens regarded as one of the most significant threats (Jones *et al.*, 2008; Smith *et al.*, 2014; Taylor *et al.*, 2001). Indeed, a list has been culminated by the World Health Organisation (WHO) of diseases which are a priority for research and development purposes. This is based on a lack of diagnostic and prophylactic treatments as well as the public health risk and epidemic potential they pose. It is comprised only of zoonotic viruses, all of which first emerged within the last century, distributed over four continents (Figure 1.1) (WHO, 2017). Zoonotic virus (re-)emergence, as either a newly recognised infection

or the rapidly increasing incidence and geographic range of an existing virus, is attributable to changes in ecological, social and environmental factors (Daszak *et al.*, 2000; Morse, 1995; Morse *et al.*, 2012). Scientific advances bringing an initial period of decline in EIDs could not compensate for other dramatic, fast moving changes which arose in the developing global community. Deforestation, rural-to-urban migration and displacement in zones of conflict, along with an increase in international connectivity through air travel and trade links, culminates in bringing humans into closer proximity with animal host reservoirs and the ability of emerging virus species to rapidly spread across continents (Gortazar *et al.*, 2014; Pybus *et al.*, 2015; Weiss & McMichael, 2004).

An example is the 1994 and 1999 emergence of henipavirus outbreaks in the Australasian region. Farming into previously uncultivated land allowed transmission to humans from equine and swine intermediary amplifying hosts, of Hendra and Nipah virus respectively, after exposure to Pteropid bats, the viral reservoir (Field *et al.*, 2001; Kuzmin *et al.*, 2011; Weiss & McMichael, 2004). Further, the 2002-3 emergence of severe acute respiratory syndrome coronavirus (SARS-CoV) rapidly resulted in an epidemic involving cases in over 30 countries, demonstrating the significance of air travel in abolishing the natural containment effect of geographical boundaries (Chan *et al.*, 2013; Cheng *et al.*, 2007). This has been further corroborated by the rapid spread of Middle East respiratory syndrome coronavirus (MERS-CoV) from the Middle East to Europe in 2012 and the proceeding nosocomial outbreak in South Korea during 2015, with air travel responsible for the introduction into each location (Anderson & Baric, 2012; Su *et al.*, 2015; de Wit *et al.*, 2016). Additionally, during the 2013-16 West African Ebola virus outbreak, the worldwide threat posed from its spread via international air travel drew much attention and saw the implementation of air travel restrictions, along with exit and entry screening (Bogoch *et al.*, 2015; To *et al.*, 2015). These events act to highlight the need for global collaboration on epidemiology and surveillance in order to rapidly respond to developing pandemic threats.

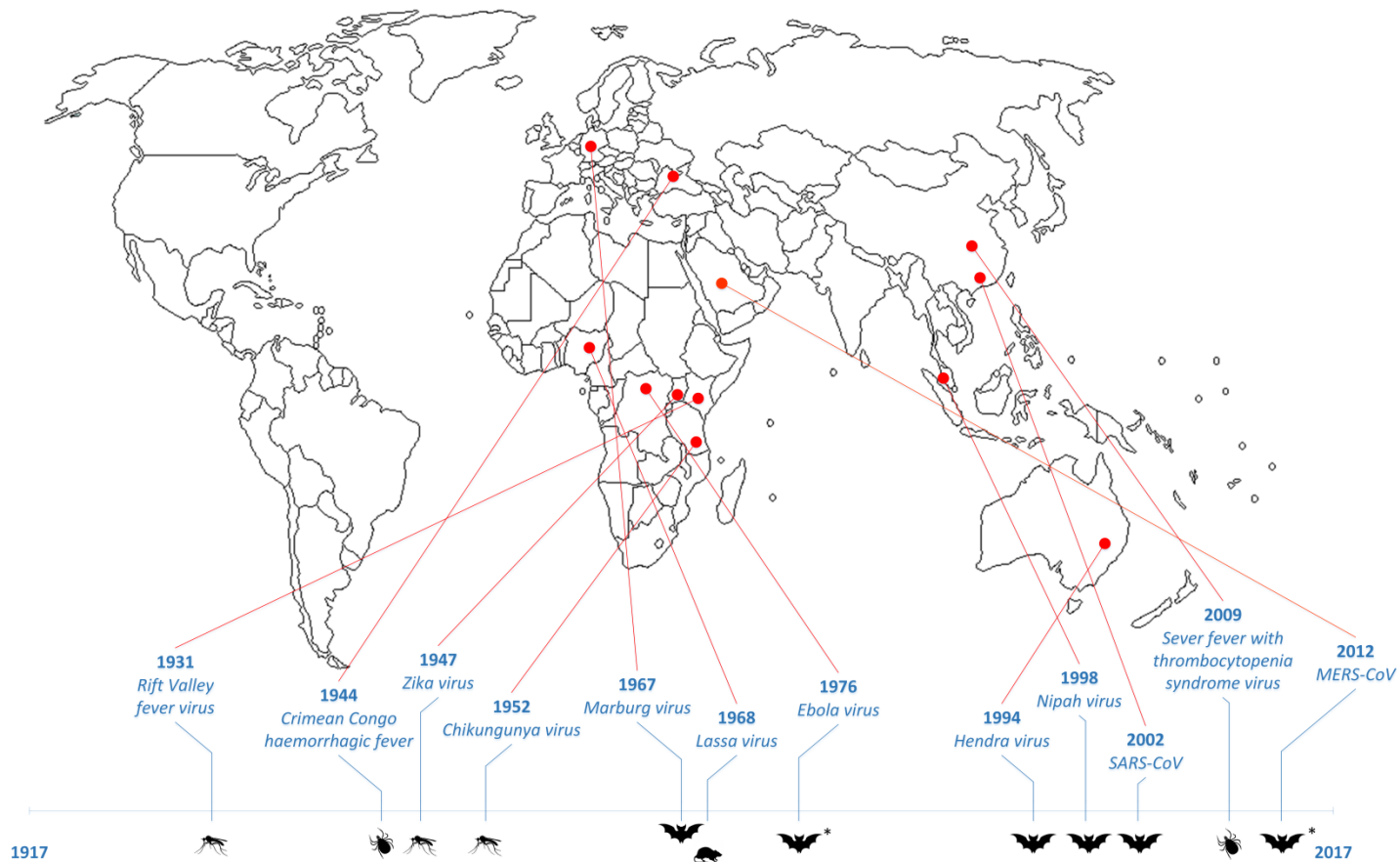


**Figure 1.1 Timeline Mapping the Emergence of Viruses Considered a Research and Development Priority by the WHO**

The year of first isolation, location and key host reservoirs/vectors are indicated for emerging viruses which are currently considered a priority by the WHO due to the potential to cause a public health emergency, requiring urgent research and development to produce effective diagnostic tests and prophylaxis. The timeline is representative of the past century (1917 – 2017) and arrowheads indicate the region where the virus emerged. \* Likely host reservoir.

It is not only mankind's encroachment and technological advances that have exacerbated the burden caused by emerging viruses, but also the ability of the viruses themselves to adapt and evolve to these anthropogenic drivers of emergence. Chikungunya virus, an arbovirus spread by the *Aedes aegypti* mosquito, was first documented in the 1950s in Africa but has re-emerged in the last decade to cause a series of major epidemics in Africa, Asia and more recently Europe (Caglioti *et al.*, 2013). During outbreaks in the Reunion Islands (2005-6) and Kerala, India (2009) the virus has evolved to contain specific mutations in its envelope glycoprotein that allow it to now be effectively transmitted by the *Aedes albopictus* mosquito (Tsetsarkin *et al.*, 2007; Tsetsarkin & Weaver, 2011), thereby giving it access to new environmental niches and increasing the severity of outbreaks in existing endemic areas. Similarly, it has recently been suggested that co-evolution of Zika virus with its *Aedes* mosquito host species, acquiring a mutation in a non-structural protein, lead to its enhanced infectivity and prevalence within mosquitoes, which may have contributed to its recent re-emergence and spread (Liu *et al.*, 2017). First isolated in Uganda in 1947, Zika virus caused only sporadic cases prior to outbreaks in western, followed by southern, Pacific islands and the French Polynesia between 2007-13. Then, geographical expansion in 2015 led to its emergence in the Americas and the resulting epidemic which spread across three continents. It was declared a public health emergency of international concern by the WHO in February 2016 due to its association with an alarming increase in cases of microcephaly (Baud *et al.*, 2017; McCloskey & Endericks, 2017). In each of these cases, economic growth in the developing countries driving urbanisation gave rise to an increase in mosquito populations and human contacts. A higher number of transmission events fuel the probability of the virus evolving genetically favourable adaptations.

The majority of emerging zoonotic viruses, and indeed those accountable for some of the most threatening outbreaks, are RNA viruses. High error rates of virus-encoded RNA polymerase allows for frequent mutations during genome replication, with additional genetic recombination or reassortment possible in positive-sense RNA viruses and those with segmented genomes respectively in particular (Chan *et al.*, 2013; Nichol *et al.*, 2000). The ability to rapidly adapt and

exploit the evidenced environmental and social worldwide developments has facilitated their successful transmission. They are further able to overcome selective pressures of the immune response and adaptation of the host. An additional feature advantageous to their success is asymptomatic carriage in reservoir host species, demonstrated by bat species which are implicated as the reservoir of many zoonotic RNA viruses. Bats demonstrate persistent viral shedding despite a lack of notable pathology, a phenomenon tentatively accounted for by characteristics of their immune system (Chan *et al.*, 2013; Kuzmin *et al.*, 2011; Zhang *et al.*, 2013). There is additional speculative theory on the role of flight, unique to these mammals, which is metabolically demanding resulting in body temperatures in the range of those seen during fever, associated with shortened disease duration and improved recovery, yet studies to substantiate this further are needed (O'Shea *et al.*, 2014; Wang *et al.*, 2011). Indeed there is constant evolutionary pressure between viruses and their hosts, adapting to have temporary genetic advantages through interactions known as arms races (Daugherty & Malik, 2012). A phenomenon defined under the Red Queen hypothesis of organisms continually evolving to gain both reproductive and status advantages over both opposing organisms and the changing environmental landscape.

Influenza A virus is a prime example of a zoonotic virus which undergoes continual evolution events, producing new antigenic variants to evade host immune recognition under a diverse environmental and host landscape, with global transmissibility (Pybus *et al.*, 2015; Smith *et al.*, 2014). Aquatic birds are considered the primary host reservoir of influenza A viruses, which also circulate between humans and several other mammalian and avian hosts (Webby & Webster, 2001). Annual human influenza epidemics arise from antigenic drift events within circulating strains, whereby mutations occur primarily in the haemagglutinin (HA) but also neuraminidase (NA) envelope proteins driven by an error prone RNA polymerase. More critical, although less frequent, are antigenic shift events which arise upon co-infection of a cell with two or more influenza viruses, leading to re-assortment of the segmented RNA genome to form an antigenically distinct variant. Such antigenic shift events gave rise to pandemic events in 1918, 1957, 1968 and

2009; with the 1918 (Spanish) influenza pandemic causing a devastating 50-100 million deaths (Johnson & Mueller, 2002). Signifying how devastating such pandemic events can be.

### **1.1.2. Significance and Future Direction of the Emerging Virus Field**

Outbreaks of emerging zoonotic viruses have repeatedly demonstrated catastrophic implications for human and animal populations, with a significant economic burden. The 2002-3 SARS-CoV outbreak infected more than 8,000 people and caused 774 deaths, with an estimated cost of USD\$40 billion. It has been estimated that the cost of a pandemic scenario during the 21<sup>st</sup> century could amount to more than USD\$60 billion per year (National Acadamey of Medicine, 2016). Animal losses can also be high; between 2006-9 OIE-WAHID veterinary services reported that 55% of livestock loss was a result of zoonosis (The World Bank, 2012). A response to the 1999 emergence of Nipah virus in Malaysia was the mass culling of more than 1 million pigs, causing significant economic implications (Lam & Chua, 2002). As a consequence of evolutionary pressures and the drivers of emergence, the threat of further emerging virus outbreaks is constant. Indeed, since a framework was introduced in 2007 for WHO epidemic alert and response activities, detailed under International Health Regulations (IHR), there have been 4 public health emergencies of international concern (PHEIC), with 3 attributed to zoonotic emerging viruses. The third declared PHEIC was in response to the 2013 Ebola virus outbreak, which devastatingly resulted in more than 11,000 deaths (WHO, 2016). Despite recognising the need to direct a coordinated, international, response to an outbreak threatening global public health, improvements are needed. It has also been widely recognised that having a responsive approach alone is limited in effectiveness, and the capacity to mitigate future threats will be greatly improved by investing in relevant public health infrastructure and research.

It is proposed that an investment of USD\$4.5 billion a year should be made towards a framework building global capabilities to counter the threats of infectious diseases, which is a relatively small sum when compared to the predicted cost of a pandemic (National Acadamey of Medicine, 2016).

The key aims are outlined as strengthening and regularly assessing public health capabilities and infrastructure under IHR legal regulations, with improved WHO leadership of better integrated global and regional activities, along with an accelerated research and development programme overseen by a dedicated committee. Public health strategies to reduce threats include surveillance programmes supported by robust high-throughput diagnostic capabilities for early diagnosis and clear infection control and isolation measures (Reperant & Osterhaus, 2017; Welfare & Wright, 2016). Contact tracing to isolate, monitor and control further transmissions is also fundamental. A tremendous example of the value of such a system was set when Ebola virus spread to Lagos, Nigeria during the recent outbreak. The country rapidly implemented intense and sustained contact tracing and control procedures, monitoring 894 contacts linked to the index case, to effectively prevent what could have been a serious outbreak in such a densely populated and connected city (Fasina *et al.*, 2014).

Active surveillance for the early detection and monitoring of these emerging zoonotic threats, which occur at the transboundary of people, animals and the ecosystem, requires a cross-sectorial, One Health approach. The benefits have been evaluated both economically, showing cost effectiveness, and in terms of public health benefits, measuring a reduction in Disability Adjusted Life Years (DALYs) as a result of disease burden (Baum *et al.*, 2017; The World Bank, 2012). Such an approach can help towards preventing outbreaks at the source and work towards predicting their occurrence (Morse *et al.*, 2012; Reperant & Osterhaus, 2017). A basic intervention was implemented to help prevent the spill-over of Nipah virus, from their fruit bat reservoir to humans within Bangladesh. This involved adding bamboo skirts to date palms (Khan *et al.*, 2012) to prevent bat saliva coming into contact with sap collected for human consumption, after it became clear harvests coincided with outbreaks. The control and surveillance of influenza virus is another good example of effective One Health measures. Live poultry markets were identified as a major transmission route for avian influenza within the crowded city of Hong Kong during an outbreak in 1997. Subsequent market closures, as well as implementing better cleaning practices and inspections has led to a greatly reduced risk of emergence (Sims & Peiris, 2013). Further,

surveillance of poultry as well as wild birds and swine for evidence of avian and swine influenza respectively, including molecular evolution, helps pre-empt potential pandemics and contributes towards guidance on which subtypes to include in seasonal vaccines (Peiris *et al.*, 2012; Sims & Peiris, 2013).

The PREDICT project, initiated in 2009 as part of the United States Agency for International Development's (USAID) Emerging Pandemic Threats program, is using a One Health approach towards strengthening global capacities to detect known and unknown zoonotic viruses within wildlife reservoirs (Kelly *et al.*, 2017; Morse *et al.*, 2012; PREDICT, 2017). The project is vast in scale, working with over 30 countries, with surveillance programmes in many developing nations which are considered hotspots for emergence. It has collected thousands of wildlife and animal samples, identifying known and novel viruses (PREDICT, 2017). The sampling of bats is particularly prominent, due to their implication as a reservoir for many zoonotic viruses and a desire to better understand their ecology, as well as the diversity of viruses they may harbour. Projects have included identifying cost-effective strategies to quantify diversity and reviewing sample collection in bats to optimise discovery (Anthony *et al.*, 2013; Young & Olival, 2016). One outcome was the early isolation of a MERS-CoV sequence from a bat that was identical to that of the human index case during the 2012 outbreak (Memish *et al.*, 2013), with further studies providing evidence for the evolutionary mechanisms behind its possible emergence from a bat reservoir host (Anthony *et al.*, 2017). Analysis also looks at high-risk patterns of human behaviour and identifies intervention points, while providing training to the local workforce to improve continuing surveillance and diagnosis capabilities. Works include a recent review into wildlife hosts of OIE listed diseases, to encourage better documentation and surveillance of increasing global wildlife trade activities (Smith *et al.*, 2017). Further, a mobile-phone based reporting system was implemented in Uganda under an Animal Morbidity and Mortality Monitoring programme to allow local rangers to provide rapid dissemination of information to enhance surveillance of potential risks (Machalaba & Karesh, 2015). Ultimately it is hoped the improvements in zoonotic

emerging virus recognition achieved under the PREDICT programme will help inform strategy and policy to lower the risks of future pandemic events.

Finally, given many emerging viruses lack appropriate diagnostic tools and prophylaxis, there is a fundamental need to undertake research towards their development. This has been recognised in the previously mentioned blueprint established by the WHO in 2015 as a response to the Ebola virus outbreak and revised in 2017; listing diseases which require priority research and development (WHO, 2017) (Figure 1.1). Prioritisation is based on a lack of, or insufficient countermeasures, taking into account the public health risk posed and potential to cause an epidemic. A target product profile is issued with the aim to fast-track the development of a pipeline of products fulfilling the set requirements. As set out in a case study on the WHO consultation activities for MERS-CoV research and product development, success requires a global dialogue between public health agencies, scientists, product developers and funders (Modjarrad *et al.*, 2016). The Ebola virus vaccine development field greatly benefitted from this coordinated, global collaboration. Working in PHEIC scenario, the accelerated regulatory and ethical approval of clinical studies, along with the provision of funding and manufacturing support, enabled several phase I and II clinical trials to be undertaken and impressively, the completion of a phase III clinical trial (Lambe *et al.*, 2017; Venkatraman *et al.*, 2017). This clearly demonstrated the potential of working to fast-track development when public health risks are high and acted to offer the necessary focus towards vaccine development for other high priority emerging viruses.

### **1.1.3. Lyssaviruses**

Rabies is one of the oldest and most deadly zoonotic diseases of mankind, causing an invariably fatal encephalitic disease in all warm-blooded mammals. It is caused by members of the *Lyssavirus* genus, belonging to the *Rhabdoviridae* family, with rabies virus (RABV) constituting the type species and thought to be responsible for the majority of human cases. Bats are considered the reservoir host of lyssaviruses, with all but two species having been associated with a species of bat

(Banyard & Fooks, 2017). However, RABV is only detected in bats within the Americas (New World), yet circulates globally within terrestrial carnivores (Figure 1.2). Indeed bites from rabid dogs is the principle transmission reservoir, responsible for 99% of human cases and causing almost 60,000 deaths a year, which predominantly occur in Africa and Asia (Fooks *et al.*, 2014; WHO, 2013). The theory is that RABV emerged within terrestrial mammals following a spill-over event, which led to its subsequently geographic expansion (Badrane *et al.*, 2001). Distinct lineages of RABV are also maintained within various wildlife carnivores, such as racoons and foxes in certain geographic locations (Troupin *et al.*, 2016). Canine rabies is estimated to cost 3.7 million DALYs and USD8.6 billion annually (Hampson *et al.*, 2015). It is considered that under reporting of rabies, partly due to the lack of effective surveillance and laboratory infrastructure (Banyard *et al.*, 2013; Sudarshan *et al.*, 2007), resulted in a lack of realisation as to its burden and historical policies were insufficient towards its elimination.

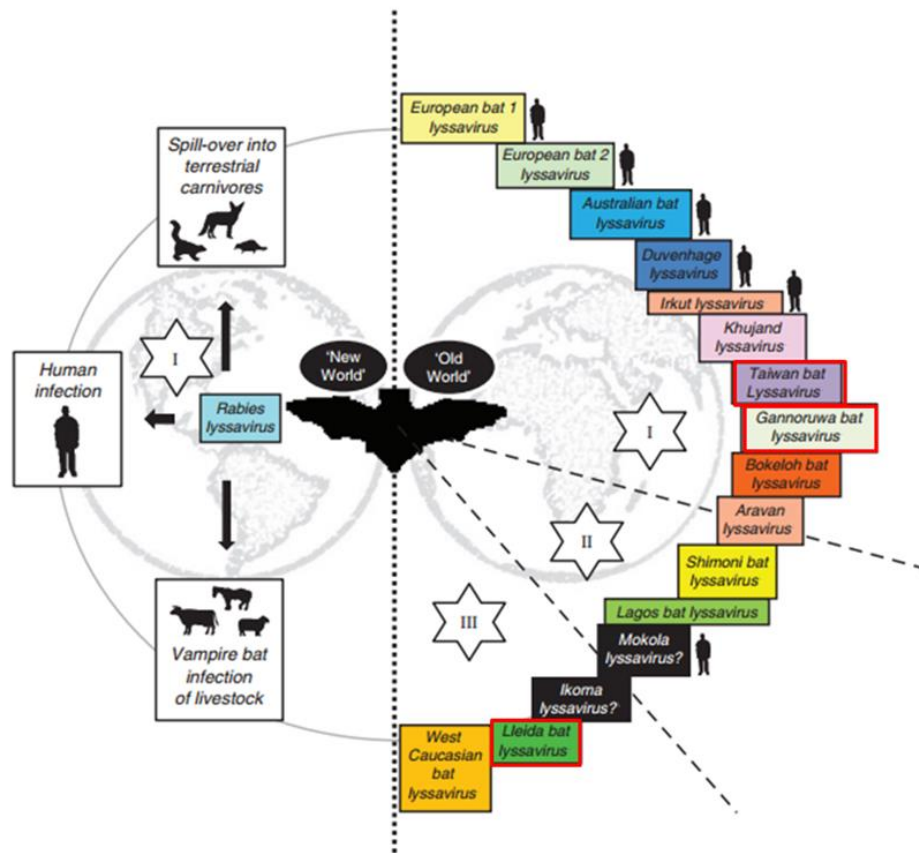


**Figure 1.2 Diversity with the *Lyssavirus* Genus**

Representation of the current global diversity within the *Lyssavirus* genus, divided into antigenically distinct phylogroups I, II and III with a human silhouette representing species associated with human fatalities. Species marked by a red boarder are awaiting classification. Adapted from (Banyard & Fooks, 2017).

Although efforts to control canine rabies have seen it successfully eliminated across many developed countries, it remains endemic across large regions of the developing world. Effective vaccines derived against RABV are available and post-exposure prophylaxis can prevent rabies if administered promptly before the onset of symptoms, however it is not always available in endemic regions and both have a high cost implication (Fooks *et al.*, 2014; Hampson *et al.*, 2008). Improving access to therapeutics certainly goes some way towards limiting its burden. Yet, the key priority towards the control of human rabies is the mass vaccination of domestic dogs, adopting a coordinated One Health approach. Investing in dog vaccination is both ethical and economically viable and effective provided at least 70% coverage is achieved (WHO, 2013; Zinsstag *et al.*, 2007). It works to avert future human exposures, decreasing medical costs and also presents a feasible method towards elimination. The cost effectiveness is calculated to be USD\$837 per averted human exposure (Zinsstag *et al.*, 2007). Such efforts have successfully eliminated dog rabies in Europe and the Americas (Muller *et al.*, 2012; Vigilato *et al.*, 2013). Further, wildlife rabies control via oral vaccination schemes has progressed towards eliminating rabies from foxes within Europe (Freuling *et al.*, 2013). In 2015, a joint WHO-OIE global framework was set for the elimination of canine rabies by 2030 (WHO & OIE, 2015). Key obstacles include the need to collect high quality surveillance data, with in-field diagnostic capabilities and the maintenance of political and social awareness (Banyard *et al.*, 2013; Fahrion *et al.*, 2017; Fooks *et al.*, 2014). Further, surveillance to better document and understand rabies circulation within wildlife species will remain important to assessing the human rabies risk.

A different challenge is posed by the non-RABV lyssaviruses, which have been detected within bats across Africa, Europe and Asia (Old World) but have rarely been documented in non-flying species (Fooks *et al.*, 2014) (Figure 1.2). The first to be identified was Lagos bat virus (LBV), isolated in 1956 in Nigeria (Boulger & Porterfield, 1958) and since then an increasing number of novel lyssaviruses continue to be discovered, circulating in distinct geographical regions. Currently 14 species are classified within the *Lyssavirus* genus, which are separated within 3 phylogroups based on antigenic and genetic distance, with a further three putative species awaiting classification

(Banyard & Fooks, 2017; Dietzgen *et al.*, 2011) (Figure 1.2). While both Mokola virus (MOKV) and Ikoma virus (IKOV), isolated from a shrew and civet respectively, have not been detected in bats, their ecology and circumstances of detection mean a bat reservoir is likely (Evans *et al.*, 2012; Horton *et al.*, 2014). These novel lyssaviruses cause an indistinguishable clinical disease, and although only a small number of human cases have been documented, routine diagnosis does not differentiate the causative species and thus the disease burden could be higher (Evans *et al.*, 2012; Fooks, 2004). Significantly, it has been shown that existing vaccines and post-exposure prophylaxis are ineffective at affording protection against more divergent species in phylogroups II and III (Brookes *et al.*, 2005; Hanlon *et al.*, 2005; Horton *et al.*, 2010). Consequently there is a drive towards the urgent development of more broadly neutralising prophylaxis. The number of human rabies cases caused by non-RABV lyssaviruses also needs to be better characterised. Given the maintenance of lyssaviruses within bats, there is an inability to eradicate rabies and once again bats are constituting a risk for spill-over events leading to infectious disease emergence (Fooks, 2004; Kuzmin *et al.*, 2011). As ever, there is a need for improved knowledge of the ecology of bats and their role in the maintenance and circulation of lyssaviruses to fully understand future risks of rabies emergence, particularly after elimination from the canine reservoir.

#### **1.1.4. Filoviruses**

Members of the *Filoviridae* family have been a known cause of severe haemorrhagic fever in humans since first emerging as the etiological agent responsible for an outbreak in 1967. Laboratory workers in Germany had become infected handling African green monkeys imported from Uganda, there were 31 cases with a 23% fatality rate and the species responsible falls within the *Marburgvirus* genera (Leroy *et al.*, 2011; Smith *et al.*, 1967). The second defined genus, *Ebolavirus*, emerged 10 years later in almost simultaneous outbreaks in Sudan and the Democratic Republic of Congo. They were each responsible for over 200 cases and found to be caused by the species *Sudan ebolavirus* and *Zaire ebolavirus*, with an 88% and 53% fatality rate respectively (Leroy *et al.*, 2011; WHO, 1978a, b). Since their emergence there have been numerous sporadic outbreaks of Marburg and Ebola virus disease (M/EVD) across remote villages in Central Africa,

limited to at most a few hundred cases, with variable fatality rates (Leroy *et al.*, 2011; To *et al.*, 2015). EVD has occurred most frequently and of the five species within the *Ebolavirus* genus, *Sudan* and *Zaire ebolavirus* are often responsible. Of the other species, just one human case has been associated with *Tai Forest ebolavirus*, when an ethnologist fell sick after performing an autopsy on a chimpanzee (Le Guenno *et al.*, 1995) and *Bundibugyo ebolavirus* has caused two outbreaks, in 2007 and 2012 which had relatively low fatality rates (To *et al.*, 2015; Towner *et al.*, 2008). Distinctly, the *Reston ebolavirus* species circulates within the Philippines and has not caused human disease (Leroy *et al.*, 2011; Miranda *et al.*, 1999).

All the filoviruses originating in Africa cause haemorrhagic fever of varying severity within humans and have shown a similarly high pathogenicity in non-human primates (NHPs). A large epizootic outbreak of *Zaire ebolavirus* has contributed to a decline in great ape numbers in Gabon and the Republic of Congo (Bermejo *et al.*, 2006; Walsh *et al.*, 2003). Frequently, the emergence of M/EVD within human populations has been linked to contacts with infected NHPs, acting as an intermediate host. For a long time the natural reservoir of these filoviruses has remained elusive, however it seems likely that bats act as a reservoir following the isolation of *Marburgvirus* from a bat species (Towner *et al.*, 2007, 2009) and demonstration that others harboured antibodies and genetic material specific to *Zaire ebolavirus* (Leroy *et al.*, 2005). It has also been shown that during an outbreak of *Zaire ebolavirus* in 2007, humans were likely directly infected following contact with migratory fruit bats which were hunted for consumption (Leroy *et al.*, 2009). Although a better understanding of the transmission cycle is required, it has become clear that direct contact with tissues of infected wildlife also constitutes a risk for human infection. Subsequent transmission between humans occurs via direct contact with bodily fluids of symptomatic individuals. As for *Reston ebolavirus*, it was identified after causing a haemorrhagic fever outbreak with high mortality in NHPs imported to the US, which were traced back to the Philippines (Miranda *et al.*, 1999). The source of infection was not identified, yet it has subsequently been found that domestic swine within the Philippines act as a host (Barrette *et al.*, 2009) and it has also been detected in pigs in China (Pan *et al.*, 2014). Humans in contact with the infected NHPs and

swine were found to have antibodies against the virus without clinical disease, thus asymptomatic infection is assumed. Perhaps unsurprisingly, bats seropositive for *Reston ebolavirus* have been implicated as a reservoir in the Philippines (Taniguchi *et al.*, 2011). Intensified studies into bat ecology have further found evidence of species seropositive for both *Zaire* and *Reston ebolavirus* in Bangladesh (Olival *et al.*, 2013) and China (Yuan *et al.*, 2012). Lastly, following a large die-off of bats in Spain they were found to be infected with a novel, genetically distinct, filovirus (Negredo *et al.*, 2011). The species, *Lloviu cuevavirus* has been classified under the *Cuevavirus* genus. There is speculation as to whether it was the cause of the bat deaths.

The recent, historical, outbreak of EVD within West Africa is suspected to have infected more than 28,000 people (WHO, 2016). The index case occurred in Guinea in December 2013 and by March 2014, when the WHO was notified of a communicable disease outbreak, there were already 111 suspected cases and *Zaire ebolavirus* was identified as the cause (Baize *et al.*, 2014). By this time the virus was already spreading to highly populated and well connected areas in bordering Liberia and Sierra Leone, which went on to report EVD cases in March and May 2014 respectively (To *et al.*, 2015). When, on 8<sup>th</sup> August 2014 the WHO declared a PHEIC, there were already 1,070 confirmed cases within the three countries (WHO, 2014). The West African region was eventually declared free of EVD in June 2016 (WHO, 2016). Some of the implications of this outbreak included the pandemic risks associated with international connectivity and the lack of available prophylaxis. As mentioned (Section 1.1.2), the establishment of the WHO blueprint of priority pathogens helped coordinate and facilitate vaccine clinical trials during the outbreak. Efforts to mitigate the risk of future outbreaks should include strengthening the healthcare infrastructure within the regions affected, including differential diagnosis of cases of viral haemorrhagic fever given Lassa virus is endemic in the same region (Baize, 2015). The location of the recent outbreak was of interest, given that it was so far from the central African regions where EVD outbreaks had until now occurred and the spill-over event that lead to the outbreak is unknown. The role of bats in filovirus ecology needs to be better understood, which has been outlined in a review by the PREDICT consortium (Olival & Hayman, 2014). Several questions also remain to be answered

towards vaccine development, such as determining the immune correlate of protection by which to measure vaccine efficacy and the durability of protection afforded by vaccines (Lambe *et al.*, 2017; Venkatraman *et al.*, 2017). Given that the recent outbreak has expanded the geographic area associated with EVD outbreaks, with predictive mapping estimating 22 countries are at risk of outbreaks (Pigott *et al.*, 2014), further research efforts to widen the understanding of filoviruses are prudent.

## **1.2. The Viral Envelope Protein**

### **1.2.1. Importance and Structure of the Viral Envelope Protein**

Structurally, many mammalian RNA viruses and all zoonotic RNA viruses consist of a viral envelope, a lipid membrane acquired during budding from host cell intracellular or extracellular membranes, which surrounds the core proteins. Protruding from this lipid membrane are viral envelope proteins, involved in attachment to host cell receptors and mediating viral entry during the process of infection, which is the initial stage of the viral replication cycle. Following conformational changes leading to irreversible binding of receptors to envelope proteins, the viral genome and capsid enters after membrane fusion has occurred, either at the host cell surface or internally after endocytosis. Envelope proteins comprise two properties to mediate this, domains which recognise and bind specifically to cell receptors and a specialised fusion domain. These are generally the same within a viral family and are responsible for initiating membrane penetration and entry of the viral genetic material post-fusion (Cosset & Lavillette, 2011). Based on structural features three classes of fusion protein have been described, class-I, II and III. The fusion domain is often hidden, becoming exposed as a result of conformational changes. This is either a direct result of envelope protein binding to the host cell receptor, allowing membrane fusion at the cell surface, or in a pH-dependent fashion, requiring entry via endocytosis with conformational changes by acidification (Cosset & Lavillette, 2011). As a result of their central role in attachment and entry into the host cell, they are considered to play a major role in determining pathogenicity. Further to

this, being the most exposed protein on the surface of the virus results in them being the major target of the humoral immune response.

Structurally, viral envelope proteins are generally type I transmembrane proteins, spanning the lipid envelope and comprising an N-terminal ectodomain, transmembrane domain and C-terminal cytoplasmic tail. It is thought an interaction between the cytoplasmic tail and the underlying matrix protein of the core may guide incorporation of the envelope protein during viral budding at the plasma membrane (Harrison, 2013). They can also contain trafficking signals, directing the envelope protein to the site of viral budding, and contribute to the fusion process (Cosset & Lavillette, 2011; White *et al.*, 2008). The ectodomain of envelope proteins directs the functions of receptor binding and fusion. For most viruses these functions are combined onto a single envelope protein, such as those of the *Rhabdoviridae* and *Filoviridae* family. However for the *Paramyxoviridae* they are split between two proteins with one directing receptor binding (H) and the other carrying out fusion activities (F). All three classes of fusion protein act to bring about fusion of the viral and host cell membranes in the same sequence; upon activation by receptor binding, a low pH, or a combination of both, a conformational change exposes a fusion domain which interacts with the cell membrane, the protein then refolds into a post-fusion structure to bring the membranes into a hemifusion state before further refolding results in the formation of a fusion pore (Figure 1.3) (Harrison, 2008; White *et al.*, 2008). The three classes are based on distinct structural features of the pre- and postfusion proteins. A key feature of class I fusion proteins is their synthesis as a precursor with two subunits, which often requires proteolytic cleavage in the producer cell for activation, as with the well characterised influenza virus HA. Alternatively, as has been demonstrated for the envelope protein (GP) of ebolavirus, cleavage of the GP<sub>1</sub> and GP<sub>2</sub> subunits is not required for cell entry (Neumann *et al.*, 2007; White *et al.*, 2008). However, rather uniquely, proteolysis of GP<sub>1</sub> by endosomal cathepsin proteases is a necessary priming step for exit from the endosome (Schornberg *et al.*, 2006). Class I fusion proteins are trimers in both pre- and post-fusion states with an  $\alpha$ -helical structure and refold into a stable rod like structure to mediate fusion (Figure 1.3A). On the other hand, class II fusion proteins are anti-parallel dimers in their

pre-fusion state, folded low on the virion surface, and upon activation refold as trimers extending towards the cell membrane and are formed of  $\beta$ -sheets (Figure 1.3B). They are synthesised in association with a chaperone protein, which regulates folding and transport and is proteolytically cleaved during maturation. In the absence of cleavage viral infectivity is reportedly reduced (Cosset & Lavillette, 2011). The class III proteins share features of the previous two; however do not undergo proteolytic processing. Like class I proteins, they are trimers in the pre-fusion state, yet have a fusion domain resembling that of class II proteins and both  $\alpha$ -helix and  $\beta$ -sheets (Figure 1.3C). Envelope proteins of the *Rhabdoviridae* family are class III fusion proteins.

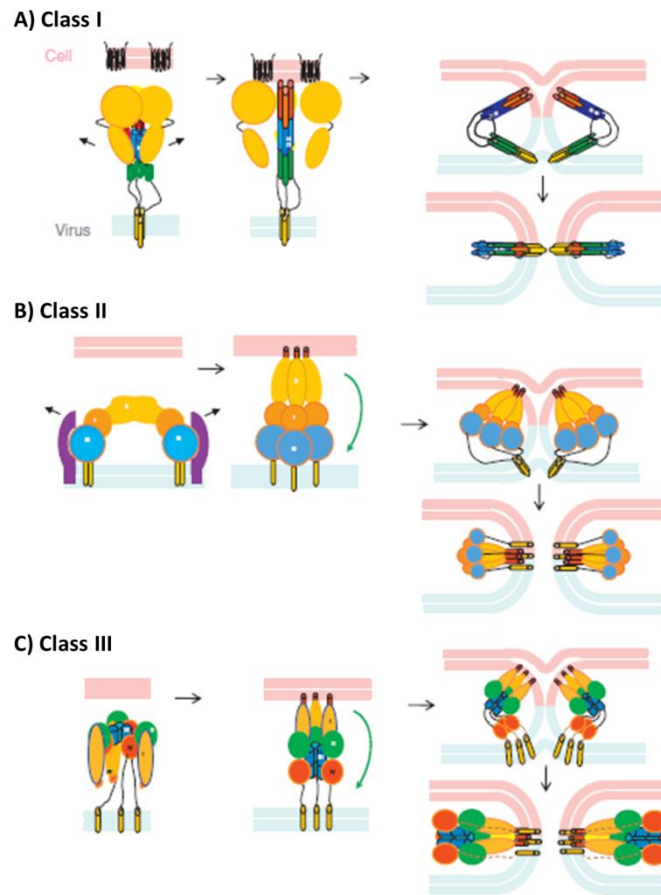


**Figure 1.3 Schematic Representation of Conformational Rearrangements for Different Classes of Viral Fusion Protein during Viral and Cell Membrane Fusion**

Fusion between viral and cell membranes, creating a fusion pore for viral entry follows the same sequence for each class of fusion protein but their conformational rearrangements differ. **(A)** Class I fusion proteins are trimers in the virus envelope pre-fusion, which upon activation directs the fusion peptide to the cell membrane. Initial refolding brings the membranes into a hemifusion state, before further folding opens a fusion pore with the fusion protein anchored as a trimer in a stable rod like structure. **(B)** Class II fusion proteins are presented in an anti-parallel dimer formation in the viral envelope, which transitions to a trimer formation and extends towards the cell membrane on activation, before folding back to create a fusion pore. **(C)** Class III fusion proteins are trimers pre- and post-fusion, like class I proteins, and present a fusion domain similar in conformation to class II proteins following activation, which also folds back to create a fusion pore for viral entry. (Cosset & Lavillette, 2011)

### **1.2.2. The Viral Envelope Protein as a Target**

Studying these envelope proteins, which constitute the primary viral surface antigen, can provide important information to assist development of prophylaxis. For example, current rabies vaccines only afford protection against lyssaviruses within phylogroup I, with studies finding no cross-protection is provided against those in phylogroups II and III (Brookes *et al.*, 2005; Fooks, 2004; Hanlon *et al.*, 2005). This is due to the antigenic distance of these lyssaviruses from the vaccine strain. By comparing identified antigenic sites mapped to the envelope protein, which are important immune targets to block functionality, it is possible to gather information to assist with the development of a vaccine which affords a greater level of cross-protection (Evans *et al.*, 2012). This also feeds into new approaches to evaluate vaccine protection, with knowledge of the envelope protein antigenic variation helping predict the level of protection afforded (Horton *et al.*, 2010). Efforts to develop an efficacious vaccine against Ebola virus have focused on methods of presenting the GP envelope protein to the immune system, as a key antigenic target for the development of immunity. Many vaccine regimes have entered clinical trials, which are predominantly based on using recombinant viral vectors to present the GP, with others employing virus like particles as well as DNA based vaccines which work to deliver the GP envelope protein in isolation of other viral presentation components (Gilbert, 2015; Lambe *et al.*, 2017; Wang *et al.*, 2017). Assessment of the magnitude and durability of the response evoked against the GP envelope protein, along with how the response correlates with protection, informs suitability of a vaccine regime to progress through development.

In addition to raising an antibody response via vaccination, the envelope protein also constitutes a target for the development of antiviral drugs. The administration of convalescent serum post-infection has long been used as a passive immunisation route, which can afford immediate protection in previously unvaccinated individuals. However, replacing these polyclonal preparations with monoclonal antibody (mAb) can offer a more potent and specific response (Both *et al.*, 2013a). It is during the development and isolation of mAb targeting the envelope protein, that a detailed assessment of antigenic sites is used to construct an antigenic map. The antigenic

structure of the rabies virus envelope protein was initially defined by Lafon *et al.*, (1983) and current antigenic maps evolved over several development studies (Kuzmina *et al.*, 2013; Marissen *et al.*, 2005). Structural studies of mAb bound to the ebolavirus envelope protein have helped the understanding of important targets to prevent infection, as well as the receptor binding and fusion mechanisms of the envelope protein (Bale *et al.*, 2012; Lee *et al.*, 2008a; Murin *et al.*, 2014). Additionally, knowledge of the receptor binding and fusion processes of an envelope protein can also be exploited to develop chemical and peptide inhibitors of entry. By targeting these viral processes, rather than being specific to a viral species, offers a broad spectrum antiviral approach (Vigant *et al.*, 2015). Inhibitors of the cathepsin proteases, which are required for envelope protein cleavage and activation for the entry of filoviruses, coronaviruses and henipaviruses, is an example of an antiviral that could have a broad spectrum mode of action (Vigant *et al.*, 2015; Zhou & Simmons, 2012). Careful assessment of the therapeutic index of such antivirals is required due to the risk of side effects from their broad action as well as often having a low potency. However, they are considered less susceptible to the development of resistance owing to not being encoded by the viral genome, and if developed, have value in rapidly offering an effective treatment for a newly emerging virus.

### **1.3. Serology**

#### **1.3.1. Serological Investigations**

Serum antibodies are produced as part of the adaptive humoral immune response either to infection or following vaccination. Serological methods for their detection can be used to provide indirect evidence of acute, current infection with a pathogen or past exposures and immune status. IgM class antibodies are produced during the acute phase of infection, before a transition to IgG class antibodies which provide longer-lasting protection and can persist for a life-time. Diagnosis of an acute viral infection can be made by detecting virus specific IgM, or by detecting a four-fold rise in antibody titres between an acute and convalescent serum sample. Detecting IgG antibodies alone

signifies past infection or vaccination. However, the onset of antibody responses can occur at variable time points during acute infections and so serology may not always be appropriate for diagnosis. Further, the advent of molecular techniques such as real-time PCR to give direct evidence of current viral infection has led to a gradual reduction in the use of serology. Both of these situations are true for rabies and EVD, with molecular detection of virus RNA being employed for diagnosis (Broadhurst *et al.*, 2016; Fooks *et al.*, 2009). Although this is only recommended for rabies *intra vitam*, with antigen detection in tissue samples the gold standard OIE prescribed test. Despite this, in instances where viremia is transient and virus isolation is either impractical or slow the detection of virus specific antibodies is highly valuable (Storch & Wang, 2013). As a result serology still remains useful to assist diagnosis and allows identification of the risk of viral infection.

When deciphering the immune status of individuals to identify the risk of infection and evaluate the efficacy of vaccines, the detection and quantification of neutralising antibodies (NAbs) is fundamental. NAbs act to block infectivity and for enveloped viruses are targeted towards the envelope protein - blocking receptor binding and/or fusion and therefore the processes of entry and uncoating within the cell. They are often the best correlate of protection following vaccination (Klasse, 2014). During the ongoing development of a vaccine against EVD, assessment of its efficacy in producing a humoral immune response and the power of NAbs against the envelope protein in preventing infection are essential (Feldmann *et al.*, 2003; Lambe *et al.*, 2017; Ye & Yang, 2015). Further, studies investigating the efficacy of current rabies vaccines against novel lyssaviruses by quantifying NAbs has been key to determining the lack of protection afforded to those in phylogroups II and III (Brookes *et al.*, 2005; Hanlon *et al.*, 2005). Their quantification will also be a key part of studies being carried out towards the development of new, broadly neutralising vaccine formulations.

Serology also provides the ability to track the spread of emerging viruses, with the advantage of detecting antibodies when the symptomatic stage of infection and viral clearance has occurred.

Such serosurveillance provides valuable epidemiological and public health information on emerging viruses, such as the health risk posed, geographic distribution and prediction of its epidemic potential. As examples, a serosurveillance study highlighted the longstanding disease burden of important emerging viruses circulating in Sierra Leone and the need for better surveillance as well as differential diagnosis (O’Hearn *et al.*, 2016). In others, the frequency of Ebola virus seropositive, asymptomatic individuals, was shown to be low during the recent outbreak (Glynn *et al.*, 2017), even though it has previously been suggested to occur at a high frequency (Becquart *et al.*, 2010). Further, upon the recent emergence of Schmallenberg virus, a member of the *Bunyaviridae* family causing congenital malformations in ruminants, development of a serological assay was required for serosurveillance studies. This helped to quickly establish it had a high prevalence among livestock in the Netherlands (Beer *et al.*, 2013; Elbers *et al.*, 2012). It was also possible to determine it posed a low zoonotic risk, with no detectable antibodies in a serosurvey of farmers known to be exposed to the virus (Tarlinton *et al.*, 2012). Serology is also frequently applied to studying the circulation of emerging viruses in their wildlife reservoir hosts, where sample volumes can be limited (Gilbert *et al.*, 2013). Several studies into bat populations which are an important reservoir of emerging viruses have been carried out, including isolating NAbs to henipaviruses (Peel *et al.*, 2012) and lyssaviruses (Arguin *et al.*, 2002; Kuzmin *et al.*, 2006; Schatz *et al.*, 2014).

### **1.3.2. Serological Assays**

Several different formats of serological assay are available for the detection of virus specific antibody within serum. Most typically they can be divided within two categories, either binding or functional assays. Binding assays measure the attachment of antibody to viral antigen which has been attached to a solid surface. Common formats include the indirect immunofluorescent antibody assay (IFA) and the enzyme-linked immunosorbent assay (ELISA). Using the IFA, viral antigen is attached to a microscope slide and incubated with serum to allow binding of antiviral antibody. A fluorescently labelled secondary antibody, which has specificity to the species being tested, is then

added and binding detected using a fluorescent microscope. The ELISA works in a similar way, but is performed in a microtiter plate and uses enzyme-conjugated antibody requiring the addition of a substrate, which most commonly emits a colourimetric or fluorescent signal. Signal intensity indicates the presence or absence of antibody depending on which format of ELISA is used. Binding assays can be used to differentiate between IgM and IgG antibodies by using a class specific secondary antibody.

Functional assays work on the basis of measuring specific activities resulting from the binding of antibody to viral antigen. This could be agglutination, such as with the haemagglutination-inhibition assay (HI) whereby antibodies to viruses which are able to agglutinate erythrocytes are measured from the action of preventing agglutination. This is usually operated on the basis of testing acute and convalescent sera in parallel to detect a rise in antibody titres. Yet the most important functional assay is the virus neutralisation assay (VNA), which measures the ability of antibodies to block viral infectivity. The assay is performed by preparing serial dilutions of serum for incubation with a standardised quantity of virus. Following a short incubation the mixture is added to a confluent monolayer of permissive cells and incubated for a period sufficient for infection to have occurred. Virus infection is either observed as plaques of virus-induced cytopathic effect, or using fluorescently labelled virus specific antibodies to detect infected cells for viruses which do not cause cytopathic effect. The value in being able to quantify NAbs makes this widely regarded as the serological assay to which others should be measured (Storch & Wang, 2013).

Serology to assist diagnosis is mainly undertaken with binding assays, commonly ELISA, based on the fact they are relatively low cost and rapid. They also have utility in differentiating antibody responses raised to infection or vaccination as part of the Differentiating Infected from Vaccinated Animals (DIVA) approach when a subunit vaccine has been used, with the ability to select the target viral antigen (Mather *et al.*, 2013; Uttenthal *et al.*, 2010). However, in comparison to the VNA their specificity is limited by potential cross-reactivity of secondary antibodies, as well as the use of purified or recombinant proteins as antigen, which may not have authentic conformation.

Overall, when evaluating vaccine efficacy the VNA is considered a gold standard and information on the protective capacity of antibodies is highly valued for serosurveillance studies. Indeed, two variations of a VNA, the rapid fluorescent focus inhibition test (RFFIT) (Smith *et al.*, 1973) and fluorescent antibody virus neutralisation test (FAVN) (Cliquet *et al.*, 1998), are the OIE endorsed gold standard serological tests for rabies. However limitations in performing a VNA include its cost, a laborious technique as well as often needing several days incubation for virus growth, which slows the collection of results, and most importantly the requirement to use infectious virus. This presents a major limitation in the ability to measure NAbs for pathogenic viruses which require high biosafety level (BSL) 3 or 4 containment facilities, hampering the performance of vaccine efficacy and serosurveillance studies. This is a particular constraint for emerging viruses which are often highly pathogenic and endemic in less developed countries which do not have access to high containment facilities. This is true of both lyssaviruses and filoviruses which are BSL 3 and 4 pathogens respectively. Consequently, a robust serological assay to measure NAbs which does not require handling live virus is of great value.

## **1.4. Pseudotyped Virus**

### **1.4.1. Pseudotyped Virus Definition**

Pseudotyped viruses (PVs) are defined as viral particles which consist of a core (matrix, capsid, nucleocapsid) originating from one virus, which is surrounded by a lipid envelope comprising envelope proteins protruding from the outer surface. In most cases the genome is engineered to incorporate a transfer/reporter gene and lacks the genetic elements required for replication. This offers a safe system to study properties related to the viral envelope proteins, with the ability to act as surrogates to pathogenic viruses. Upon PV transduction of susceptible cells, detection of reporter gene expression can be used to infer envelope protein interaction with cell receptors and viral entry.

With an equivalent serological profile, PV has proven to be a robust alternative to wildtype emerging viruses when applied to serological assays and addresses the limitations to their use (Mather *et al.*, 2013). They can be handled in low containment BSL 1 or 2 laboratories to measure NAbs as part of vaccine efficacy and serosurveillance investigations, with a lower associated cost as well as result turnaround time than some VNAs using live virus. This enables them to be used in a wider range of laboratory environments, including those in less developed countries where emerging viruses are often endemic. Consequently, PV has established itself as an attractive alternative to live virus within the emerging virus field.

#### **1.4.2. History of Pseudotyped Virus**

Retroviruses have widely been used as cores for PVs and current production protocols are based on several decades of retroviral vector development (Temperton *et al.*, 2015a). This development is closely allied to the gene therapy field, where retroviral vectors are favoured due to the ability to stably integrate transfer genes into the cell genome without transferring viral genes (Naldini, 1998; Sakuma *et al.*, 2012). This is attributable to the unique property of retroviruses to reverse transcribe their single stranded RNA genome to a double stranded DNA provirus, with viral integrase subsequently directing its integration into the chromosome of target cells. Early retroviral vectors were based on gammaretroviruses, often murine leukemia virus (MLV); however their utility was restricted by only being able to transduce dividing cells. Consequently, the system was soon expanded to include lentiviruses, most commonly human immunodeficiency virus (HIV), which due to infecting non-dividing tissue macrophages has evolved the ability to infect cells in the absence of division. This would allow *in vivo* integration into non-dividing cells such as hepatocytes, haematopoietic stem cells and neurons (Naldini *et al.*, 1996).

Initial efforts in the use of retroviral vectors for gene therapy applications in the early 1990s were based on the use of stable cell lines. These cells expressed packaging components, with the retroviral genome being introduced within a plasmid by transfection, where the packaging genes

were replaced by a transfer gene (Miller, 1990; Pear *et al.*, 1993). Unfortunately, recombination events between the newly produced retroviral vectors and the integrated packaging genes meant replication-competent viruses could be detected. Safety of the system was greatly improved by moving away from stable cell lines and instead adopting a method which separated the structural and enzymatic genes, envelope protein and transfer genes onto three separate plasmids, which were transiently transfected into producer cells (Naldini *et al.*, 1996; Soneoka *et al.*, 1995). Their simultaneous expression produced replication-defective retrovirus which would require at least two recombination events to revert to a pathogenic variant. Lentiviral vector systems based on HIV have undergone several rounds of development to further improve upon the safety of the 'first-generation' vectors (Sakuma *et al.*, 2012).

Safety precautions employed within the first-generation vector system involved only including the *cis*-acting elements required for packaging ( $\Psi$ ) and the long terminal repeats (LTRs) and response element (RRE) required for reverse transcription and integration on the transfer gene plasmid, excluding the expression of lentiviral proteins within target cells (Figure 1.4) (Naldini *et al.*, 1996; Sakuma *et al.*, 2012). Pseudotyping the vectors, including an envelope protein from an unrelated virus, further reduced the chance of recombination by removing homologous sequences with the transfer plasmid. Second-generation vectors offered enhanced safety by removal of lentiviral accessory protein genes (Vif, Vpu, Vpr and Nef) from the lentiviral structural plasmid (Figure 1.4). Although required during natural infection, they were found to be dispensable during replication (Zufferey *et al.*, 1997). This left only four (*gag*, *pol*, *tat* and *rev*) of the nine lentiviral genes within the system when incorporating a foreign envelope. This system was further adapted by the introduction of self-inactivating (SIN) transfer vectors. LTRs contain three regions (U3, R and U5) and flank the transfer gene, becoming integrated within the target cell genome and regulating transcription and polyadenylation of transfer gene mRNA. A deletion in the 3'-LTR U3 region was found to disrupt the generation of potentially packageable transfer RNA as genomes in progeny virions (Sakuma *et al.*, 2012; Zufferey *et al.*, 1998). Further, risks associated with rescue of the transfer gene into new viral particles if subsequent infection with wild-type lentivirus occurs,

and the possibility of insertional activation of nearby proto-oncogenes (Hacein-Bey-Abina *et al.*, 2003) by residual promoter activity of the LTR, were also prevented. Finally, a third-generation vector system was developed where the *rev* gene on the lentiviral structural plasmid, which is involved in nuclear export of transcripts, was placed on a separate plasmid (Figure 1.4) (Dull *et al.*, 1998). Additionally the *tat* regulatory gene, required for viral transcription, was removed by replacing the 5'-LTR U3 promoter region on the transfer gene plasmid with a strong viral promoter (Dull *et al.*, 1998). This system results in at least three recombination events being required to generate replication competent virus, which would still lack active LTRs and accessory proteins. However, lower pseudotyped vector yields as a consequence of transfecting an additional plasmid are a disadvantage and have limited its use (Sakuma *et al.*, 2012).

Further modifications to improve the performance of the transfer gene plasmid, which are widely used, include the addition of a central polypurine tract (cPPT) (Demaison *et al.*, 2002) and the woodchuck hepatitis virus post-transcriptional regulatory element (WPRE) (Zufferey *et al.*, 1999). They function to increase vector transduction efficiency by facilitating nuclear import and enhance transfer gene expression in target cells, respectively. Additionally alterations to improve safety and performance are continually being proposed (Sakuma *et al.*, 2012). Within this work, the three plasmid lentiviral vector system is used for PV production. While not conforming to the defined four plasmid third-generation system, the transfer gene plasmid employs additional safety features and improvements introduced beyond the second-generation system (Figure 1.4).

When producing PV with different viral envelope proteins, the efficiency of production with different vector systems alters dependent on factors such as the site of envelope protein accumulation and parental virus budding, and the ability of the envelope protein to interact with the viral core component (Sandrin & Cosset, 2006; Steffen & Simmons, 2016). The generation of a rhabdoviral vector system based on vesicular stomatitis virus (VSV), is so far proving to be the second most popular system to retroviral vectors for pseudotyping. While acclaimed for having

superior pseudotyping efficiency, with the ability to readily incorporate envelope proteins of different viruses, establishment of the system is far more complex (King *et al.*, 2016; Whitt, 2010).

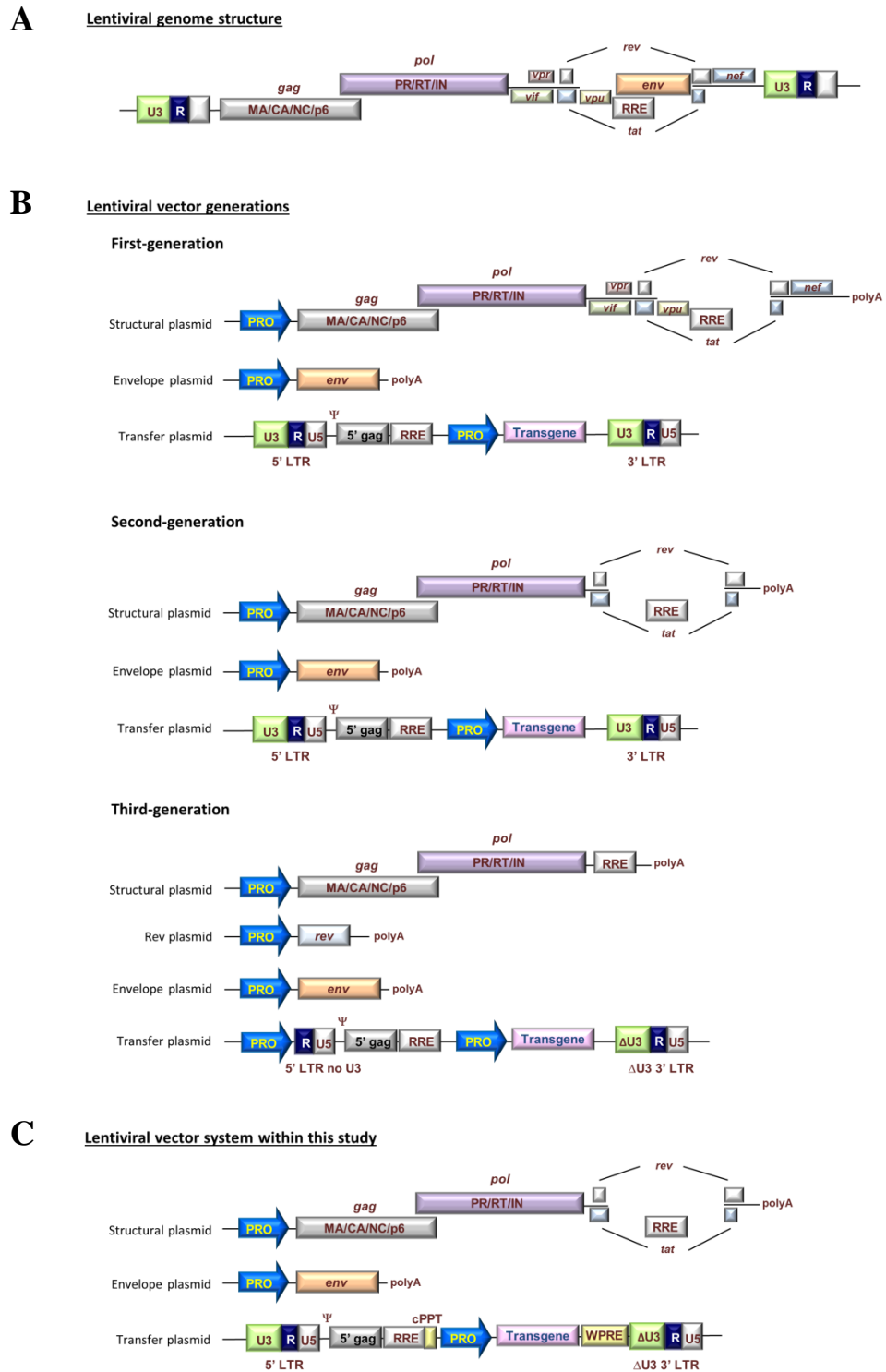


**Figure 1.4 Schematic Representation of the Lentiviral Genome and Vector System**

(A) The lentiviral viral genome encodes three structural (*gag*, *pol* and *env*), two regulatory (*rev* and *tat*) and four accessory (*vif*, *vpr*, *vpu* and *nef*) genes which are flanked by LTRs. The *gag* gene encodes the matrix (MA), capsid (CA), nucleocapsid (NC) and p6 proteins and the *pol* gene encodes the enzymatic proteins to process them; protease (PR), reverse transcriptase (RT) and integrase (IN). The *rev*-response element (RRE)

located in the *env* gene is also depicted. **(B)** First-generation lentiviral vectors include all elements of the genome, except *env* which is depicted here as a VSV envelope protein. The LTRs and packaging signal ( $\Psi$ ) are on the transgene plasmid, so viral genes are not packaged or expressed in target cells. Genes are expressed under strong viral promoters (PRO). Second-generation vectors lack the lentiviral accessory genes on the structural plasmid. Third-generation vectors include a separate plasmid encoding the *rev* gene and the *tat* gene is removed after including a strong viral promoter in place of the 5' LTR U3 promoter. Additionally, the system is self-inactivating (SIN) after including a deletion in the 3' LTR U3 region. **(C)** The lentiviral vector system used in this study employs a second generation packaging plasmid and an upgraded SIN transfer plasmid which includes a central polypurine tract (cPPT) and the woodchuck hepatitis virus post-transcriptional regulatory element (WPRE) to enhance transduction and expression of the transfer gene. Adapted from (Sakuma *et al.*, 2012).

### 1.4.3. Pseudotyped Virus Production

The production of retroviral PV is achieved by the concurrent transfection of plasmids separately comprising retroviral structural genes, envelope protein and transfer genes, such as detailed for the lentiviral vector system in Section 1.4.2, into a readily transfectable producer cell line (Figure 1.5A). The human embryonic kidney 293 T-cell line (HEK 293T) is highly transfectable and thus commonly used for this purpose (Pear *et al.*, 1993; Temperton *et al.*, 2015a). The retroviral structural plasmid encodes the structural proteins of the viral core (matrix, capsid and nucleocapsid) along with the enzymatic proteins to process them on the *gag* and *pol* genes respectively; with the regulatory *tat* and *rev* genes also expressed from this plasmid. The retroviral core component (depicted in grey, Figure 1.5B) may be produced without supplying the envelope protein ( $\Delta env$ ) for use as a transduction control. The transfer gene, commonly encoding a reporter protein, is incorporated within the PV core as an RNA dimer (depicted in pink, Figure 1.5B), facilitated by a packaging signal ( $\Psi$ ) which is included only on the transfer plasmid so that packaging of viral sequences supplied on other plasmids does not occur. The PV core, incorporating two copies of a RNA reporter gene, is trafficked to the producer cell plasma membrane which contains the foreign viral envelope protein, introduced via the plasmid expressing the envelope protein gene. Following extracellular budding, the retroviral PV becomes encased in the producer cell plasma membrane, studded with the foreign viral envelope protein (depicted in orange, Figure 1.5B). Released into the producer cell culture medium, the supernatant containing PV can be harvested and titrated onto a permissive target cell line.

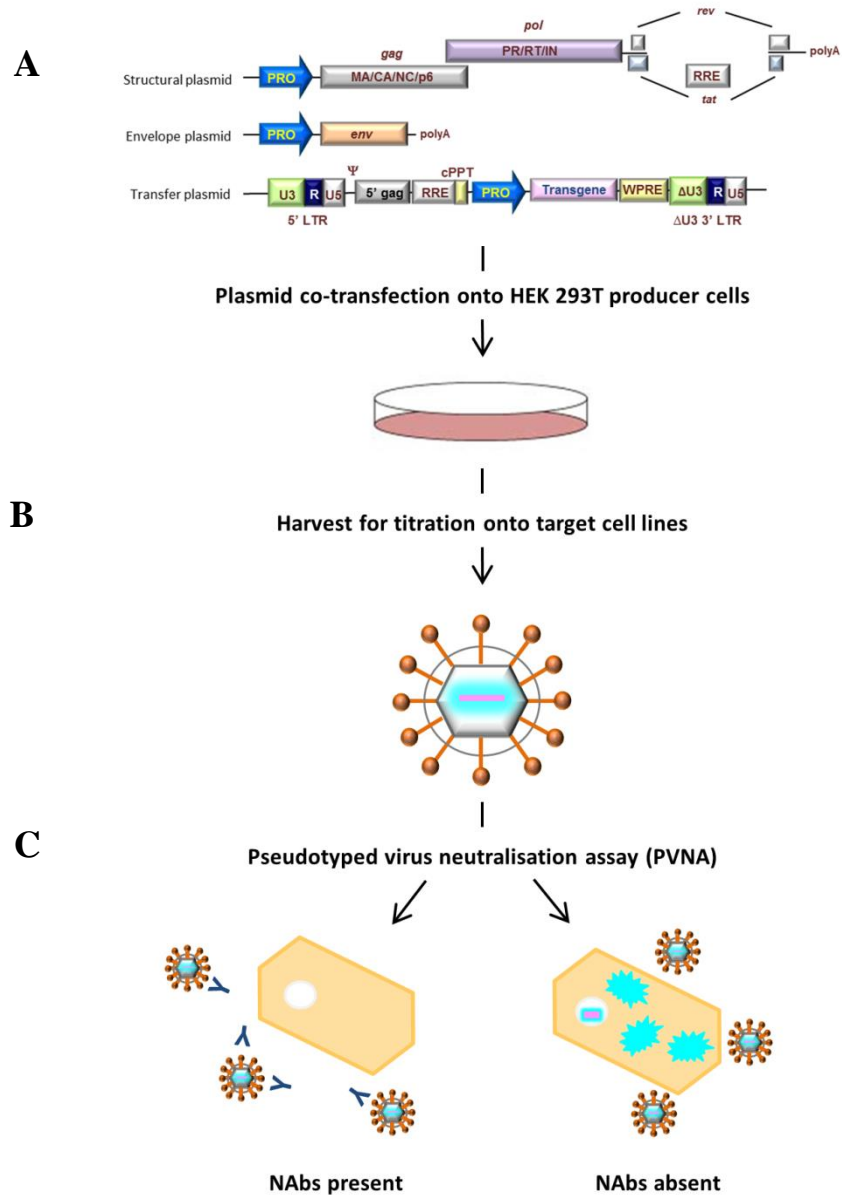


**Figure 1.5 Schematic Representation of the Three Plasmid Transfection System for Retroviral Pseudotyped Virus Production and Use in a Neutralisation Assay**

(A) As part of the retroviral vector system for PV production, three plasmids separately expressing retroviral genes (*gag-pol*) required for core formation, a viral envelope protein (*env*) and a reporter gene for packaging ( $\Psi$ ) within the PV core are concurrently transfected into a producer cell line such as HEK 293T cells. (B) PV is harvest from the producer cell culture medium and can then be titrated onto permissive target cells, where reporter gene expression is measured to assign a titre. (C) Used in a PV neutralisation assay (PVNA), the correlation between reporter gene expression and cell transduction can be used to detect for the presence of neutralising antibodies (NAb) in serum samples.

Transduction of target cells is dependent upon envelope protein interaction with appropriate cell receptors, which leads to membrane fusion and internalisation (Temperton *et al.*, 2015a). The PV reporter gene becomes integrated within the target cell genome; facilitated by the LTRs and the reverse transcriptase and integrase of the retroviral core. Given that only the reporter gene is included within the PV core; viral proteins required for replication are not able to be produced within the target cell, preventing replication. This is the central reason for their safety in comparison to working with wildtype virus. Detection of reporter expression from the target cells acts to provide a quantitative measure as to the level of PV transduction, allowing a titre to be assigned which can be used to control input into downstream assays. When undertaking serological evaluation via a PV neutralisation assay (PVNA), this positive correlation between reporter expression and cells transduced can be used to infer the presence of NAb (Figure 1.5C).

There is inherent flexibility in this retroviral pseudotype system to tailor for end user requirements, with the nature of the three plasmid system facilitating simplicity in altering the various components. A variety of reporter genes have been incorporated within the platform, which offer outputs over a range of time, cost and sensitivity constraints (Figure 1.6) (Wright *et al.*, 2009). The use of luciferase and green fluorescent protein reporters is popular due to their high throughput capabilities as well as offering good sensitivity; however they both require expensive reagents or equipment. Using the lower cost *lacZ* reporter gene, which doesn't require advanced laboratory equipment or expensive reagents, expands the utility of PV to resource limited settings, such as within less developed countries where outbreaks of highly pathogenic emerging viruses have frequently occurred. Further, PV has previously demonstrated good stability, with a half-life of 1-2 or 2-4 weeks at room temperature or 4°C respectively, as well as withstanding lyophilisation (Mather *et al.*, 2014; Wright *et al.*, 2009). This permits its use in settings with less reliable infrastructure.

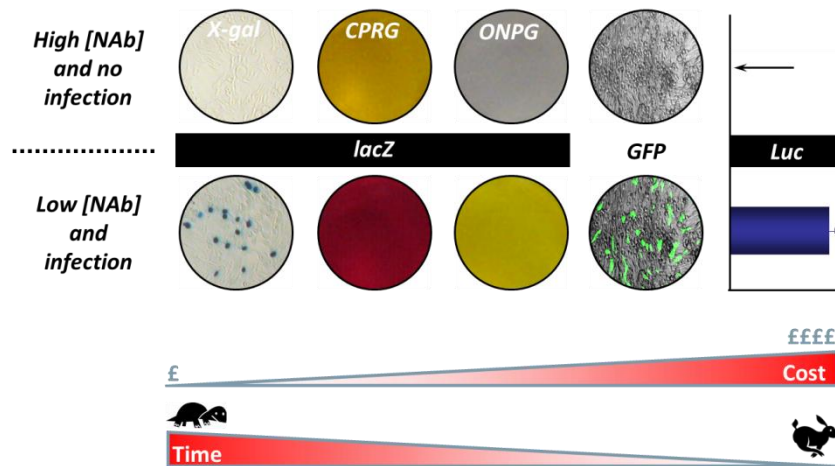


**Figure 1.6 Representation of Cost and Time Constraints of Reporter Genes Incorporated with the Retroviral Pseudotyped Virus Platform**

The *LacZ* reporter gene is low cost and colourimetric readouts can be provided via addition of X-gal, CPRG or ONPG  $\beta$ -gal substrates. The green fluorescent reporter gene (GFP) is a mid-range reporter, while the luciferase (*luc*) reporter has the highest cost and also offers high-throughput results. The readout in the presence of high and low neutralising antibody concentrations [NAb] is represented, luciferase only offers quantitative results. Image drawn by E. Wright.

As has already been mentioned, the efficiency of viral envelope protein incorporation into PV produced based on different vector systems can vary. Producing PV via the retroviral system has generally proven successful for RNA viruses which bud from the plasma membrane, with lentiviral vectors proving to be those most commonly used (Temperton *et al.*, 2015a). In some cases a source of protease is required for envelope protein cleavage during maturation to become fusion competent. This is the case for the production of influenza PV, with a protease encoding plasmid commonly being transfected during production (Carnell *et al.*, 2015; Ferrara *et al.*, 2012). Efforts to produce PV for internally budding viruses, which traffic envelope proteins to the golgi complex rather than the cell plasma membrane, have proven to be problematic. This includes viruses within the *Flaviviridae* and *Bunyaviridae* families, with only hepatitis C virus successfully producing PV using a retroviral core (Bartosch *et al.*, 2003b; Tarr *et al.*, 2007; Urbanowicz *et al.*, 2016a). Using alternative cores, such as those based on VSV which has been used to produce Crimean-Congo haemorrhagic fever PV (Shtanko *et al.*, 2014), may offer a way to overcome difficulties in their production.

#### 1.4.4. Pseudotyped Virus Applications

The use of PV to study serological aspects of emerging viruses is becoming well established, offering a low containment platform to answer important research and development questions, which is both efficient and accessible. Yet their use is not limited to serological evaluation, they are also applicable to studies of viral entry or exit, elucidating cell surface receptors or investigating innate antiviral responses. This includes the screening of antiviral drugs targeting entry or exit processes. Additionally, the use of PV as a vaccine immunogen has been explored. Several reviews highlight these various applications (Cosset & Lavillette, 2011; King *et al.*, 2016; Steffen & Simmons, 2016; Temperton *et al.*, 2015a). Overall, the flexibilities of PV allow it to be exploited to undertake high-throughput screening of neutralising antibodies and antivirals towards the development of both natural and artificial therapeutics.

The use of PV for serological evaluation is widely reported and increasing, with neutralisation assays to detect NAbs targeted towards the viral envelope protein having been developed for many species, providing both sensitive and specific results which correlate with live virus assays (Mather *et al.*, 2013; Temperton *et al.*, 2015a). Pseudotypes have previously been produced for different *Lyssavirus* species, acting as surrogates for live virus to evaluate levels of cross-neutralisation afforded by current rabies virus vaccines against the emerging European bat lyssavirus (EBLV) -1 and -2, using sera from vaccine recipients (Wright *et al.*, 2008). The assay was further applied in a larger serosurveillance study in Africa, a developing country where rabies is endemic, detecting rabies antibodies within field serum samples from vaccinated dogs. Further to this a further three lyssaviruses, LBV, MOKV and Duvenhage lyssavirus (DUVV) were incorporated into the pseudotype platform to increase its specificity (Wright *et al.*, 2009). In each case, the PVNA was shown to be able to distinguish between lyssavirus species and results were found to correlate with, or in some cases were more sensitive than, the validated live virus FAVN assay (Wright *et al.*, 2008, 2009). Additionally, it was demonstrated how serological studies via a PVNA only require a small volume of serum for each assay, which is 5-10 fold lower than assays with live virus, with

further benefits attributed to their relative low cost and suitability to be used in a wide range of laboratory environments (Wright *et al.*, 2009).

Further serological studies, applying a PVNA to detect NAbs and demonstrating correlation with the corresponding wildtype virus assay, showing good sensitivity and specificity, have been performed for SARS-CoV, MERS-CoV, influenza virus and hepatitis C virus, which included evaluating suitability for serosurveillance (Bartosch *et al.*, 2003a; Molesti *et al.*, 2013; Perera *et al.*, 2013; Temperton *et al.*, 2005, 2007; Yang *et al.*, 2014). The ease of PV production, along with the speed, reproducibility and safety of the PVNA make it amenable to a high-throughput format when conducting serological investigations, such as serosurveillance or vaccine clinical trials which involve a large number of samples. An automated PV production system, which can produce one litre of cell culture supernatant containing PV a week under Good Clinical Laboratory Practice (GCLP) guidelines, has been described to meet this purpose (Schultz *et al.*, 2012). These same features make PV a valuable resource in the response to outbreaks of novel, highly pathogenic viruses. Once the sequence of the viral envelope protein is known, it can be rapidly synthesised and PV produced, providing an accessible platform to begin serological screening. This was applied in response to the 2012 emergence of MERS-CoV, with a PVNA being rapidly produced and used to evaluate seroprevalence in both livestock and human populations within Saudi Arabia (Gierer, *et al.*, 2013; Hemida, *et al.*, 2013). Additionally, maintaining a library of emerging virus pseudotypes for important strains of circulating species, such as that being developed for influenza virus (Bentley *et al.*, 2015), provides an outbreak preparedness resource.

By exploiting the flexibility of the pseudotype system a further advantage has been demonstrated in the ability to develop a multiplex PVNA, detecting NAbs directed against two viral envelope proteins in a single volume of sera. In one study the PVNA was used to detect NAbs against the lyssaviruses LBV and MOKV from a single sample of bat sera by using PV incorporating a renilla and firefly luciferase reporter gene respectively (Wright *et al.*, 2010). This helps maximise the amount of data that can be collected in serosurveillance studies, such as those of bats, where only

small volumes of sera can be collected. The multiplex platform has also been adapted to the detection of antibodies directed towards different subtypes of influenza PV (Molesti *et al.*, 2014a). Further, it was used to include PV with unrelated envelope proteins as internal controls for a high-throughput PV assay screening for entry inhibitors of SARS-CoV (Zhou *et al.*, 2011).

The high-throughput format of the PVNA has also seen it widely applied to the screening of antiviral drugs against emerging viruses (Steffen & Simmons, 2016; Temperton *et al.*, 2015a; Wang *et al.*, 2014; Zhou & Simmons, 2012). Not long before the 2014 Ebola virus outbreak a study was undertaken using PV to screen >1000 FDA approved compounds for antiviral activity against Ebola virus, Marburg virus and Lassa virus, in an effort to identify therapeutic options against these high-priority bioterrorism agents (Madrid *et al.*, 2013). The study identified 24 compounds that were broadly active against two or more of the viruses. During the outbreak a further study was rapidly undertaken, looking to confirm the mechanism of entry inhibition for currently licenced drugs which had shown therapeutic potential against Ebola virus to help inform their safe administration (Long *et al.*, 2015). This screening approach has also recently been applied to identify monoclonal antibodies (mAbs) which could broadly neutralise non-RABV lyssaviruses in phylogroup I, as well as having activity across the other phylogroups (De Benedictis *et al.*, 2016). A panel of 22 PVs incorporating the envelope protein of one or more isolates of each *Lyssavirus* species were used to screen 16 mAbs. As well as identifying entry inhibitors, PV has been applied to a study looking at influenza virus neuraminidase inhibitors (NAI) to prevent virus release from cells (Su *et al.*, 2008). Given PV with a HA envelope protein requires NA cleavage of surface sialic acid molecules for their release, a different approach was taken, measuring the inhibition of PV production at different concentrations of NAI.

Further work demonstrating advantages of the inherent flexibility provided by the pseudotype system has been in the ability to manipulate envelope proteins incorporated within PV. The interaction of rabies mAbs with epitopes on the envelope protein has been characterised by incorporating envelope protein with mutated antigenic sites into PV and evaluating its effect on

neutralisation (De Benedictis *et al.*, 2016; Both *et al.*, 2013b). This allowed the epitope specificity of mAbs undergoing development to be better defined. Taking this further, a study by Evans, *et al.*, (2013) switched each of the five defined antigenic sites of the lyssavirus envelope protein between a phylogroup I and II species and investigated the effect on PV neutralisation by polyclonal sera. The evaluation of the immunological importance of the antigenic sites between different lyssavirus phylogroups will act to assist the development of more broadly neutralising vaccines.

Viral tropism and cell surface receptor interactions with viral envelope proteins, initiating target cell entry, can also be elucidated using the pseudotype system. Much of the work into filovirus virus entry has been undertaken with PVs, alleviating the need for BSL 4 containment of this highly pathogenic virus. Measurement of PV transduction was initially used to identify cell lines susceptible and refractory to infection, revealing filoviruses to have a broad host range with only lymphoid cells being resistant to infection (Chan *et al.*, 2000; Wool-Lewis & Bates, 1998). They were then further used to screen cells to assist in eliminating the involvement of cell receptors initially thought to be involved in entry. This provided confirmation that the Niemann-Pick C1 receptor is required for exit from the late endosome (Côté *et al.*, 2011; Simmons *et al.*, 2003a, b). A significant study, again using the flexibility of the pseudotype system to mutate the envelope protein, looked at the impact on viral tropism of lineage-defining amino acid substitutions circulating during the recent Ebola virus outbreak (Urbanowicz *et al.*, 2016b). Using a panel of PV with mutant envelope proteins representative of the lineages, specific amino acid changes were experimentally shown to have increased tropism in human cells which in turn reduced in bat cells. Moving on, in addition to studies of virus entry, PV has utility in elucidating the action of innate antiviral responses targeted against the envelope protein. Studies have recently been conducted using PV with lyssavirus and influenza virus envelope proteins to investigate activity of the restriction factor interferon-inducible transmembrane protein 3(IFITM3), which acts to block cytosolic entry of these and other enveloped viruses, in chickens, bats and pigs (Benfield *et al.*, 2015; Smith *et al.*, 2013).

While the use of PV to study the serological aspects of vaccine efficacy, antiviral activity and serosurveillance, as well as properties of the envelope protein is well established; select studies have shown PV can be used as a platform for antigen delivery in order to stimulate an immune response. Concentrated influenza PV, when injected into mice, lead to seroconversion of the animals and the production of humoral and cellular neutralising responses against homo- and heterotypic influenza HA moieties (Powell *et al.*, 2012; Szécsi *et al.*, 2006). Therefore, PV not only provides a valuable platform for undertaking studies that elucidate data on epitope antigenicity and the generation of antigenically optimised antigens, but also as a vehicle for the administration of these proteins as vaccine immunogens.

Each study reported PVs as a robust tool to study highly pathogenic emerging viruses, urgently requiring therapeutic interventions at low containment levels. Thus having applicability to enable a wider range of research groups to undertake such work and offering a flexible platform for future research, including use in less developed countries where emerging zoonotic viruses often occur.

## 1.5. Aims and Objectives

Given the continuing threat posed by the emergence of zoonotic viruses, which are often highly pathogenic with a lack of effective prophylaxis and validated diagnostic assays, there is an unquestionable need for research advances aimed at mitigating the resulting social and economic burdens. More recently there has been an increasing recognition in the need to strengthen global capabilities to respond and be better prepared to prevent outbreaks. To this end, PVs are proving to be a valuable tool, circumventing the need to handle highly pathogenic emerging viruses, and thus increasing accessibility to serology studies detecting NAb and assessing antivirals, as well as being applicable to answering cell biology questions. In working to continue expanding the utility of the pseudotype platform, studying aspects relating to the flexibility of the system and efforts towards the standardisation of PV based assays will help inform validation of its use.

Therefore, the first aim of this project was to exploit novelties in the flexibility of the pseudotype system to develop neutralisation assays for emerging zoonotic viruses and quantify NAb responses raised against the envelope protein, including determining the importance of antigenic sites.

### *Objectives:*

- To generate new PV incorporating the envelope protein of important emerging zoonotic virus species.
- Develop a neutralisation assay to evaluate the efficacy of available prophylaxis, or that undergoing development, against the newly generated PV.
- Continually monitor the status of emerging viruses, responding to the Ebola virus outbreak to generate a filovirus PVNA, making it available for serological studies.
- Investigate the manipulation of lyssavirus and filovirus envelope proteins to produce a higher titre of PV for serological evaluation.
- To use PV incorporating lyssavirus envelope proteins with altered antigenic sites to investigate their immunological importance via a PVNA.

The second aim of this project was to expand the repertoire of reporter genes incorporated within the pseudotype platform and evaluate alternative ways to quantify PV, to assist the standardisation of input into downstream assays.

*Objectives:*

- To incorporate and test new PV reporter genes against the existing repertoire.
- Investigate whether the disparate readout units of fluorescent and luminescent reporter genes can be correlated.
- Test alternative methods for PV quantification, which measure different structural components, in addition to biological titre that is currently used.

## Chapter 2. Materials and Methods

### 2.1. Materials

#### 2.1.1. Bacterial Strains and General Media

**Table 2.1** *Escherichia coli* Strain and Associated Genotype

Strain	Genotype	Source
<b>OneShot™ TOP10</b>	F- mcrA Δ( mrr-hsdRMS-mcrBC) Φ80lacZΔM15 Δ lacX74 recA1 araD139 Δ( araleu)7697 galU galK rpsL (StrR) endA1 nupG	Invitrogen

**Table 2.2** Bacterial Culture Media

Name	Composition	Source
<b>Luria Broth (LB), Miller</b>	10 g/L Tryptone, 10 g/L NaCl, 5 g/L yeast extract	Sigma
<b>LB Agar</b>	Luria Broth supplemented with 15 g/L agar	Sigma
<b>SOC Media</b>	20 g/L Tryptone, 5 g/L yeast extract, 10 mM NaCl, 2.5 mM KCl, 10 mM MgCl <sub>2</sub> , 10mM MgSO <sub>4</sub> , 20 mM glucose	Sigma

#### 2.1.2. Virus Envelope Protein and Reporter Protein Sequences

Full details of the accession number, source and sequence of the virus envelope proteins and reporter proteins used within this study are provided partially within the relevant results chapter and in full in Appendix I.

#### 2.1.3. Plasmids and Primers

Envelope protein genes used in this study were inserted into multiple cloning sites within the pI.18 or pCAGGS expression plasmid (Table 2.3 and 2.4). Both are pUC-based plasmids, encoding a

bacterial origin of replication and an ampicillin resistance gene for growth and selection in *E. coli*. The pI.18 plasmid comprises a human cytomegalovirus promoter, truncated enhancer region, intron A gene and terminator sequence (Cox *et al.*, 2002). The pCAGGS plasmid has a full chicken  $\beta$ -actin promoter and an efficient poly(A) signal from a rabbit  $\beta$ -globin gene (Niwa *et al.*, 1991). Plasmid maps are available in Appendix I.

New reporter protein sequences were inserted into the pCS[reporter]W plasmid (Appendix I) using primers detailed in Table 2.5. Expression of the reporter protein is driven by the U3-LTR and spleen focus forming virus (SFFV) promoter, which is enhanced by a Woodchuck hepatitis virus posttranscriptional regulatory element (WPRE) lacking the oncogenic X protein (Demaison *et al.*, 2002). Constructs with a firefly luciferase (FLuc), enhanced green fluorescent protein (GFP), emerald GFP (emGFP) and *LacZ* reporter protein which had previously been cloned were used and referred to as pCSFLW (Wright *et al.*, 2008), pCSGW (Demaison *et al.*, 2002), pCSemGW (kindly provided by Greg Towers, UCL) and pCSLZW (Wright *et al.*, 2009) respectively. A second reporter protein expression plasmid, pDUAL, was used within this study (Table 2.6). Based on pCS[reporter]W, a ubiquitin promoter is incorporated to create a dual promoter expression plasmid (Escors *et al.*, 2008). These reporter protein plasmids form part of the self-inactivating (SIN) system for pseudotyped virus production applied within this study and used in combination with the plasmid p8.91 which provides the retroviral *gag* and *pol* genes (Zufferey *et al.*, 1997). When producing pseudotyped virus with a gammaretroviral core, the plasmid pCMVi was used to provide *gag* and *pol* genes (Towers *et al.*, 2000) and a pCNC[reporter] plasmid to supply the reporter protein, where expression is driven by a human cytomegalovirus promoter (Beeck *et al.*, 2004). Confirmation of genes cloned within expression plasmids was carried out using the appropriate sequencing primers (Table 2.7) as detailed in Section 2.2.8.

**Table 2.3 Primers and Cloning Sites for Envelope Protein Genes Inserted into the pI.18 Expression Plasmid**

Construct	Gene	Cloning Site	Flanking Primers (5' → 3')			
			Forward (F)	Reverse (R)		
C1.1	CVS-11	<i>KpnI/XhoI</i>	GCGCGGGTACCGCCACCATGGTTCCTCAAGTTCTT	GCGGCCTCGAGTTACAGTCTGATCTCACCTC		
C1.2	RV61	<i>KpnI/XhoI</i>	GCGCGGGTACCGCCACCATGGTTCCTCAAGTTCTT	GCGGCCTCGAGTCACAGTCTGGTCTCACC		
C1.3	RV193	<i>KpnI/XhoI</i>	GCGCGGGTACCGCCACCATGGTTCCTCAGTTCTT	GCGGCCTCGAGTCACAGTCTGGTCTCACC		
C1.4	RV250	<i>KpnI/EcoRI</i>	GCGCGGGTACCGCCACCATGGTTCCTCAAGCTCTT	GCGCGGAATTCTCACAGTCTGGTCTCACC		
C1.5	RV277	<i>KpnI/XhoI</i>	GCGCGGGTACCGCCACCATGGTTCCTCAGTTCTT	GCGGCCTCGAGTCACAGTCTGGTCTCACC		
C1.6	WCBV	<i>KpnI/XhoI</i>	GATCATGGTACCGCCACCATGGCTTCTACTTTGCG	GATCATCTCGAGTTATTGGGCAGTTTGTCCCT		
C1.7	CVStoWCBV FSS	<i>KpnI/XhoI</i>	*C1.1	*C1.1		
C1.8	WCBVtoCVS FSS	<i>KpnI/XhoI</i>	*C1.6	*C1.6		
			Flanking Primers (5' → 3')		Internal (int) Primers (5' → 3')	
			Forward (F)	Reverse (R)	Fint	Rint
C1.9	RV61etmCVS-11c	<i>KpnI/XhoI</i>	*C1.2	*C1.1	ACATGTTGC AGAAGAGCCAAT	GGCTCTTCT GCAACATGTTAT
C1.10	RV193etmCVS-11c	<i>KpnI/XhoI</i>	*C1.3	*C1.1	ACATGTTGC AGAAGAGCCAAT	GGCTCTTCT GCAACATGTTAT
C1.11	RV250etmCVS-11c	<i>KpnI/EcoRI</i>	*C1.4	GAGCGGAATTCTTAC AGTCTGATCTCACCTC	GACATGTTGT AGAAGAGCCAA	GGCTCTTCT ACAACATGTCATT
C1.12	RV277etmCVS-11c	<i>KpnI/XhoI</i>	*C1.5	*C1.1	ACATGTTGC AGAAGAGCCAAT	GGCTCTTCT GCAACATGTCATT
C1.13	CVS-11etmVSVc	<i>KpnI/XhoI</i>	*C1.1	GATCATCTCGAGTTAC TTTCCAAGTCGGTTCA	GACATGGTGC CGAGTTGGTATCCAT	TACCAACTCG GCACCATGTCATTAG

<b>C1.14</b>	RV61etmVSVc	<i>KpnI/XhoI</i>	*C1.2	*C1.13	AACATGTTGC CGAGTTGGTATCCAT	TACCAACTCG GCAACATGTTATTATG
<b>C1.15</b>	RV193etmVSVc	<i>KpnI/XhoI</i>	*C1.3	*C1.13	AACATGTTGC CGAGTTGGTATCCAT	TACCAACTCG GCAACATGTTATTATG
<b>C1.16</b>	RV250etmVSVc	<i>KpnI/EcoRI</i>	*C1.4	GATCATGAATTCTTAC TTTCCAAGTCGGTTCA	GACATGTTGT CGAGTTGGTATCCAT	TACCAACTCG ACAACATGTCATTAAG
<b>C1.17</b>	RV277etmVSVc	<i>KpnI/XhoI</i>	*C1.5	*C1.13	GACATGTTGC CGAGTTGGTATCCAT	TACCAACTCG GCAACATGTCATTATG
<b>C1.18</b>	CVStoWCBVIIb	<i>KpnI/XhoI</i>	*C1.1	*C1.1	ACAACCTGAACAAAGCATAA CCTACATGGAACCTCAAAG	GCTTTGTTTCAGTTGTACAA TATTCATCCTCCACAACCA GG
<b>C1.19</b>	CVStoWCBVIIa	<i>KpnI/XhoI</i>	*C1.1	*C1.1	GCAGAGGGAAACTAGTC TCCAAAGG	CCTTTGGAGACTAGTTT CCCTCTGC
<b>C1.20</b>	CVStoWCBVI	<i>KpnI/XhoI</i>	*C1.1	*C1.1	ATATGCGGTAGGCAG GGACTTAGACTTATGG	CCTACCGCATATTGA GAGCCTGCATGCTCCT
<b>C1.21</b>	CVStoWCBVIV	<i>KpnI/XhoI</i>	*C1.1	*C1.1	ACATCAAGTC AGACGAGATTGAGC	GACTTGATGT CGTGCAAATTCACC
<b>C1.22</b>	CVStoWCBVIII	<i>KpnI/XhoI</i>	*C1.1	*C1.1	GTAGAGAATTGGTCAGAGG TCATCCCCCAAAAAG	TGACCAATTCTCTACCTTG ATGTAGTGAGCATCAG
<b>C1.23</b>	WCBVtoCVSIIb	<i>KpnI/XhoI</i>	*C1.6	*C1.6	ACCAACCTGTCCGAGTTCT CCTACACAGAGTTGAAGG	CTCGGACAGGTTGGTACAT CCAGAGGCATCAGTATAA
<b>C1.24</b>	WCBVtoCVSIIa	<i>KpnI/XhoI</i>	*C1.6	*C1.6	GCAGAGGGAAACTAGTC TCCAAAGG	CGGTTCTTGCTCTCTT CCCTCTAC
<b>C1.25</b>	WCBVtoCVSI	<i>KpnI/XhoI</i>	*C1.6	*C1.6	TTATGTGGAGTTCTT GGAATCCGTTTAGTGG	AACTCCACATAACTT TATTTTGCATGCTCCT
<b>C1.26</b>	WCBVtoCVSIV	<i>KpnI/XhoI</i>	*C1.6	*C1.6	ATCAACACGCACGAC TTTCACTCGATGAGCTGG	CCAGCTCATCGACGTGAAA GTCTGCGTGTGAT
<b>C1.27</b>	WCBVtoCVSIII	<i>KpnI/XhoI</i>	*C1.6	*C1.6	GTCCGGACCTGGAATGAGA TCATCCCACAAAAG	ATTCCAGGTCCGACTGAC TTGTAGTGAGCATCTG

\* Indicates when the primer used is the same as that detailed for another construct

**Table 2.4 Primers and Cloning Sites for Envelope Protein Genes Inserted into the pCAGGS Expression Plasmid**

Construct	Gene	Cloning Site	Flanking Primers (5' → 3')	
			Forward (F)	Reverse (R)
<b>C2.1</b>	EBOV/MAY	<i>KpnI/XhoI</i>	GATCATGGTACCGCCACCATGGGCGTTACAGGAATATTGC	GATCATCTCGAGCTAAAAGACAAATTTGCA
<b>C2.2</b>	EBOV/MAK	<i>KpnI/XhoI</i>	GATCATGGTACCGCCACCATGGGCGTGACCGGAAT	GATCATCTCGAGTCAGAACACGAACTTGCAG
<b>C2.3</b>	BDBV	<i>KpnI/XhoI</i>	GATCATGGTACCGCCACCATGGTTACATCAGGAATTC	GATCATCTCGAGTTAGAGTAGAAATTTGC
<b>C2.4</b>	TAFV	<i>KpnI/BglIII</i>	GATCATGGTACCGCCACCATGGGGGCTTCAGGGATTCT	GATCATAGATCTTCACAGCATAAACTTACAG
<b>C2.5</b>	SUDV	<i>KpnI/NheI</i>	GATCATGGTACCGCCACCATGGAGGGTCTTAGCCTACT	GATCATGCTAGCTCAACAAAGCAGCTTGCA
<b>C2.6</b>	RESTV	<i>EcoRI/XhoI</i>	GATCATGAATTGCCACCATGGGGTCAGGATATCAACT	GATCATCTCGAGTCAACACAAAATCTTACATA
<b>C2.7</b>	EBOV/MAYetmRAVVc	<i>KpnI/BglIII</i>	*C2.1	GATCATAGATCTTCATCCAATGTATTTAGTGAAGATACG GCATATACAGAATAAAGCG
<b>C2.8</b>	EBOV/MAKetmRAVVc	<i>KpnI/BglIII</i>	*C2.2	*C2.7
<b>C2.9</b>	SUDVetmRAVVc	<i>KpnI/NheI</i>	*C2.5	GATCATGCTAGCTCATCCAATGTATTTAGTGAAGATACG GCAGACGCAAAGAAGAGCA
<b>C2.10</b>	EBOV/MAYetm	<i>KpnI/BglIII</i>	*C2.1	GATCATAGATCTCTAGCATATACAGAATAAAGCGAT
<b>C2.11</b>	EBOV/MAKetm	<i>KpnI/BglIII</i>	*C2.2	*C2.10
<b>C2.12</b>	SUDVetm	<i>KpnI/NheI</i>	*C2.5	GATCATGCTAGCTCAGCAGACGCAAAGAAGAGCA
<b>C2.13</b>	EBOV/MAKetmHAc	<i>KpnI/BglIII</i>	*C2.2	GATCATAGATCTTTAAATGCAAATCTGCATTGTAACGA

				CCCATTGGAGCAGCATATACAGAATAAAGC		
C2.14	SUDVetmHAc	<i>KpnI/NheI</i>	*C2.5	GATCATGCTAGCTTAAATGCAAATCTGCATTGTAACGA		
				CCCATTGGAGCAGCAGACGCAAAGAAGAGC		
				<b>Flanking Primers (5' → 3')</b>		
				<b>Internal (int) Primers (5' → 3')</b>		
				<b>Forward (F)</b>		
				<b>Reverse (R)</b>		
C2.15	EBOV/MAYetmVSVc	<i>KpnI/XhoI</i>	*C2.1	GATCATCTCGAGTTAC TTTCCAAGTCGGTTCA	<b>Fint</b>	<b>Rint</b>
C2.16	EBOV/MAKetmVSVc	<i>KpnI/XhoI</i>	*C2.2	*C2.15	CTGTATATGC CGAGTTGGTATCCAT	TACCAACTCG GCATATACAGAAT
C2.17	SUDVetmVSVc	<i>KpnI/NheI</i>	*C2.5	GATCATGCTAGCTTACTTTC CAAGTCGGTTCA	*C2.15	*C2.15
C2.18	EBOV/MAKetmHIVc	<i>KpnI/NheI</i>	*C2.2	GATCATGCTAGCTTATAGCA AAATCCTTTC	TTGCGTCTGC CGAGTTGGTATCCAT	TACCAACTCG GCAGACGCAAAG
C2.19	SUDVetmHIVc	<i>KpnI/NheI</i>	*C2.5	*C2.18	CTGTATATGC AATAGAGTTAGGCA	TAACTCTATT GCATATACAGAATAA

\* Indicates when the primer used is the same as that detailed for another construct

**Table 2.5 Primers and Cloning Sites for Reporter Protein Sequences Inserted into the pCS[insert]W Expression Plasmid**

Construct	Gene	Cloning Site	Flanking Primers (5' → 3')			
			Forward (F)	Reverse (R)		
<b>C3.1</b>	Cypridina Luciferase	<i>Bam</i> <i>HV</i> / <i>Not</i> <i>I</i>	GATAGGATCCGCCACCATGAAGACCTTAATTCT	GATAGCGGCCGCTATTTGCATTTCATC		
<b>C3.2</b>	NanoLuc Luciferase	<i>Bam</i> <i>HV</i> / <i>Not</i> <i>I</i>	GATCGAGGATCCGCCACCATGGTCTTCACACTCGAAG	GATCGAGCGGCCGCTTACGCCAGAATGCGTTCGC		
<b>C3.3</b>	SEAP	<i>Bam</i> <i>HV</i> / <i>Not</i> <i>I</i>	GATCGAGGATCCGCCACCATGCTGCTGCTGCTGCTGCT	GATCGAGCGGCCGCTTAACCCGGGTGCGCGGCGT		
<b>C3.4</b>	SEAP2	<i>Bam</i> <i>HV</i> / <i>Not</i> <i>I</i>	*C3.3	GATCGAGCGGCCGCTCATGTCTGCTCGAAGC		
	Dual-Nuclear					
<b>C3.5</b>	Localised (dNG) Dual-Nuclear	GFP <i>Bam</i> <i>HV</i> / <i>Not</i> <i>I</i>	GATCGAGGATCCGCCACCATGCCAAGAAAAAGCG	GATCGAGCGGCCGCTTAGCCGCTCTTATACAG		
<b>C3.6</b>	Localised tdTomato (dNT)	<i>Bam</i> <i>HV</i> / <i>Not</i> <i>I</i>	GATCGAGGATCCGCCACCATGGTGAGCAAGGGCGAGG	GATCGAGCGGCCGCTTATCTTGATCCGGTCGATCCTACCT		
			Flanking Primers (5' → 3')			
			Forward (F)	Reverse (R)		
			Internal (int) Primers (5' → 3')			
			Fint	Rint		
<b>C3.7</b>	FLuc – T2A – GFP	<i>Bam</i> <i>HV</i> / <i>Not</i> <i>I</i>	GATCATGGATCCACCGGTCG CCACCATGGAAGATGCC	GATCATGCGGCCGCTTT ACTTGTA	AGGAAGTCTTCTAACATGCGGT GACGTGGAGGAGAATCCCGGCC CTTCCGGGCATTTAAATGTGAG CAAGGGCGAGG AGGAAGTCTTCTAACATGCGGT	CTCCTCCACGTCACCGCATG TTAGAAGACTTCTCTGCCC TCTCCAGACCCGTTAATTAA CACGGCGATCTTGCC CTCCTCCACGTCACCGCATG
<b>C3.8</b>	GFP – T2A – FLuc	<i>Bam</i> <i>HV</i> / <i>Not</i> <i>I</i>	GATCATGGATCCACCGGTCG CCACCATGGTGAGCAAGG	GATCATGCGGCCGCTTA CACGGCGATC	GACGTGGAGGAGAATCCCGGCC TCTCCAGACCCGTTAATTAA TGCCAAAAACATTAAG	CTCCTCCACGTCACCGCATG TTAGAAGACTTCTCTGCCC TCTCCAGACCCGTTAATTAA CTTGTACAGCTCGTCC

**Table 2.6 Primers and Cloning Sites for Reporter Protein Sequences Inserted into the pDUAL Expression Plasmid**

Construct	Gene	Cloning Site	Flanking Primers (5' → 3')	
			Forward (F)	Reverse (R)
C4.1	LacZ	<i>KpnI/XhoI</i>	GATCGAGGTACCGCCACCATGGCGCCAAAAAAGAAGAGAA	GATCGACTCGAGTTATTTTTGACACCAGACCAACT
C4.2	FLuc	<i>KpnI/XhoI</i>	GATCGAGGTACCGCCACCATGGAAGATGCCAAAAACATTAAGA	GATCGACTCGAGTTACACGGCGATCTTGCCGCCCTTC
C4.3	GFP	<i>KpnI/XhoI</i>	GATCGAGGTACCACCGGTCGCCACCATGGTGAGCAAGGGCGA	GATCGACTCGAGTTACTTGTACAGCTCGTCCATGC

**Table 2.7 Sequencing Primers**

Plasmid	Primers (5' → 3')	
	Forward (F)	Reverse (R)
pI.18	GGTGGAGGGCAGTGTAGTCT	GAAGACACGGGAGACTTAGT
pCAGGS	TTCGGCTTCTGGCGTGTGA	CAGAAGTCAGATGCTCAAGG
pCS[reporter]W	AAAGAGCTCACAAACCCTCA	AAGCTTGCATGCCTGCAGGT
pDUAL ( <i>KpnI/XhoI</i> site)	GGTCAATATGTAATTTTCAGTG	GCTAAGATCTACAGCTGC
pCSFLuc-T2A-W	TTGCACGAGATCGCCAG	
pCS-T2A-FLucW	ATAGCTTGCAGTTCTTCATGC	

## **2.2. Methods**

### **2.2.1. Chemically Competent TOP10 *E. coli* Cell Preparation**

An LB agar plate streaked with a loop of competent TOP10 *E. coli* cells was incubated overnight at 37°C. The following day, several colonies were inoculated into 10 mL LB broth in a sterile 50 mL falcon tube and incubated overnight at 37°C, 330 rpm. On day three, 1 mL of the overnight culture was inoculated into 50 mL of pre-warmed LB broth in a sterile conical flask. This was left to grow at 37°C, 220 rpm until the O.D.<sub>600nm</sub> reached 0.3 – 0.4. At this point the culture was transferred to a pre-chilled 50 mL falcon tube and left to chill on ice for 20 minutes. Cells were harvested via centrifugation for 5 minutes at 3,000 rpm, 4°C. After discarding the supernatant the cell pellet was gently resuspended in 5 mL ice cold, filter sterile 0.1 M CaCl<sub>2</sub> and left on ice for 30 minutes. After a repeat centrifugation, the supernatant was discarded and the cell pellet gently resuspended in 2 mL ice cold, filter sterile 0.1 M CaCl<sub>2</sub> and 15% glycerol and left on ice for a minimum of 30 minutes. 100 µL aliquots were prepared in pre-chilled eppendorfs and stored at -80°C.

### **2.2.2. Agarose Gel Electrophoresis**

Agarose gels were prepared by dissolving 1g agarose (Sigma) in 100 mL 1x TAE buffer (40 mM Tris, 1 mM EDTA, 20 mM acetic acid) to give a 1% w/v ratio and heating in a microwave until dissolved. Prior to pouring, SYBR<sup>TM</sup> Safe DNA gel stain (Life Technologies; used at 50,000x) was added to the gel. Gels were submerged in 1x TAE buffer and Quick-Load® purple 2-log DNA ladder was loaded as a marker (as per the manufacturer's instructions; New England Biolabs (NEB)). Where gel bands were cut for purification, gels were briefly visualised on a Safe Imager<sup>TM</sup> 2.0 Blue Light Transilluminator (Invitrogen) and the correct size bands excised using a sterile scalpel blade. DNA was purified from the gel using the QIAquick Gel Extraction kit (Qiagen) or GeneJet Gel Extraction kit (Thermo Scientific), eluting in 25 – 35 µL elution buffer. Concentrations and A260/A280 purity ratios were assessed using a NanoDrop Lite (Thermo Scientific). Where bands were not excised, gel images were captured using an Omega Fluor<sup>TM</sup> Gel Documentation system (Aplegen).

### **2.2.3. cDNA PCR Amplification**

The constructs listed in Table 2.3 – 2.6 were amplified using flanking oligonucleotide primers designed to incorporate a 5' overhang followed by a restriction enzyme site for sub-cloning, which in the forward primer was followed by a Kozak consensus sequence (GCCACCATG). PCR reactions were performed using the high fidelity, proofreading enzyme AccuPrime<sup>™</sup> Pfx SuperMix (Life Technologies,) or Q5<sup>®</sup> Hot Start High-Fidelity 2x Master Mix (NEB). Following manufacturer instructions, 25 µL reactions were set up and run following the cycling conditions in Table 2.8 and 2.9. A gradient of four temperatures with 5°C increments, selected according to the melting temperature (T<sub>m</sub>) of the primer pair, was used at the annealing step. Reactions were run on a Veriti<sup>®</sup> Thermal Cycler (Applied Biosystems). To confirm amplicon size, PCR products were resolved by agarose gel electrophoresis, loading with 10x loading dye (0.25% bromophenol blue, 50% glycerol) and purified as detailed in Section 2.2.2.

**Table 2.8 PCR Cycling Conditions for AccuPrime Pfx SuperMix**

<b>Step</b>	<b>Temperature</b>	<b>Time</b>
<b>Initial Denaturation</b>	95°C	5 minutes
<b>35 Cycles of:</b>		
Denaturation	95°C	15 seconds
Annealing	50 - 70°C	30 seconds
Extension	68°C	1 minute per kb

**Table 2.9 PCR Cycling Conditions for Q5 Hot Start High-Fidelity 2x Master Mix**

<b>Step</b>	<b>Temperature</b>	<b>Time</b>
<b>Initial Denaturation</b>	98°C	30 seconds
<b>30 Cycles of:</b>		
Denaturation	98°C	10 seconds
Annealing	50 - 70°C	30 seconds
Extension	72°C	30 seconds per kb
<b>Final Extension</b>	72°C	2 minutes

#### **2.2.4. Splicing by Overlap Extension (SOE) PCR Amplification**

The modification of gene sequences, to produce chimeric genes, splice together gene segments and carry out site-directed mutagenesis was undertaken via an adapted SOE PCR protocol, working on the basis of extending overlapping gene segments (Heckman & Pease, 2007) (Figure 2.1). All PCR reactions were performed as detailed in Section 2.2.3 unless stated otherwise.

To produce chimeric constructs C1.9 – 1.17 (Table 2.3) and C2.15 – C2.19 (Table 2.4), internal oligonucleotide primers b and c (Figure 2.1A) were designed with a 5' overhang of 8 – 12 nucleotides complementary to the gene sequence being introduced. Flanking primers a and d (Figure 2.1A) were designed as per standard PCR amplification, described in Section 2.4. Initial PCR reactions were performed to separately amplify gene segments through the pairing of oligonucleotide primers a with b and c with d, as depicted in Figure 2.1A, producing two gene fragments with a region of complementary nucleotides spanning their junction. In a second PCR, 50 ng of each of the complementary gene fragments was added as template, hybridisation of the overlapping regions brought together the entire open reading frame and amplification was facilitated by the flanking primers a and d (Figure 2.1A).

The production of the linked constructs C3.7 and 3.8 (Table 2.5) and site-directed mutations of the constructs C1.18 – 1.27 (Table 2.3) followed the same protocol as that detailed to produce the chimeric constructs above; however the design of internal primers differed. To insert a nucleotide sequence (red broken line in Figure 2.1B) between two genes, internal primers b and c were designed with 5' overhangs of equal lengths of the sequence to be inserted with a complementary region spanning the central section of the insert sequence (Figure 2.1B). Internal primers to generate specific nucleotide substitutions were designed as a complimentary pair, with nucleotide sequence flanking the substituted nucleotides, when the region containing the substitutions was less than 10 nucleotides in length (Figure 2.1C). When the region containing the substitutions was greater than 10 nucleotides, internal primers b and c were designed with a complementary 5' overhang comprising the substituted nucleotides.

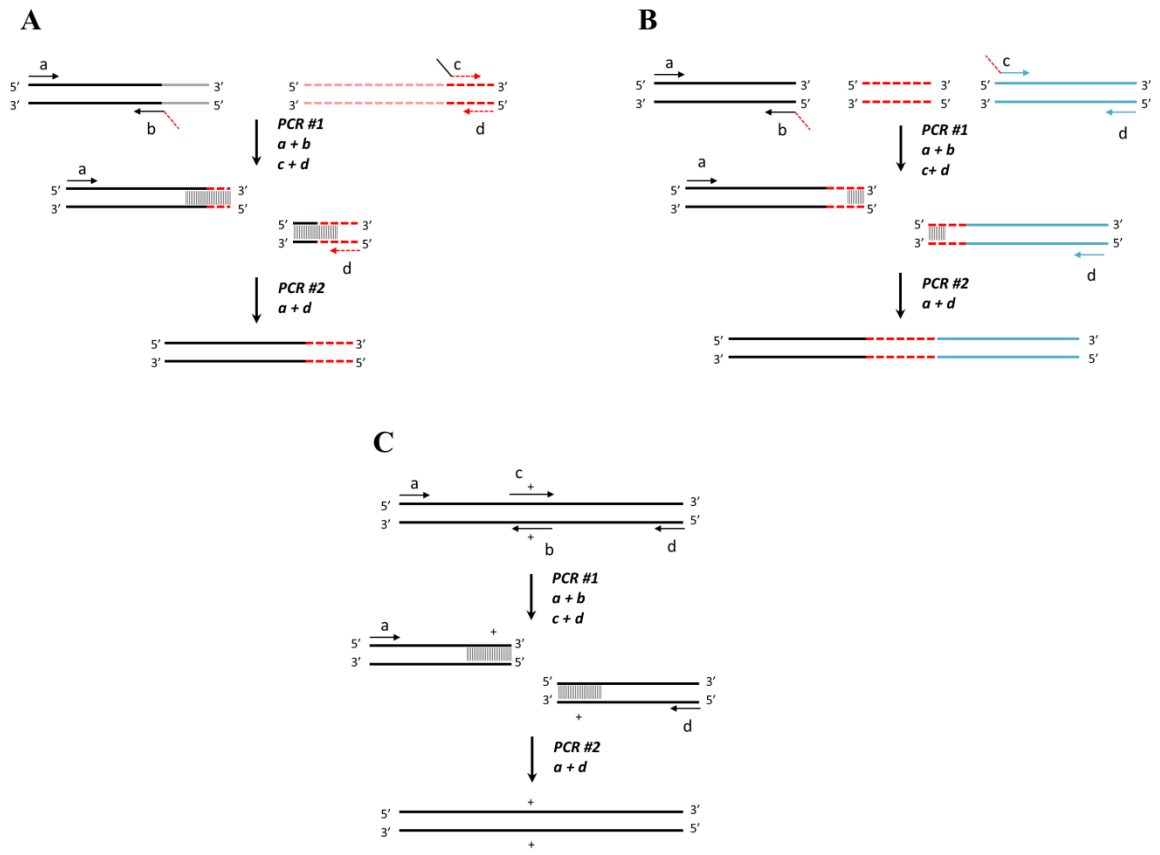


**Figure 2.1 Primer Design for Splicing by Overlap Extension (SOE) PCR**

PCR amplification using primers a-d extends overlapping gene segments to produce chimeric genes, spliced gene segments or site directed mutagenesis. **(A)** Chimeric genes are produced by designing internal primers b and c with overlapping sequences spanning the junction of the two sequences to be joined. The first PCR uses primers a + b and c + d to produce intermediate sequences with complementary regions. Both products are used as template in a second PCR where they denature and hybridise at the complementary region and the chimeric sequence is amplified by flanking primers a + d. **(B)** Spliced gene segments are also produced by two PCRs, except internal primers b and c have an overhang of equal length to a sequence to be inserted, including a complementary region that will allow the PCR products to hybridise in the second PCR. **(C)** Site directed mutagenesis follows the same PCR protocol, yet uses a complementary pair of internal primers c and b with sequence either side of the substituted nucleotides to produce intermediate products with a complementary region containing the mutated site.

### **2.2.5. Restriction Enzyme Digestion and Cloning into Plasmid Vector**

To create sticky ends for ligation, gene sequences with PCR inserted restriction enzyme sites were double-digested with 1  $\mu\text{L}/\mu\text{g}$  FastDigest<sup>TM</sup> restriction enzyme per  $\mu\text{g}$  of DNA in 10x Green buffer (Thermo Scientific) at 37°C for 30 minutes. 2 – 3  $\mu\text{g}$  plasmid DNA was digested in parallel. Digested gene inserts and linearised plasmid DNA were gel purified following agarose gel electrophoresis as detailed in Section 2.2.2.

Ligations were set up with T4 DNA ligase (1 Unit/ $\mu\text{L}$ ) in 10x T4 DNA ligase buffer (Thermo Scientific) with 50 – 100 ng linearised plasmid DNA and 100 – 300 ng digested insert sequence in a 1:3 plasmid-to-insert ratio, incubating for 1 hour at room temperature and heat inactivating at 70°C for 5 minutes. Ligation products were transformed into competent TOP10 *E. coli* cells.

### **2.2.6. Transformation of Chemically Competent Cells**

Competent TOP10 *E. coli* cells were removed from -80°C storage and thawed on ice for at least 5 minutes. 5  $\mu\text{L}$  (10% v/v) ligation product, or 10 ng plasmid DNA, was added to 50  $\mu\text{L}$  of competent cells and incubated on ice for 30 minutes. The cells were heat shocked at 42°C for 42 seconds and placed back on ice for 2 minutes. Cells were then incubated with 200  $\mu\text{L}$  SOC media (Sigma) at 37°C, 300 rpm for 30 – 60 minutes. 150  $\mu\text{L}$  of transformed cells were then plated onto an LB agar plate containing antibiotic corresponding to the plasmid's resistance marker (Ampicillin-Nafcillin 50  $\mu\text{g}/\text{mL}$ ; Sigma) and left to grow at 37°C for 20 hours, or room temperature for 72 hours.

### **2.2.7. Plasmid Propagation**

To screen clones following transformation, three colonies were picked from the LB agar plate and inoculated into separate 6 mL LB broth cultures containing antibiotic (Ampicillin-Nafcillin 50  $\mu\text{g}/\text{mL}$ ; Sigma). Cultures were incubated overnight at 37°C, 300 rpm (Incubating Mini Shaker, VWR). The following day glycerol stocks were prepared for long term storage at -80°C, mixing

800  $\mu\text{L}$  of the overnight culture with 200  $\mu\text{L}$  of 50% filter (0.2  $\mu\text{M}$ ) sterile glycerol solution. Cells in the remaining culture were pelleted by centrifugation at 3,000 rpm for 10 minutes (Heraeus Megafuge 1.0R) and plasmid DNA purified using the PureLink® Quick Plasmid Miniprep kit (Invitrogen), eluting into 30 – 40  $\mu\text{L}$   $\text{dH}_2\text{O}$  (Molecular Grade, Eppendorf). Concentrations and A260/A280 purity ratios were assessed using a NanoDrop Lite (Thermo Scientific).

To prepare plasmid DNA from glycerol stocks, a loop of the frozen culture was inoculated into a 1 mL LB broth starter culture containing antibiotic (Ampicillin-Nafcillin 50  $\mu\text{g}/\text{mL}$ ) and incubated for 5 – 7 hours at 37°C, 300 rpm. An overnight culture was then prepared by transferring 0.5 – 1 mL of the starter culture to a 6 mL pre-warmed LB broth culture and incubating at 37°C, 300 rpm as detailed above.

### **2.2.8. Confirmation of Cloned Gene Sequences**

To confirm the correct gene sequences were cloned into expression plasmids, following plasmid DNA purification 300 ng was double-digested with the restriction enzymes used for cloning as detailed in Section 2.2.5. A gel image captured following agarose gel electrophoresis was used to establish the presence and size of the insert gene sequence (Section 2.2.2). Finally, 100 ng/ $\mu\text{L}$  of plasmid DNA containing the correct size insert gene was sequenced using 3.2 pmol/ $\mu\text{L}$  of plasmid sequencing primers (Table 2.7) (SourceBioscience). Chromatogram files were analysed to confirm the correct gene sequence using DNADynamo software (v.1.387, Blue Tractor Software Ltd).

### **2.2.9. Cell Culture**

All cell lines except CHO-K1 cells (Table 2.10) were cultured in Dulbecco's Modified Eagles Medium (DMEM) high glucose (Gibco), supplemented with 10% heat inactivated foetal bovine serum (FBS; Gibco) and 1% penicillin-streptomycin (10,000 Units/mL penicillin, 10,000  $\mu\text{g}/\text{mL}$  streptomycin; Sigma):complete media. The CHO-K1 cell line was cultured in Ham's F-12 medium (Gibco), supplemented with 10% FBS and 1% penicillin-streptomycin. When reviving cells from

liquid nitrogen, vials were quickly thawed in a 37°C, 5% CO<sub>2</sub> incubator (Sanyo MCO-15AC Incu-Safe) and washed in 10 mL cold complete media followed by centrifugation at 2,000 x g for 10 minutes (MSE Centaur 2). Cell pellets were re-suspended in 7 mL complete media and seeded into a 6-cm culture dish (TPP) before incubating at 37°C, 5% CO<sub>2</sub> until confluent.

Cells were passaged tri-weekly or frozen for storage upon reaching 80 – 90% confluence. To passage, cells were briefly washed and subsequently incubated with pre-warmed 0.05% Trypsin-EDTA (1x; Sigma) for 5 minutes at 37°C, 5% CO<sub>2</sub> or until detached from the culture dish. The trypsin was neutralised with pre-warmed complete media and cells seeded into a fresh 10-cm culture dish (TPP or Nunc for HEK 293T/17 cells only) with 8 mL complete media. Depending on the cell line growth rate, they were passaged between 1:5 and 1:12. When freezing cells for storage, cells were pelleted by centrifugation at 2,000 x g for 10 minutes and re-suspended in FBS containing 10% DMSO (Hybri-Max™, Sigma) and 1 mL aliquots prepared. Cells were frozen gradually, at -80°C in a cryo-freezing container for a minimum of 48 hours, before transferring to liquid nitrogen.

**Table 2.10**      **Cell Lines**

<b>Cell Line</b>	<b>Description</b>	<b>ATCC® Number</b>
HEK 293T/17	Human embryonic kidney 293T clone-17	CRL-11268
BHK-21	Baby hamster kidney-21 clone-13	CCL-10
CHO-K1	Chinese hamster ovary	CCL-61
CRFK	Feline kidney	CCL-94
A549	Human lung carcinoma	CCL-185
Vero-E6	African green monkey kidney clone-E6	CRL-1586
HeLa05 <sup>1</sup>	Human cervix adenocarcinoma	
E-SIAT MDCK (EBOV GP) <sup>2</sup>	Canine kidney overexpressing sialic acid, stably expressing Ebola glycoprotein	

<sup>1</sup>Cell line kindly provided by Greg Towers, UCL. <sup>2</sup>Cell line kindly provided by Alain Townsend, University of Oxford.

### 2.2.10. Transfection for Pseudotyped Virus Production

HEK 293T/17 cells were seeded 24 hours prior to transfection into a 6-well culture plate ( $\sim 2 \times 10^5$  cells/well; TPP) or 10-cm culture dish ( $\sim 2 \times 10^6$  cells; Nunc) to be 60 – 80% confluent at the point of transfection. Prior to transfection cell media was replaced, adding 1.5 mL and 5 mL complete media to cells on a 6-well plate and 10-cm dish respectively. Either polyethylenimine (PEI; Sigma) or FuGENE® 6 transfection reagent (Promega) was used. A plasmid DNA mix was prepared as detailed in Table 2.11 along with the transfection reagent which was prepared separately, as detailed in Table 2.12. Both the plasmid DNA mix and transfection reagent were left to incubate at room temperature for 5 minutes before combining and incubating for a further 15 or 20 minutes for Fugene-6 or PEI transfection reagent respectively. The resulting solution was frequently mixed. The transfection mix was then added dropwise to the cells to evenly distribute and the cells left to incubate at 37°C, 5% CO<sub>2</sub>. After 18 – 20 hours the cell media was replaced with the equivalent volume of complete media. At 48 and 72 hours post-transfection cell media containing pseudotyped virus was harvest, filtering through a 0.45 µM filter (Millipore), replacing with the equivalent volume of complete media at 48 hours. The two harvests were combined and stored short term (up to 4 weeks) at 4°C and long term (no maximum) at -80°C.

**Table 2.11 Plasmid DNA Mix for Transfection**

Culture dish	Plasmid DNA			Transfection Reagent	
				PEI	Fugene-6
	<i>Gag-pol</i>	<i>Reporter</i>	<i>Envelope</i>	<i>OptiMEM</i>	<i>dH<sub>2</sub>O</i>
<b>6-well</b>	0.6 µg	0.9 µg	0.6 µg	100 µL	Up to 10 µL
<b>10-cm</b>	1 µg	1.5 µg	1 µg	200 µL	Up to 15 µL

**Table 2.12 Transfection Reagent**

Culture dish	PEI		Fugene-6	
	<i>1 mg/mL PEI</i>	<i>OptiMEM</i>	<i>Reagent</i>	<i>OptiMEM</i>
<b>6-well</b>	20 µL	100 µL	9 µL	100 µL
<b>10-cm</b>	60 µL	200 µL	18 µL	200 µL

## **2.2.11. Pseudotyped Virus Titration**

### **2.2.11.1. Infection Assay**

On a 96-well culture plate harvested pseudotyped virus was titrated on a susceptible target cell line to assess the infectious titre. A 2-fold serial dilution of pseudotyped virus was prepared starting at a 1:4 dilution, in duplicate. 100 µL complete media was added to wells 1-12 and 100 µL pseudotyped virus serially diluted across the plate from the first well before the addition of 100 µL of target cells ( $2 \times 10^5$  cells/mL) to each well. Controls of target cells and pseudotyped virus alone were set up in quadruplet, and the infection assay incubated at 37°C, 5% CO<sub>2</sub> for 48 hours. Results for infection plates were read according to the reporter gene incorporated within the pseudotyped virus (Section 2.2.12). Titrations of pseudotyped virus with a luminescent reporter gene were prepared in a 96-well opaque (white) culture plate (Nunc). All other titrations were prepared on clear 96-well culture plates (TPP).

For flow cytometry analysis, four replicates of an infection with pseudotyped virus at a 1:4 dilution was set up, adding 50 µL of pseudotyped virus to 50µL of complete media on a 96-well culture plate. Target cells were added to each well, including six target cell alone controls and the plate incubated as described above.

### **2.2.11.2. Titre Designation Assay**

An assay was set up with pseudotyped virus preparations to determine the 50% tissue culture infective dose per mL (TCID<sub>50</sub> / mL) which was used to standardise input. A 5-fold serial dilution of pseudotyped virus was prepared, starting at a 1:10 dilution, in four replicates across wells A - D, 1 - 11 of a 96-well culture plate. 100 µL complete media was added to wells A - D, 1 - 12 and 25 µL pseudotyped virus serially diluted across from well 1 – 11. The titration plate was then incubated at 37°C, 5% CO<sub>2</sub> for 30 – 60 minutes. Following incubation, 100 µL of target cells ( $2 \times 10^5$  cells/mL) were added to each well, with wells A12 - D12 acting as target cell alone controls.

The TCID<sub>50</sub> titration plate was then incubated at 37°C, 5% CO<sub>2</sub> for 48 hours and read according to the pseudotyped virus reporter gene.

The TCID<sub>50</sub>/mL value was calculated from the data using the Reed-Muench endpoint method (Condit, 2001; Reed & Muench, 1938). Firstly the cumulative number of wells positive or negative for pseudotyped virus infection at each dilution was counted and the percentage negative calculated for each. The negative cut-off was set at 2.5x the average of the cell alone control wells. The proportionate distance between the dilutions either side of the 50% point was then calculated and the Reed-Muench formula applied:

$$\text{Proportionate distance} = \frac{(\% \text{ positive above } 50\%) - 50\%}{(\% \text{ positive above } 50\%) - (\% \text{ positive below } 50\%)}$$

$$\log_{10} \text{TCID}_{50} = \log_{10} \text{dilution above } 50\% \\ - (\text{proportionate distance} \times \log_{10} \text{dilution factor})$$

## **2.2.12. Titration Readout**

### **2.2.12.1. Luminescence**

Pseudotyped virus titrations with a firefly luciferase, NanoLuc or renilla luciferase reporter gene were read via the Bright-Glo™, Nano-Glo® and Dual-Glo® assay systems (Promega) respectively, prepared following manufacturer's instructions. After incubation, cell media was removed from the 96-well culture plate and 50 µL of 50% v/v assay reagent in DMEM added to each well, incubating on a shaking platform for 3 minutes. The plate was then read using a GloMax®-Multi+ microplate luminometer (Promega) using the manufacturer's Bright-Glo protocol. Each well of the 96-well culture plate was assigned a value in relative light units (RLU) according to the intensity of luminescence detected by the luminometer. Data was exported as a Microsoft™ Excel file for analysis.

Titration data for pseudotyped virus with a cypridina luciferase reporter gene was read using the BioLux® cypridina luciferase assay (NEB) prepared following manufacturers instructions. After incubation, cell media was carefully removed from the titration and transferred to clean wells on the 96-well culture plate. 50 µL of BioLux® reagent was added to each well, incubating on a shaking platform for 3 minutes. The plate was read using the GloMax®-Multi+ microplate luminometer using the luminescence protocol with the integration time set to 2 seconds. Data was collected as described above.

### **2.2.12.2. Colourimetric**

#### **2.2.12.2.1. β-Galactosidase Assay**

Titration of pseudotyped virus with a lacZ reporter gene were read by first fixing cells in the 96-well titration plate by removing cell media and adding 0.5% glutaraldehyde (in 1x PBS) and incubating for 10 minutes at 4°C. After discarding, cells were incubated with 1x PBS for 5 minutes at 4°C. The cells were then washed twice with 1x PBS before staining by adding 50 µL X-gal (1 mg/mL) diluted in X-gal buffer for 30 – 60 minutes at 37°C protected from light. After staining, cells were washed once with 1x PBS with 100 µL added and left on each well. The plate was read using a light microscope (Wilovert, Will Wetzlar) and the 10x objective. Cells infected with pseudotyped virus had blue stained nuclei and were counted as positive, recording the total number of infected cells for each well.

#### **2.2.12.2.2. Alkaline Phosphatase Enzymatic Assay**

Titration of pseudotyped virus with a secreted alkaline phosphatase (SEAP) reporter gene were read using 2 mg/mL p-Nitrophenyl Phosphate (pNPP) substrate (5 mg pNPP in 2.5 mL Trizma® base, 0.2 M, pH 9.8; Sigma). 50 µL cell media was transferred to a clean well in a 96-well culture plate and incubated with an equal volume of pNPP substrate for 30 minutes – 1 hour at room temperature. The plate was read at A<sub>405</sub> on a SpectroStar Nano microplate reader (BMG Labtech, Germany). Data was exported as a Microsoft™ Excel file for analysis.

### **2.2.12.3. Fluorescence**

#### **2.2.12.3.1. Microscopy**

Pseudotyped virus titrations with a fluorescent protein reporter gene were read after fixing cells in the 96-well titration plate by removing cell media and incubating with 0.5% glutaraldehyde (in 1x PBS) for 10 minutes at 4°C. After discarding, cells were incubated with 1x PBS for 5 minutes at 4°C. The cells were then washed once with 1x PBS with 100 µL added and left on each well. The plate was read using an Axiovert S100 inverted microscope with fluorescence (Carl Zeiss), using the 10x objective and a blue filter to visualise green fluorescent protein (GFP;  $Ex_{max}$  488 nm,  $Em_{Max}$  509 nm) and a green filter to visualise tandem tomato fluorescent protein (tdTomato;  $Ex_{Max}$  554 nm,  $Em_{Max}$  581 nm). Cells emitting fluorescence were counted as positive for infection with pseudotyped virus and the total number of infected cells per well recorded. Images were captured using AxioCam HRc camera attachment and ZEN v.2.3 (blue addition) software (Carl Zeiss).

#### **2.2.12.3.2. Flow Cytometry**

Following an infection assay (Section 2.2.11.1) cells were prepared for flow cytometry analysis by removing the cell media, washing with 50 µL 1x PBS and incubating with 50 µL 0.05% Trypsin-EDTA (1x; Sigma) for 3 minutes at 37°C, 5% CO<sub>2</sub>. The trypsin was neutralised with 200 µL 1x PBS and the cells resuspended, combining the four replicates. Cells were pelleted by centrifugation at 2000 x g for 3 minutes and resuspended in 500 µL 1x PBS. Using a Dako CyAn™ ADP cytometer (Beckman Coulter) a total of 100,000 cells were counted for each sample using protocols with the fluochrome channel parameters detailed in Table 2.13, using the FITC protocol to detect GFP and PE-Texas Red protocols to detect tdTomato. Uninfected cell controls were used to set gates for the main cell population, removing cell debris or multiple cell events during acquisition. Data was analysed using the Summit™ v.4.4 software (Beckman Coulter).

**Table 2.13** Flow Cytometry Flurochrome Channel Parameters

	<b>FITC</b>	<b>PE-Texas Red</b>
<b>Excitation Laser (nm)</b>	488	488
<b>Emission Filter (nm)</b>	530/40 (FL1)	613/20 (FL3)
<b>FS Threshold (%)</b>	1.5	1
<b>FS Gain</b>	10	10
<b>SS Volts</b>	420 <sup>1</sup> / 460 <sup>2</sup>	450
<b>Channel Volts</b>	460	550

<sup>1</sup>BHK-21 or <sup>2</sup>HEK 293T/17 cells

### 2.2.13. Neutralisation Assay

The ability of mAb or sera samples to neutralise pseudotyped virus with a firefly luciferase reporter gene was assessed by a doubling serial dilution of samples in complete media across wells 1 – 12 of a 96-well culture plate, in duplicate, with a final volume of 50  $\mu$ L per well. Pseudotyped virus was diluted in complete media to add 50 – 100 TCID<sub>50</sub> per well in 50  $\mu$ L. Culture plates were centrifuged at 500 rpm for 5 minutes (Heraeus Megafuge 1.0R) before incubating for 30 minutes – 1 hour at 37°C, 5% CO<sub>2</sub>. Following incubation, 100  $\mu$ L target cells were added to each well (2 x 10<sup>5</sup> cells/mL) and the plate incubated for a further 48 hours. Controls of pseudotyped virus with target cells, along with each alone, were set up in four replicates. Plates were read as described in section 2.13.1. Neutralisation titres of the samples tested were recorded as full or half maximum inhibitory concentrations (IC<sub>100</sub>/IC<sub>50</sub>). Where IC<sub>100</sub> end-point titres varied by more than one doubling dilution the assay was repeated and the geometric mean recorded. To calculate IC<sub>50</sub> titres, percentage neutralisation at each dilution was calculated relative to the control of target cells infected with pseudotyped virus and plotted in GraphPad Prism® v.5.02 where values were interpolated from the non-linear fit of transformed data.

### 2.2.14. Sucrose Purification

Prior to RT-qPCR or nanoparticle tracking analysis pseudotyped virus was purified from cell media using a sucrose cushion and centrifugation. Samples to be purified were first subject to DNase

treatment, incubating 1 mL of the sample with DNase I at a final concentration of 500 U/mL for 1 hour at 37°C (Life Technologies). Following DNase treatment, 900 µL of the sample was overlaid onto 400 µL of 20% filtered sucrose in 1x PBS and centrifuged at 13,000 xg for at least 2 hours at 4°C. After centrifugation the pellet was resuspended in 900 µL filtered 1x PBS. Samples were either analysed immediately or stored overnight at 4°C.

## **2.2.15. Pseudotyped Virus Genome Analysis**

### **2.2.15.1. RNA Extraction**

The RNA genome was extracted from purified (Section 2.2.14) and un-purified lentiviral pseudotyped virus samples using the QIAamp® viral RNA mini kit (Qiagen). Prior to extraction, un-purified pseudotyped virus samples were diluted 1:2 in 1x filtered PBS. Extraction was performed using 140 µL of sample following manufacturers instructions, eluting with 60 µL of the provided 'AVE' buffer.

### **2.2.15.2. Quantitative Reverse Transcription PCR (RT-qPCR)**

Prior to setting up the reaction, a dilution series of the firefly luciferase expressing reporter plasmid, pCSFLW, was prepared for use as a template to generate a standard curve. A 10-fold dilution series of the plasmid vector was prepared, diluting in 1 mg/mL UltraPure Salmon Sperm DNA solution (Life Technologies) to achieve  $1 \times 10^{10}$  –  $1 \times 10^1$  plasmid copies/well in the reaction (adding 2.5 µL) after calculating copy numbers (plasmids/µL) using the formula:

$$\text{molecular weight (g/mol)} = \text{Length (bp)} \times 660 \text{ g/mol (av. weight of dsDNA bp)}$$

$$\text{moles dsDNA/}\mu\text{L} = [\text{Vector}] \text{ (g/}\mu\text{L)} \div \text{molecular weight (g/mol)}$$

$$\text{plasmid copies/}\mu\text{L} = 6.0221 \times 10^{23} \text{ molecules/mol (Avogadro's number)} \times \text{moles dsDNA/}\mu\text{L}$$

RT-qPCR was performed targeting the LTR region of the RNA genome extracted from lentiviral pseudotyped virus samples using the RNA UltraSense™ One-Step Quantitative RT-PCR system (Life Technologies). 25 µL reactions were set up, using RNA UltraSense™ 5x master mix containing reverse transcriptase and ROX reference dye (0.05 µL) according to the kit guidelines,

along with 0.1  $\mu\text{M}$  HIV-LTR TaqMan<sup>TM</sup> probe and 0.2  $\mu\text{M}$  HIV-LTR forward and reverse primers (Table 2.14), adding 2.5  $\mu\text{L}$  extracted RNA. Reactions were run on MicroAmp® Optical 96-well plates (Applied Biosystems) in triplicate, including no template controls where 2.5  $\mu\text{L}$  of 1 mg/mL UltraPure Salmon Sperm DNA solution (Life Technologies) was added in place of extracted RNA. The standard was run in duplicate on each plate. A second reaction was prepared as a reverse transcriptase negative control, inactivating the enzyme at 75°C for 15 minutes prior to preparing the master mix. Reactions were run on a Mx3005p qPCR instrument (Stratagene) following the cycling conditions in Table 2.15 and analysed using MxPro v.4.1 software.

**Table 2.14 HIV-LTR Primer and Probe Sequence for RT-qPCR**

<b>Primer / Probe</b>	<b>Sequence (5' → 3')</b>
<b>HIV-LTR Forward</b>	GCTCTCTGGCTARCTAGGG
<b>HIV-LTR Reverse</b>	GTTACCAGAGTCACACAACAGA
<b>HIV-LTR TaqMan™ probe (5' – FAM and 3' – BHQ1)</b>	GCTTCAAGTAGTGTGTGCC

**Table 2.15 RT-qPCR Cycling Conditions for RNA UltraSense™ Master Mix**

<b>Step</b>	<b>Temperature</b>	<b>Time</b>
<b>Reverse Transcription<sup>1</sup></b>	50°C	30 minutes
<b>Taq Initial Activation</b>	95°C	10 minutes
<b>40 Cycles of:</b>		
Denaturation	95°C	30 seconds
Annealing & Extension	60°C	1 minute 30 seconds
<b>Melt Curve Analysis</b>		

<sup>1</sup>Step excluded for reverse transcriptase negative control reaction

### **2.2.16. SYBR Green Product-Enhanced Reverse Transcriptase (SG-PERT)**

#### **Assay**

The reverse transcriptase (RT) activity of lentiviral pseudotyped virus samples was quantified via an SG-PERT assay adapted from (Pizzato *et al.*, 2009; Vermeire *et al.*, 2012). Pseudotyped virus samples were lysed prior to addition to the reaction by incubating a 50% v/v mix of 10x diluted sample (in ultrapure (18 M $\Omega$ ) H<sub>2</sub>O) with 2x lysis buffer (100 mM TrisHCl, 50 mM KCl, 0.25% Triton X-100, 40% glycerol) supplemented with 0.8 U/ $\mu$ L RiboLock RNase inhibitor (Thermo Scientific) prior to use, for 10 minutes at room temperature. Following incubation samples were further diluted to give 100x pseudotyped virus lysate.

HIV RT (500U; Merck-Milipore), used to prepare a standard curve, was diluted to 10 mU/ $\mu$ L in storage buffer (10 mM potassium phosphate, 1 mM DTT, 20% glycerol, pH 7.4) and 10  $\mu$ L single use aliquots stored at -80°C. A standard curve was generated by preparing a 10-fold serial dilution of 10 mU/ $\mu$ L HIV RT to achieve  $1 \times 10^9 - 1 \times 10^3$  pU/well in the reaction (when adding 2  $\mu$ L per well). 25  $\mu$ L reactions were set up, using QuantiTect SYBR<sup>TM</sup> Green 2x master mix (Qiagen) containing 0.2 U/mL RiboLock RNase inhibitor (Thermo Scientific), 3.5 pmol/mL MS2 RNA (Sigma) and 0.5  $\mu$ M MS2 cDNA forward and reverse primers (Table 2.16), adding 12  $\mu$ L of 100x pseudotyped virus lysate. Reactions were run in triplicate on MicroAmp® Fast Optical 96-well plates (Applied Biosystems) and master mix, primer and diluent (ultrapure H<sub>2</sub>O) controls set up in duplicate. The HIV RT standard dilution was run in duplicate, adding 2  $\mu$ L to the master mix along with 10  $\mu$ L of ultrapure H<sub>2</sub>O. Reactions were run on a 7500 Fast RT-PCR instrument (Applied Biosystems) following the cycling conditions in Table 2.17 and analysed using 7500 v.2.3 software.

**Table 2.16 MS2 cDNA Primer Sequence for SG-PERT Assay**

<b>Primer</b>	<b>Sequence (5' → 3')</b>
<b>MS2 cDNA Forward</b>	TCCTGCTCAACTTCCTGTGAG
<b>MS2 cDNA Reverse</b>	CACAGGTCAAACCTCCTAGGAATG

**Table 2.17 SG-PERT Assay Cycling Conditions**

<b>Step</b>	<b>Temperature</b>	<b>Time</b>
<b>Reverse Transcription</b>	42°C	20 minutes
<b>Taq Initial Activation</b>	95°C	15 minutes
<b>40 Cycles of:</b>		
Denaturation	95°C	10 seconds
Annealing	60°C	30 seconds
Extension & Acquisition	72°C	30 seconds
<b>Melt Curve Analysis</b>		

### **2.2.17. Nanoparticle Tracking Analysis**

Sucrose purified pseudotyped virus samples (Section 2.2.14) were analysed using a NanoSight LM10 instrument (Malvern). Before and between sample acquisition the instrument was calibrated with polystyrene latex microspheres diluted in 1x PBS. The camera level was set to 15, with a detection threshold of 4. As optimal acquisition required a particle concentration of approximately  $10^8$  particles/mL, samples were 10-fold serially diluted in 1x PBS from 100 – 10000x and tested on the instrument. Samples 100x diluted had an optimal particle concentration and 1 mL was injected for analysis, acquiring 5 times for 90 seconds each. Data was analysed using Nanoparticle Tracking Analysis v.2.3 software (Malvern).

# Chapter 3. Production of Chimeric Arctic-like Rabies Virus Glycoproteins to Improve Pseudotyped Virus Titres and Permit Serological Studies

## 3.1. Introduction

Rabies, a neglected zoonotic disease caused by members of the *Lyssavirus* genus, poses a significant public health threat with a near 100% case fatality rate in individuals who develop clinical disease (Fooks *et al.*, 2014). Globally rabies virus (RABV), the type species of the *Lyssavirus* genus, is accountable for approximately 60,000 human deaths per year, having a higher mortality rate than any other zoonotic disease (Fooks *et al.*, 2014). Effective pre and post-exposure prophylaxes regimens have long been well defined, however high cost implications and the geographical distribution of rabies, present on all continents except Antarctica, represents a challenge to its control (Fooks, 2004; Warrell, 2012). As such, serological studies, monitoring responses to pre and post-exposure treatments and undertaking widespread sero-surveillance, are vital aspects in the implementation of control programmes aimed at lowering rabies incidence (Banyard *et al.*, 2013; Brookes *et al.*, 2005; Wright *et al.*, 2009). However, as many rabies-endemic areas are in the developing world, they lack the infrastructure to be able to undertake these routine serological techniques which can require use of BSL 3 containment facilities or specialised equipment.

At present, 14 species are classified within the *Lyssavirus* genus, with a further three putative members awaiting classification (Figure 1.2) (Banyard & Fooks, 2017; Dietzgen *et al.*, 2011). They cause clinically indistinguishable disease, with techniques to differentiate between causative species not routinely employed during diagnosis, particularly in endemic regions, thus the true burden of species other than classical RABV remains undefined (Fooks, 2004). Arctic-like rabies virus (AL RABV) forms one of seven geographically and genetically distinct viral lineages of the

RABV species, determined via phylogenetic analysis (Kuzmin *et al.*, 2008; Nadin-Davis *et al.*, 2007). Endemic across the Middle East and Asia, AL RABV is likely responsible for a significant proportion of rabies cases in this region, which results in greater than 20,000 human fatalities each year in India alone (Sudarshan *et al.*, 2007). Yet with inadequate reporting systems and a weak healthcare infrastructure across this region, the true burden of rabies could be far higher (Banyard *et al.*, 2013; Pant *et al.*, 2013). A lack of accurate data has resulted in the low prioritisation of control programmes by policy makers and public health professionals (Fooks *et al.*, 2014; Sudarshan *et al.*, 2007). While there is no evidence to indicate AL RABV has an altered pathogenicity, its infection dynamics and epidemiology are under studied together with the protection afforded by current vaccines and antivirals. Undertaking a comprehensive analysis of currently circulating RABVs, as well as monitoring for the emergence of new variants, forms a vital aspect in limiting rabies incidence (Matsumoto *et al.*, 2013). Thus, it is important to fully understand the public health threat posed by the AL RABV lineage.

The development of a pseudotyped virus neutralisation assay (PVNA) for the measurement of anti-rabies virus neutralising antibodies (NAbs) in vaccine recipients, along with further large scale in-field serosurveillance within a developing country has previously been described (Moeschler *et al.*, 2016; Wright *et al.*, 2008, 2009, 2010). These provided sensitive and specific results which correlated with the WHO and OIE endorsed fluorescent antibody virus neutralisation test (FAVN), a live virus assay, and distinguished between lyssavirus species. As the use of PV allows neutralisation assays to be undertaken in BSL 1 or 2 laboratories, along with having a lower cost implication, the serological study of rabies is expanded to resource-limited laboratories in regions where the virus is endemic.

While *Lyssavirus* isolates have previously pseudotyped efficiently, initial attempts to produce AL RABV pseudotypes found titres were inadequate to allow downstream neutralisation assay studies to be undertaken. The flexibility of using a chimeric envelope glycoprotein to study rabies has been demonstrated in a study, albeit based on a recombinant rabies virus system, using a chimeric VSV

envelope glycoprotein with a RABV cytoplasmic domain to determine the importance of the RABV envelope glycoprotein in eliciting an immune response (Foley *et al.*, 2000). Additionally, studies looking at the use of RABV pseudotypes in gene therapy, targeting the central nervous system, reported that the pseudotyping efficiency of a RABV envelope glycoprotein could be increased by replacing the cytoplasmic domain with that of a VSV glycoprotein, which pseudotypes highly effectively (Carpentier *et al.*, 2011; Kato *et al.*, 2011). The work described in this chapter aimed to adapt this approach and produce a chimeric AL RABV glycoprotein in an attempt to increase PV titre and allow the efficacy of current vaccines and antivirals against the AL RABV lineage to be tested via a PVNA.

## 3.2. Results

### 3.2.1. Chimeric AL RABV Envelope Glycoprotein Construction

Chimeric envelope glycoprotein (G) constructs were generated for four AL RABV isolates, RV61, RV193, RV250 and RV277 using G cDNA sequences within a pI.18 expression plasmid, previously amplified from viral RNA by the Animal and Plant Health Agency (APHA, UK) (Table 3.1). The isolates were selected to represent three genetically distinct clades of the Arctic-related lineage (Table 3.1), which included the isolate (RV61) linked to a clinical, transplant associated, outbreak (Ross *et al.*, 2015) as well as two (RV193 and RV277) reported to grow poorly in live viral cultures by the reference laboratory source (APHA, UK).

**Table 3.1 Arctic-like Rabies Virus Isolates**

Details of the phylogenetically determined Arctic-related clade of the isolates used and GenBank accession numbers for the G sequences. All G cDNA sequences were provided by APHA, UK.

Isolate	Arctic-related Clade <sup>1</sup>	GenBank Accession Number
India.human.87.RV61	Arctic-like 1a	KU534939
Pakistan.dog.89.RV193	Arctic-like 1a	KU534940
Russia.squirrel.RV250	Arctic 2	KU534941
Pakistan.goat.RV277	Arctic-like 1b	KU534942

<sup>1</sup>Determined via phylogenetic analysis (Appendix II)

Using splicing by overlap extension (SOE) PCR (Section 2.2.4) the cytoplasmic (c) domain sequence of the four AL RABV isolates was replaced with that of a laboratory strain of RABV, challenge virus standard 11 (CVS-11; EU352767), or VSV (J02428) G, which had both previously produced high titre PV (Wright *et al.*, 2008). The ecto-transmembrane (etm) domain was not altered. Primers used (C1.9 – 1.17, Table 2.3) were designed based on mapping the cytoplasmic domain of the AL RABV and CVS-11 G to amino acids 481 – 526 and that of the VSV G to amino acids 483 – 512, following those defined in the Carpentier, *et al.* (2011) study. A chimeric CVS-11 G with a VSV cytoplasmic domain (CVS-11etmVSVc) G was also produced to act as a control. All the constructs produced are depicted in Figure 3.1 and were cloned into the pI.18 expression plasmid and sequencing verified (Section 2.2.8).

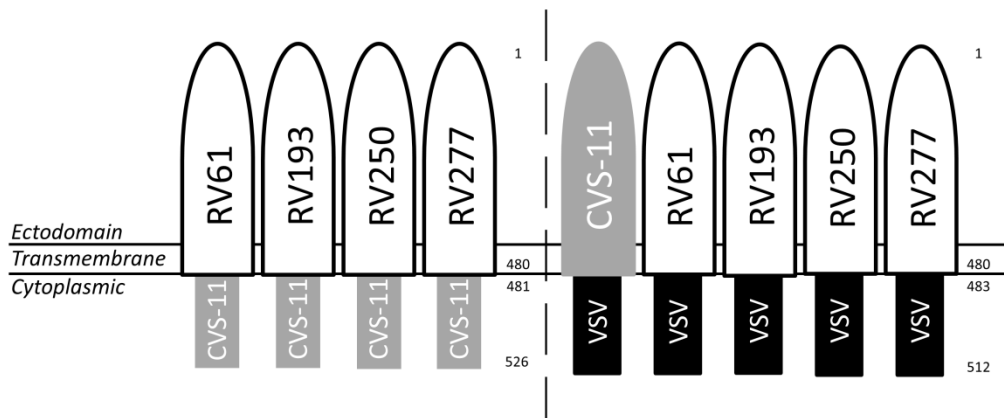


**Figure 3.1 Schematic Representation of Chimeric Envelope Glycoprotein Constructs**

The chimeric envelope glycoprotein constructs produced by switching the cytoplasmic domain are depicted. Numbers represent the amino acids of the respective full length glycoprotein for the AL RABV and CVS-11 ecto-transmembrane domain and CVS-11 or VSV cytoplasmic domain.

### 3.2.2. Production of Arctic-like Rabies Virus Pseudotyped Virus

Lentiviral PV was produced with a firefly luciferase reporter gene, comprising the wildtype AL RABV isolate and CVS-11 G, as well as the chimeric G constructs generated in Section 3.2.1, by transfecting HEK 293T/17 cells (Section 2.2.10). To determine whether the chimeric G had increased the PV titre, an infection assay was set up (Section 2.2.11.1) with four replicates of 1:4 diluted PV titrated onto the BHK-21 cell line, previously determined to be permissive to lyssavirus infection (Wright *et al.*, 2008). The level of infection was recorded in relative light units (RLU; Section 2.2.12.1). It was found that PV with a chimeric CVS-11 cytoplasmic domain G caused a decrease (RV61: -15.7 fold,  $p = 0.2$ ; RV250: -10.6 fold,  $p = 0.0007$ ; RV277: -1.4 fold,  $p = 0.7$ ) or insignificant increase (RV193: 1.2 fold,  $p = 0.7$ ) in titre (Figure 3.2). However, PV with a chimeric VSV cytoplasmic domain G gave a significant increase ( $p < 0.0005$ ) in titre for three of the AL RABV isolates (RV61, RV193 and RV277) and CVS-11 control (Figure 3.2). The fold increase in titre between PV with a wildtype and chimeric VSV cytoplasmic domain G was calculated (Table 3.2), showing a small (1.1 fold,  $p = 0.3$ ) increase in titre for the RV250tmVSVc G PV.

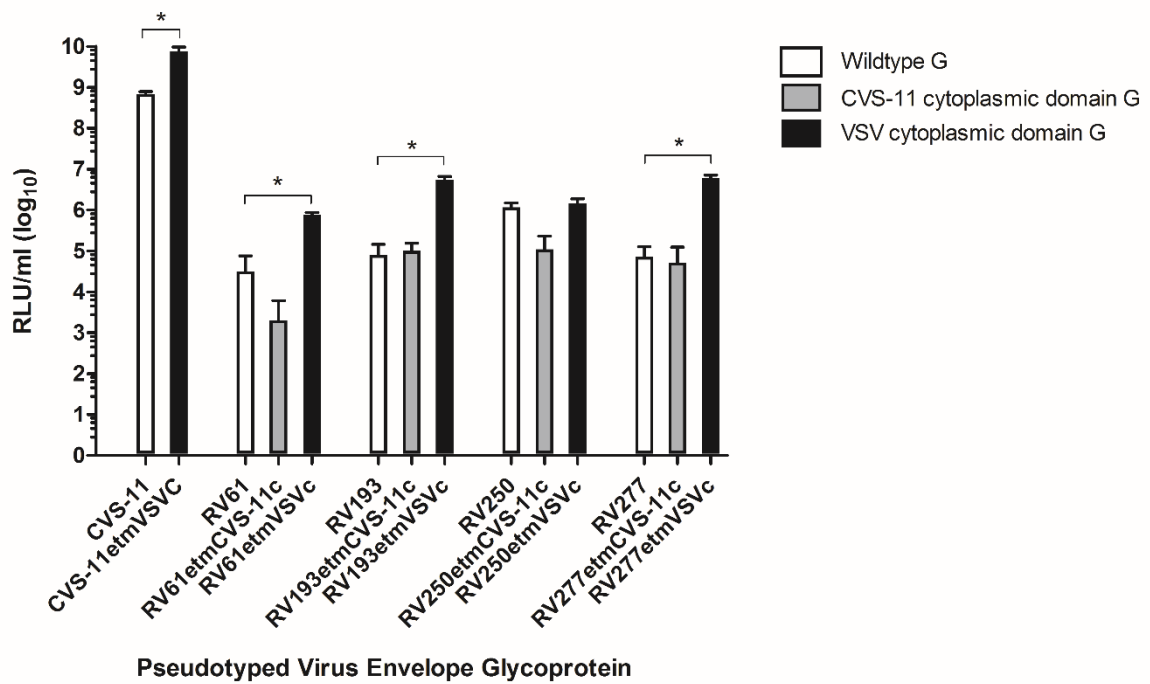


**Figure 3.2 Comparison of Pseudotyped Virus Titres using Wildtype and Chimeric Envelope Glycoproteins**

PV with a luciferase reporter gene titrated on BHK-21 cells, with titres calculated as relative light units per ml (RLU/ml) to determine if a chimeric glycoprotein with a CVS-11 or VSV cytoplasmic domain increased titres. (\* $p < 0.0005$ ; two-tailed  $t$ -test) Error bars show SD (n = 4).

**Table 3.2 Fold Increase in Pseudotyped Virus Titre using a Chimeric VSV Cytoplasmic Domain Envelope Glycoprotein**

Fold increase calculated in comparison to PV with a wildtype glycoprotein using RLU/ml values plotted in Figure 3.2.

Envelope Glycoprotein	Fold Increase
CVS-11etmVSVc	11.3
RV61etmVSVc	24.2
RV193etmVSVc	67.9
RV250etmVSVc	1.1
RV277etmVSVc	83.3

To corroborate the increase in titre observed, lentiviral PV was produced with the wildtype and chimeric VSV cytoplasmic domain G incorporating an emerald green fluorescent protein (emGFP) reporter gene. Infection assays were set up for imaging cells via fluorescent microscopy, as well as to undertake flow cytometry analysis. Using fluorescent microscopy a visibly apparent increase in cells infected with PV was observed with the chimeric VSV cytoplasmic domain G in comparison to those infected with wildtype G PV (Figure 3.3). Analysis of flow cytometry data collected using the FITC protocol (Section 2.2.12.3) was carried out by applying a gate to remove cell or other debris from the analyses (Figure 3.4A). A second gate was applied to the FITC channel at the end of the first log-decade to count the percentage of cells from the population emitting fluorescence above the background level (Figure 3.4B). The fold increase in titre values calculated for PV with a chimeric VSV cytoplasmic domain G (Table 3.3) were found to be in line with those previously calculated for PV with a luciferase reporter gene. This acted to confirm the use of a chimeric VSV cytoplasmic domain G to increase the titre of AL RABV PV.

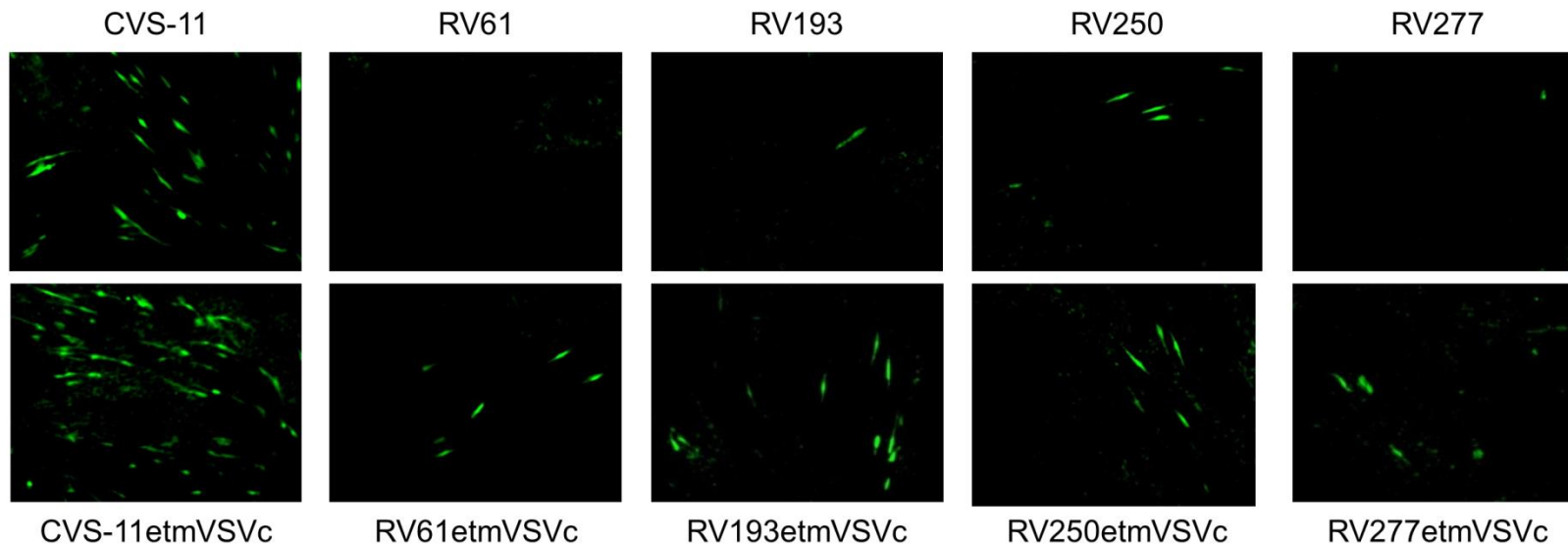


**Figure 3.3 Comparison of Cell Infection by Pseudotyped Virus Bearing Wildtype versus Chimeric Envelope Glycoprotein**

Fluorescent microscopy images of BHK-21 cells infected with PV bearing wildtype CVS-11 or AL RABV isolate glycoprotein (top row) in comparison to that bearing chimeric VSV cytoplasmic domain glycoprotein (bottom row). An emGFP reporter gene was used and images captured using the x10 objective.

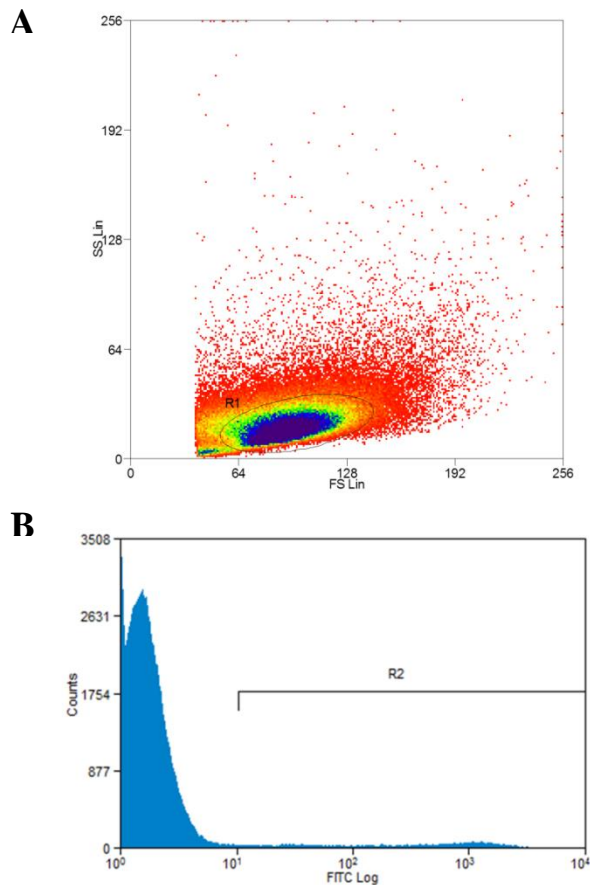


**Figure 3.4 Gating of Cells for Flow Cytometry Analysis**

Example of gates set for analysis of BHK-21 cells infected with an emGFP reporter gene PV with. (A) A gate (R1) was placed over the cell population to exclude larger cells or any cell debris from the analysis. (B) Using the FITC channel a gate (R2) was from the end of the first log-decade to count the percentage cell population expressing fluorescence above background.

**Table 3.3 Fold Increase in Titre of Pseudotyped Virus with a Chimeric VSV Cytoplasmic Domain Glycoprotein Measured Using Flow Cytometry Analysis**

Fold increase calculated in comparison to PV with a wildtype glycoprotein from flow cytometry data on the percentage of cells emitting fluorescence.

Envelope Glycoprotein	Fold Increase
CVS-11etmVSVc	2.2
RV61etmVSVc	54.5
RV193etmVSVc	27.0
RV250etmVSVc	8.0
RV277etmVSVc	19.0

### **3.2.3. Neutralisation Assays to Evaluate the Efficacy of Existing Prophylaxis against the Arctic-like Rabies Virus Lineage**

The increased PV titre achieved for the AL RABV isolates by using a chimeric VSV cytoplasmic domain G enabled serology studies to be undertaken via a PVNA to assess the efficacy of currently used vaccines and post-exposure prophylaxes. As both receptor-binding domains and antigenic sites are known to be mapped to the ectodomain (Evans *et al.*, 2012; Kuzmina *et al.*, 2013), switching of the cytoplasmic domain in the generation of the chimeric G constructs should not have influenced the serological profile. Further, sequence comparison was undertaken for the G domains of the AL RABV isolates and that of CVS-11 G, constructing a radial phylogenetic tree following ClustalW sequence alignment using the MEGA6 maximum likelihood method, based on the JTT matrix model (Figure 3.5A) (Tamura *et al.*, 2013) and nucleotide and amino acid sequence identities determined using the BLAST® Global Alignment tool on the NCBI database (Figure 3.5B). The high levels of homology observed via this analysis acted to suggest the neutralisation profiles should be similar, yet only offered a crude estimate due to the potential disproportionate effect individual amino acid substitutions can have on antigenic properties.

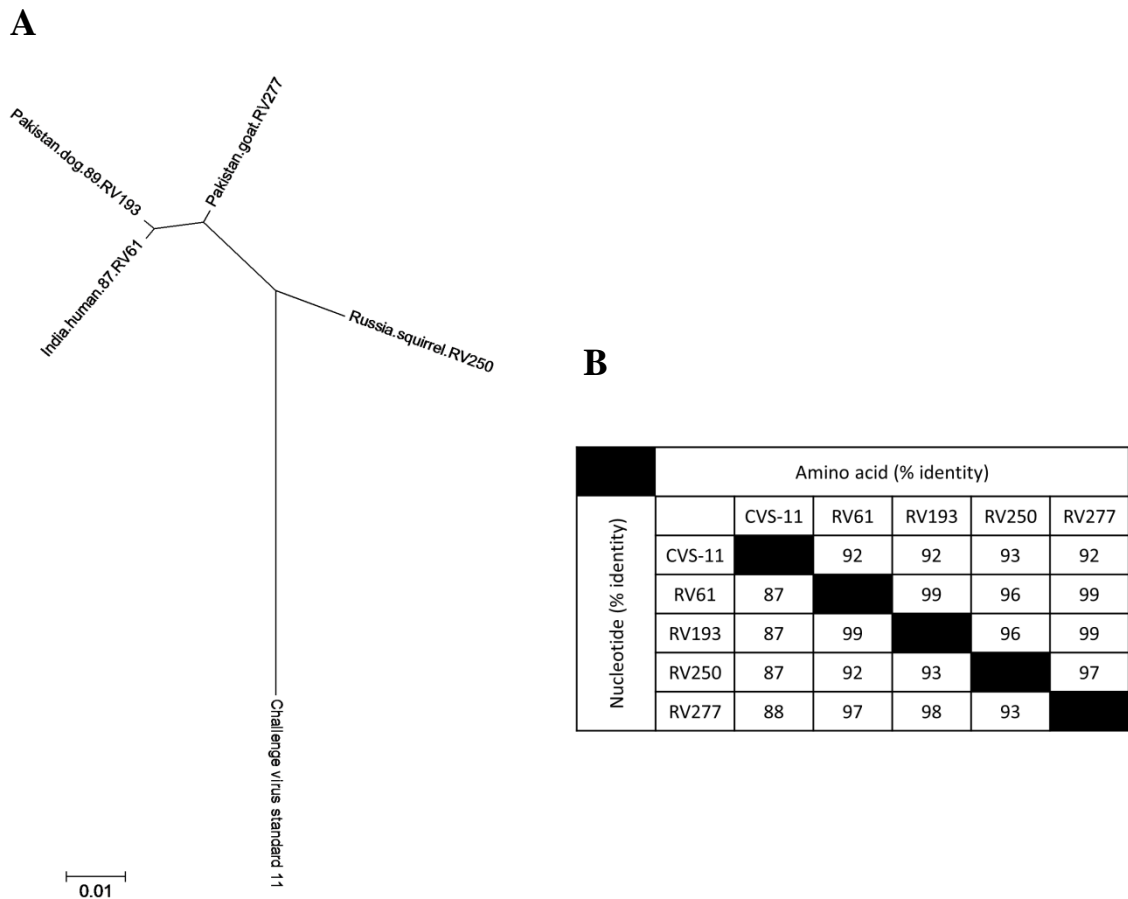


**Figure 3.5 Degree of Nucleotide and Amino Acid Sequence Identity Between Arctic-like Rabies Virus and CVS-11 Envelope Glycoprotein Ecto-Transmembrane Domain**

(A) Radial phylogenetic tree constructed using the MEGA6 maximum likelihood method, based on the JTT matrix model, following ClustalW sequence alignment of the envelope glycoprotein ecto-transmembrane domain amino acid sequences. Scale corresponds to amino acid substitutions per site. (B) Nucleotide and amino acid percentage sequence identities determined using the BLAST® Global Alignment tool on the NCBI database.

Initially, a PVNA was performed (Section 2.2.13) testing the chimeric G PV alongside wildtype CVS-11 G PV using the OIE standard reference dog serum (0.5 international units per mL (IU/mL)), as well as the WHO 2<sup>nd</sup> international human anti-rabies Ig reference serum (2 IU/mL; NIBSC, UK) over a 2-fold serial dilution, starting at 1:20. An input of 50 TCID<sub>50</sub> of PV was used for neutralisation assays based on the results of a titration assay (Section 2.2.11.2) and results were recorded as IC<sub>100</sub> end-point titres. Results showed that chimeric CVS-11etmVSVc G PV had an IC<sub>100</sub> titre matching or within one doubling dilution of that for wildtype CVS-11 G PV for the OIE (IC<sub>100</sub> = 80) and WHO (IC<sub>100</sub> = 269 and 453) standards respectively (Figure 3.6). This suggested switching the cytoplasmic domain of the G had not altered the neutralisation profile. Further to this, each of the AL RABV chimeric G PV were neutralised at an equivalent or more potent level by each standard than that recorded for CVS-11 G PV (Figure 3.6).

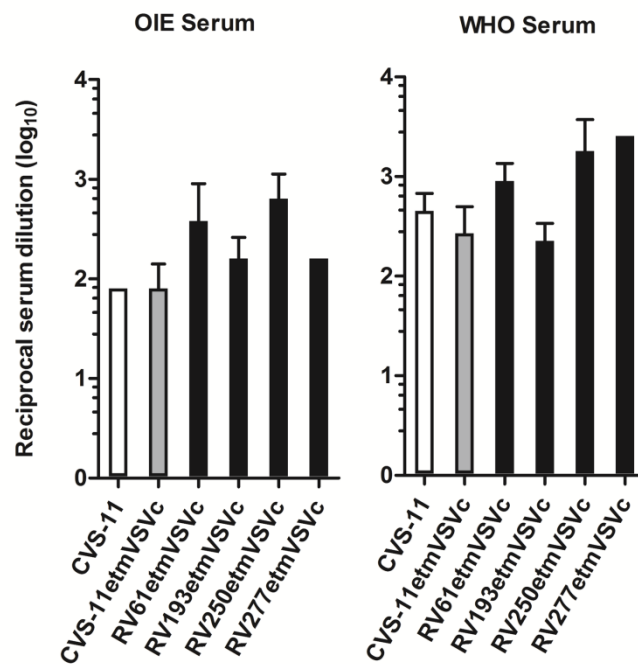


**Figure 3.6 Neutralisation of Pseudotyped Virus by OIE and WHO Serum Standards**

The OIE is a standard reference dog serum (0.5 IU/mL) and the WHO is the 2<sup>nd</sup> international human anti-rabies Ig reference serum (2 IU/mL). Values are reported as IC<sub>100</sub> endpoint reciprocal serum dilutions (geometric mean ± SD). Where error bars are absent, replicates produced the same IC<sub>100</sub> endpoint dilution.

Analysis of the neutralisation afforded against these AL RABV isolates by pre-exposure vaccination was undertaken by assessing a blinded panel of serum samples (n = 20) taken from RABV-vaccinated humans (Rabipur, Novartis) and domestic animals (dogs and cats) vaccinated (Rabvac, Fort Dodge; Nobivac, Intervet; Rabisin, Merial; Quantum, Schering Plough) as part of the UK pet travel scheme (PETS) (Ramnial *et al.*, 2010) (Appendix II). The samples had been assigned a titre (IU/mL) using the FAVN test method for detecting rabies specific antibodies, a score of 0.5 IU/mL is considered the cut-off for adequate sero-conversion for protection (Cliquet *et al.*, 1998; WHO, 2013). When un-blinded, four human serum samples (H1, H5, H6, H7) with NAb levels of 0.03 – 0.1 IU/mL, had not neutralised any PV tested (data not presented) and one sample with a NAb level just below 0.5 IU/mL (H61, 0.38 IU/mL) had neutralised all PV tested (Figure 3.7A). All samples with a NAb titre above 0.5 IU/mL produced good levels of neutralisation for the CVS-11 and CVS-11etmVSVc G PV (IC<sub>100</sub> titres of 160 – 640) along with comparable levels for the chimeric AL RABV G PV (Figure 3.7A). The same cut-off is used to assign a satisfactory vaccination response in canine and feline recipients. All animal serum samples with an adequate level of sero-conversion produced a robust neutralising response (Figure 3.7B). Of the four samples tested which had been assigned NAb titres between 0.07 – 0.38 IU/mL on FAVN testing (Figure 3.7B; PET-5531,-5545,-5734,-5896) a low level of PV neutralisation was detected (IC<sub>100</sub> titres of 12 – 57).

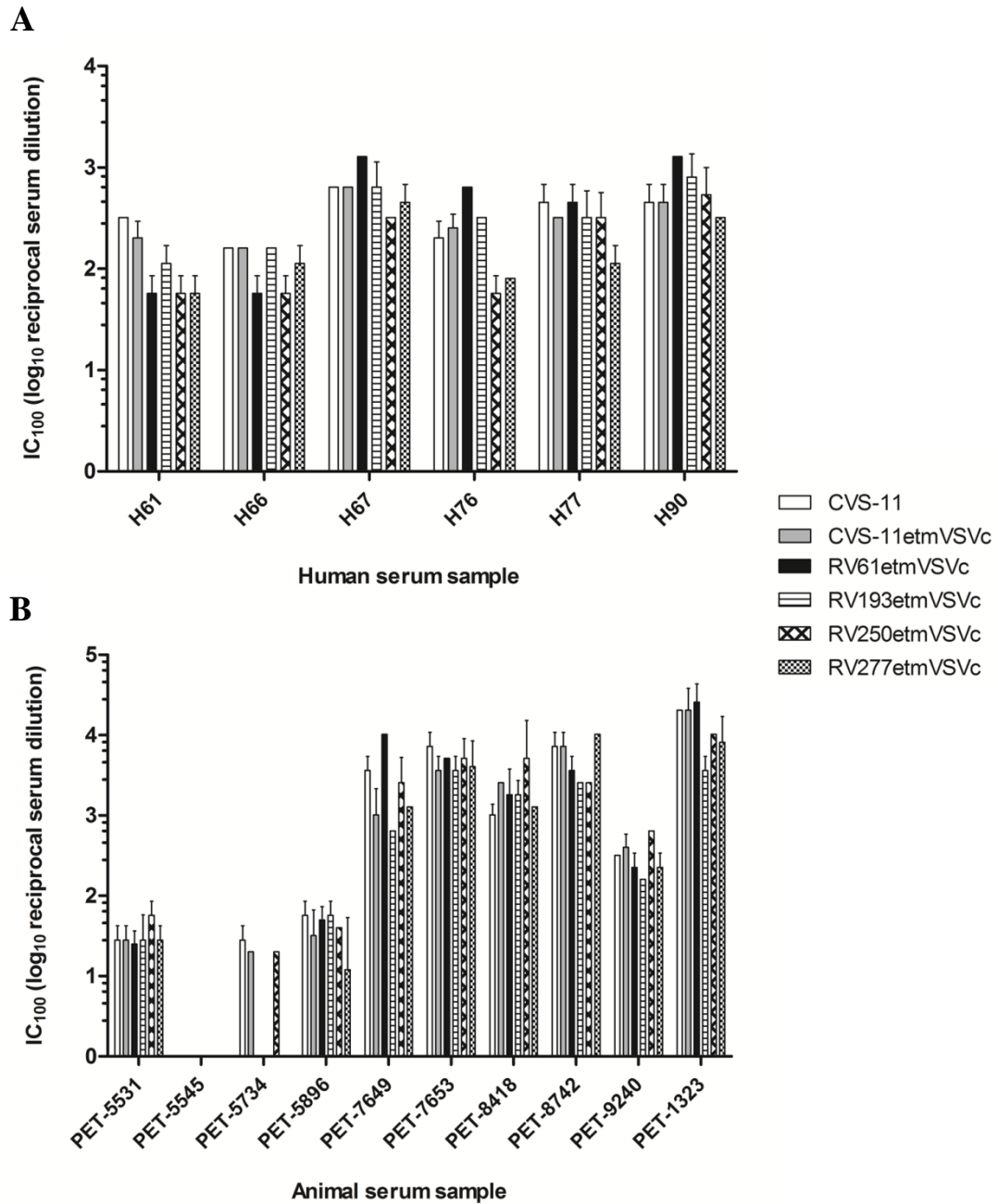


**Figure 3.7 Pseudotyped Virus Neutralisation IC<sub>100</sub> Endpoint Dilutions for Human and Animal Serum Samples**

Neutralisation of CVS-11, CVS-11etmVSVc and chimeric AL RABV G PV reported as the reciprocal serum dilution of IC<sub>100</sub> endpoints. **(A)** Human serum samples are from RABV vaccine recipients, sample H61 was assigned a FAVN titre of 0.38 IU/mL and the remaining samples a titre > 0.5 IU/mL. **(B)** Animal serum samples are from vaccinated dogs or cats, four samples with FAVN titres between 0.07 – 0.38 IU/mL (PET-5531,-5545,-5734,-5896) are shown. The remaining samples have a titre > 0.5 IU/mL. Values are the geometric mean ± SD. Where error bars are absent, replicates produced the same IC<sub>100</sub> endpoint dilution.

Biologics used for post-exposure prophylaxis (PEP) were also tested for their efficacy against the AL RABV isolates. Human rabies immunoglobulin (HRIG), in the form of commercial samples released for the European market (provided by NIBSC, UK), were tested by PVNA with a starting concentration of 2 IU/mL. Results showed each sample provided a good level of neutralisation for the PV tested ( $IC_{100}$  titre of  $1.9 \times 10^{-3} - 7.6 \times 10^{-6}$  IU/mL; Figure 3.8). In addition, monoclonal antibody (mAb) preparations were tested (CR57, CR4098, RVC20 and RVC58), which are directed against various neutralising antigenic sites on the RABV G and are being considered for development to replace HRIG in PEP (Bakker *et al.*, 2005; De Benedictis *et al.*, 2016). Used at a starting concentration of 15  $\mu$ g/mL, each mAb neutralised the chimeric AL RABV G PV ( $IC_{100}$  titre of 1.1 – 662.3 ng/mL), with CR4098 and RVC20 offering the most potent levels of neutralisation across all PV preparations ( $IC_{100}$  titres between 1.1 – 35.6 and 1.3 – 106.9 ng/mL respectively; Figure 3.8).

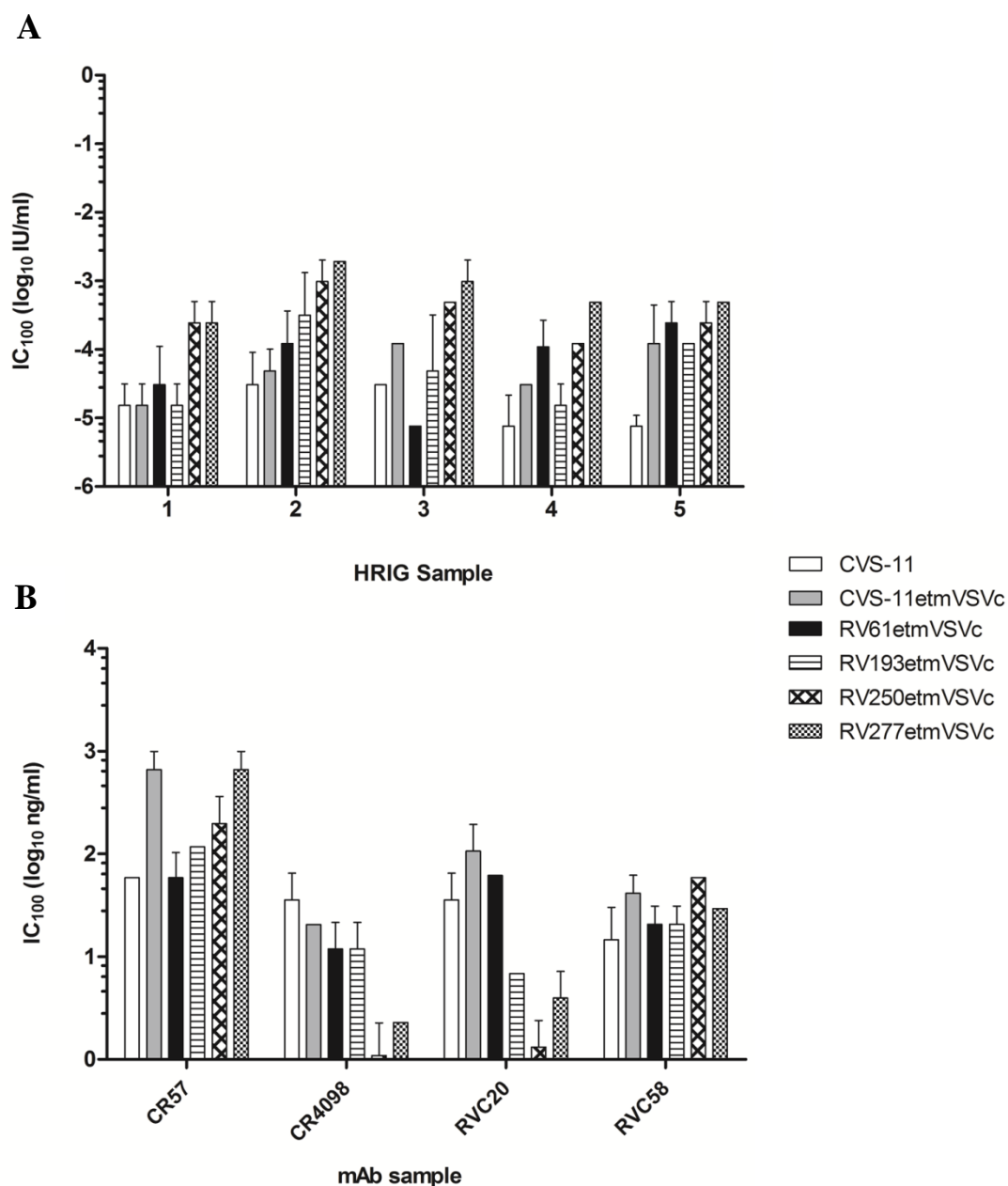


**Figure 3.8 Pseudotyped Virus Neutralisation IC<sub>100</sub> Endpoint Dilutions for HRIG and mAb Samples**

Neutralisation of CVS-11, CVS-11etmVSVc and chimeric AL RABV G PV reported as IC<sub>100</sub> endpoint dilutions. (A) HRIG samples were tested at a starting concentration of 2 IU/mL. (B) mAb samples derived against different neutralising epitopes were used at a starting concentration of 15 µg/mL. Values are the geometric mean ± SD. Where error bars are absent, replicates produced the same IC<sub>100</sub> endpoint dilution.

To further ensure switching the cytoplasmic domain of the G had not influenced the neutralisation profile, IC<sub>100</sub> endpoint titres obtained by the PVNA for wildtype CVS-11 G PV were correlated with those for CVS-11etmVSVc G PV. Analysis by Pearson's correlation using GraphPad Prism® (v.5.02) showed a strong level of correlation between the PVNA results ( $r = 0.99$ ,  $p < 0.0001$ ; Figure 3.9) and thus switching the G cytoplasmic domain had not altered its antigenicity.

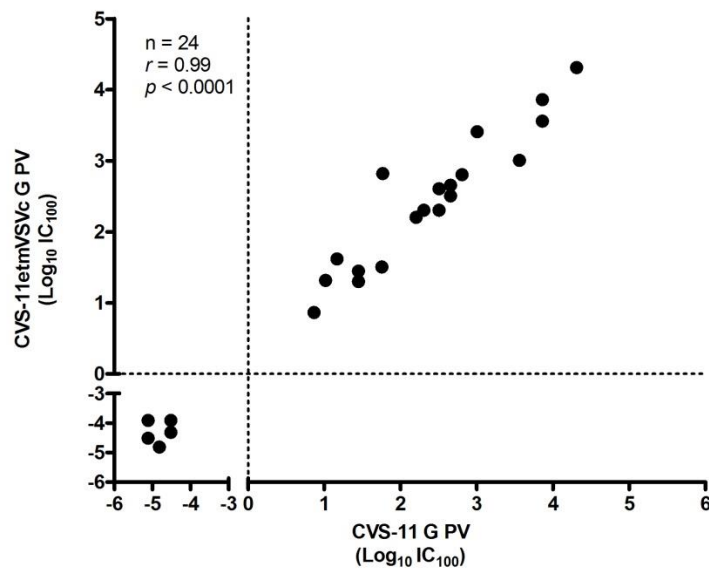


**Figure 3.9 Comparison of the Neutralisation IC<sub>100</sub> Endpoint Titres for Wildtype CVS-11 G PV Compared to Chimeric CVS-11etmVSVc G Pseudotyped Virus**

A high correlation ( $r$ ) is observed between the IC<sub>100</sub> endpoint titres for CVS-11 G and CVS-11etmVSVc G PV. Pearson's product-moment correlation was used to calculate  $r$  and  $p$  values.

### 3.3. Discussion

Serological studies are required to define NAb titres as part of vaccination and antiviral development and treatment schedules, while also allowing surveillance of the epidemiological spread of emerging viruses. As PV incorporate envelope proteins representative of the wildtype virus in their envelope they are antigenically similar, mimic the action of live virus in neutralisation tests and have proven to be a safe, robust and flexible alternative for use in serological assays (Mather *et al.*, 2013; Steffen & Simmons, 2016; Temperton *et al.*, 2015b). It has also been shown that using a CVS-11 G PV the PVNA proved to be 100% specific and equally sensitive to the WHO and OIE endorsed FAVN method of rabies NAb detection (Wright *et al.*, 2008, 2009). The results of this study substantiates its use and demonstrates the inherent flexibility of the platform, allowing manipulation of the envelope G to increase PV titre, permitting serological studies to determine the protection conferred by vaccines and antivirals against AL RABV isolates.

Chimeric AL RABV envelope G sequences were constructed with either a CVS-11 or VSV G cytoplasmic domain in an attempt to increase PV titre. As both CVS-11 and VSV G routinely produce high titre PV with the pseudotype system used in this study, it was of interest to establish if splicing in the cytoplasmic domains from these G could increase PV titre for other G. However, it was found that only the chimeric VSV cytoplasmic domain envelope G resulted in a significant increase in PV titre for three of the AL RABV isolates (RV61, RV193 and RV277). The lower increase in titre for the RV250 isolate is thought to be attributed to a difference in its glycoprotein structure, as phylogenetic analysis showed greater sequence homology between the other isolates, which formed a separate cluster. Previously, the use of a chimeric CVS (B2c strain) envelope G with a VSV cytoplasmic domain was described (Carpentier *et al.*, 2011), reporting a two fold increase in titre. In a similar study by Kato, *et al.* (2011) a 13 fold increase in titre was reported for a CVS strain envelope G of RABV. This is in line with that observed for the CVS-11etmVSVc G used within this study. The mechanism behind this effect remains to be fully elucidated, yet studies have described that the assembly of viable virions requires a direct or indirect interaction between the lentiviral matrix protein and envelope protein cytoplasmic domain (Cosson, 1996; Freed, 1998;

Sandrin *et al.*, 2004; Yu *et al.*, 1992). Thus it is possible the cytoplasmic domain of VSV G interacts more effectively with the lentiviral core compared to that of the CVS-11 G. Alternatively, it has been suggested a truncated or shorter cytoplasmic domain, as with VSV G, may cause a reduced steric hindrance or allow incorporation into lentiviral particles independent of matrix protein interaction (Freed & Martin, 1995). This is further supported by the report that truncation of the measles virus fusion (F) protein cytoplasmic domain lead to an increased PV titre (Frecha *et al.*, 2008).

Both CVS-11 and VSV constitute well studied prototypes of the lyssavirus and vesiculovirus genera respectively, within the *Rhabdoviridae* family. Importantly, there is good consensus within the literature of the defined regions of the lyssavirus G domains (Evans *et al.*, 2012; Kuzmina *et al.*, 2013). The position of the VSV G cytoplasmic domain is also well defined and the crystal structure of the G ectodomain has been derived (Roche *et al.*, 2006; Rose *et al.*, 1980). Due to the predictive nature of structural models to define transmembrane and cytoplasmic domains, which often are not present in crystal structures, there can be variability in the reported domain regions of less studied envelope proteins. It has also been demonstrated that the hydrophobic transmembrane domain can affect folding and incorporation into the viral membrane, as well as being involved in fusion (White *et al.*, 2008). There are residues in the transmembrane domain of the VSV G which are critical for fusion (Cleverley & Lenard, 1998). Further, the membrane proximal region of the ectodomain of envelope fusion proteins play a critical role in conformational changes during membrane fusion and constitute a target for entry inhibition (Cosset & Lavillette, 2011). Consequently, caution is needed when designing chimeric sequences as alterations may result in loss of function, particularly the transmembrane domain which is functionally important.

While current vaccines provide protection against RABV, the high level of sequence identity between the AL RABV isolates and CVS-11 G is not sufficient to definitively predict their neutralisation profile, as the effect of individual amino acid substitutions on antigenic variation has in some cases proven substantial (Horton *et al.*, 2010). Also, with the advent of mAbs for PEP,

point mutations within the binding sites of mAbs can result in viral escape from neutralisation and thus the identification of these critical residues, assessing the neutralisation of generated escape viruses, forms a vital aspect in the development of effective, broadly neutralising, therapeutics (Bakker *et al.*, 2005; Marissen *et al.*, 2005). Direct measures of antigenic variation by serology are fundamental yet can prove difficult to quantify. The use of antigenic cartography has added power to the interpretation of antigenic data, enabling the generation of an antigenic map for a global panel of lyssaviruses, instrumental for predicting antigenicity based on the envelope G gene sequence (Horton *et al.*, 2010). The PVNA platform has previously been used in the collection of antigenic data in a cross-species comparison of lyssavirus neutralisation, showing suitability as a high-throughput screening method to complement quantification of antigenic differences (Wright *et al.*, 2008, 2009). This study demonstrates the inherent flexibility of the PVNA in the creation of chimeric viral envelope protein PV without disruption to the neutralisation profile and therefore the envelope protein function. This enabled the determination of sero-status, and by extrapolation, protection afforded by current vaccines and prophylaxis against the AL RABV isolates.

The AL RABV isolates were found to be effectively neutralised by human and mammalian serum samples, conferring adequate protection by current pre-exposure vaccine formulations. As more than 99% of human rabies cases occur from contact with rabid dogs, the control of rabies within this population is of high priority (Banyard *et al.*, 2013; WHO, 2013). The annual economic cost of canine rabies alone is estimated to be USD\$8.6 billion, highlighting the severe economic and societal implications of endemic rabies (Hampson *et al.*, 2015; Pant *et al.*, 2013). Mass vaccination campaigns of dog populations are highly effective and thus monitoring levels of protection afforded by animal vaccine formulations is of equal importance to the prevention of human rabies infections. All licenced vaccine preparations are derived from inactivated preparations of classical RABV, which has shown to confer protection against viruses in phylogroup I but offer limited or no protection against those in phylogroups II and III (Evans *et al.*, 2012; Fooks, 2004; Hanlon *et al.*, 2005). Since AL RABV is a lineage of classical RABV, the protection observed follows this accepted consensus and while rabies cases are poorly characterised in the regions where AL RABV

circulate, unexplained vaccine failures have not been reported. However, due to poor growth of these AL RABV isolates in live viral cultures, which could suggest a different envelope G structure, and the implication of one isolate in a transplant-associated rabies outbreak in Germany (Ross *et al.*, 2015), it was important to be able to undertake serological evaluation. Further studies into cross-protection of rabies vaccines against more divergent lyssaviruses, such as those within phylogroups II and III, using this PVNA could assist in the development of a more broadly cross reactive vaccine formulation.

PEP regimes have long been effective in preventing rabies virus infection in the event of exposure. For previously un-vaccinated individuals this consists of wound cleansing, vaccination and the administration of rabies immunoglobulin (RIG) to provide passive immunity in the interval before vaccine induced active immunity is achieved (Fooks *et al.*, 2014). RIG of human (H) or equine (E) origin is available. While HRIG is preferred due to its longer half-life, it is expensive compared to the more immunogenic ERIG, which is primarily used in the developing world; yet both are in short supply (WHO, 2013). The AL RABV isolates were neutralised by all HRIG preparations, however alternative means of PEP are now being sought by the development of mAb cocktails. This study tested four mAbs, RVC20 and CR57, and RVC58 and CR4098, which target antigenic site I and III respectively of the RABV G (Bakker *et al.*, 2005; De Benedictis *et al.*, 2016; Marissen *et al.*, 2005). In order to meet WHO guidelines, which suggest RABV PEP should contain at least two antibodies to lower the probability of immune escape, CR57 and CR4098 have been combined into the CL184 mAb cocktail and undergone phase II clinical trials (Bakker *et al.*, 2008; Nagarajan *et al.*, 2014; WHO, 2013). The mAbs RVC20 and RVC58 are in earlier stages of development, having demonstrated good broad-spectrum potency by neutralising non-RABV lyssaviruses (De Benedictis *et al.*, 2016). In this study, each mAb effectively neutralised the AL RABV isolates, which can further serve as an indication that both antigenic sites are conserved across the AL RABV lineage.

Ultimately, the flexibility of using PV demonstrated within this study can be further extended. The generation of antigenic escape mutant envelope protein for incorporation into the PV platform will enable evaluation of mAb cocktails undergoing development. Likewise, switching of epitopes between lyssavirus envelope G can allow further cross neutralisation studies to be undertaken, an important aspect in vaccine design. The ability to switch domains of the lyssavirus envelope G has already been explored, highlighting its potential for use in antigenic studies (Jallet *et al.*, 1999). This will enable the level of protection afforded against other divergent lyssaviruses in phylogroup II and III to be evaluated. This is of great interest from a public health perspective due to their unknown disease burden.

Using the approach of generating a chimeric envelope glycoprotein with a VSV cytoplasmic domain resulted in high titre PV without affecting their neutralisation profile. These data also provide evidence of the flexibility pseudotyped virus-based assays provide when undertaking serological studies of highly pathogenic viruses. In conclusion, it was determined the AL RABV isolates are not likely to pose a significant public health risk because they are neutralised by available vaccines and post-exposure prophylaxis.

# **Chapter 4. Using Pseudotyped Virus to Study the Antigenicity of Phylogroup I and III Lyssaviruses by Switching Antigenic Sites of the Envelope Glycoprotein**

## **4.1. Introduction**

The *Lyssavirus* genus, which includes 14 classified species and three putative members awaiting classification, is divided into three phylogroups based on genetic and antigenic distance (Figure 1.2) (Banyard & Fooks, 2017; Dietzgen *et al.*, 2011; Evans *et al.*, 2012). Phylogroup I includes rabies virus (RABV), which is the type species for the lyssavirus genus, while phylogroup II includes Mokola virus (MOKV), Lagos bat virus (LBV) and Shimoni bat virus (SHIV). Phylogroup III comprises the most divergent lyssaviruses, with West Caucasian bat virus (WCBV) and Ikoma virus (IKOV) currently classified within this category. All current pre- and post-exposure prophylaxes are derived against live attenuated strains of classical RABV to produce inactivated human vaccines, or anti-RABV antibodies for the development of immunoglobulin treatments. Despite lyssaviruses causing an indistinguishable and invariably fatal disease, it has been demonstrated that while these prophylaxes confer protection against phylogroup I lyssaviruses, they do not effectively neutralise those within phylogroups II and III due to the antigenic distance of lyssaviruses from the vaccine strain (Brookes *et al.*, 2005; Evans *et al.*, 2012; Fooks, 2004; Hanlon *et al.*, 2005; Horton *et al.*, 2010). As most lyssaviruses seem able to cause rabies, which is invariably fatal following the onset of clinical symptoms (Johnson *et al.*, 2010a, b), it is prudent to further understand the antigenicity of the envelope glycoprotein to assist the development of more broadly neutralising prophylaxis.

The lyssavirus envelope glycoprotein is the primary surface antigen, involved in cell attachment and entry, and the target of neutralising antibodies. Antigenic sites on the envelope glycoprotein have been mapped through the use of mutagenesis and monoclonal antibodies (mAbs), identifying

both major sites (I - IV) and minor site 'a' (Benmansour *et al.*, 1991; Evans *et al.*, 2012; Kuzmina *et al.*, 2013). Alignment of these antigenic sites for different lyssavirus species, together with the genetic identity at the amino acid level in comparison to RABV, has been used to demonstrate the possibility of quantitatively predicting neutralisation efficacy (Badrane *et al.*, 2001; Evans *et al.*, 2012; Horton *et al.*, 2010). However, as the effect of individual amino acid substitutions can be unpredictable, sequence analysis should be used in combination with serology, or the higher resolution method of antigenic cartography, which has been used to build an antigenic map for a panel of lyssaviruses (Horton *et al.*, 2010). In addition to predicting neutralisation efficacy for newly discovered lyssaviruses, identifying the importance of individual antigenic sites in neutralisation is also valuable to the development of more broadly neutralising vaccine preparations. The importance of individual antigenic sites has previously been assessed using mAbs, however not by polyclonal antibodies produced in response to vaccination. The value of pseudotyped virus (PV), with the flexibility to readily manipulate the envelope glycoprotein, was first utilised to study lyssavirus antigenicity by Evans, *et al.*, (2013); producing a panel of PV with antigenic sites switched between the phylogroup I RABV and phylogroup II LBV and investigating their pattern of neutralisation by sera samples.

It is equally important to consider phylogroup III lyssaviruses in the production of broadly neutralising vaccines and antivirals. As the most divergent lyssaviruses, WCBV and IKOV share 50% or less amino acid identity with RABV and have both shown significantly reduced or no neutralisation by sera samples derived against RABV (Hanlon *et al.*, 2005; Horton *et al.*, 2014; Kuzmin *et al.*, 2005). This study looked to expand upon the approach by Evans, *et al.*, (2013), switching the antigenic sites between RABV and WCBV envelope glycoprotein and producing PV for neutralisation studies by sera samples, identifying antigenic sites of importance for these phylogroup I and III lyssaviruses.

## 4.2. Results

### 4.2.1. Antigenic Site Swapping and Pseudotyped Virus Production

The envelope glycoprotein (G) cDNA sequences of the challenge virus standard 11 (CVS-11;) isolate of rabies virus (RABV; EU352767) and the single known isolate of West Caucasian bat virus (WCBV; RUS-02; EF614258) were within a pI.18 expression plasmid, and represent lyssavirus species of phylogroups I and III respectively. Sequence alignment was carried out to identify the amino acid residues and corresponding nucleotide sequence at each of the six defined antigenic sites which differed between the species (Table 4.1). As previously highlighted (Evans *et al.*, 2012), site 'a' is conserved yet several residues differ at other sites. Notably, the glycine-cysteine (GC) sequence at position 34-35 in site IIb of the RABV sequence is almost universally conserved between phylogroups (Evans *et al.*, 2012), yet glycine is replaced by a tyrosine (Y) within the WCBV site. However, the largest universally conserved motif of leucine/isoleucine-cysteine-glycine (LCG/ICG) at position 227-229 in site I is present. To switch each of the disparate antigenic sites, individually, between the RABV and WCBV envelope glycoprotein, primers were designed (C1.18 – C1.27, Table 2.3) to undertake site directed mutagenesis of codons via SOE PCR (Section 2.2.4). Additionally, G cDNA sequences with full antigenic site swaps (FSS) were obtained via gene synthesis (GeneArt, Invitrogen). Each of the constructs produced, depicted in Figure 5.1, were cloned within the pI.18 expression plasmid and sequencing verified (Section 2.2.8).

**Table 4.1 Sequence Alignment of Rabies Virus and West Caucasian Bat Virus Envelope Glycoprotein Antigenic Sites**

Antigenic sites of the rabies virus (RABV) and West Caucasian bat virus (WCBV) lyssavirus species envelope glycoprotein (G). Amino acid sequences are numbered after removal of the signal peptide (19 amino acids), with residues that differ underlined.

Virus	Antigenic Site					
	<b>IIb</b> (34 – 42)	<b>IIa</b> (198 – 200)	<b>I</b> (226 – 231)	<b>IV</b> (263 – 264)	<b>III</b> (330 – 338)	<b>a</b> (342 – 343)
<b>RABV</b> <b>(CVS-11)</b>	GGA TGT ACC AAC CTG TCC GAG TTC TCC <u>G</u> C T <u>N</u> <u>L</u> <u>S</u> <u>E</u> <u>F</u> <u>S</u>	AAG AGA GCA K <u>R</u> <u>A</u>	AAG TTA TGT GGA GTT CTT <u>K</u> <u>L</u> C G <u>V</u> <u>L</u>	TTT CAC <u>F</u> <u>H</u>	AAG TCA GTC CGG ACC TGG AAT GAG ATC <u>K</u> <u>S</u> V <u>R</u> <u>T</u> W <u>N</u> E <u>I</u>	AAA GGG K G
<b>WCBV</b> <b>(RUS-02)</b>	TAT TGT ACA ACT GAA CAA AGC ATA ACC <u>Y</u> C T <u>T</u> <u>E</u> <u>Q</u> <u>S</u> <u>I</u> <u>T</u>	AAA CTA GTC K <u>L</u> <u>V</u>	TCA ATA TGC GGT AGG CAG <u>S</u> <u>I</u> C G <u>R</u> <u>Q</u>	ATC AAG <u>I</u> <u>K</u>	ATC AAG GTA GAG AAT TGG TCA GAG GTC <u>I</u> <u>K</u> V <u>E</u> <u>N</u> W <u>S</u> E <u>V</u>	AAA GGA K G

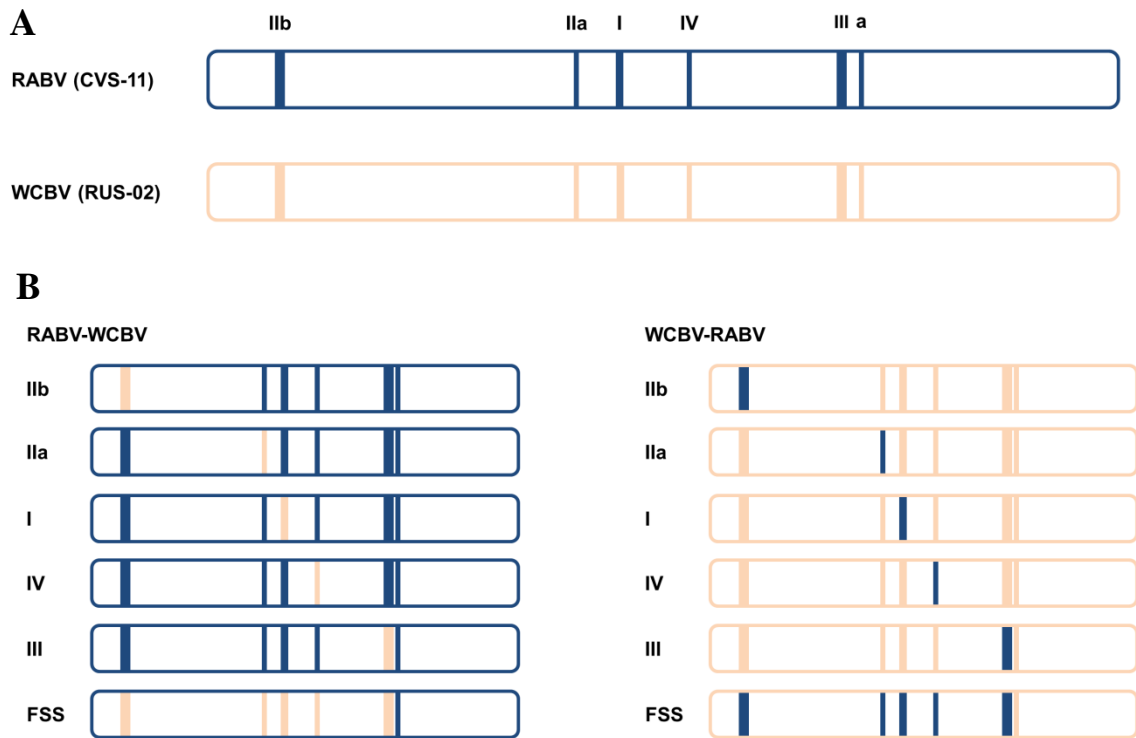


**Figure 4.1 Schematic Representation of the Antigenic Site Swapped Envelope Glycoproteins Produced**

(A) The wildtype envelope glycoproteins of the rabies virus (RABV) CVS-11 isolate and West Caucasian bat virus (WCBV) RUS-02 isolate, depicting the position of the defined antigenic sites. (B) Constructs produced switching each antigenic site individually from the RABV to WCBV sequence and vice-versa, as well as envelope glycoproteins with full antigenic site swaps (FSS).

Each of the envelope glycoprotein constructs (Figure 4.1) was used to produce lentiviral PV incorporating a firefly luciferase reporter gene by transfecting HEK 293T/17 cells (Section 2.2.10). The titre of each of the PV constructs and the TCID<sub>50</sub> was determined via a titration assay (Section 2.2.11.2) on the BHK-21 cell line. Titres were recoded as relative light units (RLU; Section 2.2.12.1) and comparisons made to determine whether switching the antigenic sites had negatively impacted PV production, which could indicate disruption to the folding of the envelope glycoprotein. Results showed that titres >10<sup>7</sup> RLU/ml were achieved for all PV produced (Figure 4.2). While some titres were reduced compared to that of PV comprising RABV and WCBV wildtype G, with the largest decrease being 6-fold for RABV-WCBV I Ib G PV and 64-fold for WCBV-RABV I Ia G PV, the titres were high enough to demonstrate the envelope glycoprotein was still functional.

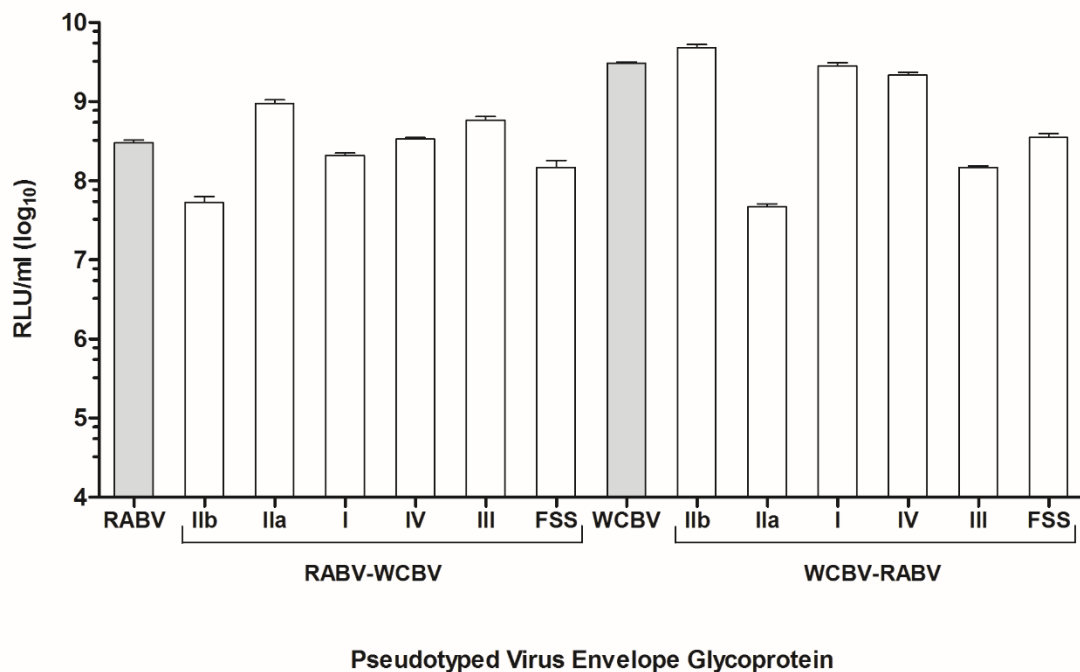


**Figure 4.2 Comparison of Titres of Pseudotyped Virus Produced Comprising Wild Type and Antigenic Site Swapped Envelope Glycoproteins**

PV with a luciferase reporter gene and comprising wildtype and antigenic site swap G, titrated on BHK-21 cells with titres calculated as relative light units per ml (RLU/ml) to determine the impact of switching the antigenic sites on PV titre. Error bars show SD (n = 4).

#### **4.2.2. Characterising Neutralisation of RABV and WCBV Antigenic Variants by Serum Samples**

The impact of switching the antigenic sites on neutralisation by serum samples was investigated via a PVNA (Section 2.2.13) with an input of 100 TCID<sub>50</sub> of PV. Samples tested included a serum sample taken from a RABV-vaccinated human (Rabipur, Novartis), which is known to afford protection against phylogroup I lyssaviruses, and had previously been assigned a titre of 17.8 IU/ml (H85) by a FAVN test, along with a sample with a titre of 0.03 IU/ml (H46) which was used as a negative due to previously finding samples with this NAb level failed to neutralise RABV G PV (Chapter 3). Further, the WHO 2<sup>nd</sup> international human anti-rabies Ig reference serum (WHO IS; prepared by NIBSC, UK), which is assigned a titre of 2 IU/ml and also known to neutralise phylogroup I lyssaviruses was used. Finally, a rabbit serum sample derived against WCBV (WCBV #827; produced by CDC) was used, which when previously tested potently neutralised the WCBV G PV (E. Wright, unpublished data). Sera were tested over a 2-fold dilution series, starting at a 1:40 dilution for the human sera (H85 & H46), a 1:20 dilution for the WHO IS and a 1:640 dilution for the WCBV serum, with IC<sub>100</sub> endpoint titres recorded.

Results showed that after switching individual antigenic sites, a significant drop in the neutralisation IC<sub>100</sub> endpoint for the RABV G PV occurred when switching site III to that of WCBV (RABV-WCBV III), with a 5.7-fold drop ( $p = 0.05$ ) in neutralisation by the H85 serum sample and a 7.9-fold drop ( $p = 0.03$ ) for the WHO IS serum (Table 4.2, Figure 4.3A). Additionally, switching antigenic site IIa caused a small 3.0 and 2.8-fold decrease in the IC<sub>100</sub> neutralisation titre by the H85 and WHO IS sera respectively. The H85 serum had a significantly reduced potency (50.7-fold,  $p < 0.0001$ ) in neutralising the RABV-WCBV FSS G PV and the WHO IS serum did not produce an IC<sub>100</sub> endpoint titre (Table 4.2, Figure 4.3A). The WCBV #827 and H46 sera did not give an IC<sub>100</sub> endpoint titre with any of the constructs.

**Table 4.2 Rabies Virus Antigenic Site Swap Pseudotyped Virus Neutralisation by Serum Samples**

Neutralisation of wildtype RABV G PV and RABV-WCBV antigenic site swap G PV reported as the reciprocal serum dilution of IC<sub>100</sub> endpoints. Serum samples known to neutralise phylogroup I lyssaviruses include a RABV vaccinated human serum sample, H85 (17.8 IU/ml), along with the WHO IS (2 IU/ml). The WCBV #827 is a rabbit serum sample that neutralises WCBV. Sample H46 (0.03 IU/ml) is from a human RABV vaccine recipient and was used as a negative control.

PV Envelope Glycoprotein	Serum Sample			
	H85	WHO IS	WCBV #827	H46 (Negative)
<b>RABV</b>	5120	453	-	-
<b>RABV - WCBV</b>				
<b>IIb</b>	3225	403	-	-
<b>IIa</b>	1810	226	-	-
<b>I</b>	8127	508	-	-
<b>IV</b>	4064	320	-	-
<b>III</b>	905	57	-	-
<b>FSS</b>	101	-	-	-

The results of individually switching the antigenic sites of the WCBV G showed that the highest drop in the IC<sub>100</sub> endpoint titre of the WCBV #827 serum occurred for the WCBV-RABV I G PV (8-fold; Table 4.3, Figure 4.3B). A drop in neutralisation potency of the WCBV #827 serum was also observed when switching antigenic sites IIb and IIa by 2.8 and 4.0-fold, respectively. Similar to the results for the RABV G, switching all the antigenic sites of the WCBV G prevented an IC<sub>100</sub> neutralisation titre from being achieved with the WCBV #827 serum; however in this case the H85 serum consequently gave an IC<sub>100</sub> titre at a low, 1:57 dilution (Table 4.3).

**Table 4.3 West Caucasian Bat Virus Antigenic Site Swap Pseudotyped Virus Neutralisation by Serum Samples**

Neutralisation of wildtype WCBV G PV and WCBV-RABV antigenic site swap G PV reported as the reciprocal serum dilution of IC<sub>100</sub> endpoints. Serum samples known to neutralise phylogroup I lyssaviruses include a RABV vaccinated human serum sample, H85 (17.8 IU/ml), along with the WHO IS (2 IU/ml). The WCBV #827 is a rabbit serum sample that neutralises WCBV. Sample H46 (0.03 IU/ml) is from a human RABV vaccine recipient and was used as a negative control

PV Envelope Glycoprotein		Serum Sample			
		H85	WHO IS	WCBV #827	H46 (Negative)
WCBV		-	-	5120	-
WCBV - RABV	IIb	-	-	1810	-
	IIa	-	-	1280	-
	I	-	-	640	-
	IV	-	-	6451	-
	III	-	-	4064	-
	FSS	57	-	-	-

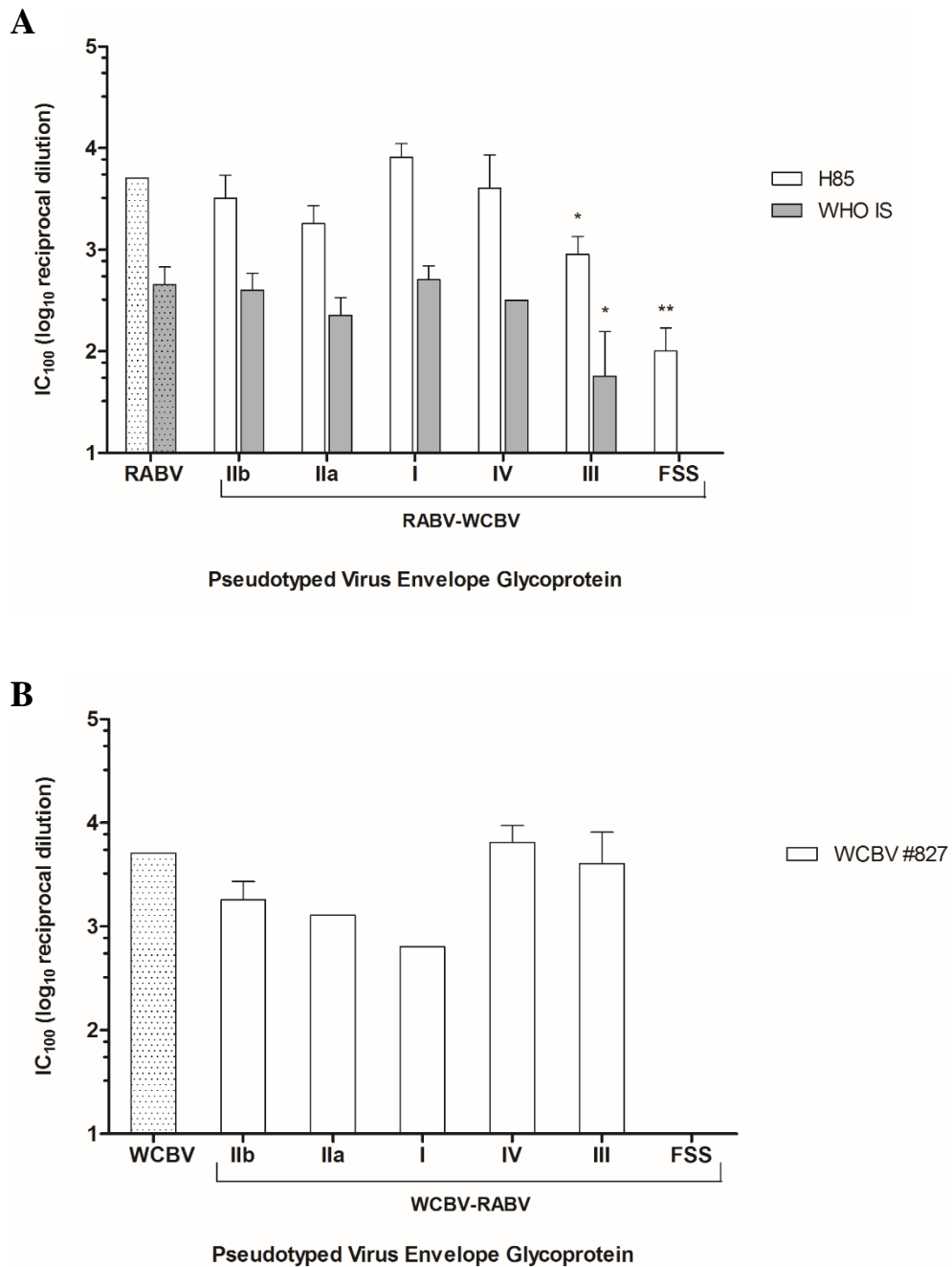


**Figure 4.3 Comparison of Serum IC<sub>100</sub> Endpoint Neutralisation of RABV and WCBV Antigenic Site Swap Glycoprotein Pseudotyped Virus**

The reciprocal serum dilution of IC<sub>100</sub> endpoints reported in Table 5.2 – 5.3 for (A) wildtype RABV G PV (dot-filled bars) and RABV-WCBV antigenic site swap G PV by the H85 and WHO IS serum samples and (B) wildtype WCBV G PV (dot-filled bars) and WCBV-RABV antigenic site swap G PV by the WCBV #827 serum sample. The WCBV-RABV FSS G PV was neutralised (IC<sub>100</sub> = 1:57) by the H85 serum sample, data not shown. \* $p \leq 0.05$  and \*\* $p < 0.0001$  by a one sample  $t$ -test comparison of antigenic site swap G PV to the respective wildtype G PV endpoint. Values are the geometric mean  $\pm$  SD, where error bars are absent, replicates produced the same endpoint and a  $t$ -test could not be performed.

### 4.3. Discussion

Current vaccines and post-exposure prophylaxis against rabies are derived against strains of the phylogroup I, RABV type species, and do not effectively neutralise more divergent lyssavirus species which have been classified within phylogroups II and III. While the true burden of non-RABV lyssaviruses is undefined due to a lack of discriminatory diagnostics and an unclear epidemiological picture, they have or are considered capable of causing the same devastating clinical disease and pose a continued threat due to the potential for spill-over events from bat reservoir species (Banyard & Fooks, 2017; Evans *et al.*, 2012; Fooks, 2004). Thus, to fully eliminate the threat of rabies it is prudent to better understand the immunological profile of divergent species, which can assist the development of broadly neutralising prophylaxis against lyssaviruses in each of the current phylogroups. The low containment level and flexibility of the pseudotype platform allows the comprehensive study of individual antigenic sites of the envelope protein through evaluation of their immunological importance in neutralisation by polyclonal sera. This study further builds upon a recent investigation into the antigenicity of phylogroup I and II lyssaviruses (Evans, *et al.*, 2013), by including a phylogroup III lyssavirus, WCBV.

While it has been shown that vaccine efficacy is likely associated with antigenic divergence from the RABV species for which they are derived, the relationship remains poorly understood. Even within phylogroup I, vaccine efficacy has been found to be reduced against some species such as Aravan and Irkut virus, although remains capable of affording protection (Brookes *et al.*, 2005; Hanlon *et al.*, 2005). Yet *in vivo* vaccine challenge experiments have shown protection is not afforded against phylogroup II (Badrane *et al.*, 2001), or the phylogroup III WCBV and IKOV (Hanlon *et al.*, 2005; Horton *et al.*, 2014). Currently phylogenetic analysis places IKOV within phylogroup III, however it has been found that no cross neutralisation occurs between WCBV and IKOV (Horton *et al.*, 2014), which supports a more complex relationship between vaccine cross protection and sequence identity. Structurally, antigenic sites are proposed to occur on exposed sites of the lyssavirus envelope glycoprotein (Buthelezi *et al.*, 2016), although structural models of RABV G are based on vesicular stomatitis virus and thus differences in antigenicity cannot be

directly linked to differences in folding. The RABV and WCBV antigenic site swap G PV in this study were produced to high titres, suggesting that function is not affected by changes which may have occurred in envelope glycoprotein folding. Using these PV antigenic variants, levels of neutralisation afforded by sera samples from vaccine recipients were measured via a PVNA.

The antigenic sites on the RABV envelope glycoprotein have been defined using mAbs and more recently by glycoprotein mutagenesis. Antigenic sites II and III were among the earliest described and a large number of mAbs are directed against these sites (Benmansour *et al.*, 1991; Kuzmina *et al.*, 2013; Lafon *et al.*, 1983). They have also previously been suggested to be most important for neutralisation of RABV (Benmansour *et al.*, 1991). Site II is a discontinuous conformational epitope, formed of two domains, IIb and IIa (Prehaud *et al.*, 1988), while site III is a continuous conformational epitope, which is considered to be part of a loop on the tertiary structure of the protein as mAb is unable to bind the unfolded protein (Benmansour *et al.*, 1991). Additionally, antigenic site III contains charged lysine (K) and arginine (R) residues at amino acid positions 330 and 333 respectively, which have a role in receptor interaction and pathogenicity (Coulon *et al.*, 1998). These two residues are not conserved within the WCBV G, however compensatory K or R residues at amino acid position 331, such as the K within the WCBV G, or at position 334 have been found to be sufficient to maintain pathogenicity (Badrane *et al.*, 2001).

Within this study, a significant drop in the potency of the anti-RABV sera was observed when antigenic site III of RABV G was replaced with that of WCBV, suggesting this site is important for neutralisation of the phylogroup I lyssavirus. Since the reciprocal swap of antigenic site III from WCBV G to RABV was not detrimental to neutralisation by the anti-WCBV serum, the same site does not have dominance in neutralisation of the phylogroup III lyssavirus. These results confer with those reported by Evans, *et al.*, (2013) which also showed site III to be important for the neutralisation of a phylogroup I lyssavirus, but similarly found it to be less important for neutralisation of the phylogroup II LBV, for which antigenic site II was immunologically dominant. Although within this study the switching of site IIa from RABV to WCBV caused a

small drop in neutralisation potency by anti-RABV sera, it was not of significance. A small drop in the IC<sub>100</sub> neutralisation titre was also observed for both sites IIb and IIa when they were switched from WCBV to RABV, which may benefit from further investigation; switching both domains to generate a WCBV-RABV site II G PV to further evaluate the importance of this antigenic site.

Antigenic site I, which is described to consist of both conformational and linear epitopes (Marissen *et al.*, 2005), was found to be immunologically dominant in the neutralisation of the phylogroup III WCBV. Work by Evans, *et al.*, (2013) found antigenic site I to be important for the neutralisation of RABV, with the site also found to be targeted by a number of mAbs and suggested to share the importance of sites II and III (Bakker *et al.*, 2005; Lafon *et al.*, 1983). Yet introducing the WCBV site I into RABV G did not cause a reduction in the potency of neutralisation by the anti-RABV sera.

Both the results of this study and that by Evans, *et al.*, (2013) have not found antigenic site IV to be immunologically dominant. Unlike the other major antigenic sites, site IV is not conformational but comprised of overlapping linear epitopes which includes amino acids 263 and 264 (Luo *et al.*, 1997) used within this study. Although other linear epitopes within this region at amino acid positions 251 and 261-262 have been defined (Bakker *et al.*, 2005; Kuzmina *et al.*, 2013).

When evaluating neutralisation against the FSS envelope glycoprotein, the sera either had a considerably reduced IC<sub>100</sub> neutralisation titre or were unable to fully neutralise the FSS G PV. As switching single antigenic sites did not cause a complete loss of neutralisation to an IC<sub>100</sub> titre, this suggests multiple antigenic sites are targeted by polyclonal sera. However, switching the antigenic sites of the RABV G to those of WCBV did not result in neutralisation by the anti-WCBV serum and only one of the anti-RABV sera were able to fully neutralise the WCBV FSS G PV. This suggests that either changing several antigenic sites causes a big change in folding so that epitopes become hidden or that regions of the envelope glycoprotein other than the defined antigenic sites are involved in neutralisation by polyclonal sera.

Employing antigenic cartography could further assist in the quantification of the immunological profile of these divergent lyssavirus species. This technique works on the basis of constructing a biological map based on data from assays measuring antigenic differences. It was first used to graphically represent binding data from the influenza haemagglutination assay which is now used by the World Health Organisation (WHO) as part of their influenza surveillance (Fouchier & Smith, 2010; Smith *et al.*, 2004). Antigenic cartography was applied to a global panel of lyssaviruses in a study by Horton, *et al.*, (2010), which among other findings demonstrated that KHUV is more closely related to RABV antigenically than phylogenetic analysis would suggest. It was further employed in the study by Evans, *et al.*, (2013) to look at the relationship between RABV, LBV, and LBV FSS G using recombinant viruses and polyclonal sera, which included a panel of sera obtained after using the antigenic site swap G PV as a vaccine immunogen. The results showed that switching all antigenic sites of the LBV G did not cause a complete phenotypic switch, with the glycoprotein instead positioned equally between RABV and LBV (E. Wright, personal communication). They also mapped the closeness of polyclonal sera to each of the viruses, to demonstrate the shift in immunogenicity caused by each antigenic site. This data supported the identification of immunologically important antigenic sites and the hypothesis that sites important for broad, cross-neutralisation may be present outside those currently mapped and known to be involved in antigenicity. Generating an antigenic map using data collected via the PVNA should be explored to allow for enhanced assessment of immunologically important sites via this low containment level, accessible platform.

In conclusion, the use of PV comprising envelope glycoprotein with antigenic sites switched between RABV and WCBV within this study allowed assessment of their neutralisation by polyclonal sera samples raised against each of these lyssavirus species. This led to the identification that antigenic site III of the RABV, phylogroup I lyssavirus, and antigenic site I of the WCBV, phylogroup III lyssavirus, are likely to be immunologically dominant. Further, it seems likely that neutralisation by polyclonal sera involves epitopes other than those identified by mAbs.

Future investigation into the importance of other antigenic sites in raising an immune response, including more divergent lyssaviruses such as IKOV and incorporating the use of antigenic cartography to assess PVNA data, will help to establish immunogens required for a broadly neutralising lyssavirus vaccine.

# Chapter 5. Optimising the Production of Filovirus Pseudotypes for Use in Serological Studies

## 5.1. Introduction

The recent outbreak of Ebola virus in West Africa, beginning in December 2013 in Guinea before spreading to neighbouring Liberia and Sierra Leone, along with imported cases in seven countries, resulted in more than 11,000 deaths and was the largest outbreak since being first isolated in 1976 (Baize *et al.*, 2014; WHO, 2016). All species within the *Ebolavirus* and *Marburgvirus* genera of the *Filoviridae* family cause haemorrhagic fever in humans and circulate within Africa, except the *Reston ebolavirus* species which is thought to be asymptomatic and reported to circulate in Filipino bat and swine populations (Baize, 2015; Barrette *et al.*, 2009). A third genera, *Cuevavirus*, was more recently described following the isolation of *Lloviu cuevavirus* from bats in a Spanish cave (Negredo *et al.*, 2011). The case fatality rate of Marburg and Ebola virus disease (M/EVD) varies between outbreaks and the causative species, with *Zaire* and *Sudan ebolavirus* outbreaks having occurred most frequently, often with fatality rates >50% (Leroy *et al.*, 2011; To *et al.*, 2015). Indeed, *Zaire ebolavirus* was the species responsible for the recent outbreak which had an estimated fatality rate of 40% (WHO, 2016). Following an exponential increase in cases and in light of the threat posed by further regional and global transmission, on 8<sup>th</sup> August 2014 the WHO declared the epidemic a public health emergency of international concern (PHEIC), with preparedness and response plans implemented globally (WHO, 2014). With no licenced vaccines or antiviral drugs available, despite the well-known public health threat ebolavirus poses, there was an unprecedented push for their fast-track development by the global public health community.

As handling live filoviruses requires biosafety level (BSL) 4 containment, the development of a pseudotyped virus neutralisation assay (PVNA) was highly valuable. It would permit widely accessible, low containment, serology studies to be undertaken to assess the efficacy of vaccines

and antivirals undergoing development and also to assist in the establishment of serological and nucleic acid standards. Further, the relatively low cost and stability of PV, which has previously been lyophilised to circumvent cold-chain storage (Mather *et al.*, 2014), means that the PVNA is applicable in the resource-limited countries where filoviruses are endemic. Whilst there were limited reports of retroviral-based filovirus PV generation prior to the recent EVD outbreak (Chan *et al.*, 2000; Simmons *et al.*, 2003a, b; Wool-Lewis & Bates, 1998), their method or components for production varied from the three plasmid retrovirus-based PV system used in these studies, for which an assay had not been established. The following study aimed to determine the optimal method for high titre filovirus PV production along with evaluating the target cell line that ensures the most consistent results in the PVNA, in response to the EVD outbreak.

## 5.2. Results

### 5.2.1. Optimal Producer and Target Cell Lines

To optimise the production of filovirus PV a panel of envelope glycoproteins (GP) were used representing each genus and species within the *Filoviridae* family (Table 5.1) and including the *Zaire ebolavirus* (EBOV) Makona isolate responsible for the recent outbreak (Baize *et al.*, 2014). This allowed any difference in PV production which could result from the diversity observed between the GP sequences of each species to be taken into account. GP identity was assessed via ClustalW sequence alignment and construction of a phylogenetic tree using the MEGA7 maximum-likelihood method, based on the JTT matrix model (Figure 5.1) (Kumar *et al.*, 2016). The GP cDNA sequences used had previously been cloned within a pCAGGS expression plasmid, which was found to offer superior PV titres in a preliminary experiment (Appendix III). So that secreted GP (sGP) could not be produced, the *Ebolavirus* and *Cuevavirus* GP sequences were derived from an edited mRNA transcript, with eight adenosines in the editing site (Sanchez *et al.*, 1996).

**Table 5.1** *Filoviridae* Isolates

Details of the genus and species of the filovirus isolates used and GenBank accession numbers for the GP sequences.

Genus	Species	Isolate	GenBank Accession Number
<i>Ebolavirus</i>	<i>Bundibugyo ebolavirus</i>	BDBV/UGA/2007	FJ217161
	<i>Reston ebolavirus</i>	RESTV/Pennsylvania/USA/1989	AY769362
	<i>Sudan ebolavirus</i>	SUDV/Boniface/SUD/1976	FJ968794
	<i>Tai Forest ebolavirus</i>	TAFV/CIV/1994	FJ217162
	<i>Zaire ebolavirus</i>	EBOV/Mayinga/COD/1976 EBOV/Makona/GIN/2014/ Kissidougou-C15	EU224440 KJ660346
<i>Cuevavirus</i>	<i>Lloviu cuevavirus</i>	LLOV/ESP/2003	JF828358
<i>Marburgvirus</i>	<i>Marburg marburgvirus</i>	RAVV/KEN/1987/KitumCave	DQ447649

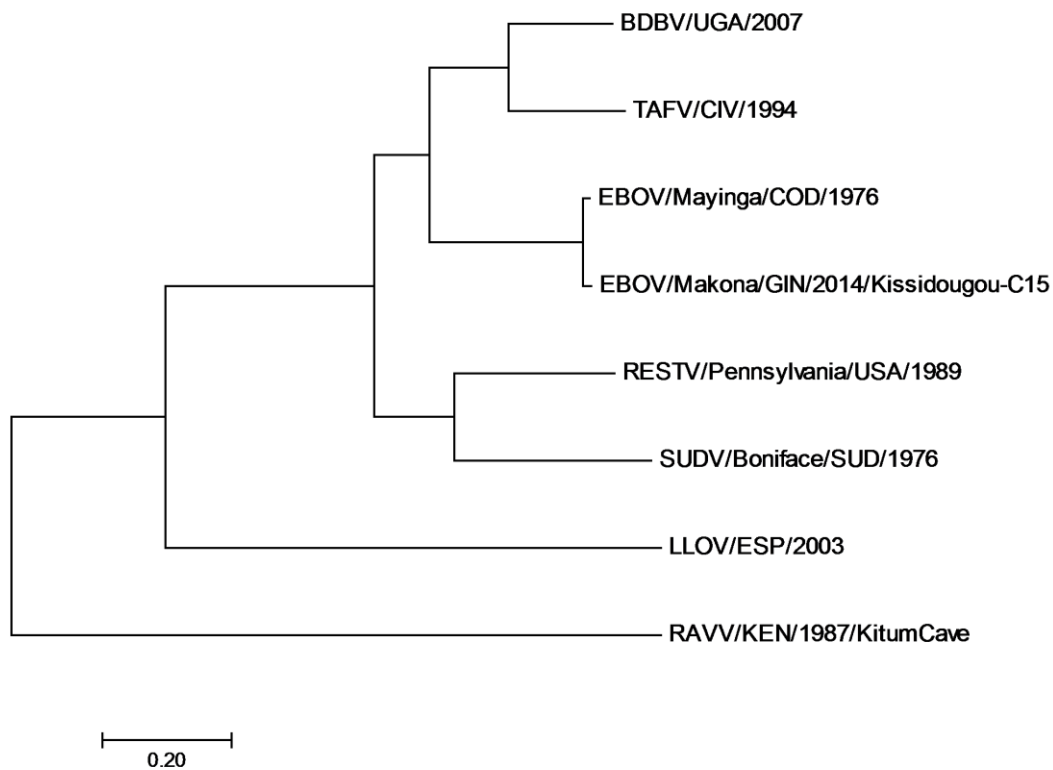


**Figure 5.1 Sequence Homology between Filovirus Envelope Glycoproteins**

Phylogenetic tree constructed using the MEGA7 maximum likelihood method, based on the JTT matrix model, following ClustalW sequence alignment of filovirus isolate envelope glycoprotein amino acid sequences. Scale corresponds to amino acid substitutions per site.

For each of the filovirus isolates, PV were produced with a gammaretroviral or lentiviral core, incorporating a firefly luciferase reporter gene, by transfecting HEK 293T/17 cells (Section 2.2.10). As a negative control a  $\Delta$ envelope PV was produced to assess background non-specific uptake, along with VSV and CVS-11 G PV as positive controls which pseudotype efficiently to give high and medium titres respectively (demonstrated in Chapter 3). To determine the cell line most permissive to infection by the gammaretroviral and lentiviral filovirus GP PV, an infection assay was performed (Section 2.2.11.1) with four replicates of 1:4 diluted PV titrated onto five different target cell lines (HEK 293T/17, A549, Vero-E6, CHO-K1, CRFK; Table 2.10). The level of infection was recorded in relative light units (RLU; Section 2.2.12.1). For PV produced with a gammaretroviral core, all filovirus GP PV except RAVV failed to infect the target cell lines or had very low infectious titres (Figure 5.2A). A cut-off of  $10^3$  RLU/ml was considered to represent the minimum titre at which a viable level of infection had taken place. The CRFK cell line was most permissive to infection by the gammaretroviral RAVV GP PV ( $3.4 \times 10^4$  RLU/ml), closely followed by the HEK 293T/17 cell line ( $3.0 \times 10^4$  RLU/ml), and the titres were in line with those of the positive control VSV and CVS-11 G PV (Figure 5.2A). However, the infectious titres for lentiviral RAVV GP PV on CRFK and HEK 293T/17 cell lines were far greater (3800 and 2000 fold, respectively), with these cell lines still being the most permissive to infection (Figure 5.2B). Viable titres were also achieved on every cell line for each of the other filovirus GP PV when using a lentiviral core, with HEK 293T/17 cells being most permissive to infection followed by CRFK and CHO-K1 cells (Figure 5.2B). From these results it was noted that GP of the *Ebolavirus* and *Cuevavirus* genus pseudotyped less efficiently than that of the *Marburgvirus* genus and also had titres lower than those of the CVS-11 G PV control. In addition, the lentiviral  $\Delta$ envelope PV titres were found to be above the threshold set to represent a viable level of infection ( $10^3$  RLU/ml). However, analysis found the titres were significantly lower ( $p \leq 0.03$ ; two-tailed  $t$ -test) than that of the filovirus GP PV with the lowest titre on each of the cell lines most permissive to infection (HEK 293T/17:  $p < 0.0001$ ; CRFK:  $p = 0.01$ ; CHO-K1:  $p = 0.03$ ).

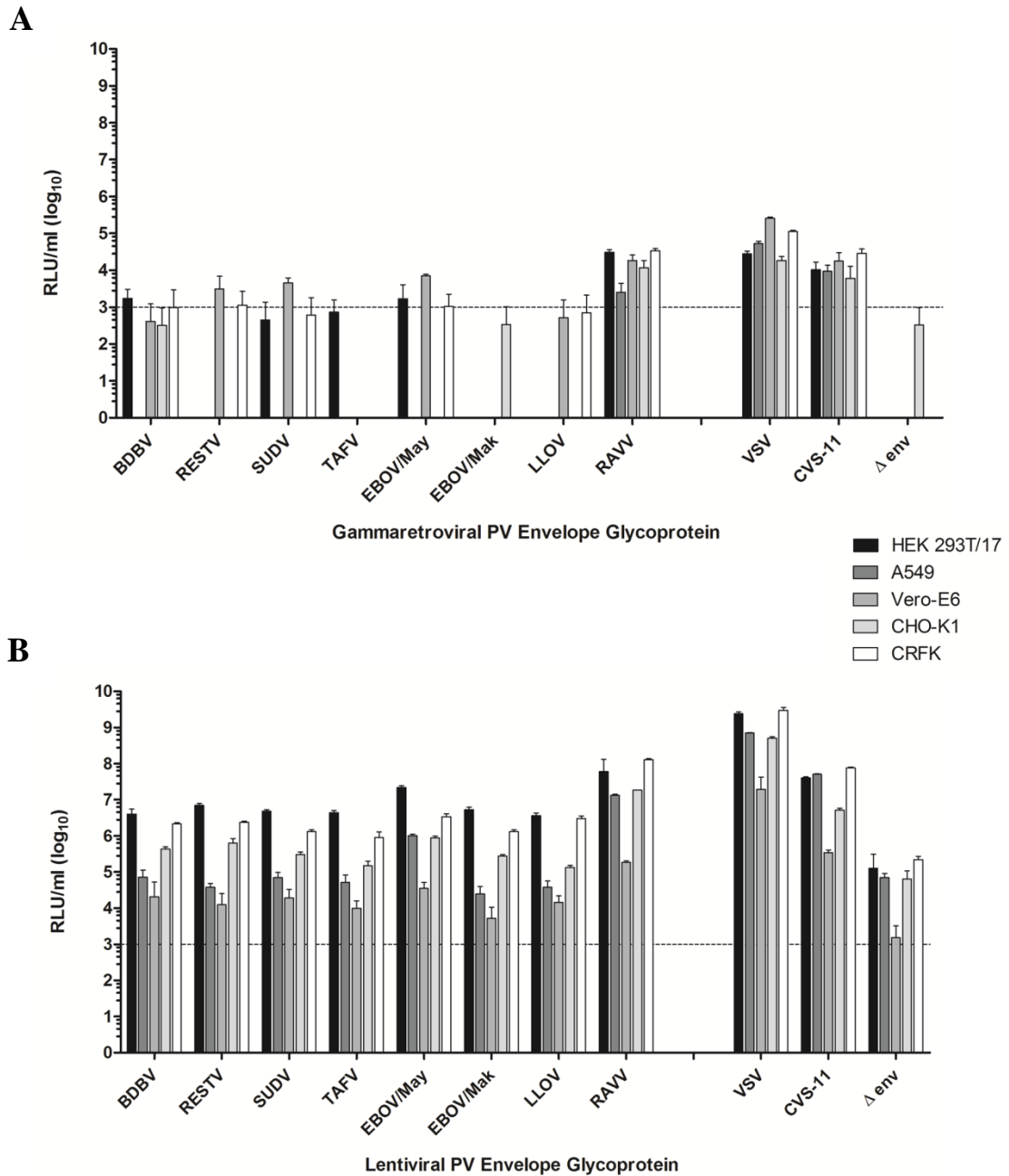


**Figure 5.2 Cell Lines Permissive to Infection by Filovirus Envelope Glycoprotein Pseudotyped Virus**

Filovirus envelope GP PV with a gammaretroviral (**A**) or lentiviral (**B**) core titrated onto five different target cell lines, with titres recorded as relative light units per ml (RLU/ml). Positive controls of VSV and CVS-11 PV are included, along with a  $\Delta$ envelope PV ( $\Delta$ env) as a control for background infection levels. A broken line at  $10^3$  RLU/ml represents the cut-off for a viable PV titre. Error bars show SD ( $n = 4$ ).

The lentiviral  $\Delta$ envelope PV titres were further evaluated to determine if they influenced which permissive cell line to use when titrating filovirus GP PV. An infection assay (Section 2.2.11.1) was performed, titrating lentiviral  $\Delta$ envelope PV in parallel to the EBOV/May GP PV on each of the three most permissive cell lines, over a 2-fold serial dilution starting at 1:4. Where  $\Delta$ envelope titres were recorded, they were considerably lower than those measured for the EBOV/May GP PV at each dilution on the HEK 293T/17 (166 – 7049 fold;  $p = 0.0005$ ), CRFK (5 – 80 fold;  $p < 0.0001$ ) and CHO-K1 (7 – 51 fold;  $p = 0.001$ ) cell lines (Figure 5.3). It was also found that for lower PV dilutions the titre of the EBOV/May GP PV remained high, yet  $\Delta$ envelope PV titres were not recorded. This highlighted that the production of high titre PV was advantageous, as lower PV input volumes into an assay would omit the potential for presence of  $\Delta$ envelope PV background titres.

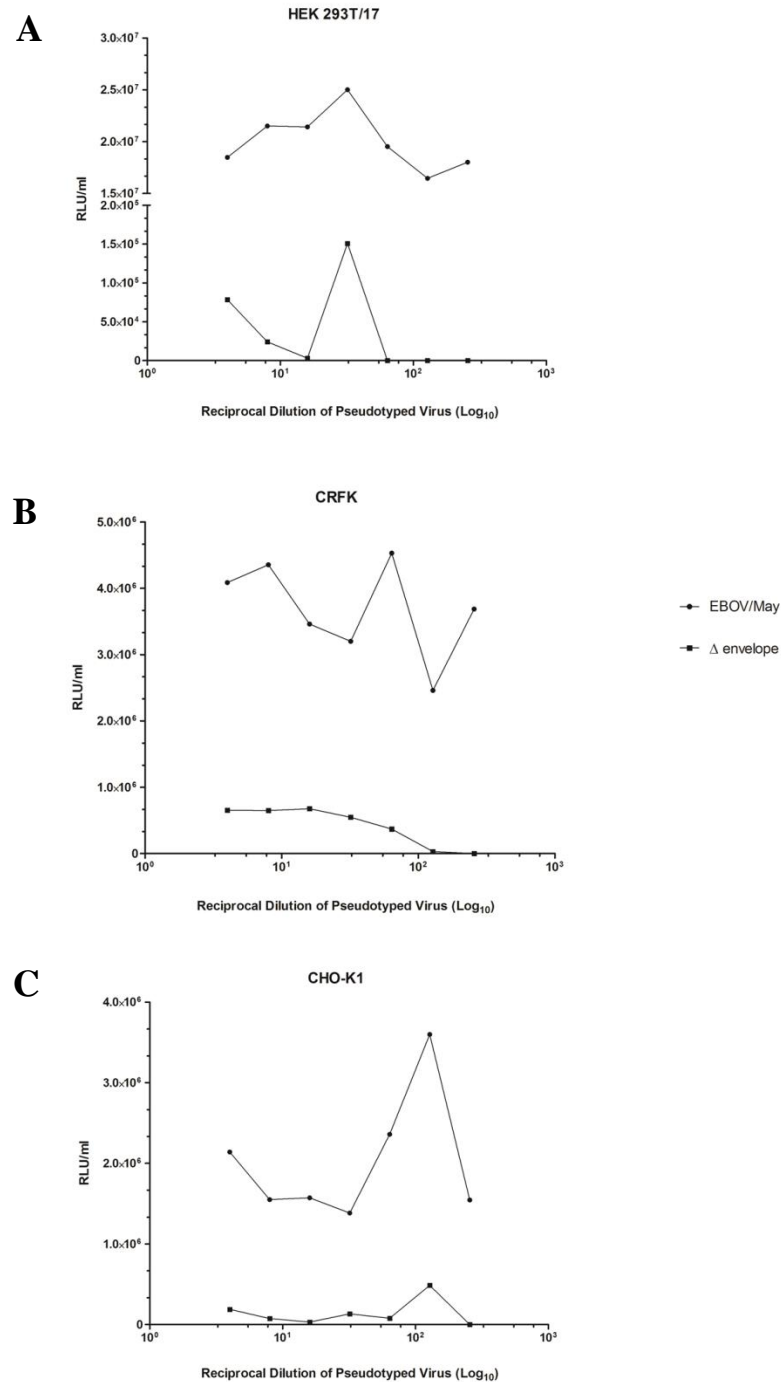


**Figure 5.3 Comparative Titration of Lentiviral Pseudotyped Virus Produced With and Without Envelope Glycoprotein on Three Cell Lines Permissive to Filovirus Infection**

Lentiviral PV produced with an EBOV/May GP was titrated in parallel to  $\Delta$ envelope PV ( $n = 2$ ) on the HEK 293T/17 (A), CRFK (B) and CHO-K1 (C) cell lines. Titres were recorded as relative light units per ml (RLU/ml). Statistical analysis of the difference between the EBOV/May GP and  $\Delta$ envelope PV titres on each cell line found they were significant ( $p \leq 0.001$ ; paired two-tail  $t$ -test).

After establishing the cell lines most permissive to filovirus GP PV infection, assessment was undertaken to determine whether there was a more efficient cell line for PV production than HEK 293T/17 cells, which are normally transfected in the pseudotype system used within this study (Temperton *et al.*, 2015b). Additionally, as HEK 293T/17 cells proved to be most permissive to infection by filovirus PV, an alternative producer cell line could alleviate potential issues such as non-specific uptake or reduced serum sensitivity in a neutralisation assay (Magre *et al.*, 2004; Voelkel *et al.*, 2012). A cell line engineered to stably express EBOV/Mak GP, E-SIAT MDCK, and the HeLa05 cell line (Table 2.10) were transfected (Section 2.2.10) alongside HEK 293T/17 cells, omitting envelope plasmid DNA for the transfection of the E-SIAT MDCK cells, to produce lentiviral EBOV/Mak GP PV with a firefly luciferase reporter gene. An infection assay, titrating onto HEK 293T/17 cells, showed transfecting both E-SIAT MDCK and HeLa05 cells had failed to produce PV (Figure 5.4).

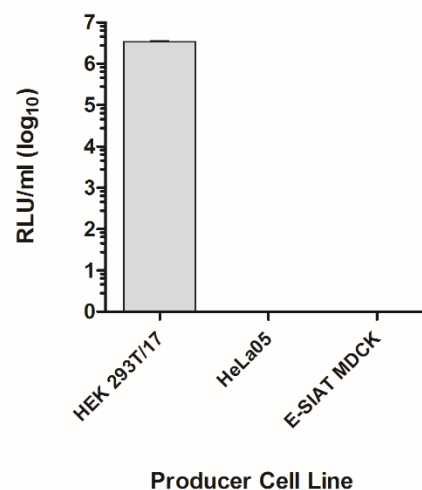


**Figure 5.4 Comparison of Cell Lines for Production of Filovirus Pseudotyped Virus**

The titres of lentiviral EBOV/Mak GP PV produced after transfection of three cell lines, HEK 293T/17, HeLa05 and E-SIAT MDCK, were tested by infection of HEK 293T/17 cells. Infectious titres were recorded as relative light units per ml (RLU/ml). Error bars show SD (n = 2).

It had been reported that lowering the quantity of envelope GP plasmid DNA used in transfections to produce an *Ebolavirus* pseudotype could increase production, while high levels of envelope GP on the PV surface can impair infectivity (Mohan *et al.*, 2015). Consequently, HEK 293T/17 cells were transfected in the 6-well format (Section 2.2.10) to produce lentiviral EBOV/May GP PV, varying the quantity of envelope plasmid DNA from the standard 0.6 µg to include three lower (0.3 µg, 0.06 µg and 0.03 µg) and two higher (1.0 µg and 2.4 µg) quantities. An infection assay, titrating onto HEK 293T/17 cells, found that each of the lower quantities of envelope plasmid DNA caused a decrease in PV titre (Figure 5.5). The decrease was significant using 0.06 µg and 0.03 µg of envelope plasmid DNA ( $p < 0.0001$ ; two-tailed *t*-test), which were in line with the quantities reported to give increased titres by Mohan *et al.* (2014). Interestingly, the highest quantity of envelope plasmid DNA used resulted in a significant, 1.5 fold, increase in PV titre ( $p = 0.0004$ ; two-tailed *t*-test) (Figure 5.5). However, the quantity of envelope plasmid DNA used in transfections for this study was not altered due to the low magnitude of the increase and concerns over the comparatively large quantity of DNA in the transfection which can cause cytotoxicity, although none was observed. Further, the morphology of EBOV/May GP PV produced using this transfection method was as expected, with a good covering of envelope GP visible, when assessed via electron microscopy as part of a collaboration (Appendix III).

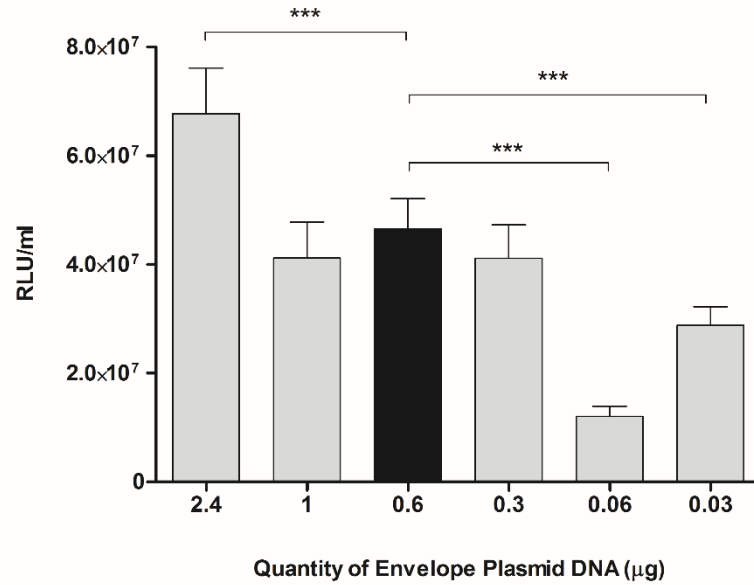


**Figure 5.5 Production of Pseudotyped Virus after Transfecting with Different Quantities of Envelope Plasmid DNA**

Titres of EBOV/May GP PV, measured by infecting HEK 293T/17 cells, following transfection using different quantities of envelope GP plasmid DNA in comparison to the standard 0.6 µg normally used. Titres are measured in relative light units per ml (RLU/ml) (\*\*\*)  $p \leq 0.0004$ ; two-tailed  $t$ -test). Error bars show SD (n = 6).

### 5.2.2. Chimeric and Truncated *Ebolavirus* Envelope Glycoprotein Construction

The lentiviral PV produced with an *Ebolavirus* GP was found to have titres lower than both *Marburgvirus* GP PV and the control CVS-11 G PV, thus requiring larger volumes be produced to perform downstream assays. As it had previously been proven that switching a RABV envelope G cytoplasmic domain to that of VSV could increase PV titres (Chapter 3), this approach was investigated for its application to the production of *Ebolavirus* GP PV. Chimeric envelope GP was generated for the SUDV, EBOV/May and EBOV/Mak isolates, covering two *Ebolavirus* species (Table 5.1). The cytoplasmic domain of the three isolate's GP was replaced with that of the VSV G using SOE PCR (Section 2.2.4) and primers designed (C2.15 – 2.17; Table 2.4) based on mapping the *Ebolavirus* GP cytoplasmic domain to amino acids 672 – 677 (UniProt: Q05320), with the VSV G cytoplasmic domain mapped to amino acids 483 – 512. As the RAVV isolate of the *Marburgvirus* genus had pseudotyped efficiently in this study, chimeric envelope GP was also produced with a RAVV GP cytoplasmic domain using primers (C2.7 – 2.9; Table 2.4) designed for standard PCR (Section 2.2.3) owing to the short length of the *Marburgvirus* cytoplasmic domain which spans amino acids 674 – 682 (Mittler *et al.*, 2013). Finally, as it had been reported that truncation of the envelope protein cytoplasmic domain could increase MeV PV titre (Frecha *et al.*, 2008), primers were designed (C2.10 – 2.12; Table 2.4) to remove the cytoplasmic domain of the envelope GP. The constructs produced are depicted in Figure 5.6 and were each cloned into the pCAGGS expression plasmid and sequencing verified (Section 2.2.8).

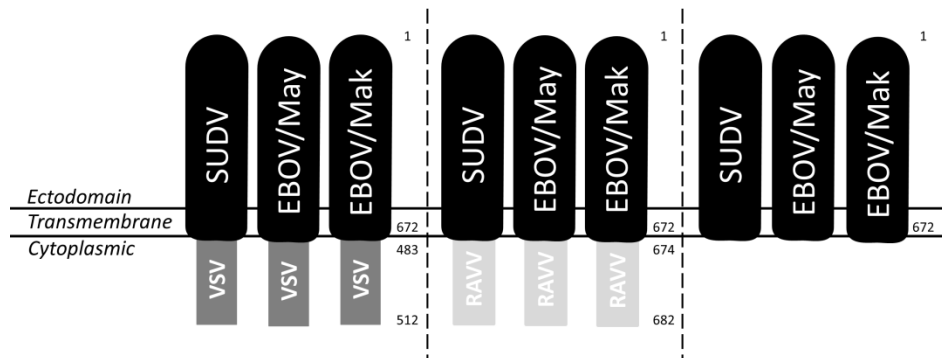


**Figure 5.6 Schematic Representation of Chimeric and Truncated *Ebolavirus* Envelope Glycoprotein Constructs**

The chimeric envelope glycoprotein constructs produced by switching or removing the cytoplasmic domain are depicted. Numbers represent the amino acids of the respective full length glycoprotein for the *Ebolavirus* ecto-transmembrane domain and VSV or RAVV cytoplasmic domain.

Lentiviral PV with a firefly luciferase reporter gene was produced comprising each of the chimeric and truncated GP constructs, alongside wildtype SUDV, EBOV/May and EBOV/Mak GP, by transfection of HEK 293T/17 cells (Section 2.2.10). To determine whether the chimeric or truncated GP had increased PV titre, an infection assay was set up (Section 2.2.11.1) titrating onto HEK 293T/17 cells. It was found that all chimeric and truncated GP, except the chimeric SUDV GP with a RAVV cytoplasmic domain (SUDV<sub>etm</sub>RAVV<sub>c</sub>), caused a substantial or complete loss in PV titre in comparison to their respective wildtype GP PV (Figure 5.7). The chimeric SUDV<sub>etm</sub>RAVV<sub>c</sub> GP PV gave a 28% (1.4 fold) increase in PV titre relative to wildtype SUDV GP PV, yet had a high level of variance ( $28.1 \pm 36.2$  %; mean  $\pm$  SD). While there was instead a loss in PV titre, this high level of variance was shared by the chimeric EBOV GP isolates with a RAVV cytoplasmic domain (EBOV/May  $-52.4 \pm 19.6$  %; EBOV/Mak  $-33.0 \pm 40.0$  %). Overall, the use of a chimeric GP with a RAVV cytoplasmic domain did not prove to be an efficient method of increasing *Ebolavirus* PV titres.

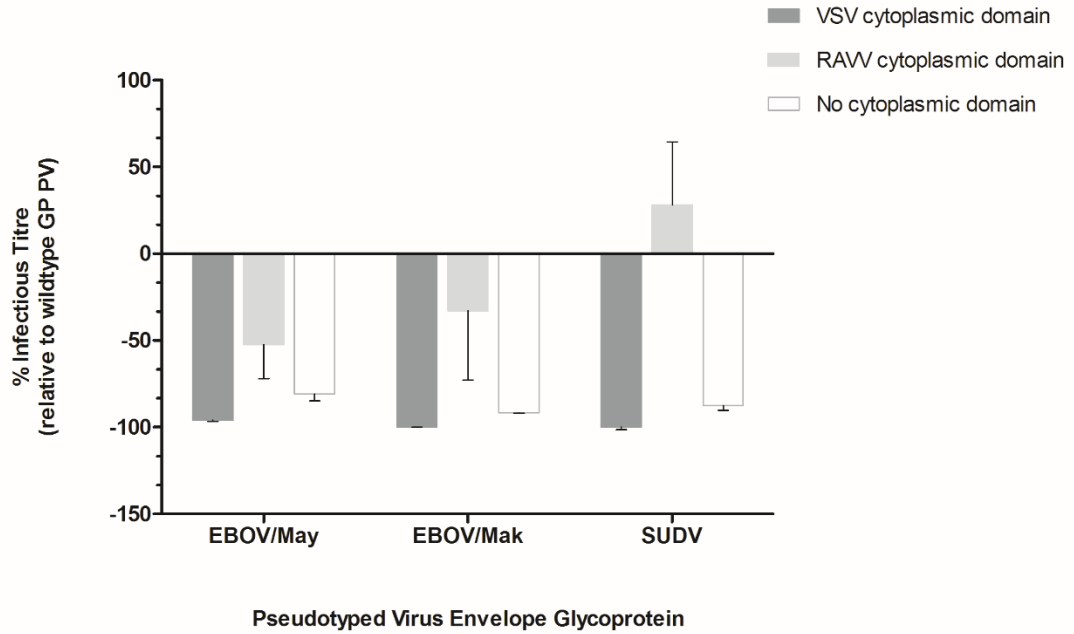


**Figure 5.7 Percentage Change in *Ebolavirus* Pseudotyped Virus Titre using a Chimeric or Truncated Envelope Glycoprotein**

Lentiviral PV with wildtype (SUDV, EBOV/May or EBOV/Mak) envelope GP was titrated onto HEK 293T/17 cells in parallel to a corresponding PV with either a truncated GP or a chimeric VSV or RAVV cytoplasmic domain GP. Titres were measured in relative light units (RLU) and the percentage change relative to PV with wildtype GP calculated. Error bars show SD (n = 6).

A further attempt to increase the titre of *Ebolavirus* PV using a chimeric envelope GP was made, using envelope fusion proteins of the same class. Two class I fusion proteins, an influenza virus haemagglutinin (HA) (A/Vietnam/1194/2004(H5N1); ABP51976) which had previously pseudotyped efficiently (Molesti *et al.*, 2014b) and the human immunodeficiency virus (HIV) gp160 envelope protein (type 1 HXB2; K03455) were used. Chimeric SUDV and EBOV/Mak GP with a HA cytoplasmic domain was produced by standard PCR (Section 2.2.3) using primers designed (C2.13 – 2.14; Table 2.4) based on the HA cytoplasmic domain spanning amino acids 577 – 569 (Scolari *et al.*, 2016) (UniProt: P03459). The chimeric SUDV and EBOV/Mak GP with a HIV cytoplasmic domain was produced via SOE PCR (Section 2.2.4), with primers designed (C2.18 – 2.19; Table 2.4) mapping the cytoplasmic domain to amino acids 706 – 857 (UniProt:

P04578). The constructs are depicted in Figure 5.8 and as before were each cloned into the pCAGGS expression plasmid and sequencing verified (Section 2.2.8).

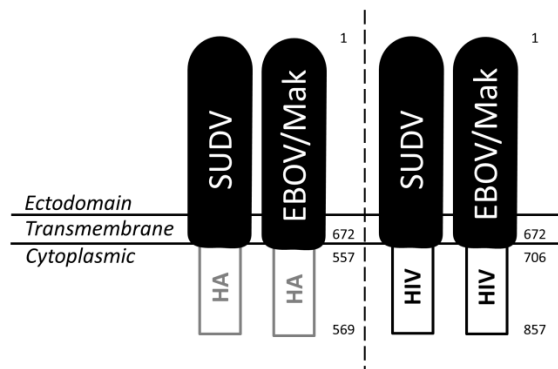


**Figure 5.8 Schematic Representation of Chimeric *Ebolavirus* Envelope Glycoprotein Constructs with a HA or HIV Cytoplasmic Domain**

The chimeric envelope glycoprotein constructs produced by switching or removing the cytoplasmic domain are depicted. Numbers represent the amino acids of the respective full length glycoprotein for the *Ebolavirus* ecto-transmembrane domain and HA or HIV cytoplasmic domain.

As before, lentiviral PV with a firefly luciferase reporter gene was produced comprising each of the chimeric and truncated GP constructs, alongside wildtype SUDV and EBOV/Mak GP, by transfection (Section 2.2.10). Following an infection assay (Section 2.2.11.1), it was found that both chimeric envelope GP with a HA and HIV cytoplasmic domain failed to increased *Ebolavirus* PV titres (Figure 5.9). The use of a chimeric HIV cytoplasmic domain GP caused a complete loss in PV titre for both the SUDV and EBOV/Mak GP.

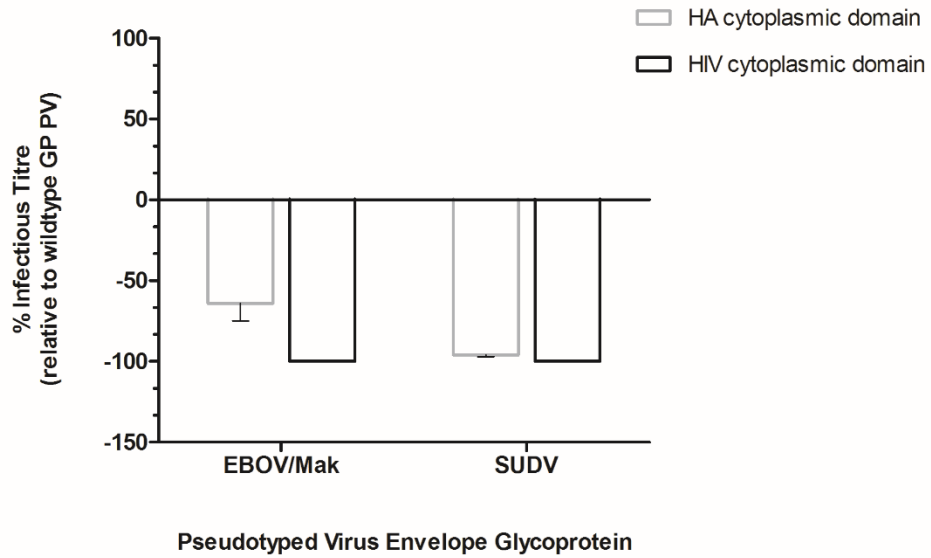


**Figure 5.9** Percentage Change in *Ebolavirus* Pseudotyped Virus Titre using a Chimeric Envelope Glycoprotein with a HA or HIV Cytoplasmic Domain

Lentiviral PV with wildtype (SUDV or EBOV/Mak) envelope GP was titrated onto HEK 293T/17 cells in parallel to a corresponding PV with a chimeric HA or HIV cytoplasmic domain GP. Titres were measured in relative light units (RLU) and the percentage change relative to PV with wildtype GP calculated. Error bars show SD (n = 6).

### **5.2.3. Influence of Target Cell Line on *Ebolavirus* Pseudotyped Virus Serology Studies**

As attempts to increase the titre of the *Ebolavirus* PV were not successful and thus larger input volumes, compared to other virus families, would be required for serology studies; a PVNA was initially performed to assess the behaviour of lentiviral  $\Delta$ envelope PV, continuing the analysis in Section 4.2.1 (Figure 5.3). The PVNA was set up (Section 2.2.13) to test the EBOV/May GP PV alongside  $\Delta$ envelope PV using a potent mAb, EVB114 (Corti *et al.*, 2016), over a 2-fold serial dilution with a starting concentration of 50  $\mu$ g/mL and using HEK 293T/17 cells as the target cell line. An input of 12.5  $\mu$ L of PV was used, equating to a 1:16 dilution. PV infection controls were included to measure infectivity in the absence of mAb. Results recorded as RLU following incubation showed that the EBOV/May GP PV titre decreased with an increasing concentration of the EVB114 mAb sample and was below that of the infection control (Figure 5.10). The  $\Delta$ envelope PV titre did not share the same correlation and had a higher level of infectivity than the infection control at several points, including the two highest concentrations of EVB114 (Figure 5.10). This showed that  $\Delta$ envelope PV was not neutralised and thus would not interfere with the serological assessment of samples via the PVNA.

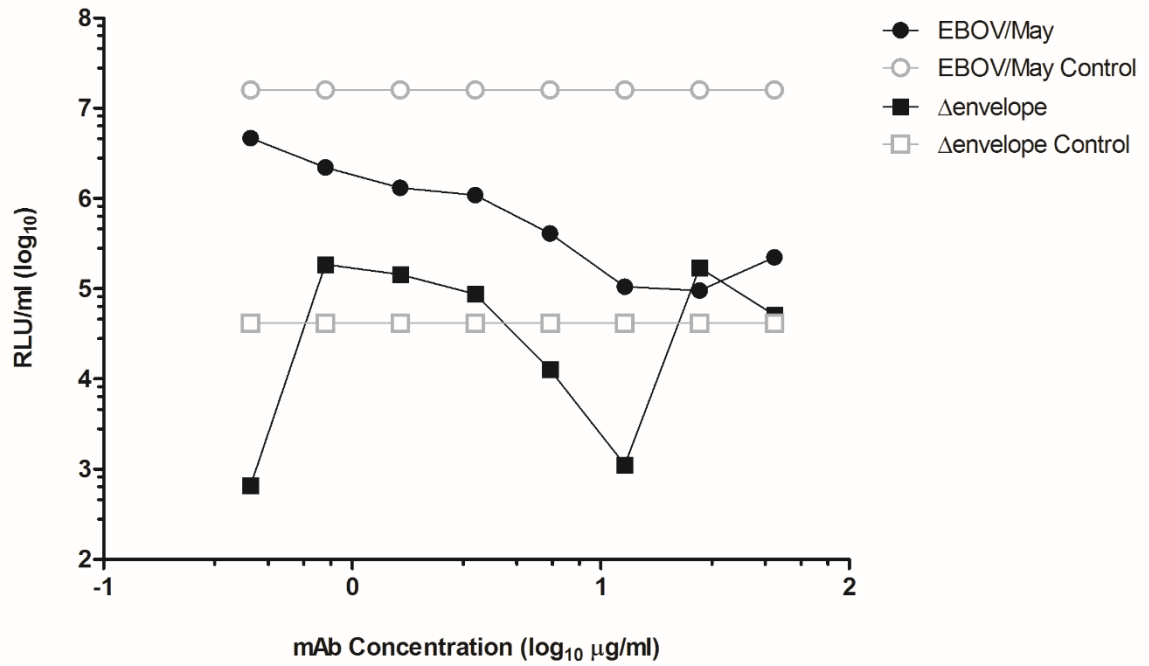


**Figure 5.10 Assessment of the Neutralisation of Lentiviral Pseudotyped Virus with and without Envelope Glycoprotein**

Neutralisation of lentiviral EBOV/May GP PV compared to that of a Δenvelope PV by the EVB114 mAb sample, titrating on HEK 293T/17 cells. EVB114 was tested at a starting concentration of 50 µg/ml. Values are reported as average relative light units per ml (RLU/ml) (n = 2). Data points for each PV infection control represent the average of four replicates of PV incubated without mAb.

To evaluate whether the target cell line influenced the collection of *Ebolavirus* PV neutralisation data, which could prove detrimental in the evaluation of antivirals and prophylaxis, a PVNA (Section 2.2.13) was performed using the three target cell lines found to be most permissive to infection (HEK 293T/17, CRFK and CHO-K1). Lentiviral EBOV/Mak GP PV was used, with an input of 50 TCID<sub>50</sub> for each cell line determined via a titration assay (Section 2.2.11.2). Three mAb samples, KZ52 (Lee *et al.*, 2008b), P6 (Dr A. Townsend, University of Oxford) and EVB114 (Corti *et al.*, 2016), were tested in parallel for neutralisation of the EBOV/Mak PV on each of the cell lines over a 2-fold serial dilution, with a starting concentration of 20 µg/mL for P6 and 40 µg/mL for each of the other mAb samples. A mAb derived against RABV, RVB492 (De Benedictis *et al.*, 2016), was used as a negative control, with a starting concentration of 40 µg/mL. PV infection controls were included by titrating the EBOV/Mak GP PV onto each of the cell lines without the addition of mAb, and used to calculate percentage neutralisation. Results showed that neutralisation with the EVB114 mAb sample produced a similar dose-response pattern on each of the target cell lines (Figure 5.11). The neutralisation data for the KZ52 and P6 mAb samples did not produce a smooth dose-response on the CRFK cell line (Figure 5.11B). To aid the comparison, IC<sub>50</sub> endpoint values were extrapolated via regression analysis, for which a value could not be determined for the KZ52 mAb on the CRFK cell line (Table 5.2). The dose-response pattern on both the HEK 293T/17 and CHO-K1 cell lines allowed extrapolation of IC<sub>50</sub> values (Table 5.2). However, as the data was cleanest on the CHO-K1 cell line (Figure 5.11C) this was considered the preferable target cell line to use for neutralisation assays.

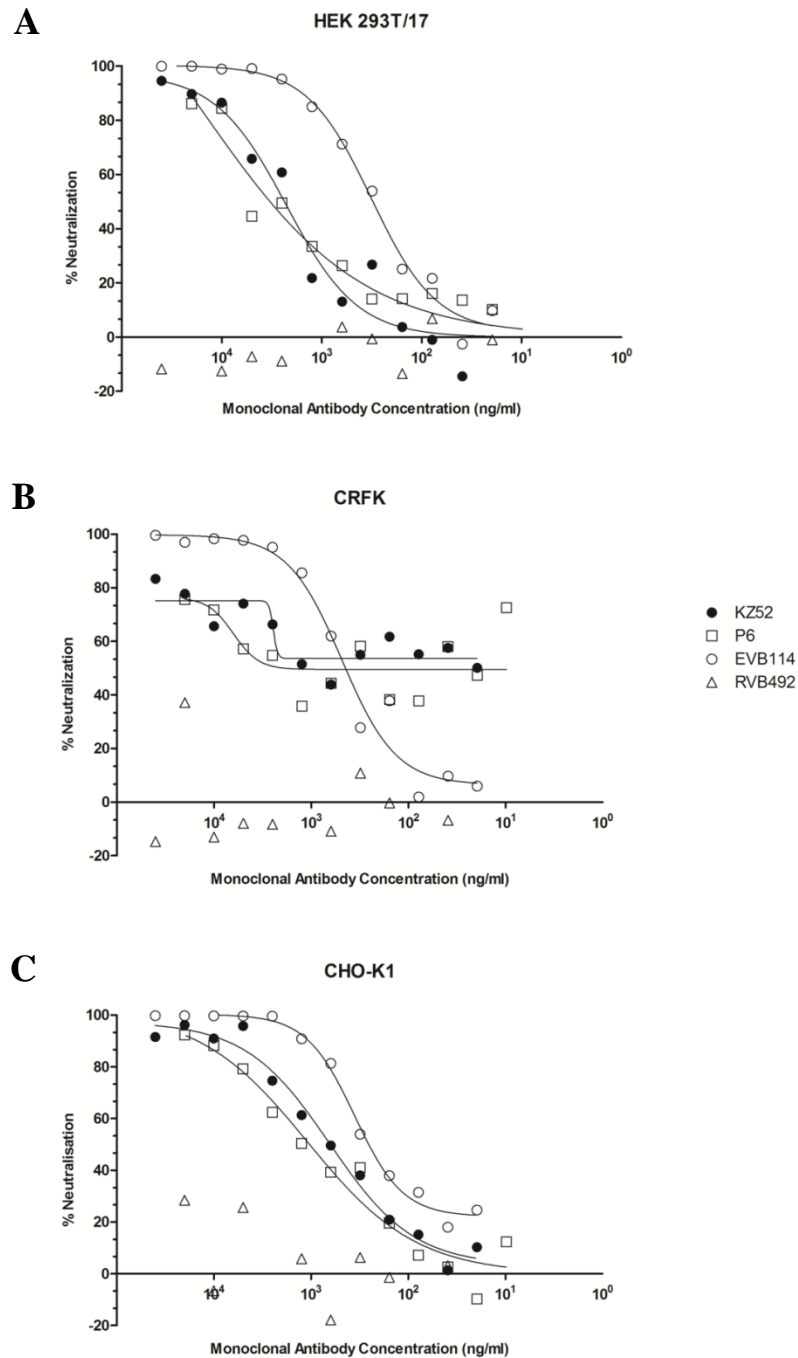


**Figure 5.11 Comparison of *Ebolavirus* Pseudotyped Virus Neutralisation by Monoclonal Antibody Samples on Three Target Cell Lines**

The percentage neutralisation of lentiviral EBOV/Mak GP PV by the monoclonal antibody samples KZ52, P6 and EVB114 was measured by comparison to a PV infection control on three target cell lines, HEK 293T/17 (A), CRFK (B) and CHO-K1 (C). Non-linear regression analysis ( $\text{Log}_{10}[\text{inhibitor}]$  vs. response) was performed, constraining the bottom value to be  $> 0\%$ . Data points are plotted for the RVB492 negative control mAb sample. ( $n = 2$ )

**Table 5.2 Neutralisation IC<sub>50</sub> Endpoint Titres of Monoclonal Antibody Samples Measured by Pseudotyped Virus Neutralisation Assay on Three Target Cell Lines**

The IC<sub>50</sub> endpoint values (ng/mL) for neutralisation of EBOV/Mak GP PV via three monoclonal antibody samples, on three target cell lines, were calculated via extrapolation from non-linear regression analysis (Log<sub>10</sub>[inhibitor] vs. response). Where the IC<sub>50</sub> endpoint could not be extrapolated, values are absent (-).

<b>Monoclonal Antibody IC<sub>50</sub> Endpoint Titre (ng/mL)</b>			
<b>Cell Line</b>	<b>KZ52</b>	<b>P6</b>	<b>EVB114</b>
<b>HEK 293T/17</b>	2360.5	3288.5	306.9
<b>CRFK</b>	-	1905.5	443.6
<b>CHO-K1</b>	632.4	1032.8	254.7

A further PVNA was performed using serum samples to assess whether the neutralisation pattern on each of the target cell lines corresponded with that found when testing the mAb samples. As before, lentiviral EBOV/Mak GP PV was used with an input of 50 TCID<sub>50</sub> for each cell line. Three serum samples were tested, which included the human convalescent plasma sample (H79; WHO anti-EBOV reference reagent) and a transchromosomal bovine sample (B31), included in a collaborative study coordinated by NIBSC (Wilkinson *et al.*, 2017), along with the transchromosomal ovine serum sample S4 (Dr T. Lambe, Jenner Institute). The samples were tested in parallel over a 2-fold serial dilution, from a starting dilution of 1:50 for the H79 and B31 sample and a 1:20 dilution for the S4 sample. A negative control serum (N36), which was also included in the NIBSC collaborative study (Wilkinson *et al.*, 2017), was used at a starting dilution of 1:50. PV infection controls were again used to calculate percentage neutralisation at each dilution of the serum samples. Due to the lower potency of the serum samples in comparison to the mAb preparations, the neutralisation data was generally less clear (Figure 5.12). A low level of neutralisation was observed for the negative serum sample N36, following the findings of the collaborative study (Wilkinson *et al.*, 2017). Overall, the position of the data points and dose response pattern was similar on the HEK 293T/17 and CRFK cell lines (Figure 5.12A and B). Low levels of neutralisation (< 50%) for some samples on these cell lines meant IC<sub>50</sub> values could only be extrapolated via regression analysis for a single serum sample on each, S4 and H79 respectively (Table 5.3). In comparison, the serum neutralisation data on the CHO-K1 cell line (Figure 5.12C) allowed IC<sub>50</sub> values to be extrapolated for each serum sample (Table 5.3), which further suggested this cell line may be more appropriate for use in the ebolavirus PVNA.

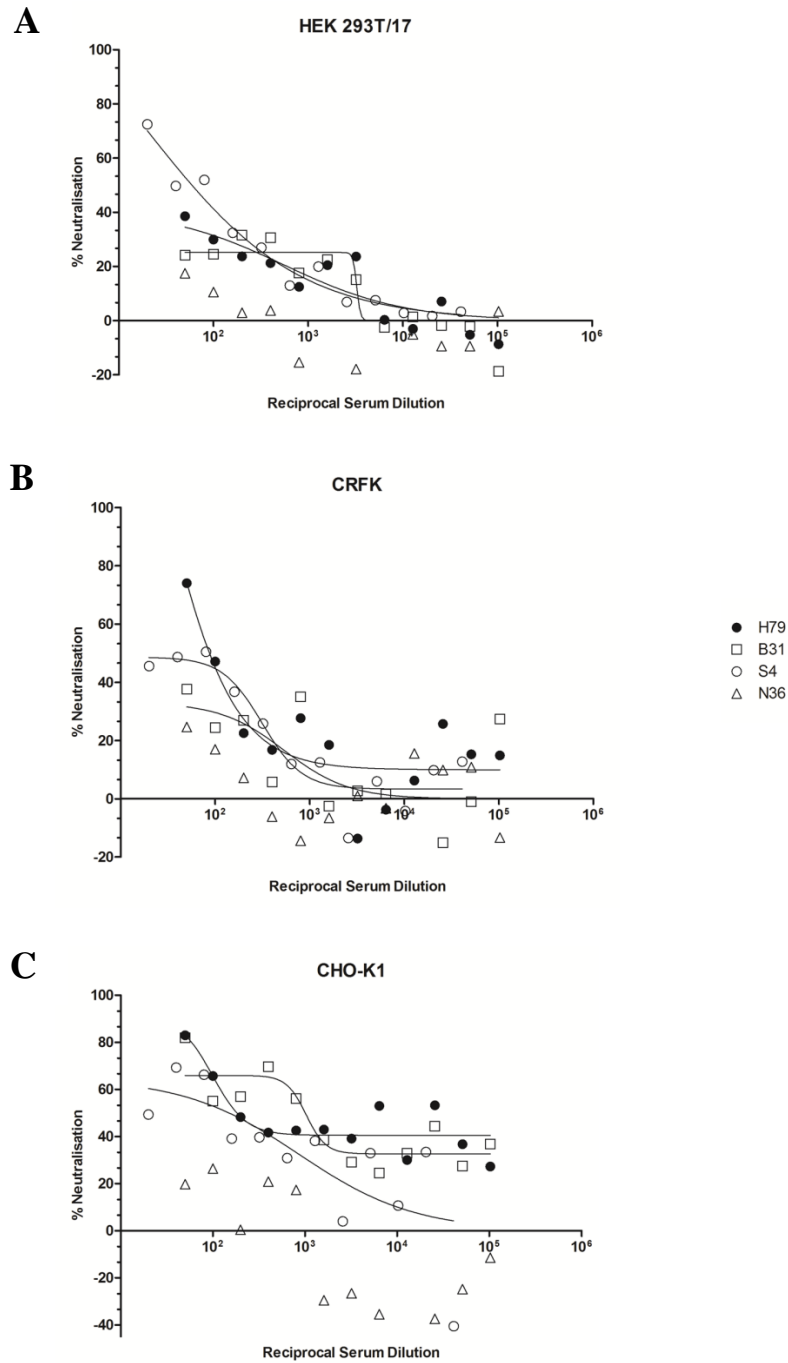


**Figure 5.12 Comparison of *Ebolavirus* Pseudotyped Virus Neutralisation by Serum Samples on Three Target Cell Lines**

The percentage neutralisation of lentiviral EBOV/Mak GP PV by the serum samples H79, B31 and S4 was measured by comparison to a control without the addition of sera on three target cell lines, HEK 293T/17 (A), CRFK (B) and CHO-K1 (C). Non-linear regression analysis ( $\text{Log}_{10}[\text{inhibitor}]$  vs. response) was performed, constraining the bottom value to be  $> 0\%$ . Data points are plotted for the N36 negative control sera sample. ( $n = 2$ )

**Table 5.3 Neutralisation IC<sub>50</sub> Endpoint Titres of Serum Samples Measured by Pseudotyped Virus Neutralisation Assay on Three Target Cell Lines**

The IC<sub>50</sub> endpoint values (reciprocal serum dilution) for neutralisation of EBOV/Mak GP PV via three serum samples, on three target cell lines, were calculated via extrapolation from non-linear regression analysis (Log<sub>10</sub>[inhibitor] vs. response). Where the IC<sub>50</sub> endpoint could not be extrapolated, values are absent (-).

Cell Line	Serum Sample IC <sub>50</sub> Endpoint Titre (reciprocal serum dilution)		
	H79	B31	S4
HEK 293T/17	-	-	59.2
CRFK	86.9	-	-
CHO-K1	182.2	1004.7	149.3

### 5.3. Discussion

The ability to rapidly develop PV, enabling highly pathogenic viruses to be handled in low containment laboratories, makes them an excellent tool to respond to emerging virus outbreaks, particularly those which pose a significant public health threat such as the recent EVD outbreak. The three plasmid transfection protocol for PV production using a retroviral core is highly successful, having been used in the development of PV for many zoonotic virus families (Temperton *et al.*, 2015b). Serology studies undertaken via a PVNA allow the inhibition of viral infectivity to be measured and are a valuable tool in the development of efficacious vaccines and antivirals. This study optimised the production of filovirus PV and its use in the PVNA, demonstrating how PV can rapidly be developed in response to an emerging virus outbreak, allowing their application to the development of efficacious vaccines and antivirals along with being applicable in the resource-limited countries where the filovirus species responsible for causing EVD circulate.

The target cell line chosen for infection assays can greatly influence the titre of PV due to a difference in the density of cell surface receptors required for transduction. Previous studies utilizing a filovirus PV have shown that while lymphoid cells are resistant to filovirus infection, they otherwise have a broad host range; infecting cells derived from different species and tissues (Chan *et al.*, 2000; Ito *et al.*, 2001; Takada, 2012; Wool-Lewis & Bates, 1998). Like many enveloped viruses, filoviruses require endocytosis to infect cells, however it is thought to occur primarily via macropinocytosis, with initial uptake occurring after a relatively non-specific interaction between host cell receptors for viral membrane phosphatidylserine and a viral GP-dependent interaction with host cell lectin receptors, expressed on a range of cell types (Moller-Tank & Maury, 2015; Nanbo *et al.*, 2010; Pöhlmann, 2013; Saeed *et al.*, 2010). Crucially, filovirus exit from the late endosome is triggered by the GP receptor binding domain, exposed following proteolytic processing by endosomal cathepsin proteases, interacting with the ubiquitously expressed fusion receptor Niemann-Pick C1 (NPC1) (Côté *et al.*, 2011; Kuroda *et al.*, 2015; Miller *et al.*, 2012; Moller-Tank & Maury, 2015). This distinct and relatively non-specific pathway is

thought to account for the wide host cell range. In this study, the highest titres of lentiviral core *Ebolavirus* PV were achieved using HEK 239T/17 cells, which were previously reported to be highly permissive to filovirus infection and had been used as target cells in pseudotyping assays (Simmons *et al.*, 2003b; Wool-Lewis & Bates, 1998). While the Vero-E6 primate cell line is commonly used to propagate wildtype filovirus due to its high permissibility (Ito *et al.*, 2001; Takada, 2012), it is not permissive to infection with lentiviral PV owing to having an intrinsic restriction factor, TRIM5 $\alpha$ , which inhibits un-coating of the genome and targets the HIV-based core for degradation (Stremlau *et al.*, 2004). Using a gammaretroviral core to overcome this was not successful. While commonly used for pseudotyping it can only infect proliferating cells, unlike lentivirus, which is detrimental to the level of transduction of target cells (Maetzig *et al.*, 2011; Temperton *et al.*, 2015b).

The infectious titres observed with  $\Delta$ envelope PV preparations are a common artifact and not cause for concern. It is thought the mechanism behind this apparent non-specific infection is accounted for by a combination of passive transfer of reporter protein trapped within the  $\Delta$ envelope PV particles (Nash & Lever, 2004), which can bind in an envelope-independent manner to the surface proteins and carbohydrate of target cells (Pizzato *et al.*, 1999; Sharma *et al.*, 2000), as well as being internalized via endocytosis (Voelkel *et al.*, 2012). Due to the high sensitivity and enzymatic nature of the luciferase assay, a small quantity of passively transferred luciferase protein is likely capable of producing the relatively high luminescence signals seen within this study. Using an alternative reporter gene with lower sensitivity, such as GFP or the *lacZ* gene, may give lower  $\Delta$ envelope PV titres. In this study it was shown that decreasing the input volume of PV into an assay caused  $\Delta$ envelope PV titres to diminish, indicating an advantage to the production of high titre PV stocks. It is also likely that a lower amount of  $\Delta$ envelope PV is produced when an envelope protein is included in transfections. Further, the  $\Delta$ envelope PV was not neutralised in the PVNA, ultimately mitigating concerns.

Generation of PV by transient transfection of HEK 293T/17 cells is widely used and highly efficient. However, using the same cell line for both production and infection studies should be avoided if possible. As retroviral-based PV bud from the producer cell, their plasma membrane forms the outer viral membrane and incorporates membrane proteins. This could lead to an increase in non-specific binding and uptake as discussed above for  $\Delta$ envelope PV, or alter sensitivity to human serum from the combination of human complement receptors on the viral surface (Magre *et al.*, 2004; Takeuchi *et al.*, 1996). The use of alternative transfection cells, such as found using HeLa cells within this study, is unlikely to lead to higher PV production titres. Both HEK 293T/17 and HeLa cells are very well studied and thought to be good transfection hosts due to the inability to sense intracellular DNA and mount an antiviral response via the cGAS-STING and RIG-I pathways, owing to interfering viral oncogenes of human adenovirus 5 (hAd5) and human papilloma virus 18 (HPV18), which were introduced during the immortalisation of each of these cell lines respectively (Lau *et al.*, 2015). However it is often found that HEK 293T/17 cells are most readily transfectable and generate high protein yields (Baldi *et al.*, 2007; Thomas & Smart, 2005) and transfection of other cell lines requires further protocol optimisation. Additionally, use of the E-SIAT MDCK cell line stably expressing the EBOV/Mak GP failed to produce infectious PV. The cell line was originally adapted for use in cell culture studies to better assess human influenza virus sensitivity to neuraminidase inhibitors, transducing MDCK cells with the gene of human SIAT-1 (2,6 - sialyltransferase) so that they stably express a higher proportion of the  $\alpha$ -2,6 sialic acid receptor required for human influenza transduction (Matrosovich *et al.*, 2003). Thus this further adapted E-SIAT MDCK cell line may be better suited to anti-EBOV antibody screening and biochemical studies.

While the *Marburgvirus* envelope GP is encoded within a single open reading frame, the expression of *Ebolavirus* envelope GP is mediated via an RNA-editing mechanism with the GP gene encoded in two overlapping reading frames (Sanchez *et al.*, 1996; Volchkov *et al.*, 1995). Unedited mRNA is translated to secreted GP (sGP) which accounts for around 80% of transcripts, while the introduction of an extra adenosine within the editing site via slippage of the viral

polymerase leads to the transcription of structural envelope GP. Additionally, transcriptional editing to insert two extra adenosines in the editing site produces a low level of small, truncated, sGP (ssGP). The more recently described *Cuevavirus* species also express GP in two open reading frames (Negredo *et al.*, 2011). While sGP has been implicated in curtailing the immune response (Ito *et al.*, 2001; Mohan *et al.*, 2012), it has also been proposed that the production of sGP acts to control expression of structural GP, which can be cytotoxic, to optimize production and infectivity of virus (Mohan *et al.*, 2015; Volchkov, 2001). Given the use of an edited mRNA transcript in this study meant that sGP was not produced, and the implication of higher expression levels of structural GP causing cytotoxicity as well as limiting infection, the infective titre of PV produce via transfection with various quantities of envelope GP DNA was investigated. Interestingly, using four times the standard quantity of envelope GP DNA gave the highest infective PV titre. This did not correlate with the results of a study by Mohan *et al.* (2015), which reported that infectivity of ebolavirus PV was maximized with a reduced input of envelope GP DNA. The same study reports that for the production of ebolavirus-like particles expression of the matrix protein VP40 is reduced when high levels of envelope GP are expressed, impairing production. Consequently, the higher quantity of envelope GP DNA was not used for transfections due to remaining concerns over production and increased cytotoxicity, as well as an increased surface density of envelope GP having the potential to impair infectivity or neutralisation. As the role of sGP is not fully understood, it could be a factor in the higher infective titres achieved for PV with envelope GP from the *Marburgvirus* species, in comparison to those using *Ebolavirus* and *Cuevavirus* envelope GP. This could otherwise be related to slight structural differences reported between the envelope GP (Feldmann *et al.*, 2001), such as the position of the cleavage site and cysteine residues.

In the previous study (Chapter 3) it was found that the use of a chimeric, VSV cytoplasmic domain, envelope G successfully increased the infectious titre of RABV PV, without altering the neutralisation profile. However, the mechanism responsible for this increase in titre has not been fully elucidated. Applying this approach to the *Ebolavirus* GP used within this study, while also creating chimeric GP with a *Marburgvirus* cytoplasmic domain or removing it entirely, proved

unsuccessful. *Marburgvirus* PV has a higher titre than *Ebolavirus* PV and a GP cytoplasmic domain three amino acids longer than the five amino acids of *Ebolavirus* GP. A direct or indirect interaction between the envelope GP cytoplasmic domain and the lentiviral matrix protein is known to be important for viral assembly (Cosson, 1996; Freed, 1998; Sandrin *et al.*, 2004; Yu *et al.*, 1992). Additionally, short or truncated cytoplasmic domains have been suggested to reduce steric hindrance or allow incorporation into lentiviral particles independent of matrix protein interaction for MeV (Frecha *et al.*, 2008; Freed & Martin, 1995). However, following this approach by truncating the *Ebolavirus* GP cytoplasmic domain within this study resulted in a failure to produce infectious PV. This can be explained by a study looking at the assembly of the *Marburgvirus* envelope GP using a recombinant virus system. It found that while truncation of the GP cytoplasmic domain did not alter incorporation into progeny virions, they were less infectious and it was demonstrated that removal of the cytoplasmic domain had caused conformational changes to the GP ectodomain (Mittler *et al.*, 2011, 2013). It was also reported that the GP transmembrane domain, rather than the cytoplasmic domain, interacted with the matrix protein VP40. Attempts to follow the previously successful method of using a chimeric VSV cytoplasmic domain, which indicated a favourable interaction with the lentiviral core (Chapter 3), also failed to increase the titre of *Ebolavirus* PV.

As filoviruses and rhabdoviruses have a different class of fusion protein, I and III respectively, and trafficking motifs are located within the cytoplasmic domain (Cosset & Lavillette, 2011), it was thought likely that correct GP folding and trafficking was abolished by switching the cytoplasmic domain between different classes of fusion protein. However, chimeric *Ebolavirus* GP PV produced with the cytoplasmic domain of the influenza HA and HIV Env (gp160) envelope proteins, which are both class I fusion proteins, caused a reduction in PV titres. High titre lentivirus PV had previously been produced using the HA envelope protein (Molesti *et al.*, 2014a) and the HIV gp160 envelope protein has a very long cytoplasmic domain which has been shown to interact with its matrix protein MA (Freed & Martin, 1995). Yet it is thought likely that each of these alternate cytoplasmic domains prevented correct folding of the ecto- and transmembrane domains

of the *Ebolavirus* GP, similar to that previously reported for the *Marburgvirus* GP (Mittler *et al.*, 2013). While structurally similar, there is still a high degree of variability between the mode of fusion within the class I proteins. Uniquely, the filovirus GP does not require proteolytic cleavage during maturation to become infectious (Ito *et al.*, 2001; Neumann *et al.*, 2002). The complex series of conformation rearrangements in the late endosome, leading to fusion and entry, involves triggering by low pH dependent cathepsin proteolysis to expose the GP receptor binding domain which interacts with NPC1 (Moller-Tank & Maury, 2015; Pöhlmann, 2013). These priming events can differ between the class I fusion proteins, indeed fusion by the HA and HIV gp160 envelope proteins is triggered solely by a low pH and receptor binding respectively (Cosset & Lavillette, 2011; White *et al.*, 2008). Additionally, the GP has a heavily glycosylated mucin like domain which plays a role in cell entry and an acylation site at the boundary between the transmembrane and cytoplasmic domain, which is thought to help anchor GP within the envelope (Mittler *et al.*, 2013; Takada, 2012). Each of these factors highlights the complexity of altering envelope protein domains and the potential to negatively impact both structure and function.

Assessment of the neutralization pattern of EBOV/Mak GP PV on the three cell lines most permissive to infection via a PVNA, revealed the CHO-K1 cell line, although less permissive to infection than HEK 293T/17 and CRFK cells, provides clearer neutralisation data and therefore may be more appropriate for use in serology studies. As mentioned above, this is further favourable as it prevents using the same cell line for PV production and infection. The limited and valuable supply of prophylactic samples at the time of this study restricted the assessment of the neutralisation pattern of PV for each filovirus species, yet the data collected on the CHO-K1 cell line is most likely attributable to the cell line rather than GP specific. The variability in neutralisation observed between the cell lines highlights the importance of including standards or reference material with a known activity or potency when assessing prophylaxis undergoing development, allowing calibration of results (Temperton & Page, 2015). Of particular importance, this will allow comparisons on the immunogenicity of vaccines undergoing development and the

correlation of protective titres (Gilbert, 2015). The correlates of protection for the *Filoviridae* are currently unknown.

Generating a library of PVs for filoviruses, and other emerging viruses, is highly effective for prior outbreak preparedness and should be prioritised in response to an emerging virus outbreak (Temperton & Page, 2015). PV can be utilized to undertake serosurveillance, antiviral screening, assess vaccine efficacy and investigate viral tropism or aspects of cell biology. More recently, they were used as a standard themselves for Ebola virus diagnostic nucleic acid tests, circumventing the need for inactivated virus, which is typically used for standardisation (Mattiuzzo *et al.*, 2015). The filovirus PVNA developed within this study was rapidly applied to a range of projects, including a phase one clinical trial testing the immunogenicity of an adenovirus vaccine encoding the *Zaire ebolavirus* GP (ChAd3 EBOZ) in a prime-boost vaccination regime, by detecting vaccine induced antibody in volunteer's sera (Ewer *et al.*, 2016). The study also correlated data collected via the PVNA with that of a live *Ebolavirus* neutralisation assay, showing a promising level of concordance between the two assays. In further studies, the PVNA was applied as part of a collaborative study coordinated by NIBSC to rapidly evaluate and develop the first anti-EBOV antibody WHO International Reference Reagent (Wilkinson *et al.*, 2017), as well as to screen repurposed drugs for their ability to block filovirus entry (Long *et al.*, 2015) and in the development of novel antibody therapeutics (Corti *et al.*, 2016). This acts to highlight the applicability of the PV platform and its value in responding to future emerging virus outbreaks.

# Chapter 6. Pseudotyped Virus Quantification and Reporter Gene Characterisation

## 6.1. Introduction

When generating lentiviral PV to study properties related to viral entry, a reporter gene is packaged as an RNA dimer by retroviral core proteins that is encapsulated by a lipid membrane bearing envelope proteins from the virus of interest (Section 1.4.3). Upon transduction of a susceptible cell line, the reporter gene is reverse transcribed and integrated into the cell genome, leading to its expression. Thus, reporter gene expression correlates with transduced cells and can be used to infer interactions between the viral envelope protein and cellular receptor or neutralising antibody function. The incorporation of multiple reporter genes within the pseudotype platform, which have a range of methods to measure gene expression, with various cost and time requirements, is fundamental to expanding the flexibility and applicability of PV assays to meet various resource requirements within different laboratory settings. Given PV technology is primarily used to circumvent the need for high containment facilities, thereby reducing risk and costs, reporters with economical readout assays which retain the sensitivity and specificity of the current repertoire are highly attractive targets.

Bioluminescent, luciferase, reporters which act to catalyse the oxidation of a light emitting luciferin substrate, have proven popular for use in the study of a wide variety of biological processes due to their good sensitivity and high-throughput capabilities (Ghim *et al.*, 2010; Kaskova *et al.*, 2016). The firefly luciferase gene, of beetle (*Photinus pyralis*) origin was first expressed in mammalian cells in 1987 (De Wet *et al.*, 1987) and is now one of the most commonly used along with renilla luciferase of sea pansy (*Renilla reniformis*) origin (Alam & Cook, 2003; Lorenz *et al.*, 1996). In keeping with this, the firefly luciferase reporter is the most popular of the current portfolio of reporter genes which have been incorporated within the pseudotype platform, with renilla

luciferase being another that has been incorporated (Temperton *et al.*, 2015a; Wright *et al.*, 2010). Output is quantified as relative light units (RLU) following the lysis of transduced cells, to release firefly or renilla luciferase, in the presence of beetle luciferin or coelenterazine substrate respectively and emission of luminescence detected using a luminometer. While the requirement for specialised equipment and high cost of the substrate limits use of luciferase reporter PV to well-resourced laboratories, its high-throughput and sensitivity coupled with the relative ease of data analysis is attractive in a research setting. Many alternative luciferases have been discovered or engineered, such as isolation of the secreted cypridina luciferase from the ostracod (*Cypridina noctiluca*) (Nakajima *et al.*, 2004). As well as the ability to measure activity without disrupting cells, it is one of the most stable luciferases and emits a high level of luminescence (Kaskova *et al.*, 2016). Alternatively, NanoLuc luciferase (Hall *et al.*, 2012) is engineered from the deep sea shrimp (*Oplophorus gracilirostris*) to offer a 150-fold increase in luminescence intensity compared to the firefly and renilla luciferases and improved stability, while being a fraction of the size. The properties of each of these luminescent reporters are attractive towards expansion of the pseudotype system and their suitability for inclusion requires investigation.

Fluorescent proteins are an equally popular choice of reporter in the study of biological processes, and like luciferases, occur naturally. They are excited by light of an appropriate wavelength, emitting a longer wavelength in response, with emission profiles of current fluorescent protein variants covering almost the entire visible light spectrum (Shaner *et al.*, 2005). The most well-known is green fluorescent protein (GFP), which was first isolated from the *Aequoria victoria* jellyfish in the 1960's but not cloned and expressed until three decades later (Chalfie *et al.*, 1994). It has undergone several modifications to improve fluorescent intensity, folding and expression within mammalian cells (Alam & Cook, 2003; Shaner *et al.*, 2005) and one such variant with improved sensitivity, enhanced GFP (referred to herein as GFP) (Zhang *et al.*, 1996), is incorporated within the pseudotype platform (Temperton *et al.*, 2015a). Further, the brighter emerald GFP (emGFP) (Cubitt *et al.*, 1998) variant was used in Chapter 3. Output is quantified as infectious units (IFU) by counting transduced cells via either fluorescent microscopy or flow

cytometry. As quantification of a fluorescent protein reporter does not require lysis of transduced cells, qualitative data can simultaneously be collected via fluorescent microscopy. As fluorescence occurs throughout the nucleus and cytoplasm of transduced cells, differentiating adjacent cells by fluorescent microscopy can be challenging. However, this could be improved through the use of localisation signals which target fluorescent proteins to cellular compartments, such as the nucleus, and are widely used for cellular trafficking and gene expression imaging studies (Alam & Cook, 2003; Wu *et al.*, 2011). Further, the incorporation of a fluorescent protein from a different spectral class, such as the red fluorescent proteins derived from *Discosoma* species which have undergone extensive optimisation to have functional utility comparable to those within the green spectrum (Shaner *et al.*, 2004), would be beneficial in expanding the utility of the current reporter gene repertoire.

Finally, colourimetric reporter readouts can make use of low cost reagents and do not require specialised equipment, thus they are favourable to resource-limited laboratory environments. This covers the final reporter incorporated within the pseudotype platform; the *lacZ* reporter gene which encodes  $\beta$ -galactosidase. This bacterial enzyme, first expressed in mammalian cells in the early 1980's (An *et al.*, 1982), acts to hydrolyse various synthetic substrates containing galactose which includes the chromogens X-gal (5-bromo-4-chloro-3-indolyl- $\beta$ -D-galactopyranoside), ONPG (*o*-nitrophenyl- $\beta$ -D-ga-lactopyranoside) and CPRG (chlorophenol red- $\beta$ -D-galac-topyranoside) that have previously been used to quantify transduction of cells by PV with a *lacZ* reporter (Wright *et al.*, 2009). X-gal is most commonly used, producing a blue precipitate at the nuclei of transduced cells, which is quantified as IFU by light microscopy. Alternatively, using the ONPG or CPRG substrates causes a colour change which can be assessed on a microplate reader at 405nm and 550nm respectively, or by eye (Wright *et al.*, 2009). An alternative colourimetric reporter which should be assessed for incorporation into the pseudotype platform is secreted alkaline phosphatase (SEAP) (Berger *et al.*, 1988; Yang *et al.*, 1997). The quantification of SEAP expression in the media of transfected cells can be performed via a high-throughput colourimetric assay and would

offer a low cost and accessible alternative to the secreted cypridina luciferase simultaneously being investigated for inclusion.

While it is possible to compare data collected when using PV with a fluorescent and some colourimetric reporters, due to both using IFU as a measure of transduction, the data cannot easily be compared to that measured as RLU for PV with a luminescent reporter gene. To be able to correlate the disparate readout units of IFU and RLU, a luminescent reporter requires packaging within the genome of PV in combination with either a fluorescent or colourimetric reporter. An adaptation to the currently used (pCS[reporter]W) reporter gene expression plasmid to generate pDUAL has been described by Escors, *et al.*, (2008). This introduced an additional promoter, ubiquitin (UBIQ), and cloning site (Site II) to allow incorporation and expression of a second gene downstream of the spleen focus forming virus (SFFV) promoter and cloning site (Site I) in the original reporter plasmid (Figure 6.1). This alternative reporter expression plasmid may be used for the packaging of two reporters within PV and thus correlation of readouts by their sequential quantification from transduced cells.

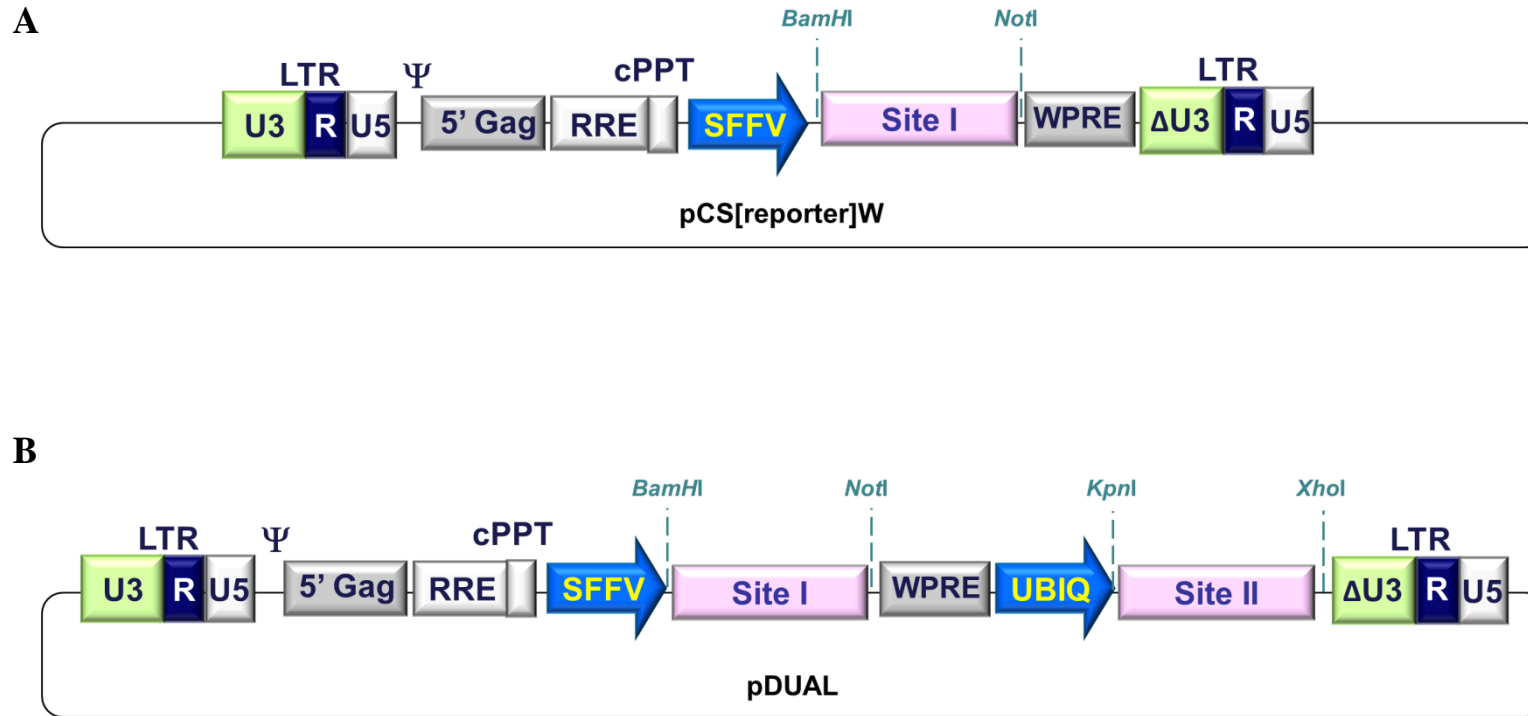


**Figure 6.1 Schematic Representation of the pCS[reporter]W and pDUAL Reporter Gene Expression Plasmids**

(A) The pCS[reporter]W expression plasmid includes a cloning site (Site I) flanked by BamHI/NotI restriction enzyme sites with expression driven by a spleen focus forming virus (SFFV) promoter and enhanced by the woodchuck hepatitis virus posttranscriptional regulatory element (WPRE) (B) The pDUAL is adapted to include a ubiquitin (UBIQ) promoter which confers expression of genes within a second cloning site (Site II) flanked by KpnI/XhoI restriction sites. Other structural elements include: LTR, long terminal repeat; Ψ, packaging signal; gag, structural proteins; RRE, Rev response element; cPPT, central polypurine tract. A deletion in the downstream LTR U3 promoter region (ΔU3) creates a self-inactivating vector.

The quantification of PV preparations via the measurement of reporter gene expression levels in transduced target cells is used to assign a biological titre, inferring the number of functional PV particles in the preparation. Yet in addition to the relatively new technology of nanoparticle tracking analysis, which enables quantification of the total number of particles within PV preparations (Filipe *et al.*, 2010; Heider & Metzner, 2014), other methods have been described to quantify different PV components in a non-functional manner. The RNA genome of PV can be quantified via an RT-qPCR reaction using primers targeting the HIV-1 long terminal repeats (LTR; Figure 6.1) (Lizée *et al.*, 2003; Mattiuzzo *et al.*, 2015) Further, the core component can separately be quantified via an RT-qPCR assay which has been adapted to measure the reverse transcriptase (RT) activity associated with the core component (Pizzato *et al.*, 2009; Vermeire *et al.*, 2012). This SYBR Green product-enhanced RT (SG-PERT) assay has been developed as a sensitive, cost effective, alternative to the use of an enzyme-linked immunosorbent assay (ELISA), which detects the HIV-1 p24 core protein and has historically been used to quantify HIV-1 virions. While it is widely reported that use of these non-functional quantification methods over-estimate, and thus cannot predict, biological titres (Geraerts *et al.*, 2006; Heider & Metzner, 2014; Lizée *et al.*, 2003; Sastry *et al.*, 2002; Scherr *et al.*, 2001), it is thought they can help evaluate the quality and composition of PV preparations and be utilised in their standardisation.

This study aimed to investigate the suitability of new reporters for incorporation into the pseudotype platform, expanding the current repertoire to improve the range of outputs available and increase its applicability to meet various laboratory resource requirements. It further aimed to determine the ratio between the disparate readout units of IFU and RLU and review alternative methods of quantifying PV, in addition to biological titre which is currently used, that could be used for standardisation and quality control.

## 6.2. Results

### 6.2.1. Incorporating New Reporters into the Pseudotyped Virus Platform

A set of six new reporter protein genes, covering the luminescent, colourimetric and fluorescent readout methods (Table 6.1) were cloned within the pCS[reporter]W expression plasmid (Section 2.1.3). Each of the reporter gene sequences were amplified via standard cDNA PCR (Section 2.2.3), introducing restriction enzyme sites for sub-cloning into pCS[reporter]W (Section 2.2.5), and all newly cloned reporter gene constructs were sequencing verified (Section 2.2.8). To assess the suitability of each of the new reporter genes, evaluating output and functionality in comparison to the existing repertoire, lentiviral PV comprising a CVS-11 G was produced incorporating each of the new reporters by transfecting HEK 293T/17 cells (Section 2.2.10).

**Table 6.1 Primers for Cloning New Reporter Genes**

Index of primers and source of reporter genes cloned into the pCS[reporter]W expression plasmid.

<b>Readout</b>	<b>Reporter Gene</b>	<b>Construct</b>	<b>Source</b>	<b>Plasmid/Accession</b>
		<b>Primers<sup>1</sup></b>	<b>Number<sup>2</sup></b>	
<b>Luminescent</b>	Cypridina Luciferase	C3.1	pCMV-CLuc 2 (NEB)	
	NanoLuc Luciferase	C3.2	pNL1.1[Nluc] JQ437370 (Promega)	
<b>Colourimetric</b>	Secreted Alkaline Phosphatase (SEAP)	C3.3	pSEAP-Basic U09660 (Clontech)	
	Secreted Alkaline Phosphatase (version 2) (SEAP2)	C3.4	pSEAP2-Basic U89937 (Clontech)	
<b>Fluorescent</b>	Dual-Nuclear Localised GFP (dNG)	C3.5	pCMS28-NLS-GFP- SAMHD1-CtD (Schwefel <i>et al.</i> , 2014)	
	Dual-Nuclear Localised tdTomato (dNT)	C3.6	ptdTomato-Nuc (Kind gift from Colin Crump, University of Cambridge)	

<sup>1</sup>Refers to Chapter 2, Table 2.5

<sup>2</sup>Further details and sequence in Appendix I

To assess the suitability of each of the new luminescent readout reporter genes, cypridina and NanoLuc luciferase, they were compared to PV comprising either the currently used firefly luciferase or renilla luciferase reporter genes. An infection assay was set up, titrating each PV in parallel across a 2-fold serial dilution from a starting dilution of 1:2 onto the BHK-21 target cell line, in duplicate (Section 2.2.11.1). The level of infection at each PV dilution was recorded in RLU via the appropriate assay system (Section 2.2.12.1). Titration of PV comprising a firefly or renilla luciferase reporter positively correlated with RLU values and the level of infection was above background levels recorded for the PV supernatant and uninfected cells (Figure 6.2A & B). Results of titrating PV comprising the newly incorporated cypridina luciferase reporter, which unlike the currently used luciferase reporters is secreted from infected cells, showed this did not positively correlate with RLU values, instead increasing up to a PV dilution of 1:128 before decreasing beyond this point (Figure 6.2C). Background RLU values were high for both the PV supernatant, which recorded an RLU ( $7.6 \times 10^4$ ) higher than that for infection with 1:2 diluted PV, and the uninfected cells ( $9.7 \times 10^3$  RLU; Figure 6.2C). This corroborated with the level of background between  $10^2 - 10^4$  RLU reported by the BioLux® cypridina luciferase assay (NEB) manufacturer for assays performed with media supplemented with 10% FBS. The titration of PV with the NanoLuc luciferase reporter similarly gave a negative correlation with RLU values at low dilutions of PV, before positively correlating at PV dilutions greater than 1:16 (Figure 6.2D). While the background RLU value for the uninfected cells read via the NanoLuc luciferase assay was in line with that for the firefly and renilla luciferase reporters, the RLU recorded for the PV supernatant was high ( $6.5 \times 10^7$  RLU; Figure 6.2D). This indicated a high level of passive transfer of the protein in the transfection supernatant. Consequently, neither the cypridina nor NanoLuc luciferase reporters were appropriate for incorporation into the PV platform.

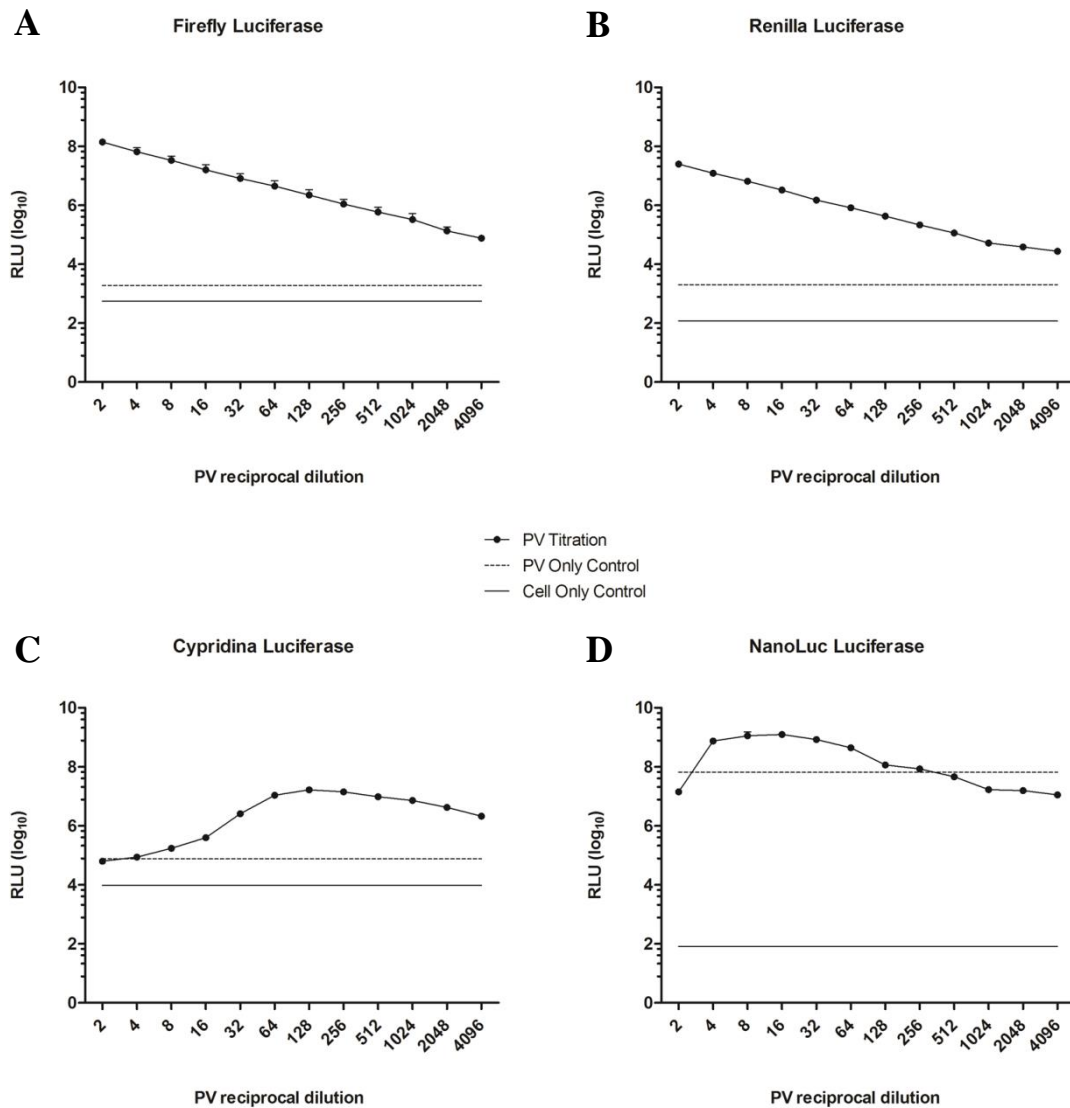


**Figure 6.2 Comparative Titration of Pseudotyped Virus Incorporating Existing and New Luciferase Reporter Genes**

Lentiviral PV produced with a CVS-11 G and incorporating either the existing firefly luciferase (A) and renilla luciferase (B) reporter genes or the newly incorporated cypridina luciferase (C) and NanoLuc luciferase (D) reporter genes were titrated onto the BHK-21 cell line, along with controls of PV supernatant alone and uninfected cells. Titres were measured as relative light units (RLU) and mean values are plotted for each dilution of PV. Error bars show SD (n = 2).

Two versions of the colourimetric secreted alkaline phosphatase reporter gene, SEAP and an updated version SEAP2, which had been modified to include a 39 nucleotide C-terminal extension (Appendix I), were compared. Initially, an infection assay was set up titrating PV with each of the reporter genes across a 2-fold serial dilution onto the BHK-21 target cell line, in duplicate (Section 2.2.11.1). The level of infection was recorded via measuring absorbance at 405 nm ( $A_{405}$ ) following an alkaline phosphatase enzymatic assay (Section 2.2.12.2). It was found that each version of the reporter gene offered approximately the same level of absorbance, which positively correlated with PV dilution (Figure 6.3A). However, undiluted PV supernatant controls gave high absorbance readings which matched the level obtained for infection with 1:2 diluted PV (Figure 6.3A). To further investigate the absorbance signal from the PV supernatant control, a repeat assay was performed titrating the PV supernatant in parallel to the infection with PV incorporating the SEAP2 reporter gene. Results of the titration showed that the absorbance signal from the PV supernatant was greater than that from the infection, measuring 3.9 and 2.4 respectively at a PV dilution of 1:4, and decreased at a similar rate (Figure 6.3B). This indicated the absorbance signal read from the infection could be a result of the passive transfer of alkaline phosphatase produced during transfection.

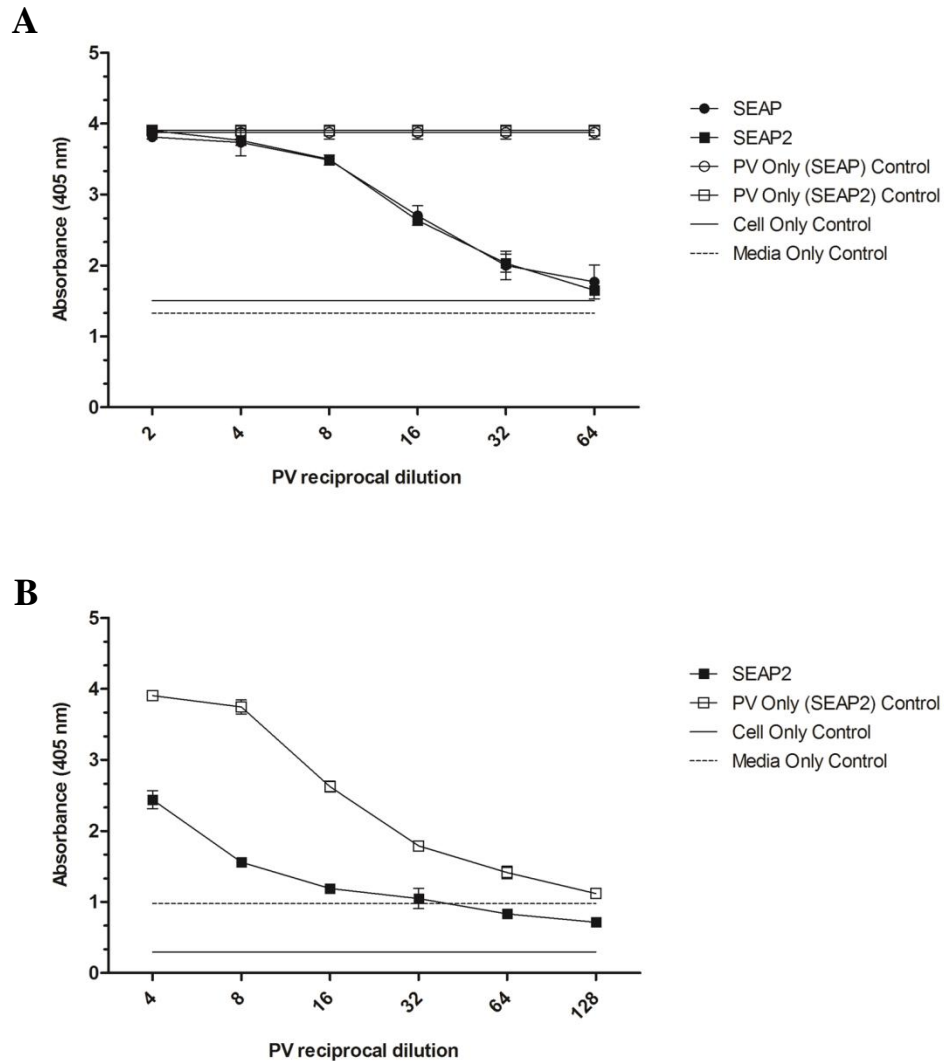


**Figure 6.3 Titration of Pseudotyped Virus Incorporating a Secreted Alkaline Phosphatase Reporter Gene**

(A) Lentiviral PV produced with a CVS-11 envelope G and incorporating either the SEAP or SEAP2 version of the alkaline phosphatase reporter gene titrated onto the BHK-21 target cell line with controls of PV supernatant alone, uninfected cells and media alone included to measure background absorbance levels. (B) CVS-11 envelope G PV incorporating an SEAP2 reporter gene titrated onto the BHK-21 target cell line along with a parallel titration of the PV supernatant and controls of uninfected cells and media alone. All titres were measured after 48 hours incubation at an absorbance of 405 nm and average values plotted for each dilution of PV. Error bars show SD (n = 2).

To further evaluate whether the signal was solely from the passively transferred alkaline phosphatase, an infection assay was performed as before, titrating PV with each SEAP reporter onto target cells in parallel to the PV supernatant as a control, however following 3 hours incubation the media was removed for incubation in a separate culture plate and replaced with fresh media. Results showed that changing the media on the transduced cells resulted in  $A_{405}$  readings in the range of 0.085 – 0.104 which were in line with those of the background measured from cell and media controls of 0.086 and 0.085 respectively (Figure 6.4A). Absorbance readings taken from the media incubated following removal after 3 hours remained above background, decreasing from 3.5 and 2.8 for 1:4 diluted PV comprising the SEAP and SEAP2 reporter gene respectively (Figure 6.4B). To ensure 3 hours incubation was long enough for PV entry to occur, an infection assay was set up, titrating CVS-11 envelope G PV incorporating a firefly luciferase reporter gene onto the BHK-21 target cell line and changing the media after 3 hours, alongside a control infection where the media was not changed. Results recorded as RLU showed that while the control infection had RLU readings on average 5-fold higher than those recorded for infection with PV where the media had been changed, 3 hours was sufficient for a significant level of infection to occur and the RLU readings from the media removed were low or level with the background recorded on the cell and media controls (Figure 6.4C). Thus, secreted alkaline phosphatase is not produced by infection of target cells with PV comprising the SEAP or SEAP2 reporter genes, but passively transferred after being produced during transfection and as a result not suitable for use as a reporter gene in the PV platform.

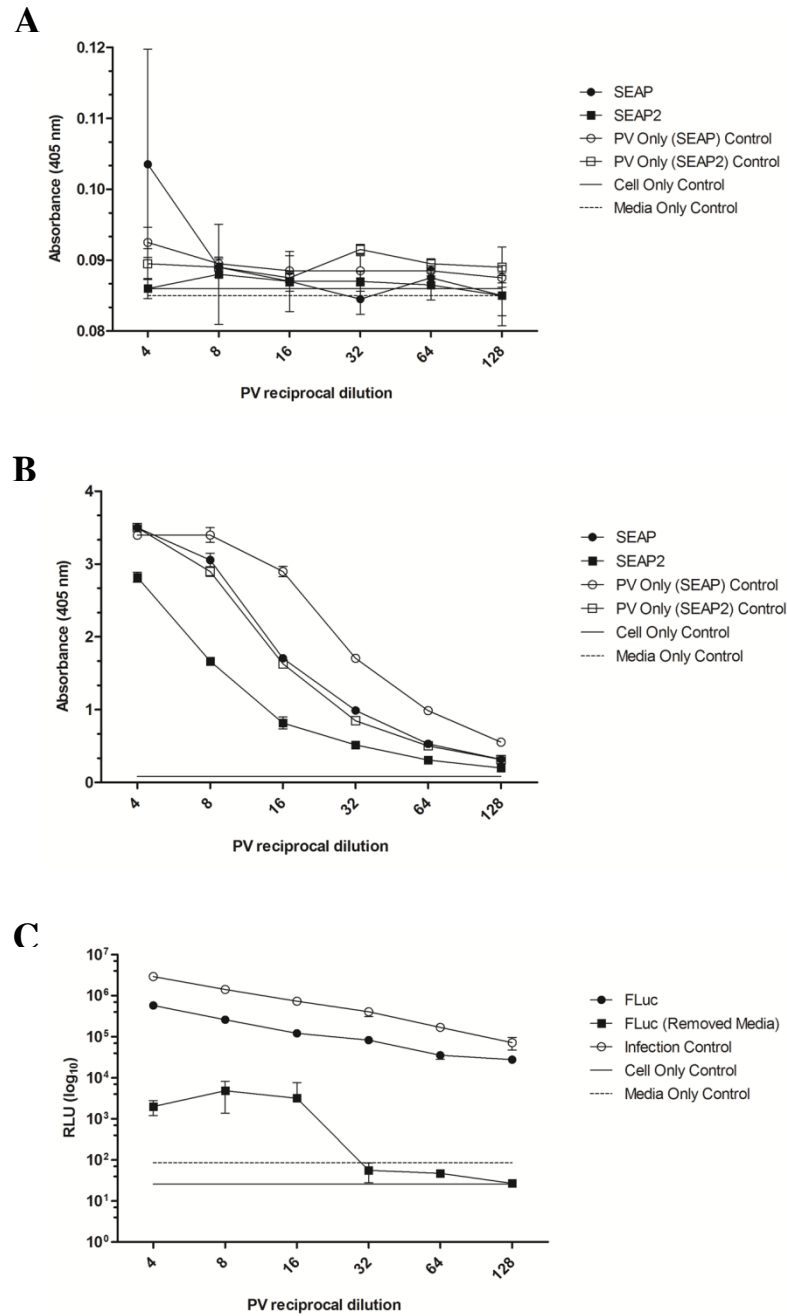


**Figure 6.4** Titres of Pseudotyped Virus Incorporating a Secreted Alkaline Phosphatase or Firefly Luciferase Reporter Gene after Changing the Media during Incubation

Lentiviral CVS-11 G PV incorporating an SEAP or SEAP2 reporter gene was titrated onto the BHK-21 cell line alongside a PV supernatant control. (A) After 3-hours incubation media was changed and 45-hours later titres were read via the absorbance at 405 nm. (B) The media removed was incubated separately and the absorbance read. (C) Lentiviral CVS-11 G PV incorporating a firefly luciferase (FLuc) reporter gene was titrated onto the BHK-21 cell line and the media changed after 3-hours, alongside an infection control where the media was not changed, measuring titres as relative light units (RLU) after a total of 48-hours incubation. In each case controls of uninfected cells and media alone were included. Error bars show SD (n = 2).

An improvement to the currently used enhanced GFP reporter gene was investigated by comparison with dual-nuclear localised versions of GFP (dNG) and tdTomato fluorescent protein (dNT). To assess each reporter gene visually, an infection assay was set up titrating PV with each of the fluorescent reporter genes over a 2-fold dilution series onto the BHK-21 target cell line and, following incubation, infected cells were fixed and visualised using the appropriate fluorescent microscope filter (Section 2.2.12.3). Visualisation of cells infected with PV incorporating a GFP reporter gene showed much of the cell monolayer emitting bright fluorescence, with a low level of definition between individually infected cells and a high level of background auto-fluorescence (Figure 6.5A). The level of definition between adjacently infected cells was greatly improved when infected with PV incorporating a dNG reporter gene, owing to the nuclear localisation signal, however fluorescence intensity was reduced and background auto-fluorescence remained high (Figure 6.5B). Infecting cells with PV incorporating the dNT reporter gene reduced background auto-fluorescence and produced an intense fluorescence signal from the nucleus of infected cells, yet a reduced number of cells appeared to be infected (Figure 6.5C).

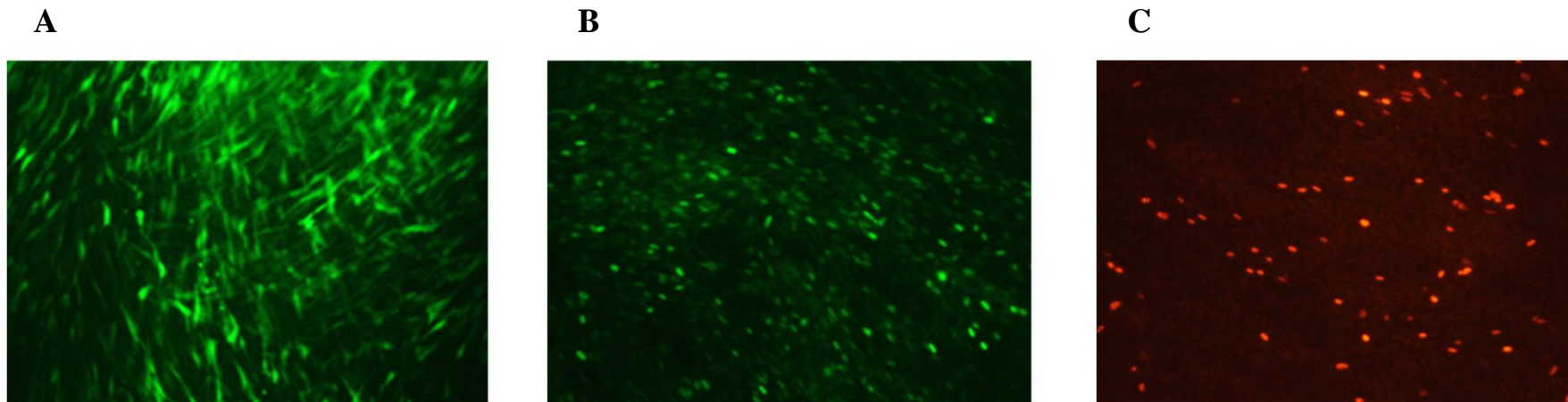


**Figure 6.5 Cell Infection by Pseudotyped Virus Incorporating New Fluorescent Reporter Protein Genes in Comparison to Standard GFP**

Fluorescent microscopy images showing BHK-21 cells infected by 1:4 diluted CVS-11 G PV incorporating (A) a standard GFP reporter gene, in comparison to (B) a dual-NLS GFP (dNG) reporter gene and (C) dual-NLS TFP (dNT) reporter gene. Images were captured using the x10 objective. Cells were at 100% confluence.

To quantify the level of infection for PV incorporating each of the fluorescent reporter genes, GFP, dNG and dNT, infection assays were set up to measure titres via flow cytometry and fluorescent microscopy (Section 2.2.12.3). Flow cytometry data was collected using the FITC protocol for a GFP or dNG reporter gene and the PE-Texas Red protocol for the dNT reporter gene (Section 2.2.12.3). Analysis of the data was undertaken by applying gates to the cell population, to remove cell debris, along with gates applied to count cells emitting a fluorescence signal above the background level, where the background was set to the end of the first log-decade (Figure 6.6A-D). Data was collected via fluorescent microscopy by counting cells emitting fluorescence as positive for infection. The level of infection quantified by each method was reported as infectious units per ml (IFU/ml). Comparison of the infective titres measured via flow cytometry showed that for PV incorporating a GFP or dNG reporter, the titre was significantly higher than PV with a dNT reporter by 25.5 and 29.7 fold respectively ( $p < 0.0001$ ; Figure 6.7). However, infective titres for each of the reporters measured via fluorescent microscopy were not significantly different (Figure 6.7). When comparing the two methods of quantification, titres recorded via flow cytometry were 4.5 fold higher than via fluorescent microscopy when quantifying the dNG reporter ( $p = 0.001$ ), yet conversely the dNT reporter titres were 4.5 fold higher when quantified via fluorescent microscopy ( $p < 0.0001$ ; Figure 6.7). Overall, the infective titre of PV incorporating a dNT reporter was lower than with a GFP or dNG reporter.

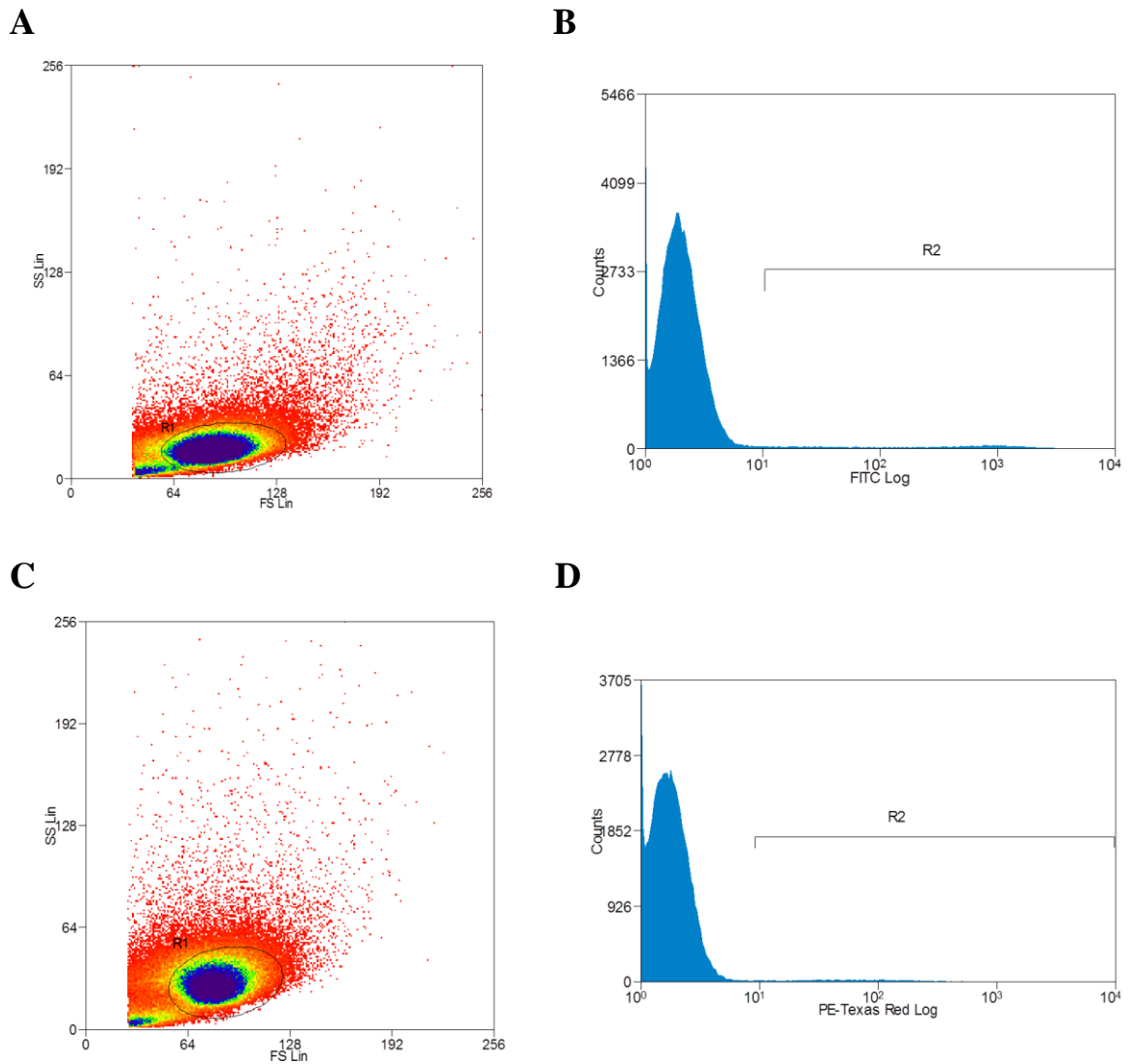


**Figure 6.6 Gating of Cells for Flow Cytometry Analysis via the FITC or PE-Texas Red Channel**

Example of gates set for analysis of BHK-21 cells infected with GFP or dNG reporter gene PV via the FITC channel, with (A) the gate R1 placed over the main cell population and (B) a second gate, R2, applied to count cells emitting fluorescence above background, from the end of the first log-decade. To analyse BHK-21 cells infected with dNT reporter gene PV via the PE-Texas red channel, (C) the gate R1 was placed over the main cell population and (D) a second gate, R2, applied as per the FITC channel, to count cells emitting fluorescence above background.

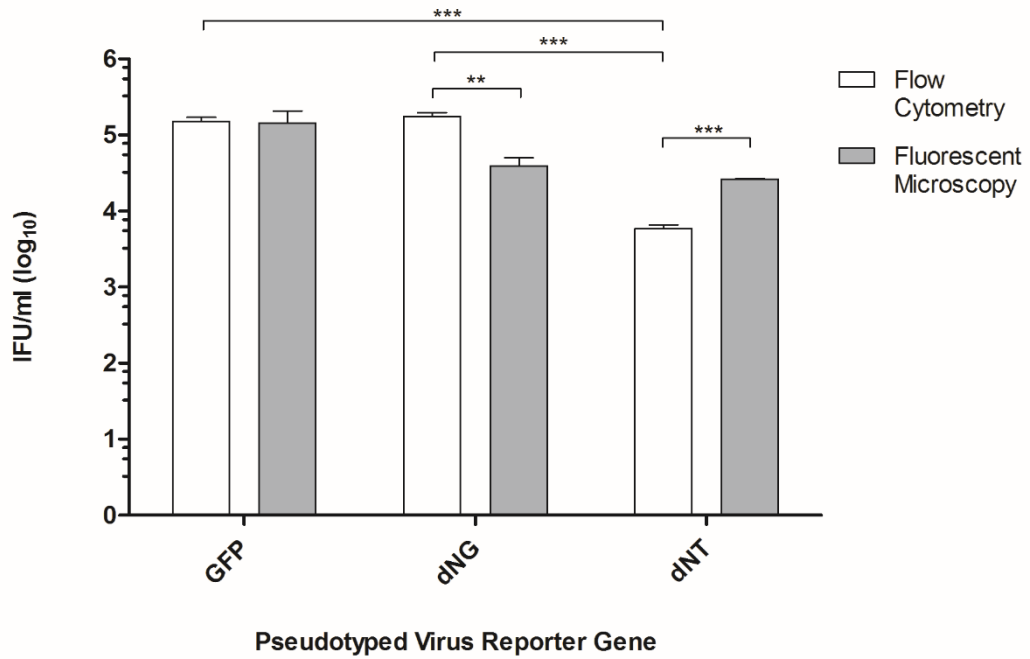


**Figure 6.7 Comparison of Infective Titres Measured for Pseudotyped Virus Incorporating New and Existing Fluorescent Reporter Genes**

Infective titres of CVS-11 G PV incorporating a GFP, dNG or dNT reporter gene and titrated onto BHK-21 target cells were measured via flow cytometry analysis or counted via fluorescent microscopy and reported as infectious units per ml (IFU/ml). (\*\* $p = 0.001$  and \*\*\* $p < 0.0001$ ; two-tailed  $t$ -test) Error bars show SD (via flow cytometry  $n = 4$  and via fluorescent microscopy  $n = 2$ ).

## 6.2.2. Comparison and Correlation of the Disparate Readout Units of Pseudotyped Virus Reporters

To compare the disparate readout units of luminescent reporters, measured as RLU, with those of fluorescent or colourimetric reporters, measured as IFU, the ability to incorporate two reporter genes within the PV core and their equal expression from transduced cells was investigated. Using the pDUAL expression plasmid (Figure 6.1B) the reporter genes firefly luciferase (FLuc), GFP and *LacZ* which cover the luminescent, fluorescent and colourimetric readout methods respectively, were paired and incorporated within the pDUAL cloning sites (Site I & II) in each orientation, producing six constructs (Figure 6.8). For cloning into Site I the reporter genes were digested and subsequently ligated (Section 2.2.5) using *Bam*HI/*Not*I restriction enzyme sites previously introduced for cloning into pCS[reporter]W. To insert each reporter gene into Site II, the sequences were amplified via standard cDNA PCR (Section 2.2.3) using primers for constructs C4.1 – 4.3 (Table 2.6, Section 2.1.3) to introduce *Kpn*I/*Xho*I restriction enzyme sites for sub-cloning. All pDUAL reporter constructs were verified by sequencing (Section 2.2.8).

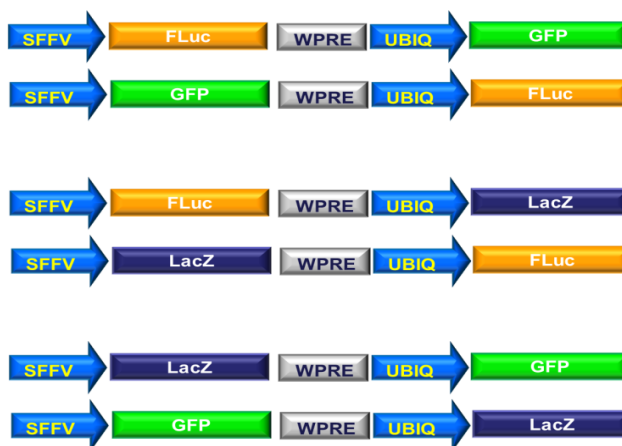


**Figure 6.8 Schematic Representation of the Orientation of Reporter Genes Incorporated within the pDUAL Expression Plasmid**

Reporter constructs produced by pairing the reporter genes, firefly luciferase (FLuc), green fluorescent protein (GFP) and *LacZ* and inserting them into cloning site I and site II of the pDUAL expression plasmid in each orientation. Expression of genes in site I is driven by the spleen focus forming virus (SFFV) and enhanced by the woodchuck hepatitis virus posttranscriptional regulatory element (WPRE), while a ubiquitin (UBIQ) promoter confers expression of genes within site II.

To evaluate the functionality of each of the pDUAL reporter constructs (Figure 6.8B), they were incorporated within CVS-11 G PV produced via the transfection of HEK 293T/17 cells (Section 2.2.10). As a control, CVS-11 G PV was also produced incorporating an FLuc, GFP or *LacZ* reporter gene separately by transfection within the pCS[reporter]W expression plasmid. Infection assays were performed, titrating each PV over a 2-fold dilution series, in duplicate, onto the BHK-21 target cell line (Section 2.2.11.1), to allow evaluation of each reporter gene incorporated within the PV core via the pDUAL expression plasmid. The infective titres were quantified as RLU/ml when detecting the FLuc reporter via luminescence (Section 2.2.12.1) and as IFU/ml when detecting the GFP or *LacZ* reporters via fluorescent microscopy (Section 2.2.12.3) or the  $\beta$ -galactosidase assay (Section 2.2.12.2) respectively. Results showed that for each of the paired reporters, the infective titre measured for the reporter when it was in Site I of the pDUAL expression plasmid was higher than when it was in Site II (Figure 6.9A-C). An exception was observed for the detection of fluorescence from GFP when paired with *LacZ*, which gave a higher infective titre when in Site II (Figure 6.9C); however this was not the case when GFP was paired with FLuc (Figure 6.9A). Interestingly, no signal was detected via the colourimetric assay for *LacZ* when it was in Site II when paired with both FLuc and GFP (Figure 6.9B&C). Together, this data showed that there were not equal levels of expression of reporter genes in Site I and II of the pDUAL expression plasmid and as a result infective titres from the two reporter genes incorporated could not be correlated.

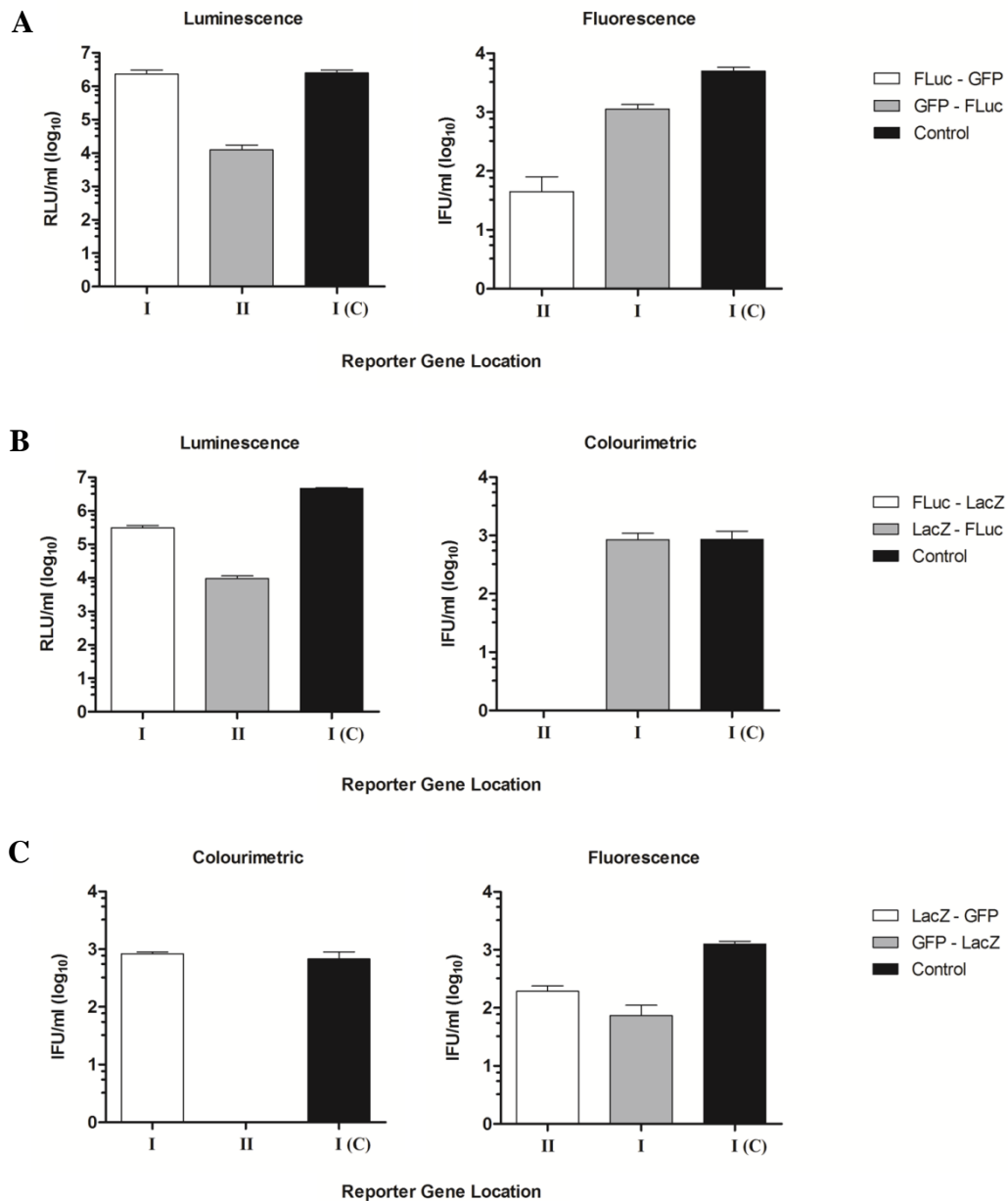


**Figure 6.9 Infective Titres to Evaluate Incorporating Two Reporter Genes within the Pseudotyped Virus Core via a pDUAL Expression Plasmid**

Titres from BHK-21 cells infected with CVS-11 G PV incorporating two reporter genes (**A**) FLuc and GFP, (**B**) FLuc and *LacZ* and (**C**) *LacZ* and GFP which had been paired and cloned into the pDUAL expression plasmid Site I and Site II and were tested in both orientations (Site I – Site II). Titres were measured individually via luminescence for FLuc, fluorescence for GFP and a colorimetric assay for *LacZ*, which were within Site I of the control (C) pCS[reporter]W expression plasmid. Luminescence results are reported as relative light units per ml (RLU/ml) while fluorescence and colourimetric assay results are in infectious units per ml (IFU/ml). Controls represent titres from BHK-21 cells infected with CVS-11 G PV incorporating a single reporter FLuc, GFP or *LacZ* corresponding to the readout assay. Error bars show SD (n = 2).

Therefore, to explore an alternative system of incorporating and expressing two reporter genes from a single PV, the use of a 2A peptide which mediates protein cleavage from a single open reading frame via a ribosomal skip mechanism was investigated. The mechanism works by preventing a normal peptide bond forming between a 2A glycine and 2B proline residue without affecting the downstream translation of the 2B peptide and thus allows concordant expression of genes placed either side (Donnelly *et al.*, 2001; Szymczak *et al.*, 2004). Of several 2A peptide sequences identified, the well-studied and comparatively short T2A sequence (EGRGSLLTCGDVEENPG\*P) from the insect *Thosea asigna* virus (TaV) was selected and used to generate an adapted pCS[reporter]W expression plasmid which incorporated cloning sites for two genes separated by the T2A peptide with expression driven by the SFFV promoter (pCS-T2A-W, Figure 6.10A). The construct was designed to include a flexible Gly-Ser-Gly (GSG) linker upstream of the T2A peptide sequence due to a reported enhancement of cleavage efficiency to near 100% (Szymczak-Workman *et al.*, 2012) and for this reason a shorter Ser-Gly (SG) linker was also included downstream of the T2A peptide (Figure 6.10A). Restriction enzyme sites were incorporated either side for simplicity of cloning of future genes into Site I and II by *BamHI/PacI* and *SmiI/NotI* digestion respectively. Importantly, all sequences were kept in frame with the T2A peptide sequence, with stop codons omitted from the 3' end of genes in Site I and start codons not included at the 5' end of genes in Site II. The pCS-T2A-W expression plasmid was produced to include the FLuc and GFP reporter genes in each orientation (Figure 6.10B) by the use of SOE PCR amplification (Figure 2.1B, Section 2.2.4) and primers for the constructs C3.7 and C3.8 (Table 2.5, Section 2.1.3) to produce FLuc-T2A-GFP and GFP-T2A-FLuc respectively, which were then cloned into the pCS[reporter]W vector using the flanking *BamHI/NotI* restriction sites. Each construct was sequencing verified (Section 2.2.8) using pCS[reporter]W primers and the appropriate pCSFLuc-T2A-W or pCS-T2A-FLucW primer dependant on the position of the FLuc gene (Table 2.7, Section 2.1.3).

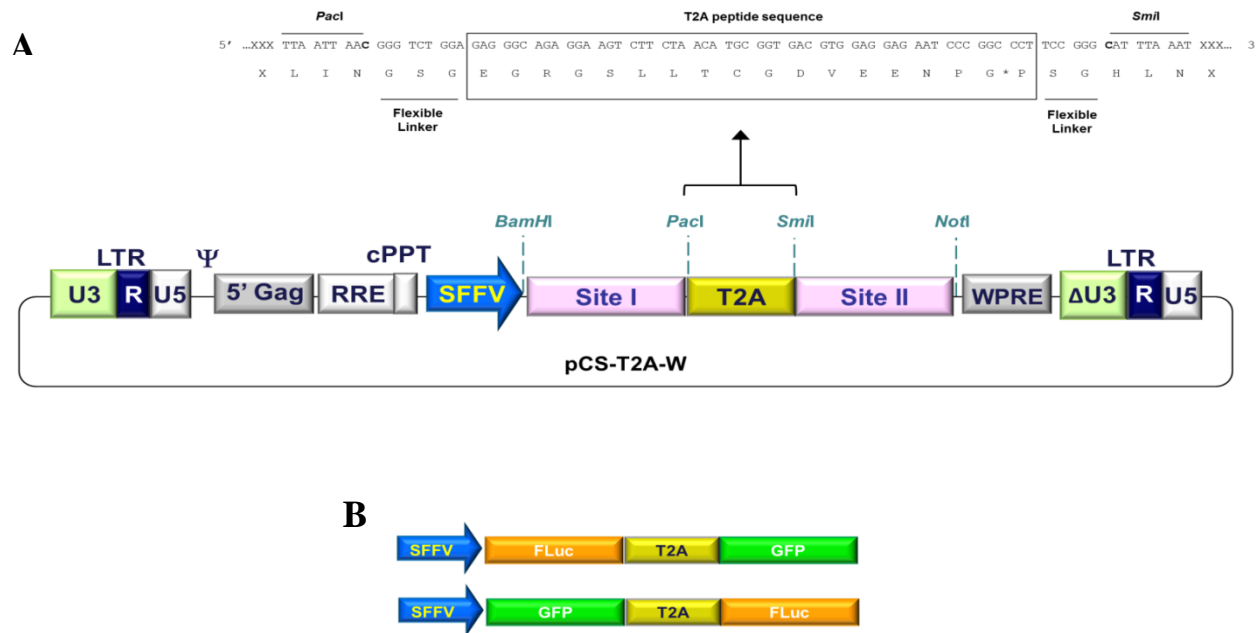


**Figure 6.10 Schematic Representation of the T2A Peptide Sequence and Orientation of Reporter Genes Incorporated within the pCS-T2A-W Expression Plasmid**

(A) The incorporated T2A peptide sequence is shown boxed with the point of cleavage (\*) and flanking flexible linker sequences indicated. *Pacl* and *SmiI* restriction enzyme sites were included to produce cloning sites (Site I and Site II) either side of the T2A peptide, with additional ‘C’ nucleotides to keep the sequence in-frame. The position of hypothetical genes is shown by ‘X’ which would omit a stop codon at the 3’ end of the gene within Site I and a start codon at the 5’ end of the gene within Site II. Expression of both genes is driven by the spleen focus forming virus (SFFV) promoter. Other structural elements include: LTR, long terminal repeat;  $\Psi$ , packaging signal; gag, structural proteins; RRE, Rev response element; cPPT, central polypurine tract; WPRE, woodchuck hepatitis virus posttranscriptional regulatory element. A deletion in the downstream LTR U3 promoter region ( $\Delta$ U3) creates a self-inactivating vector. (B) Position of the firefly luciferase (FLuc) and green fluorescent protein (GFP) reporter genes, incorporated in both orientations, in the pCS-T2A-W constructs produced.

Initially, CVS-11 envelope G PV incorporating each of the pCS-T2A-W constructs (Figure 6.10B) was produced and an infection assay undertaken to determine whether the reporter genes within each position were expressed. Following positive early results, in depth evaluation was undertaken through the production of a panel of PV comprising a VSV G, RABV (CVS-11) G and EBOV (Makona) GP envelope protein to cover high, medium and low titre PV respectively, incorporating each of the pCS-T2A-W constructs via transfection of HEK 293T/17 cells (Section 2.2.10). As before, controls were produced incorporating an FLuc or GFP reporter gene within the pCS[reporter]W expression plasmid. Infection assays were performed in triplicate on three occasions, titrating over a 2-fold dilution series onto either BHK-21 cells (VSV and RABV G PV) or HEK 293T/17 cells (EBOV GP PV) (Section 2.2.11.1). The assays were set up to first evaluate expression of the GFP reporter by fluorescent microscopy, cells were not fixed but washed and PBS added (Section 2.2.12.3), recording results as IFU/ml. Expression of the FLuc reporter was then evaluated by assaying for luminescence, transferring the supernatant to an opaque culture plate prior to reading (Section 2.2.12.1) and reporting results as RLU/ml. The results showed that there were near equal levels of expression of each of the reporters, GFP and FLuc, when cloned into Site I compared to Site II of the pCS-T2A-W expression plasmid (Figure 6.11A&B). Lower titres were consistently observed when using the adapted pCS-T2A-W expression plasmid in comparison to controls incorporating a single reporter gene into the PV core using the pCS[reporter]W expression plasmid, however this did not impact on the ability to correlate titres.

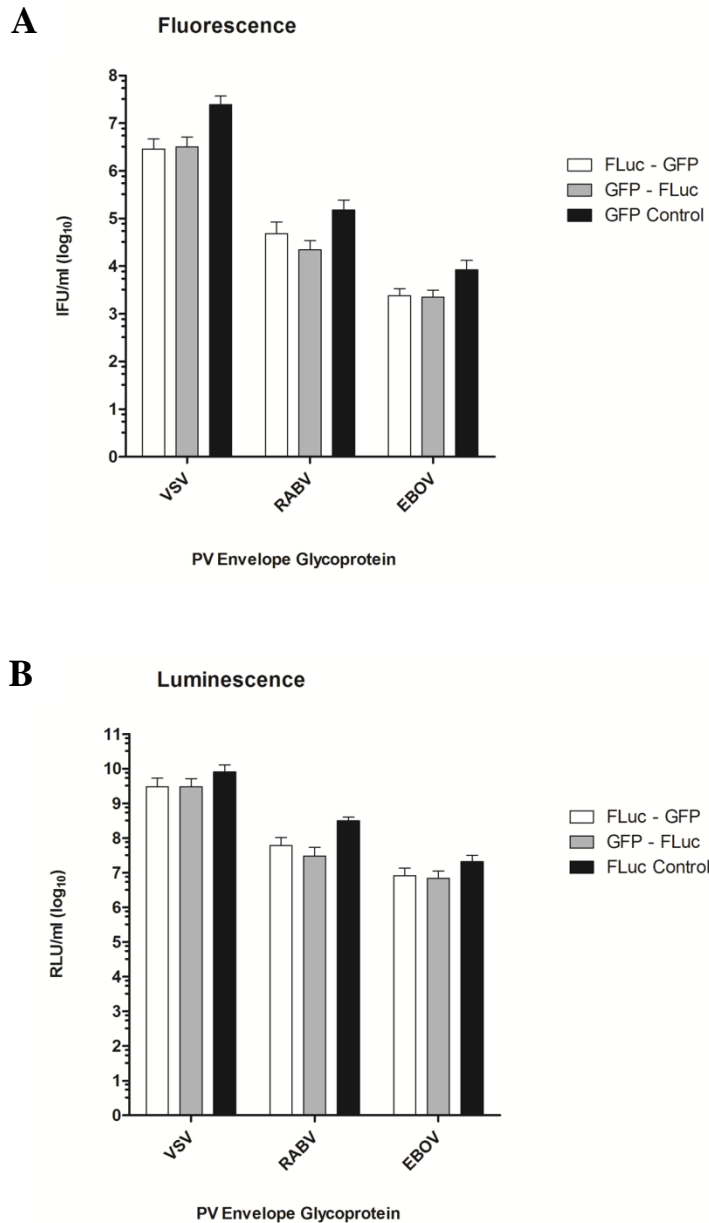


**Figure 6.11 Infective Titres to Evaluate Incorporating Two Reporter Genes within the Core of Pseudotyped Virus with a VSV, RABV or EBOV Envelope Glycoprotein via the pCS-T2A-W Expression Plasmid**

Titres from BHK-21 cells infected with VSV and RABV (CVS-11) G PV and HEK 293T/17 cells infected with EBOV (Makona) GP PV incorporating an FLuc and GFP reporter gene cloned in each orientation (Site I – Site II) within the pCS-T2A-W expression vector. PV controls were included for each comprising a single FLuc or GFP reporter. **(A)** First titres were measured as fluorescence to detect expression of the GFP reporter and recorded as infectious units per ml (IFU/ml). **(B)** Titres were then measured via luminescence to detect the FLuc reporter and results recorded at relative light units per ml (RLU/ml). Average titres are plotted and error bars show SD (n = 3).

To compare the disparate readout units of the two reporter genes the ratio between RLU and IFU titres (RLU:IFU) was determined by combining average values for the T2A peptide linked FLuc and GFP reporter genes in each orientation, after calculating ratios at single PV dilution points. For comparison, ratios were also calculated from matched dilutions of the separately titrated, single FLuc and GFP reporter, control PV. The average ratio of RLU to IFU for VSV G PV was 1417:1 while for RABV G PV it was calculated to be 1101:1 and in each case this was significantly different to the ratio calculated using the control PV titration data (539:1,  $p = 0.0012$  and 2016:1,  $p = 0.0355$  respectively; Figure 6.12). Unexpectedly, the ratio for EBOV GP PV was significantly higher at 2601:1 ( $p < 0.0007$ ) and not found to be significantly different to that calculated for the corresponding control PV ( $p = 0.3155$ ; Figure 6.12). This result was considered to arise from a difference between the HEK 293T/17 cell line used to titrate EBOV GP PV compared to the BHK-21 cell line used for both the VSV and RABV G PV titrations. Combining the calculated ratios for the VSV and RABV G PV arises at approximately 1259 RLU equating to 1 IFU on the BHK-21 cell line.

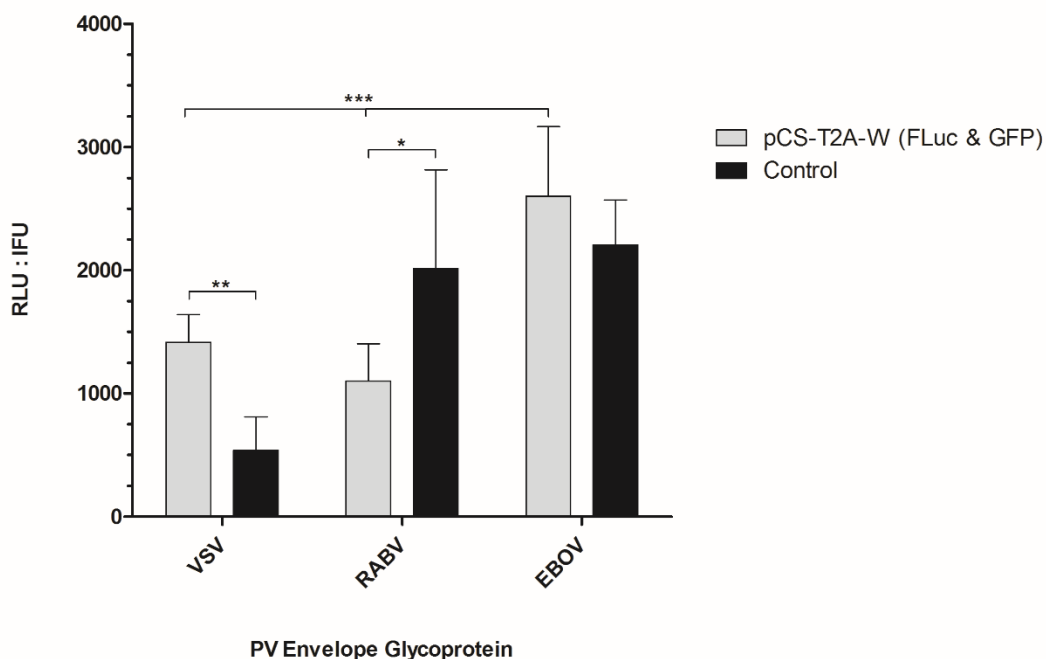


**Figure 6.12 Ratio between Luminescent (RLU) and Fluorescent (IFU) Readout Units Using Reporter Genes Linked by a T2A Peptide**

From infection assay data for VSV G, RABV G and EBOV GP PV incorporating both an FLuc and GFP reporter gene via the pCS-T2A-W expression plasmid, the ratio between RLU and IFU (RLU:IFU) was calculated from titres measured at single PV dilutions and averages for both orientations of FLuc and GFP combined.  $*p = 0.0355$  and  $**p = 0.0012$  when comparing samples with corresponding controls and  $***p < 0.0001$  when comparing EBOV GP PV sample to both VSV and RABV G PV samples (two-tailed *t*-test). Error bars show SD ( $n = 6$  for samples and  $n = 3$  for controls).

### 6.2.3. Quantification of Pseudotyped Virus

In order to evaluate four methods of quantifying PV preparations, and to account for any variance associated with the reporter gene or titre, a panel of lentiviral PVs were produced comprising a VSV G, RABV (CVS-11) G and EBOV (Makona) GP envelope protein and incorporating a firefly luciferase, GFP or *LacZ* reporter gene via the transfection of HEK 293T/17 cells (Section 2.2.10). Single use aliquots of the PV harvest were prepared for each quantification method and stored at -80°C. The biological titre of the different preparations was assessed via an infection assay, titrating each PV over a 2-fold dilution series onto either BHK-21 cells (VSV and RABV G PV) or HEK 293T/17 cells (EBOV GP PV) (Section 2.2.11.1) and measured as previously detailed (Section 2.2.12). The number of particles that were approximately 100 nm in size, corresponding to the diameter of lentivirus, were counted via nanoparticle tracking analysis and recorded as particles/ml (Section 2.2.17). Quantification of the number of genome copies was undertaken via an RT-qPCR reaction, reported as genome copies/ml (Section 2.2.15), and the RT activity measured via an SG-PERT assay and reported as pU/ml (Section 2.2.16) (Standard curves; Appendix IV).

Analysis of the quantification of PV incorporating a firefly luciferase reporter showed that the pattern of highest to lowest biological titres for PV with different envelope proteins (VSV > RABV > EBOV; Figure 6.13A) was inverted when measuring the number of particles (EBOV > RABV > VSV; Figure 6.13B). However, the genome copies and RT activity of the PV preparations correlated with the biological titre rankings (Figure 6.13C&D). For PV incorporating a GFP reporter gene, the biological titre and particle counts mirrored those of PV with a firefly luciferase reporter gene, with an inverse relationship between biological titre and particle count (Figure 6.14A&B); yet this was not the case for the genome copies and RT activity data. Preparations of PV comprising a RABV G or EBOV GP and incorporating a GFP reporter gene consisted of greater genome copies ( $8.7 \times 10^8$  and  $9.5 \times 10^8$  genome copies/ml, respectively) and higher RT activity ( $9.0 \times 10^{10}$  and  $7.0 \times 10^{10}$  pU/ml, respectively) than those with a VSVG ( $2.8 \times 10^8$  genome copies/ml and  $1.5 \times 10^{10}$  pU/ml; Figure 6.14C&D). Finally, the quantification data collected for PV with a *LacZ* reporter showed the same inverse relationship between biological titre and the number

of particles (Figure 6.15A&B). Further, as seen with the firefly luciferase reporter, the quantity of genome copies and RT activity was found to correlate with biological titre (Figure 6.15C&D). In all instances, the number of particles, genome copies and RT activity was lowest when incorporating a *LacZ* reporter, with the biological titres also being lower in comparison to PV with a GFP reporter.

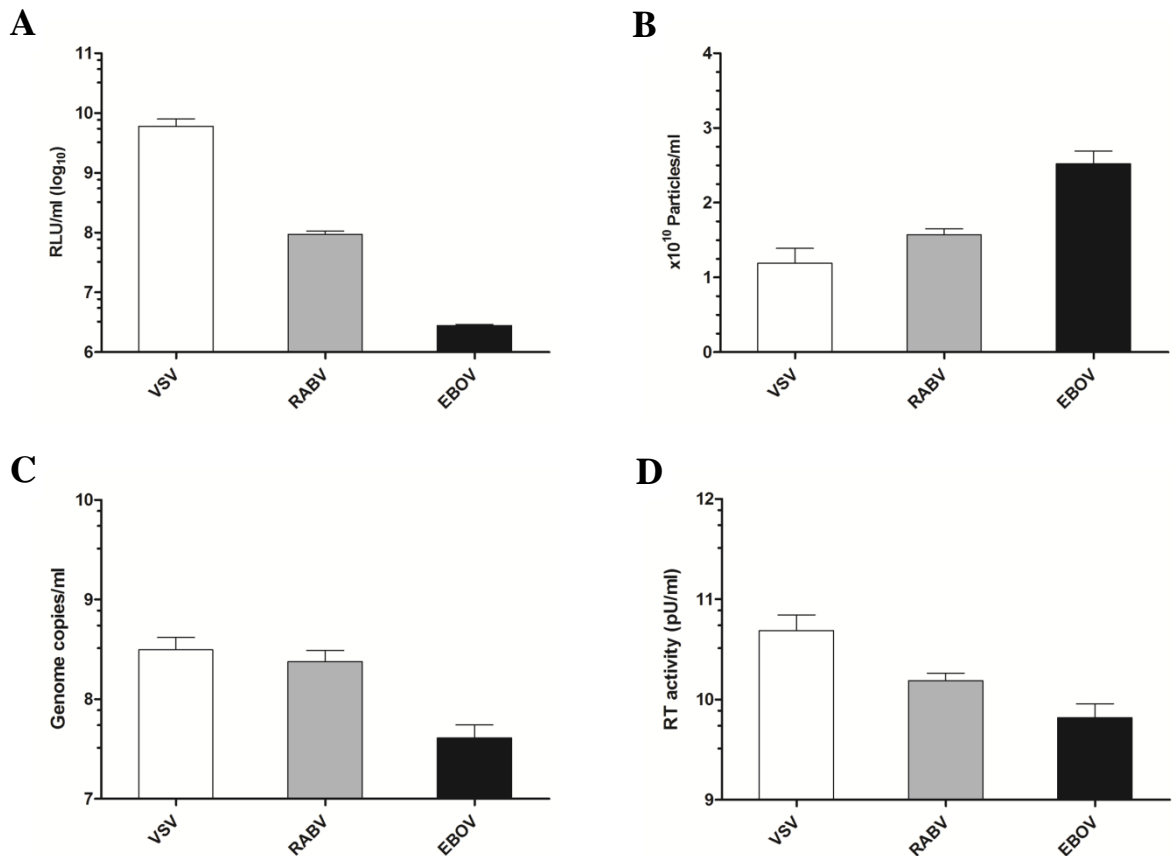


**Figure 6.13 Quantification of Firefly Luciferase Reporter Gene Pseudotyped Virus Comprising a VSV, RABV or EBOV Envelope Glycoprotein**

For the quantification of PV comprising a VSV G, RABV (CVS-11) G or EBOV (Makona) GP and incorporating a firefly luciferase reporter gene (A) biological titres were measured via luminescence and reported as relative light units per ml (RLU/ml) from BHK-21 cells infected with VSV G and RABV G PV and HEK 293T/17 cells infected with EBOV GP PV (n = 2). (B) The number of particles measuring ~100 nm in size were counted via nanoparticle tracking analysis (n = 5). (C) Genome copies were quantified via an RT-qPCR reaction targeting the HIV-1 LTR region (n = 2) and (D) the RT activity was quantified via an SG-PERT assay and reported as pU/ml (n = 2). In all cases error bars represent SD.

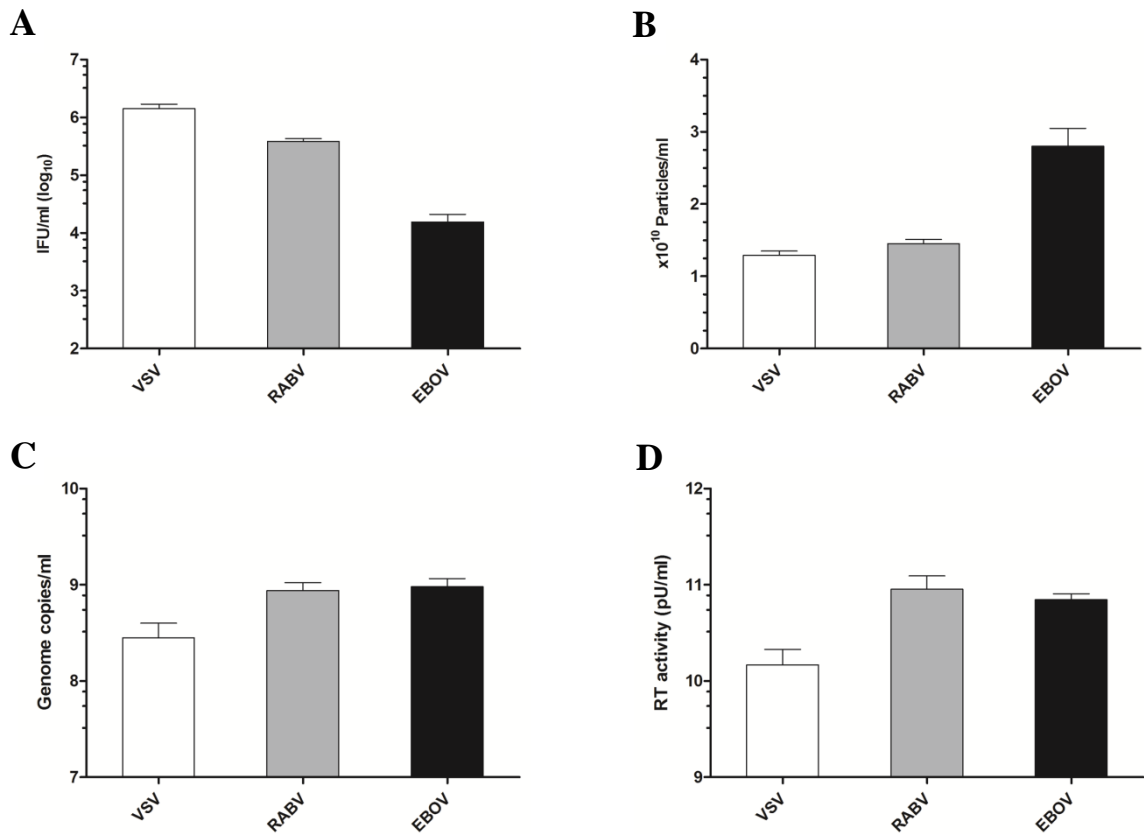


**Figure 6.14 Quantification of Green Fluorescent Protein Reporter Gene Pseudotyped Virus Comprising a VSV, RABV or EBOV Envelope Glycoprotein**

For the quantification of PV comprising a VSV G, RABV (CVS-11) G or EBOV (Makona) GP and incorporating a GFP reporter gene (A) biological titres were measured via fluorescent microscopy and reported as infectious units per ml (IFU/ml) from BHK-21 cells infected with VSV G and RABV G PV and HEK 293T/17 cells infected with EBOV GP PV (n = 2). (B) The number of particles measuring ~100 nm in size were counted via nanoparticle tracking analysis (n = 5). (C) Genome copies were quantified via an RT-qPCR reaction targeting the HIV-1 LTR region (n = 2) and (D) the RT activity was quantified via an SG-PERT assay and reported as pU/ml (n = 2). In all cases error bars represent SD.

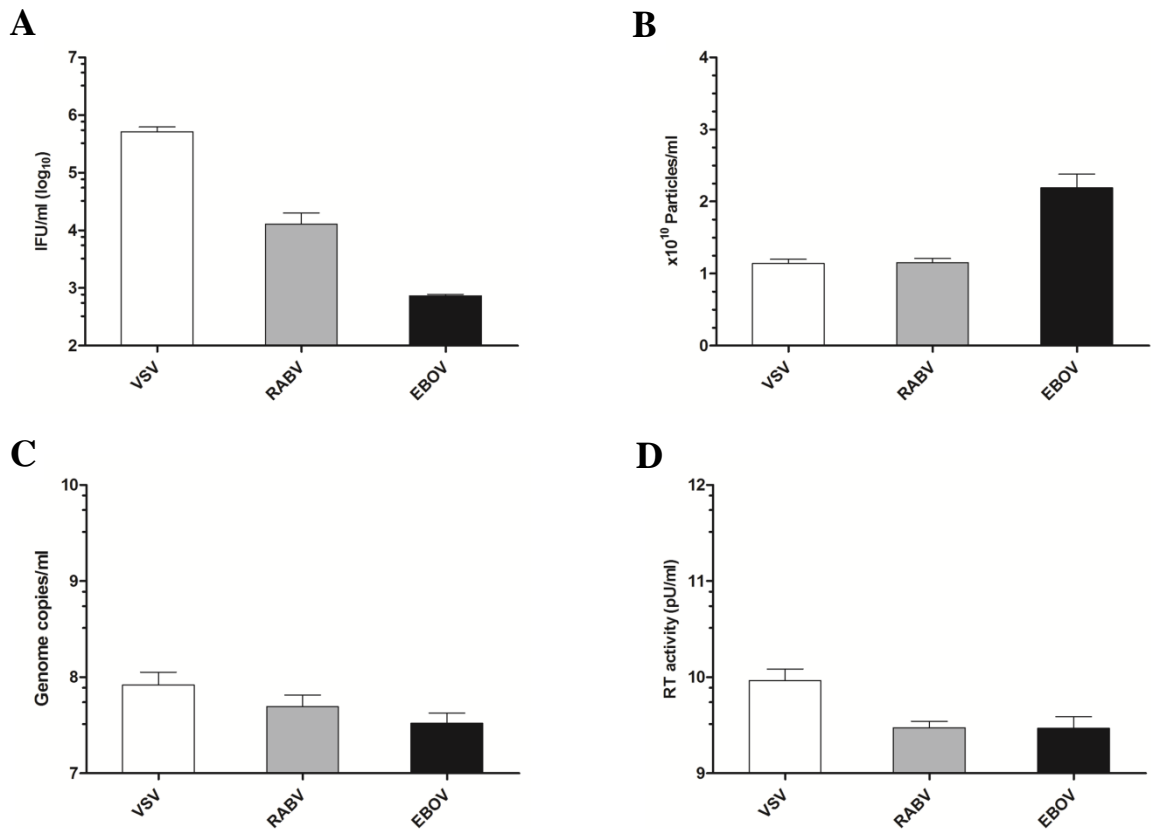


**Figure 6.15 Quantification of *LacZ* Reporter Gene Pseudotyped Virus Comprising a VSV, RABV or EBOV Envelope Glycoprotein**

For the quantification of PV comprising a VSV G, RABV (CVS-11) G or EBOV (Makona) GP and incorporating a *LacZ* reporter gene (A) biological titres were measured via light microscopy and reported as infectious units per ml (IFU/ml) from BHK-21 cells infected with VSV G and RABV G PV and HEK 293T/17 cells infected with EBOV GP PV (n = 2). (B) The number of particles measuring ~100 nm in size were counted via nanoparticle tracking analysis (n = 5). (C) Genome copies were quantified via an RT-qPCR reaction targeting the HIV-1 LTR region (n = 2) and (D) the RT activity was quantified via an SG-PERT assay and reported as pU/ml (n = 2). In all cases error bars represent SD.

To determine if there was a direct relationship between the quantification of PV particles and biological titre; the ratio of particles counted, genome copies and RT activity compared to the measured biological titre was calculated (Table 6.2). It can be seen that the ratios are subject to variation between the different titre (envelope protein) PV preparations and thus these non-functional quantification methods cannot be used to predict the biological titre. The highest titre, VSV G PV, was found to have the lowest ratio in each instance, which demonstrates that the non-functional quantification of PV can be used to indicate for the presence of unviable particles. Interestingly, there is a low level of ratio variance between PV with a GFP versus a *LacZ* reporter which further suggests the envelope protein to be the source of variance.

**Table 6.2 Ratio of Pseudotyped Virus Quantified by Counting Particles, Genome Copies and RT Activity to Biological Titre**

Ratios are calculated for each method of quantification in comparison to the biological titre measured as either RLU/ml or IFU/ml.

<b>Reporter</b>	<b>Envelope Glycoprotein</b>	<b>Ratio of Quantification Data to Biological Titre (QD:BT)</b>		
		<b>Particles</b>	<b>Genome Copies</b>	<b>RT Activity</b>
<b>Firefly Luciferase</b>	<b>VSV</b>	$2.0 \times 10^0$	$1.0 \times 10^{-1}$	$8.1 \times 10^0$
	<b>RABV</b>	$1.7 \times 10^2$	$2.5 \times 10^0$	$1.6 \times 10^2$
	<b>EBOV</b>	$9.0 \times 10^3$	$1.5 \times 10^1$	$2.4 \times 10^3$
<b>GFP</b>	<b>VSV</b>	$9.2 \times 10^3$	$2.0 \times 10^2$	$1.0 \times 10^4$
	<b>RABV</b>	$3.8 \times 10^4$	$2.3 \times 10^3$	$2.3 \times 10^5$
	<b>EBOV</b>	$1.8 \times 10^6$	$6.2 \times 10^4$	$4.5 \times 10^6$
<b>LacZ</b>	<b>VSV</b>	$2.2 \times 10^4$	$1.6 \times 10^2$	$1.8 \times 10^4$
	<b>RABV</b>	$9.0 \times 10^5$	$3.8 \times 10^3$	$2.3 \times 10^5$
	<b>EBOV</b>	$3.0 \times 10^7$	$4.5 \times 10^4$	$4.0 \times 10^6$

### **6.3. Discussion**

The pseudotype platform requires the incorporation of reporters which can be easily detected and measured quantitatively when expressed in transduced cells. The current range of reporters offers the choice of three outputs; luminescence, fluorescence and colourimetric as well as having different cost and resource requirements. Yet the assessment of new reporter genes, which could offer an improvement to the existing portfolio or alternative readout methods, is important to enhance the flexibility of the system. With an increasing uptake in pseudotype technology further characterisation for instance, by determining the correlation between disparate readout units of the different reporter outputs, will enhance their utility. Further, the evaluation of alternative methods to quantify the composition of PV preparations, to provide information on their quality, is highly valuable for the future implementation of standardisation and quality control. This study looked to address each of these aspects; investigating the suitability of new bioluminescent, fluorescent and colourimetric reporters for their incorporation within the pseudotype platform, developing a system to allow correlation of the disparate readout units of reporters and evaluating alternative methods of PV quantification towards future standardisation.

Assessment of the two bioluminescent reporter genes, secreted cypridina luciferase and NanoLuc luciferase, demonstrated they were not suitable for incorporation into the pseudotype platform. The BioLux® cypridina luciferase assay (NEB) was found to have background luminescence activity with just cell culture media that was approximately 100-fold higher than that for currently used assays for the firefly and renilla luciferase reporter gene. This reduces the lower limit of detection and useable dynamic range of the assay. Further, there was not a linear relationship between the volume of PV and cypridina luciferase activity, with an initial negative correlation before turning positive once PV input volumes became lower. While not fully understood, this could be due to contaminants in the PV harvest impairing cell transduction or cytotoxicity that was not detected due to using opaque culture plates, which was overcome by dilution at lower volumes of the PV supernatant. However due to the unfavourably high background luminescence levels this was not investigated further. While the background luminescence from cell media via the Nano-Glo® assay

(Promega) for NanoLuc luciferase was in line with that seen for firefly and renilla luciferase, there was a considerably high level of luminescence from the supernatant containing harvested PV. This was in line with that produced from transduced cells and thus rendered the NanoLuc luciferase unsuitable for the pseudotype platform. The luminescence intensity of NanoLuc is described to be approximately 150-fold more than that of firefly and renilla luciferase, which correlated with the luminescence measured in this study, as well as having a higher physical stability and being only 19 kDa in size compared to the 61 kDa and 36 kDa of firefly and renilla luciferase respectively (Hall *et al.*, 2012). The phenomenon of passively transferred reporter protein was previously discussed (Chapter 4), with some reporter protein thought to be incorporated into PV during their formation (Nash & Lever, 2004). It is suspected the small size of NanoLuc luciferase could favour a higher level of passive incorporation into PV, with the additional factors of its stability and luminescence intensity each contributing to the high level of luminescence observed from the PV supernatant.

Results generated from the incorporation of the colourimetric SEAP into the pseudotype platform, which like cypridina luciferase is secreted, proved it too was not appropriate for use in the PV system. When assaying the culture media of target cells for the presence of SEAP, it was determined the secreted reporter was not being produced yet high levels were detected within the PV supernatant. During transient transfection for PV production, reporter protein expression will be detected as a result of translation and also from transduction of cells by newly generated PV. In fact, the advantage of not requiring disruption of producer cells to detect a secreted reporter protein means SEAP is cited for use to monitor successful transfection (Berger *et al.*, 1988; Cullen & Malim, 1992; Yang *et al.*, 1997). However, secreted SEAP has previously been described as a PV reporter using alternative pseudotyping systems, initially via a transfection method for the intracellular production of papilloma viral vectors (Pastrana *et al.*, 2004) and more recently to produce VSV pseudotyped with Nipah virus F and G proteins (Kaku *et al.*, 2012). The former involves multiple lysis and centrifugation steps to purify the intracellularly produced viral vectors which would eliminate secreted SEAP, while for the latter SEAP is supplied as a replacement to

the VSV glycoprotein within a plasmid encoding the cDNA for the VSV genome (VSV $\Delta$ G-SEAP) which could dampen its expression during transfection. The apparent complete lack of SEAP secretion from transduced cells in this study suggests the efficient packaging of SEAP as an RNA dimer within the PV core or budding of PV from the producer cell membrane during formation could be confounded by its secretion. Alternatively, it is not known whether the presence of secreted SEAP within the PV supernatant may interfere with PV transduction of target cells. It has previously been shown that a secreted proteoglycan acts to inhibit cell infection, with proposed mechanisms of either binding to the envelope protein or cellular receptors to block entry (Le Doux *et al.*, 1996). The use of secreted SEAP was not further explored in this study as additional requirements, such as a purification step, would eliminate its beneficial properties of being a high throughput and resource-sparing PV reporter. However, these results act to highlight potential issues with incorporating secreted reporters into the pseudotype platform.

Each of the fluorescent reporter proteins, dNG and dNT, were successfully incorporated into the pseudotype platform and offered improved visual differentiation of transduced target cells through the nuclear localisation of the fluorescent protein. However, the dNG reporter had a lower fluorescent intensity and both caused an apparent reduction in PV titre. Auto-fluorescence when using a fluorescent protein which emits light in the green spectrum is a common artefact impairing visual clarity, and the result of cellular components absorbing light at wavelengths close to this spectrum (Brogan *et al.*, 2012). The photostability of fluorescent proteins, which bleach upon extended excitation, is a further aspect which determines clarity when imaging and varies greatly amongst the fluorescent proteins (Shaner *et al.*, 2005). While the high fluorescent intensity of enhanced GFP generally minimises the interference of background auto-fluorescence and it also has good photostability, it was found that the dNG reporter had a lower intensity, which impaired differentiation of transduced cells from background auto-fluorescence, and poor photostability. On the other hand, the dNT reporter displayed greater fluorescence intensity and photostability than the currently used GFP. It could be that the reduced PV titre using each of these reporters may arise from their higher molecular weight, due to two copies of the fluorescent protein gene being

included within these dual reporters along with their post-translational trafficking to the nucleus. Further, the reduced number of dNT transduced cells counted via flow cytometry may arise from being unable to use the optimum excitation laser. The tdTomato fluorescent protein has an excitation peak at 554 nm (Shaner *et al.*, 2004), however a 488 nm excitation laser was used within this study. Despite a reduction in PV titre, the dNT reporter is a good addition to the range of reporters incorporated within the PV platform.

In order to correlate the disparate readout units of IFU and RLU, a pDUAL expression plasmid was initially used in an attempt to package and co-express two reporter genes from a single PV. While coincident expression of two fluorescent reporter genes was reported by Escors, *et al.*, (2008), in this study it was found that each of the promoters within the pDUAL expression plasmid, SFFV and UBIQ, did not provide equal levels of reporter gene expression. There were lower, or in the case of the *LacZ* reporter gene, no detectable levels when expression was driven by the UBIQ promoter. The functionality of promoters can be cell type specific due to variations in cell transcription machinery and regulatory factors. However, the UBIQ promoter has previously been shown to offer good gene expression levels in both haematopoietic and mesenchymal cells (Byun *et al.*, 2005), which covers the cell type used in the initial pDUAL study and this study respectively. The choice of promoter is important in the design of reporter plasmids for PV production. It has previously been reported how the transduction efficiency of lentiviral vectors can be underestimated if using a suboptimal promoter and can differ between cell lines originating from different species (Ikeda *et al.*, 2002). In fact, the SFFV promoter was introduced into the currently used pCS[reporter]W expression plasmid to replace a cytomegalovirus (CMV) promoter due to enhanced transgene expression in haematopoietic cells (Demaison *et al.*, 2002). Further, the woodchuck hepatitis virus post-transcriptional regulatory element (WPRE), which was originally found to increase expression of transgenes under the CMV promoter (Zufferey *et al.*, 1999), and subsequently also acted to increase expression when the promoter was changed to SFFV in both cell types (Clements *et al.*, 2006; Demaison *et al.*, 2002), likely contributes to the unbalanced expression between the two promoters.

However, by placing a 2A peptide sequence between two reporter gene sequences, it was possible to achieve equal levels of expression under the single SFFV promoter. The use of 2A peptide sequences has emerged as an improvement to internal ribosomal entry sites (IRES) which are widely employed to express multiple genes from a single vector but have several disadvantages, including their large size and a reported variable or unbalanced level of expression which can differ between cell types (Szymczak & Vignali, 2005). The 2A peptide cleavage mechanism operates via preventing a normal bond formation between a glycine and proline residue of a conserved peptide sequence via a ribosomal skip event during translation. It was initially identified in the foot and mouth disease virus and has since been described in other picornaviruses, insect and rotaviruses (Donnelly *et al.*, 2001; Ryan *et al.*, 1991; Szymczak & Vignali, 2005). The peptide sequences are short and have previously demonstrated equal levels of reporter gene expression, as well as the ability to efficiently express multiple genes (Ibrahimi *et al.*, 2009; Szymczak *et al.*, 2004). Through incorporating both a firefly luciferase and GFP reporter gene into PV, which were expressed in transduced cells via this mechanism, it was possible to correlate the disparate readout units of RLU and IFU. While the combination of data collected from the BHK-21 cell line transduced with a VSV G or RABV G PV indicates 1259 RLU equates to 1 IFU, the ratio was higher from the analysis of data collected from HEK 293T/17 cells transduced with an EBOV GP PV. This may be the result of differences in the efficiency of GFP post-translational modifications or folding between the two cell lines, which may result in reduced sensitivity of the reporter in the HEK 293T/17 cell lines. Further analysis of RLU and IFU ratios in additional cell lines, together with the inclusion of alternative reporters, such as *LacZ*, with the pCS-T2A-W expression plasmid constructed within this study are required to address this finding.

Results from several methods, other than biological titre, to quantify and standardise PV preparations based on targeting the core, RNA genome or evaluating the total number of particles have been shown. Within this study a full assessment of the utility of each method was assessed for PV of varying biological titres and incorporating different reporters. It was shown that when

counting total particles via nanoparticle tracking analysis, a higher particle count did not translate to a higher biological titre. The lowest titre PV preparation consisted of the highest number of particles. As this was not the case for the quantification of genome copies or RT activity which, except for with a GFP reporter, correlated with biological titres, it would suggest a higher proportion of extracellular vesicles are being produced, which shed from the membrane of healthy and virally infected cells and can contain viral protein or RNA, as well as being similar in size to lentiviral PV (Heider & Metzner, 2014; Meckes & Raab-Traub, 2011; Raposo & Stoorvogel, 2013). Therefore a limitation of quantification via nanoparticle tracking analysis is that it cannot differentiate between PV particles and extracellular vesicles. The fact low and mid-titre PV preparations incorporating a GFP reporter had a higher number of genome copies and RT activity, not following the pattern observed for those with a firefly luciferase or *LacZ* reporters, may reflect the packaging efficiency of the smaller GFP reporter gene within the lentiviral core, which could shed within extracellular vesicles. The use of nanoparticle tracking analysis is not a reliable indicator to determine the quantity of PV particles.

While previous studies have used individual assays to assess PV preparations this is the first report where the same PV preparations have been assessed by each assay simultaneously. It has previously been demonstrated that the non-functional quantification of the genome and core components overestimates the level of functional PV, capable of transducing target cells. Quantification of the RNA genome has been reported to give a 10 – 10,000 fold overestimate of the biological titre (Geraerts *et al.*, 2006; Ikeda *et al.*, 2002; Lizée *et al.*, 2003; Sastry *et al.*, 2002) and that of the core component via the SG-PERT assay by approximately 1500 fold (Vermeire *et al.*, 2012). These results are built on here, and can be explained by a multitude of factors, which includes the presence of defective interfering particles (Higashikawa & Chang, 2001; Lizée *et al.*, 2003), such as from PV produced incorporating a mutant genome (Kirkwood & Bangham, 1994) or the stability of the envelope protein which, if unstable, sheds from the PV particle and is less able to withstand freeze-thaw (Davis *et al.*, 1997). The secretion of transduction inhibitors from producer cells during PV generation has also been described, identifying the secretion of

proteoglycans as a major inhibitor (Le Doux *et al.*, 1996). Additionally, it has been shown that reporter gene integration into the genome of a transduced cell may not always result in a detectable level of the reporter being expressed (Lizée *et al.*, 2003; Martin-Rendon *et al.*, 2002; Sastry *et al.*, 2002). It should also be remembered that lentiviral cores are produced, with or without the inclusion of a reporter gene during transfection, as well as in the absence of envelope protein (Geraerts *et al.*, 2006).

While a relatively low level of variance in the non-functional quantification of separate preparations of a single lentiviral vector had been reported (Logan *et al.*, 2004; Vermeire *et al.*, 2012), this study was able to show that between PV preparations incorporating different envelope proteins there was a high level of variation. This is likely linked to the factors stated above associated with the envelope protein, with a difference in stability and level of extracellular vesicle secretion. Calculating the ratio between the non-functional quantification and biological titre was found to be a useful indicator of the quality of PV preparations, with a lower ratio indicating less non-functional particles and associated with a higher biological titre. Therefore, while quantification of genome copies or RT-activity cannot be used to standardise across PV incorporating different envelope proteins, it offers utility in the standardisation of single PV preparations and provides valuable information on their quality.

In conclusion, the current range of reporters incorporated within the pseudotype platform was expanded through the inclusion of a red fluorescent protein reporter, which is nuclear localised and enhances the detection and ability to distinguish transduced cells. Attempts to incorporate secreted reporters into the platform highlighted limitations in their use, owing to the need to purify PV to remove reporter secreted during production. The ability to correlate the disparate readout units of RLU collected using a luminescent reporter and IFU using a fluorescent reporter was achieved through joining two reporter genes with a 2A peptide sequence, for packaging with PV core and subsequent equal expression levels under a single promoter. Initial data suggests approximately 1260 RLU equates to 1 IFU when transducing the BHK-21 cell line, yet future work is required to

assess how this fluctuates between cell lines. Finally, assessment of non-functional quantification methods of multiple PV preparations showed quantifying the genome and core components provides information on the quality of preparations. However, non-functional quantification cannot be used to standardise virus input for downstream assays between PV incorporating different envelope proteins.

## Chapter 7. Conclusions and Future Work

Emerging zoonotic viruses pose a major threat to human and animal health, with significant economic implications. Often, there is a lack or shortfall of effective prophylaxis and diagnostic capabilities. Research towards their development, together with surveillance activities for early detection and an improved understanding of their persistence within host populations, are recognised as high priority activities towards preparedness and the mitigation of outbreak threats. Studies of emerging viruses are commonly limited to high BSL 3 or 4 laboratories, yet this can be circumvented by the use of PV which can be handled at low containment levels, acting as a surrogate for pathogenic viruses. The use of PV in the serological study of emerging viruses is becoming increasingly prominent and it has been reported to be as a safe, robust and flexible tool (Mather *et al.*, 2013; Steffen & Simmons, 2016; Temperton *et al.*, 2015b). This study aimed to exploit novelties in the flexibility of the pseudotype system, quantifying NAb responses raised against the envelope protein of emerging zoonotic viruses using a PVNA and determining the importance of antigenic sites. The study also looked at technical aspects towards PV production, aimed at expanding the repertoire of reporter genes and identifying alternative methods of quantification to assist the standardisation of PV assay input.

The flexibility to manipulate envelope proteins for incorporation within PV offers unique opportunities. Within Chapter 3, it was shown that the low titre of PV bearing the envelope protein of AL RABV could be increased when chimeric envelope proteins incorporating the cytoplasmic domain of VSV, which pseudotypes highly efficiently, were used. This did not alter the neutralisation profile, so permitted serological assessment to confirm the efficacy of existing rabies vaccines and post-exposure prophylaxis against the AL RABV lineage. Given the near 100% case fatality rate associated with rabies and the circulation of AL RABV across rabies endemic Middle East and Asian regions, with India alone reporting more than 20,000 fatalities annually (Kuzmin *et al.*, 2008; Sudarshan *et al.*, 2007), it was important to understand the threat it posed. Indeed, this

work further demonstrates the applicability of the pseudotype system to contribute towards serosurveillance of emerging viruses. Efforts towards rabies control require a comprehensive, high quality, analysis of circulating RABVs (Fooks *et al.*, 2014; Matsumoto *et al.*, 2013). An additional outcome of successfully increasing the titre of AL RABV PV was their inclusion in the study by De Benedictis *et al.*, (2016), screening mAb for broadly neutralising activity against all lyssavirus phylogroups.

Although using a chimeric envelope protein lead to an increase in the titre of the AL RABV PV, the mechanism responsible for this increase remains to be elucidated. As such, attempts within Chapter 5 to replicate this previous success and increase the titre of *Ebolavirus* PV were unsuccessful. This included accounting for structural differences related to alternative classes of fusion protein. The use of a truncated cytoplasmic domain was also investigated, which had been suggested in other studies to either reduce steric hindrance of the cytoplasmic domain, or eliminate an unfavourable interaction with the matrix protein (Frecha *et al.*, 2008; Freed & Martin, 1995). However *Ebolavirus* PV titres were reduced within this study. These results act to highlight the complexities in altering the domains of envelope proteins. Cytoplasmic domains may include trafficking motifs and have direct effects on fusion, while the transmembrane domain is important for correct folding and structural changes during fusion (Cosset & Lavillette, 2011; White *et al.*, 2008). Future work to better understand the reason for the sometimes varying efficiency of PV production with envelope proteins of closely related viral species, which demonstrate relatively high sequence homology, is required. It is thought differences in structural features of the envelope protein, such as glycosylation patterns, may be important factors. Both the lyssavirus and filovirus envelope proteins are glycosylated, with that of filoviruses having a heavily glycosylated mucin-like domain which has a high level of sequence variability between species (Pöhlmann, 2013; Takada, 2012).

Identifying the importance and structural location of neutralising epitopes has been an important part of mAb development. PV has been utilised in studies characterising rabies mAb for this

purpose, with the flexibility to mutate the defined antigenic sites of the rabies envelope protein (De Benedictis *et al.*, 2016; Both *et al.*, 2013b). Work initiated by Evans *et al.*, (2013) looked to use this flexibility to switch antigenic sites between a phylogroup I and II lyssavirus and investigate the effect on neutralisation by polyclonal sera from vaccine recipients. Work undertaken within Chapter 4 expands upon this investigation by including the envelope protein of WCBV, a phylogroup III lyssavirus. Assessment of polyclonal sera samples by a PVNA showed antigenic site III and I were immunologically dominant for the phylogroup I and III lyssaviruses respectively. The neutralisation data also supported the theory that other epitopes may be involved in neutralisation by polyclonal sera than those that have been defined by mAb screening. Future inclusion of other divergent lyssaviruses will help define important immunogens which could be combined to develop a more broadly neutralising vaccine. This work demonstrates how the PVNA platform can be used to perform important serological assessment of the antigenic hierarchy of neutralising epitopes on viral envelope proteins. Combining data collected via the PVNA with antigenic cartography, which constructs a biological map by combining neutralisation and sequence data, will help enhance the quantification of immunological divergence. This would enable low containment assessment of emerging virus variants to help assess vaccine escape, with the use of PV also being applicable to a high throughput approach.

As the production of PV for newly emerging viruses only requires access to the nucleotide sequence of the envelope protein, they are amenable to rapid development. This was exemplified by the work undertaken within Chapter 5 in response to the recent Ebola virus outbreak. Following a PHEIC being declared, there was an urgent call by the WHO for the priority development of efficacious vaccines, antivirals and improved diagnostics. Given members of the *Filoviridae* are BSL 4 pathogens, developing a PVNA was valuable towards the serological assessment of candidate prophylaxis. A library of filovirus PVs was quickly developed, which included the *Zaire ebolavirus* Makona isolate responsible for the outbreak. Following steps to optimise production and performance of the PVNA it was applied to a range of projects, including the assessment of a vaccine undergoing a phase I clinical trial (Ewer *et al.*, 2016). It is proposed that generating and

maintaining a library of PVs for other emerging viruses offers a highly effective outbreak preparedness tool (Temperton & Page, 2015). This would involve optimising PV production for important emerging viruses, such as those listed on the WHO blueprint of priority diseases (Figure 1.1). In future work to optimise production, it would be advisable to consider evaluating the use of alternative pseudotyping cores for improved efficiency and indeed such work has already begun (O’Keefe *et al.*, 2017). It is reported a VSV core can offer a higher incorporation efficiency for certain envelope proteins (King *et al.*, 2016; Whitt, 2010) and thus it would be worth evaluating this system, albeit being more complex to produce PV.

As part of the development of a PV library, and in light of the increasing prominence in the use of PV assays to assess vaccine and antiviral activity, it is recognised that efforts towards their standardisation are required. The work undertaken within Chapter 6 looked to evaluate alternative methods to quantify the composition of PV preparations, in addition to biological titre which is primarily used. It was found that non-functional, molecular, methods to quantify the genome and core components of PV could be used to provide information on the quality of preparations and have potential to be used to standardise input. While it was shown non-functional standardisation cannot be applied between PV incorporating different envelope proteins, it is considered to have utility to be applied as a quality control for repeat production. Additional work was undertaken in Chapter 6 towards an enhanced characterisation of outputs of the PV platform, expanding its functionality. This included incorporating an additional, red fluorescent, reporter gene which offers output in a different spectrum to current fluorescent reporters and has greater clarity for data collection owing to a nuclear localisation signal. Finally, a new construct was produced to integrate and equally express two reporters from cells transduced with PV. For the first time, this allowed a common question on the correlation between the disparate readout units of IFU and RLU to be addressed. Initial data suggest approximately 1260 RLU equates to 1 IFU. Future work to understand how this may fluctuate between target cell lines is required. Both the range of reporters available, which offer different cost and time constraints, combined with an increasing level of

standardisation, make the use of pseudotypes suitable to a range of sectors, with various resource and output requirements.

In summary, the projects undertaken as part of this thesis have exploited many novelties in the flexibility of the pseudotype platform to undertake emerging virus research. This has included manipulating the envelope protein to improve PV production and serologically determine the efficacy of existing prophylaxis, contributing towards emerging virus serosurveillance efforts. It was further exploited to determine the immunological importance of antigenic sites on the envelope protein, informing the development of broadly neutralising prophylaxis. Work to respond to an important emerging virus outbreak, rapidly developing a PVNA which was used in a range of studies, demonstrating the value of the pseudotype platform for both outbreak response and future preparedness. In contributing to technical aspects of PV production, adding to the range of reporter genes, offering a novel way to correlate disparate readout units and identifying the value of other methods of quantification, their functionality and future standardisation are strengthened. These findings have already contributed to continuing studies using PV for emerging virus research and will continue to inform development and the implementation of standardisation to enhance quality controls. Ultimately, the work presented in this thesis supports the notion that the pseudotype platform offers a safe, robust and flexible tool to undertake emerging virus research.

# Appendix I

## I.1. Virus Envelope Protein

**Genus | Species | Isolate | Abbreviation | Accession Number | Length (bp) | Obtained from | Construct ID<sup>1</sup>**

<sup>1</sup>Where applicable refers to amplification primers detailed in Chapter 2 (Table 2.3 – 2.4)

***Lyssavirus* | *Rabies lyssavirus* | Challenge virus standard 11 | CVS-11 | EU352767 | 1575 | APHA | C1.1**

```
ATGGTTCCTCAGGTTCTTTTGTGGTACCCCTTCTGGGTTTTTCGTTGTGTTTCGGGAAGTTCCTCCATTTACACGATACCAGACGAACTTGGTCCCT
GGAGCCCTATTGACATACACCATCTCAGCTGTCCAAATAACCTGGTGTGGAGGATGAAGGATGTACCAACCTGTCCGAGTTCTCCTACATGGAACCT
CAAAGTGGGATACATCTCAGCCATCAAAGTGAACGGGTTCACTTGACAGGTGTTGTGACAGAGGCAGAGACCTACACCAACTTTGTTGGTTATGTC
ACAACCACATTC AAGAGAAAGCATTTCCGCCCCACCCAGACGCATGTAGAGCCGCGTATAACTGGAAGATGGCCGGTGACCCAGATATGAAGAGT
CCCTACACAATCCATACCCCGACTACCCTGGCTTCGAACTGTAAGAACCACCAAAAGAGTCCCTCATTATCATATCCCCAAGTGTGACAGATTTGGA
CCCATATGACAAATCCCTTCACTCAAGGGTCTTCCCTGGCGGAAAGTGCTCAGGAATAACGGTGTCTCTACCTACTGCTCAACTAACCATGATTAC
ACCATTTGGATGCCCGAGGATCCGAGACCAAGGACACCTTGTAACATTTTTACCAATAGCAGAGGGAAGAGAGCATCCAAGGGAACAAGACTTGCG
GCTTTGTGGATGAAAGAGCCCTGTATAAGTCTCTAAAAGGAGCATGCAGGCTCAAGTTATGTGGAGTTCCTGGACTTAGACTTATGGATGGAACATG
GGTCGCGATGCAAACATCAGATGAGACCAATGGTGCCCTCCAGATCAGTTGGTGAATTTGCACGACTTCACTCAGACGAGATTGAGCATCTCGTT
GTGGAGGAGTTAGTCAAGAAAAGAGAGGAATGTCTGGATGCATTAGAGTCCATCATGACCACCAAGTCAGTAAGTTTCAGACGTCTCAGTCACCTGA
GAAAACCTTGTTCCAGGGTTTGGAAAAGCATATACCATATCAACAAAACCTTGATGGAGGCTGATGCTCACTACAAGTCAGTCCGGACCTGGAATGA
GATCATCCCTCAAAAGGGTGTGTTGAAAGTTGGAGGAAGGTGCCATCCTCATGTGAACGGGGTGTGTTTCAATGGTATAAATATTAGGGCCTGACGGC
CATGTCCTAATCCCAGAGATGCAATCATCCCTCCTCCAGCAACATATGGAGTTGTTGAAATCTTCAGTTATCCCCTGATGCACCCCTGGCAGACC
CTTCTACAGTTTTCAAGAAGGTGATGAGGCTGAGGATTTTGTGAAAGTTCACCTCCCGATGTGTACAAACGGATCTCAGGGGTTGACCTGGGTCT
CCCGAACTGGGAAAGTATGTATTGATGACTGCAGGGGCCATGATTGGCCTGGTGTGATATTTCCCTAATGACATGGTGCAGAAGAGCCAATCGA
CCAGAATCGAAACAACGCAGTTTTGGAGGGACAGGGAGGAATGTGTCAGTCACCTCCCAAGCGGAAAAGTCATACCTTCATGGGAATCATATAAGA
GTGGAGGTGAGATCAGACTGTAA
```

***Lyssavirus* | *Rabies lyssavirus* | India.human.87.RV61 | RV61 | KU534939 | 1575 | APHA | C1.2**

ATGGTTCCTCAAGTTCCTTTTGTGGTACCCCTTCTGGTTTTCTCAATGTGTTTTCGGGAAATTCCTATCTATACGATACCAGACAACTTGGTCCCT  
GGAGCCCGATTGACATACATCATCTCAGCTGTCCAAACAACCTGGTGTGGAAGATGAAGGATGCACTAAGTTGTGGGTTTTCTCTACATGGA  
TAAGGTGGGATACATCTCGGCCATAAAAGTAAACGGGTTACGTGCACAGGTGTGGTAACAGAGGCAGAGACTTACACTAAGTTGTGGTATGTT  
ACCACCACGTTCAAAGAAAGCATTTCCGCCAACACCAGATGCATGTGAGCTGCTTACAAGTGAAGATGGCAGGTGACCCAGATATGAAGAAT  
CGCTGCACAATCCGTACCCTGACTACCCTGGCTTCGAACCGTTAAAACCACAAAGGAGTCCCTCGTCATCATATCCCCAAGTGTAGCGGACCTGGA  
CCCATACGACAAATCCCTTCATTCGAGGGTCTTTCTAGCGGGAAGTGTGCGGAATAACAATATCATCTACTTACTGCTCTACTAACCATGATTAC  
ACAATCTGGATGCCTGAGAAATCCGAGACTGGGGACATCTTGTGACATCTTTACCAACAGTAGAGGGAAGAGAGCATCCAAAGGGGGAAAACTTGCG  
GATTTGTTGATGAAAGAGGCTTGTATAAGTCTTTGAAAGGGGCATGCAAACTCAAGTTGTGTGGAGTTCTCGGCCCTTAGACTTATGGATGGAACGTG  
GGTTGCGATGCAAAACATCGGACGAAACCAAGTGGTGTCTCCTGATCAGTTGGTAAATCTACAGACTTTTCGCTCGGACGAGATCGAACATCTTGT  
GTAGAGGAGTTGGTCAAGAAAAGAGAGGAGTGTCTGGATGCACTAGAGTCCATCATGACTACCAAGTCGGTGAGTTTCAGACGCTCTCAGCCACTGA  
GGAACTTGTCCCTGGGTTTCGAAAAGCATAACCATATTCACAAAACCTTGATGGAAGCAGATGCCCATTACAAGTCAGTCCGAACCTGGAATGA  
AATCATCCCTCCAAAGGGTGTGGAGAGTTGGAGGGAGGTGCATCCTCAGTGAAGGGGTGTTTTTAAACGGTATAATACTGGTCCCTGACGGC  
CATGTTCTAATCCAGAAATGCAATCGTCCCTCCTCAGCAGCATATGGAGTTGTGGAAATCCTCAGTTATTTCCCTGATGCACCTTTGGCAGACC  
CGTCTACAGTTTTCAAGGACGGTGTGAAGCAGAGGATTTTGTGAGGTTACACCTCCCGACGTGCACAAACAATTTCAAGTGTGACCTGGGTCT  
CCCCAGCTGGGGAAGGTATGTTTTGGTGAGTGCAGGGTCTTGGTTGTCTGATGTTGACAATTTTCATAATAACATGTTGCGGAAGAGTCCATCGA  
CCCAATCTACACAACACGGTCTCGGGGGACAGGGAGGAAGGTGTGCGGTCACTTCCCAAAGCGGGAAGGTCATATCTTCATGGGAGTCATATAAGA  
GTGGGGTGAGACCAGACTGTGA

***Lyssavirus* | *Rabies lyssavirus* | Pakistan.dog.89.RV193 | RV193 | KU534940 | 1575 | APHA |**

**C1.3**

ATGGTTCCTCAGTTCCTTTTGTGGTACCCCTTCTGGTTTTCTCAATGTGTTTTCGGGAAATTCCTATCTATACGATACCAGACAACTTGGTCCCT  
GGAGCCCGATTGACATTCATCATCTCAGCTGTCCAAACAACCTGGTGTGGAAGATGAAGGATGCACTAAGTTGTGGGTTTTCTCTACATGGA  
TAAGGTGGGATACATCTCGGCCATAAAAGTAAACGGGTTACGTGCACAGGTGTGGTGACAGAGGCAGAGACTTACACTAAGTTGTGGTATGTT  
ACCACCACGTTCAAAGAAAGCATTTCCGCCAACACCAGATGCATGTGAGCTGCTTACAAGTGAAGATGGCCGGTACCCAGATATGAAGAAT  
CGCTGCACAATCCGTACCCTGACTACCCTGGCTTCGAACCGTTAAAACCACAAAGGAGTCCCTCGTCATCATATCCCCAAGTGTAGCGGACCTGGA  
CCCATACGACAAATCCCTTCATTCGAGGGTCTTTCTAGCGGGAAGTGTGCGGAATAACAATATCATCTACTTACTGCTCTACTAACCATGATTAC  
ACAATCTGGATGCCCCGAGAAATCCGAGACTGGGGACATCTTGTGACATCTTTACCAACAGTAGAGGGAAGAGAGCATCCAAAGGGGGAAAACTTGCG  
GGTTTGTGATGAAAGAGGCTTGTATAAGTCTTTGAAAGGGGCATGCAAACTCAAGTTGTGTGGAGTTCTTGGCCCTTAGACTTATGGATGGAACGTG  
GGTTGCGATGCAAAACATCGGACGAAACCAAGTGGTGTCTCCTGATCAGTTGGTAAATCTACAGACTTTTCGCTCGGACGAAATCGAACATCTTGT  
GTGGAGGAGTTGGTCAAGAAAAGAGAGGAGTGTCTGGATGCCTAGAGTCCATCATGACTACCAAGTCGGTGAGTTTCAGACGCTCTCAGCCACTGA  
GAAAACCTTGTCCCTGGGTTTCGAAAAGCATAACCATATTCACAAAACCTTGATGGAAGCAGATGCCCATTACAAGTCAGTCCGAACCTGGAATGA  
AATCATCCATCCAAAGGGTGTGGAGAGTTGGAGGGAGGTGCATCCTCAGTGAAGGGGTGTTTTTAAACGGTATAATACTGGTCCCTGACGGC  
CATGTTCTAATCCAGAGATGCAATCATCCCTCCTCAGCAGCATATGGAGTTGTGGAAATCCTCAGTTATCCCCCTGATGCACCTTTAGCAGATC  
CGTCTACAGTTTTCAAGGACGGTGTGAAGCAGAGGATTTTGTGAGGTTACACCTCCCGACGTGCACAAACAATTTCAAGTGTGACCTGGGTCT  
CCCCAGCTGGGGAAGGTATGTTTTGGCGAGTGCAGGGTCTTGGTTGTCTGATGTTGACAATTTTCATAATAACATGTTGCGGAAGAGTCCATCGA  
CCCAAGTCTACACAACACGGTCTCGGGGGACAGGGAGGAAGGTGTGCGGTCACTTCCCAAAGCGGGAAGGTCATATCTTCATGGGAGTCATATAAGA  
GTGGAGGTGAGACCAGACTGTGA

**C1.4**

ATGGTTCCTCAAGCTCTTTTGTGGTCCCTTCTGGCTTTTCCAATGTGTTTCGGGAAATCCCCATCTACACAATACCAGACAAACTTGGTCCCT  
GGAGCCCGATTGACATACATCATCTCAGCTGTCCAAATAACTTGGTTGTGGAAGACGAAGGATGCACCAACTTGTGGGTTTCTCCTACATGGA  
TAAAGTGGGATACATTTCCGCCATAAAAAGTGAACGGGTTACGTGCACAGGTGTGGTTACAGAGGCTGAGACTTACACTAACTTTGTGGTTATGTT  
ACCACCACGTTCAAGAGAAAGCATTTCCGCCAACACCAGATGCATGTCGAGCTGCTTACAACCTGGAAAATGGCCGGTGACCCAGATATGAAGAAT  
CTCTTCATAATCCGTACCCTGACTACCATTGGCTTCGAACCGTGAACCACGAAAGGAGTCTCTCATCATATATCCCCAAGTGTAGCAGACCTAGA  
CCCATATGACAAATCCCTTCACTCGAGGGTCTTTCTAGCGGGAAGTGTGGGAATAACAATATCATCTACCTACTGCTCGACTAACCATGATTAC  
ACCATCTGGATGCCCGAGAATCTGAGATTAGGGACATCTTGTGACATCTTTACCAATAGTAGAGGGAAGAGAGCATCCAAAGGAGCAAGACTTGGC  
GATTTGTTGACGAAAGAGGCTTGTATAAGTCTTTGAAGGGGCATGCAAGCTCAAATTTATGTGGGTTCTGGGACTTAGACTTATGGACGGAACGTG  
GGTCGCGATGCAACATCGGATGAGACCAAGTGGTGTCCCTGATCAGTTGGTAAATCTACACGACTTTCGCTCGGACGAGATCGAACATCTTGT  
GTGGAGGAGTTGGTCAAGAAAAGAGAGGAGTGTCTGGATGCCCTAGAGTCCATCATGACTACCAAGTCGGTGAGTTTACAGCTCTCAGCCACTTGA  
GAAAACCTTGTCCCTGGGTTCCGAAAAGCATAACCATATTCACAAAACCTGATGGAAGCTGATGCTCACTACAAGTCAGTCAGGACCTGGAACGA  
GATCATCCCTCCAAAGGGTGTCTGAGAGTTGGAGGGAGGTGTATCCCATGTAAACGGAGTGTTTTTAACGGCATAATACTGGGCCCTGACGGC  
CATGTTTTGATCCAGAGATGCAATCATCCCTCCTCAGCAACATATGGAGTTGTTGGAAATCATCAGTTATCCCTCTGATGCATCTTTAGCAGACC  
CGTCTACAGTTTTCAAGACGGTGTGAAGCAGAGGATTTGTTGAGGTTACCTTCCCGATGTGCACAAACAATCTCAGGGGTTGACCTGGGTCT  
CCCTAACTGGGAAAGTATGCTTAATAATTGCAGGGTATGATGCCATGATATGACAATCTTCTTAATGACATGTTGTGGAAGAGGTAATCGA  
CCCAAGTCCACACAACACAGTCTTGGAGGGATAGGGAGGAAGGTGTGAGCCACTTCCCAAGCGGGAAGGTCATATCTCGTGGGAGTCATATAAAA  
CGGGGGTGAGACCAGACTGTGA

ATGGTTCCTCAGGTTCTTTTGTGGTACCCTTCTTGTCTCAATGTGTTTCGGGAAATCCCTATCTATACAATACCAGACAAACTTGGTCCCT  
GGAGCCCGATCGATATACATCATCTCAGCTGTCCAAACAATCTGGTTGTGGAAGATGAAGGATGTACCAACTTGTGGGTTTCTCCTACATGGA  
TAAAGTGGGATACATCTCGGCCATAAAAAGTAAACGGATTACGTGCACAGGTGTGGTGACAGAGGCAGAGACTTACACTAACTTTGTGGTTATGTC  
ACCACCACGTTCAAAAGAAAGCATTTCCGCCAACACCAGATGCATGTCGAGCTGCTTACAACCTGGAAGCTGGCCGGTGACCCAGATATGAAGAAT  
CTCTGCACAATCCGTACCCTGACTACCCTGGCTTCGAACCGTCAAACCCACAAAGGAGTCCCTCGTCATCATATCCCCAAGTGTAGCGGACCTGGA  
CCCATACGACAAATCCCTTCAATTCGAGGGTCTTTCTAGCGGGAAGTGTGGGAATAACAATATCATCTACTTACTGCTCTACTAACCATGATTAC  
ACAATCTGGATGCCCGAGAATCCGAGACTGGGGACATCTTGTGACATCTTTACCAACAGTAGAGGGAAGAGAGCATCCAAAGGAGCAAAACTTGGC  
GATTTGTTGATGAAAGAGGCTTGTATAAGTCTTTGAAAGGGGCATGCAAACTCAAATTTATGTGGAGTTCTTGGCCTTAGACTTATGGATGGAACGTG  
GGTTGCGATGCAACATCGGACGAAACCAAGTGGTGTCTCCTGATCAGTTGGTAAATCTACACGACTTTCGCTCGGACGAGATTGAACATCTTGT  
GTGGAGGAGTTGGTCAAGAAAAGAGAGGAGTGTCTGGATGCACTAGAGTCCATCATGACTACCAAGTCGGTGAGTTTACAGCTCTCAGCCATCTAA  
GAAAACCTTGTCCCTGGGTTCCGAAAAGCATAACCATATTCACAAAACCTTGTGGAAGCAGATGCTCATACAAGTCAGTCGGAACCTGGAATGA  
GATCATCCCTCCAAAGGGTGTGAGAGTGGGAGGGAGGTGTATCCTCAGTGAATGGGGTGTTTTTAACGGTATAATACTGGTCCCTGACGGC  
CATGTTCTAATCCAGAGATGCAATCATCCCTCCTCAGCAGCATATGGAGTTGTTGGAAATCTCAGTTATCCCTCTGATGCACCTTTAGCAGACC  
CATCTACAGTTTTAAGGACGGTGTGAAGCAGAGGATTTGTTGAGGTTACCTTCCCGACGTGCACAAACAATTTCAAGTGTGACCTGGGTCT  
CCCCAGCTGGGAAAGTATGTTTTGGTGAAGTGCAGGGTCTTGGTTGCTGATGTTGACAATTTTCATAATGACATGTTGCGGAAGAGTCCATCGA  
CCCAAGTCTACGCAACACAGTCTCGGAGGACCGGGAGGAAGGTGTGGTCACTTCCCAAGCGGGAAGGTCATATCTTCATGGGAGTCATATAAGA  
CGGGGGTGAGACCAGACTGTGA

***Lyssavirus* | *West Caucasian bat lyssavirus* | **Russia.Bat.02.WCBV** | **WCBV** | **EF614258** | **1578** |**

**GenScript** | **C1.6**

ATGGCTTCCTACTTTGCGTTGGTCTTGAACGGGATCTCTATGGTTTTTCAGTCAAGGTCTTTTCCCCTTTTACACTATCCCTGACCATCTGGGACCAT  
GGACCCCATAGATCTAAGTCACCTTCACTGCCCCGAACAATCTTTACTGATGCCTCTTATGTACAACGAACAAAGCATAACCTACACAGAGTT  
GAAGGTCCGATCATCTGTGTCAAAAAATCCCCGGATTTACATGTACGGGGTAAGAAGTGAATCTGTAAACATATACCAACTTTGTTGGCTATGTG  
ACTACCACGTTCAAGAAAAACACTTTCCTCCTAAATCCAGGGACTGTAGAGAGGCGTATGAGAGGAAGAAAGCAGGAGATCCTAGATATGAAGAGT  
CTTTAGCCACCCATATCCTGACAACAGTTGGCTGAGAACAGTGACTACAACAAAGGATTCCTGGGTGATCATCGAGCCAGTGTAGTGGAGTTAGA  
TATATACACAAGTGCCTTGTATTACCTCTTTTCAAGGATGGAACATGTTCAAAATCTAGAACATATTTCCCCTACTGTCCAACCAATCATGACTTC  
ACCATTTGGATGCCAGAGAGTGAACATAAGATCTGCCTGTAATCTGTTTTCCACAAGTAGAGGGAAACTAGTCAGGAACCGCACATCCACCTGCG  
GGATTATCGATGAGAGAGGGCTGTTGAGATCAGTTAAAGGAGCATGCAAAATATCAATATGCGGTAGGCAGGGAATCCGTTTTAGTGGATGGAACCTG  
GATGCTTTTTAGATACTCAGAGTACTTACCTGTGTGTTCTCCATCACAGTGTCAACACGCACGACATCAAGGTGATGAGCTGGAGAATGCTATA  
GTTTTAGACTTGATTAGGAGGAGAGAAGAATGTCTTGACACCCTAGAAACAATTTTGATGTCAGGATCTGTGAGTACAGGAGGCTGAGTCAATTTCA  
GAAAGCTGGTCCAGGATCTGGGAAGGCTTACTCTTATATAAAACGGCACCTTAATGGAATCAGATGCTCACTACATCAAGGTAGAGAATTTGGTCAGA  
GGTCAATCCACACAAAGGATGCTCATGGTCGGGGGCAAAATGCTATGAGCCAGTCAATGATGTGTATTTCAACGGGATCATTCGGGATTCAAATAAT  
CAGATCTTGATACCTGAGATGCGATCCAGTCTTCTCAGAGAACATGTTGACCTGTTGAAGGCTAATATAGTTCGTTCCAGGATCCAAATGTTACTTA  
GGTCTTTCACATCTGACACTGAAGAAGATATCGTCGAGTTTGTCAACCCCTCATCTCCAAGATACCCAGAAGTTGGTGTGAGATATGGATCTCGGGTT  
ATCAGACTGGAAGAGATCTACTAATTGGATCTTTGGCCGTAGGAGGAGTGGTAGCAATCTTATTATCGGAACATGTTGTCTGAGATGTAGAGCA  
GGGAGAAACAGAAGAACAATCCGATCCAATCATAGGTCATTTGCCATGACGTGGTGTCCATAAAGATAAGGATAAAGTGATTACTTCTTGGGAAT  
CTTACAAGGGACAAACTGCCAATAA

***Vesiculovirus* | *Indiana vesiculovirus* | **Vesicular stomatitis Indiana virus (San Juan 56-NM-B)****

**| VSV | M35219 | 1536 | Addgene #12259 | -**

ATGAAGTGCCTTTTGTACTTAGCCTTTTTATTTCATTGGGGTGAATTGCAAGTTCACCATAGTTTTTCCACACAACCAAAAAGGAAACTGGAAAAATG  
TTCCTTCTAATTACCATTATTGCCCGTCAAGCTCAGATTTAAATTGGCATAATGACTTAATAGGCACAGCCATACAAGTCAAATGCCCAAGAGTCA  
CAAGGCTATTCAAGCAGACGGTTGGATGTGTCTGCTTCCAAATGGGTCACTACTTGTGATTTCCGCTGGTATGGACCGAAGTATATAACACAGTCC  
ATCCGATCCTTCACTCCATCTGTAGAACAATGCAAGGAAAGCATTGAACAAACGAAACAAGGAACTTGGCTGAATCCAGGCTTCCCCTCAAAGTT  
GTGGATATGCAACTGTGACGGATGCCGAAGCAGTGAATTGTCCAGGTGACTCCTCACCATGTGCTGGTTGATGAATACACAGGAGAATGGGTTGATTC  
ACAGTTTCAACGGAATAATGCAGCAATTACATATGCCCACTGTCCATAACTCTACAACCTGGCATTTCTGACTATAAGGTCAAAGGCTATGTGAT  
TCTAACCTCATTTCCATGGACATCACCTTCTTCTCAGAGGACGGAGAGCTATCATCCCTGGGAAAGGAGGGCACAGGGTTGAGAAGTAACTACTTTG  
CTTATGAAACTGGAGGCAAGGCTGCAAAATGCAATACTGCAAGCATTTGGGGAGTCAGACTCCCATCAGGTGCTGTTGTTGAGATGGCTGATAAGGA  
TCTCTTTGCTGCAGCCAGATTCCTGAATGCCAGAAAGGTCAGATATCTCTGCTCCATCTCAGACCTCAGTGGATGTAAGTCTAATTCAGGACGTT  
GAGAGGATCTGGATTATTCCTCTGCCAAGAACTGGAGCAAAATCAGAGCGGGTCTTCCAATCTCTCCAGTGGATCTCAGCTATCTTGCTCCTA  
AAAACCCAGGAACCGGCTCTGCTTTCACCATAATCAATGGTACCCTAAAATACTTTGAGACCAGATACATCAGAGTCGATATTGCTGCTCAATCCT  
CTCAAGAATGGTCGGAATGATCAGTGAACACCACAGAAAGGAACTGTGGGATGACTGGGCACCATATGAAGACGTGGAATTTGGACCAATGGA  
GTTCTGAGGACCAGTTCAGGATATAAGTTTCCTTTATACATGATTGGACATGGTATGTTGGACTCCGATCTTCACTTAGCTCAAAGGCTCAGGTGT  
TCGAACATCCTCACATTCAGACGCTGCTTCGCAACTTCCCTGATGATGAGAGTTTATTTTTGGTGATACTGGGCTATCCAAAAATCCAATCGAGCT  
TGTAAGAGTTGGTTCAGTAGTTGAAAAGCTCTATTGCCTCTTTTTCTTTATCATAGGTTAATCATTGGACTATTCTTGGTTCTCCGAGTTGGT  
ATCCATCTTTGCATTAATTAAGCACACCAAGAAAAGACAGATTTATACAGACATAGAGATGAACCGACTTGGAAGTAA

**Graham Simmons, Bloodsystems USA | C2.1**

ATGGGCGTTACAGGAATATTGCAGTTACCTCGTGATCGATTCAAGAGGACATCATTTCTTTCTTTGGGTAATTATCCTTTTCCAAAGAACATTTTCCA  
TCCCCTTGGAGTATCCACAATAGCACATTACAGGTTAGTGATGTCGACAACTAGTTTGTCTGACAACTGTCATCCACAAATCAATTGAGATC  
AGTTGGACTGAATCTCGAAGGGAATGGAGTGGCAACTGACGTGCCATCTGCAACTAAAAGATGGGGCTTCAGGTCGGGTGCCACCAAAGTGGTC  
AATTATGAAGCTGGTGAATGGGCTGAAAACCTGCTACAATCTTGAATCAAAAAACCTGACGGGAGTGAGTGTCTACCAGCAGCGCCAGACGGGATTC  
GGGGCTTCCCCCGGTGCCGATGTGACAAAAGTATCAGGAACGGGACCGTGTGCCGGAGACTTTGCCTTCCATAAAGAGGGTGCTTTCTTCTGT  
TGATCGACTTGTCTCCACAGTTATCTACCAGGAACGACTTTTCGCTGAAGGTGTCGTTGCATTCTGATACTGCCCAAGCTAAGAAGGACTTCTTC  
AGCTCACACCCCTTGAGAGAGCCGGTCAATGCAACGGAGGACCCGCTAGTGGTACTATTCTACCACAATTAGATATCAGGCTACCGGTTTTGGAA  
CCAATGAGACAGAGTACTTGTTCGAGGTTGACAATTTGACCTACGTCCAACCTTGAATCAAGATTCACACCACAGTTTCTGCTCCAGCTGAATGAGAC  
AATATATACAAGTGGGAAAAGGAGCAATACCACGGGAAAACTAATTTGGAAGGTCAACCCGAAATGATACAACAATCGGGGAGTGGCCCTTCTGG  
GAACTAAAAAAACCTCACTAGAAAAATTCGCAGTGAAGAGTTGCTTTTACAGTTGTATCAAACGGAGCCAAAAACATCAGTGGTCAGAGTCCGG  
CGGAACTTCTCCGACCCAGGGACCAACAACAACCTGAAGACCACAAAATCATGGCTTCAGAAAATTCCTCTGCAATGGTTCAAGTGCACAGTCA  
AGGAAGGGAAGCTGCAGTGTGCACTTAACAACCCCTTGCACAATCTCCACGAGTCCCAATCCCTCACAACCAAAACAGGTCGGGACAACAGCACC  
CATAATACACCCGTGTATAAACTTGACATCTCTGAGGCAACTCAAGTTGAACAACATCACCGCAGAACAGACAACGACAGCAGCCTCCGACACTC  
CCTCTGCCACGACCGCAGCCGACCCCAAAAGCAGAGAACCAACACGAGCAAGAGCACTGACTTCCTGGACCCCGCCACCAACAAGTCCCA  
AAACCACAGCGAGACCCTGGCAACAACAACACTCATACCAAGATACCGGAGAAGAGAGTCCAGCAGCGGGAAGCTAGGCTTAATTACCAATACT  
ATTGCTGGAGTTCGAGGACTGATCACAGGCGGGAGAAGAATCGAAGAGAAGCAATTTGTCATGCTCAACCCAAATGCAACCCCTAATTTACATTACT  
GGACTACTCAGGATGAAGGTGCTGCAATCGGACTGGCTGGATACCATATTTTCGGCCAGCAGCCGAGGGAATTTACATAGAGGGGCTAATGCACAA  
TCAAGATGGTTAATCTGTGGGTTGAGACAGCTGGCCACGAGACGACTCAAGCTCTTCAACTGTTCTGAGAGCCACAACCTGAGCTACGCACCTTT  
TCAATCTCAACCGTAAGGCAATTGATTTCTTGTGTCAGCGATGGGGCGCACATGCCACATCTGGGACCGGACTGCTGTATCGAACCACATGATT  
GGACCAAGAACATAACAGACAAAATGATCAGATTATTCATGATTTTGTGATAAAACCCCTCCGGACCAGGGGACAAATGACAATTTGGTGGACAGG  
ATGGAGACAATGGATACCGGCAGGTATTGGAGTTACAGGCGTTGTAATTGCAGTTATCGCTTTATTCTGTATATGCAAATTTGTCTTTTAG

**KJ660346 | 2031 | Alain Townsend, University of Oxford | C2.2**

ATGGGCGTGACCGGAATCCTGCAGCTGCCAGAGACAGGTTCAAGCGGACCAGCTTCTTCTGTGGGTGATCATCCTGTTCCAGCGGACCTTCAGCA  
TCCCCTTGGGCGTGATCCACAACAGCACCCTGCAGGTCTCCGACGTGGACAAGCTCGTGTGCCGGGACAAGCTGAGCAGCACCAACAGCTGCGGAG  
CGTGGGCTGAACCTGGAAGGCAACGGCGTGGCCACCGATGTGCCAGCGCCACCAAGAGATGGGGCTTCAGATCCGGCGTGCACCCAAAGTGGTG  
AACTACGAAGCCGCGAGTGGCCGAGAAGTGTACAACCTGAAATCAAGAAGCCGACGGCAGCGAGTGCCTGCCTGCCCTCTGATGGCATCC  
GGGGCTTCCCAGATGCAGATACGTGCACAAGGTGTCGGCCACCGCCCTGTGTGGCGACTTCGCTTTACAAAGAGGGCGCTTTTCTCTGT  
CGACCGGCTCGCCAGCACCCTGATCTACCGGGCACCCTTTGCCGAGGGCGTGGTGGCTTCTGATCTGCCCCAGGCCAAGAAGGACTTCTTC  
AGCAGCCACCCTCTGCGGAGCCGTGAACGCCACAGAAGATCCAGCAGCGGCTACTACAGCACCACCATCAGATACCAGGCCACCGGCTTCGGCA  
CCAACGAGACAGAGTACCTGTTCGAGGTGGACAACCTGACCTACGTGACGCTGGAAGCCGGTTACCCCTCAGTTTCTGCTGCAGTGAACGAGAC  
AATCTACGCCAGCGGCAAGCGGAGCAACACCACCGCAAGCTGATCTGAAAAGTGAACCCCGAGATCGACACCACAATCGGAGAGTGGCCCTTCTGG  
GAGACAAAGAAGAACCTGACCCGGAAGATCAGAAGCGAGGAAGTGAAGCTTACCCGCGTGTCCAACGGCCCCAAGAACATCAGCGGCCAGAGCCCCG  
CCAGAACCAGCAGCAGCCCCGAGACAAAACACCACCAACGAGGACCACAAGATCATGGCCAGCGAGAACAGCAGCGCCATGGTGCAGGTCCACAGCCA  
GGGCAGAAAAGGCCCGTGTCTCACCTGACCACCTCGCCACCATCAGCACCAGCCCTCAGAGCTGACCACCAAGCTGGCCCCGACAACCTCCACC  
CACAACACCCCTGTGTACAAGCTGGACATCAGCAGGACCACCAAGTGGGACAGCACCACAGACGGGCCGACAACGACAGCACCGCCAGCGATACCC  
CTCCAGCCACAACAGCCGCCGACCCCTGAAGGCCGAGAACCAACACCAGCAAGAGCGCGACAGCCTGGATCTGGCCACCACAACAGTCTCTCA  
GAATCTCCGAGACAGCCGGAACAACAACACCACCACAGGACACCGGCGAGGAAAGCGCCAGCTCTGGCAAGCTGGCCCTGATCACCACAACA  
ATCGCCGCGTGGCCGACTGATCACCAGGAGCAGCAGGACCAGACGGGAAGTGTGTAACGCCAGCCAAAGTGAACCCCAACCTGCACTACT  
GGACCACCAGGACGAGGGCGCTGCTATCGGCTGGCTGGATTCCTTACTTCGGCCCTGCCCGGAGGGCATCTACCCGAGGGCTGATGCACAA  
CCAGGACGGCCTGATCTGCGGCTGCGGACGCTGGCCAAAGAGAACACCAGGCCCTGCAGCTGTTCTGCGGGCCACCACCAGGCTGCGGACCTTC  
TCCATCTGAACGAAAAGCCATCGACTTCTGTGTCAGCGTGGGAGGACCTGTACATCTGGGCCCGACTGCTGCATCGAGCCCCACGACT  
GGACCAAGAATATCACCGACAAGATCGACCAGATCATCCAGACTTCGTGGACAAGACCCCTGCCCGACAGGGGACAAACGATAAAGTGGTGGACCGG  
CTGGCGCAGTGGATTCCAGCCGGAATCGGAGTGACCGCGTGTATTCGCGTGTATCGCCCTGTTCTGCATCTGCAAGTTCGTGTTCTGTA

**Synthesised, BioBasic | C2.3**

ATGGTTACATCAGGAATTCTACAATTGCCCGTGAACGCTTCAGAAAAACATCATTTTTTGTGGGTAATAATCCTATTTCCAAAGTTTTCCCTA  
TCCCATTGGGCGTAGTTCACAACAACACTCTCCAGGTAAGTGATATAGATAAAATTGGTGTGCCGGGATAAACTTCTCCACAAGTCAGCTGAAATC  
GGTCGGGCTTAATCTAGAAGGTAATGGAGTTGCCACAGATGTACCAACAGCAACGAAGAGATGGGGATTCCGAGCTGGTGTCCACCCAAAGTGGTG  
AACTACGAAGCTGGGAGTGGGCTGAAAACCTGTACAACCTGGACATCAAGAAAGCAGATGGTAGCGAATGCCTACCTGAAGCCCCTGAGGGTGTAA  
GAGGCTTCCCTCGCTGCCGTTATGTGCACAAGGTTTCTGGAACAGGGCCGTGCCCTGAAGGTTACGCTTTCACAAAAGAAGCGCTTCTTCTCTGTA  
TGATCGACTGGCATCAACAATCATCTATCGAAGCACCACGTTTTTCAAGGTTGTGTGGCTTCTTGATCTCCCCGAAACTAAAAAGGACTTTTTTC  
CAATCGCCACCCTACATGAACCGGCAATATGACAACAGCCATCCAGCTACTACCACACAGTCACTTAATTATGTGGCTGACAATTTTGGGA  
CCAATATGACTAACTTTCTGTTTCAAGTGGATCATCTAAGTATGTGCAACTTGAACCAAGATTACACCCACAATTTCTGTCCAACCTCAATGAGAC  
CATTATACTAATGGGCGTCGCAGCAACACCACAGGAACACTAATTTGGAAAGTAAATCCTACTGTTGACACCGCGGTAGGTGAATGGCCCTTCTGG  
GAAAATAAAAAAACTTCACAAAAACCCCTTCAAGTGAAGAGCTGTCTGTATATTTGTACCAAGAGCCCAGGATCCAGGCAGCAACCAGAACGGA  
AGGTCACCTCCACCAGCTTCGCCAACCAACCAACCTCCAAGAACCACGAAGACTTGGTTCAGAGGATCCCGCTTCAGTGGTCAAGTGCAGACCT  
CCAGAGGGAAAAACAGTGCAGCCACCCACCCAGACACAGTCCCAACAACCTGATCCCCGACACAATGGAGGAACAAACCACAGCCACTACGAA  
CCACCAAAACATTTCCAGAAAACCATCAAGAGAGGAACAACACCCGCACACCCCGAAACTCTCGCCAACAATCCCCAGACAACCAACCCCGTCGACAC  
CACCTCAAGACGGTGAGCGGACAAGTTCCACACAACACCCCTCCCCCGCCAGTCCCAACCAGCAATCCATCCACCACACGAGAGACTCACAT  
TCCCACCACAATGACAACAAGCCATGACACCCAGCAGCAATCGACCAACCAATTTGACATCAGCGAGTCTACAGAGCCAGGACCCTCACCAACACC  
ACAAGAGGGGCTGCAATCTGTGTGACAGGCTCAAGAAGAACCAGGAAATCACCTGAGAACACAAGCAAATGCAACCCAAACCTACACTATT  
GGACAACCAAGATGAAGGGGCTGCCATTGGTTAGCTGGATACCTTACTTCGGGCCCGCAGCAGAGGGAATTTATACGGAAGGGATAATGCACAA  
TCAAAATGGGCTAATTTGCGGTTGAGGCAGCTAGCAATGAGACGACTCAAGCCCTACAGTTATTTCTGCGTGTACCACGGAATTCGCGACTTTC  
TCTATATTGAATCGAAAAGCCATCGACTTTTTACTCCAAGATGGGAGGAACGTGCCACATCTTAGGCCAGATTGCTGTATTGAGCCCATGATT  
GGACTAAGAACATTACTGACAAAATAGATCAAATCATTCATGATTTTATTGATAAACTCTACCAGATCAAACAGATAATGACAATTTGGTGGACAGG  
GTGGAGGCAATGGGTTCTGCGGGGATCGGGATCACGGGGTAATAATCGCAGTTATAGCACTGCTGTGTATTGCAATTTCTACTCTAA

**Simmons, Bloodsystems USA | C2.4**

ATGGGAGCGTCAGGGATTCTGCAATTGCCCGTGAACGCTTCAGAAAAACATCTTTCTTTGTTGGGTAATAATCCTATTTCCATAAAGTCTTTTCAA  
TCCCCTGGGGGTTGTACACAACAATACCCATCAAGTGAAGTATTTGACAAGTTTGTGTGCCGAGACAAACTCTCTTCAACTAGCCAAATGAAGTC  
AGTCGGGTTGAACCTGGAGGGCAATGGAGTAGCAACTGATGTACCAACGGCAACCAAAAGATGGGGTTTTCCGAGCTGGTGTCCACCAAAAGTGGTA  
AATTGCGAAGCTGGAGAAATGGGCTGAGAAGTGTATAACCTGGCTATAAAGAAAGTTGATGGTAGTGAAGTCCACCAGAGCCCTGAGGGAGTGA  
GGGATTTTCCCCTGTTGCCGCTATGTACACAAAGTCTCAGGAAGTGGACCATGCCAGGAGGACTCGCTTTCACAAAGAAGGAGCTTCTTCTCTGTA  
TGACCGACTCGCATCAACAATCATTTATCGGGGTACAACCTTCCGCAAGGAGTTATTGCATTTCTGATCTTGCTTAAGGCGCAAGGATTTTTTC  
CAGTCTCCTCCATTCGATGAGCCTGCCAACATGACCACGGATCCCTCCAGTTACTATCACACGACAACAATAAACTACGTGGTTGATAATTTGGAA  
CCAACACCACAGAGTTTCTGTCCAAGTGCATCATTTGACGTATGTGCAGCTCGAGGCAAGATTACACCCACAATTCCTGTCTCTTAAATGAAAC  
CATCTACTCTGATAACCCGAGAAGTAACACAACAGGAAAACCTAATCTGAAAAATAAATCCCACTGTTGATACCAGCATGGGTGAGTGGGCTTTCTGG  
GAAAATAAAAAAACTTCACAAAAACCCCTTCAAGTGAAGAGTTGTCTTTCGTACCTGTACCAGAAAACCCAGAACCCAGGTCCTTGACACGACAGCGA  
CGGTCTCTCTCCATCTCCGCCACAACCACGACGCGAAGACCACAAAGAATTGGTTTCAGAGGATTCCACTCCAGTGGTTGAGATGCAAAACAT  
CAAGGAAAAGGACACAATGCCAACCAACAGTGACGGGTGTACCAACAACCACACCTCTCCATTTCCAATCAATGCTCGCAACACTGATCATACAAA  
TCATTTATCGCCCTGGAGGGGCCCAAGAAGACCACAGCACCACACAGCTGCCAAGACCACAGCCAAACCAACAGCAGACAATAATCGACGACAC  
TAAACCAACATCAGAGCCCTCCAGTAGAGGCACGGGACCATCCAGCCCACGGTCCCAACACCACAGAAAGCCAGCCGAACTTGGCAAGACAAC  
CCCAACCACACTCCAGAACAGCACAACCTGCCCCAGTGCATTTCAAGAGCCGTGCACCCGACGAACTCAGTGGACCTGGCTTCTGACGAACACA  
ATACGGGGGGTTACAATCTCCTGACAGGATCCAGAAGAAAGCGAAGGGATGTCACTCCCAATACACAACCCAAATGCAACCCAAACCTGCACTATT  
GGACAGCCTTGGATGAGGGTGTGCCATAGGTTTAGCTGGATACCACTTCCGGCCAGCAGCTGAGGGAATTTACTGAAAGGCAATAATGGAGAA  
TCAAAATGGATTGATCTGTGGATTGAGGCAGCTGGCCAACGAAACGACACAAGCTCTCAATGTTCTTAAGGGCAACTACTGAGTTGCGTACATTC  
TCTATACTAAATCGAAAAGCAATAGACTTCTGTCTCAAAGATGGGAGGAACATGTACATTTCTAGGGCTGATTGTTGCATTGAACCCCAAGATT  
GGACCAAAAATATCACTGATAAAATGATCAAATAATCCATGACTTTGTGATAATAATCTTCCAATCAGAATGATGGCAGCAACTGGTGGACTGG  
ATGGAACAATGGGTTCTGCTGGAATAGGAATCACAGGAGTAATCATTGCTATTATTGCTTGTGTGATTTGCAATTCATGCTTTGA

***Ebolavirus* | *Sudan ebolavirus* | SUDV/Boniface/SUD/1976 | SUDV | FJ968794 | 2031 | Graham**

**Simmons, Bloodsystems USA | C2.5**

ATGGAGGGTCTTAGCCTACTCCAATTGCCAGAGATAAAATTCGAAAAGCTCTTCTTTGTTGGGTCATCATCTTATTTCAAAGGCCTTTTCCA  
TGCCTTTGGGTGTGTGACCAACAGCACTTTAGAAGTAACAGAGATTGACCAGCTAGTCTGCAAGGATCATCTTGCATCCACTGACCAGCTGAAATC  
AGTTGGTCTCAACCTCGAGGGGAGCGGAGTATCTACTGATATCCCATCTGCGACAAAGCGTTGGGGCTTCAGATCTGGTGTGCCCTCCAAGTGGTC  
AGCTATGAAGCAGGAGAATGGGCTGAAAATTCGTACAATCTTGAATAAAGAAGCCGGACGGGAGCGAATGCTTACCCCCACCGCCGGATGGTGTCA  
GAGGCTTTCCAAGGTGCCGTATGTTTCAAAAGCCCAAGGAACCGGGCCCTGCCCGGGTGACTATGCCTTTTCAAGGATGGAGCTTTCTTCTCTA  
TGACAGGCTGGCTTCAACTGTAATTTACAGAGGAGTCAATTTTGTGAGGGGTAATTTGCATTTCTTGATATGGCTAAACCAAGGAAACGTTTCTT  
CAATCACCCCCATTCGAGAGGCAGTAAACTACACTGAAAATACATCAAGTTACTATGCCACATCCTACTTGGAGTACGAAAATCGAAAATTTTGGTG  
CTCAACACTCCAGACCCCTTTTCAAATTAACAATAACTTTTGTCTTCTGGACAGGCCCCACAGCCCTCAGTTCCTTTTCCAGCTGAATGATAC  
CATTACCTTCACCAACAGTTGAGCAACACAACCTGGGAACTAATTTGGACACTAGATGCTAATATCAATGCTGATATTGGTGAATGGGCTTTTGG  
GAAAATAAAAAAATCTCTCCGAACAACCTACGTGGAGAAGAGCTGTCTTTGAAAACCTTATCGCTCAACGAGACAGAAGACGATGATGCGACATCGT  
CGAGAACTACAAAGGGAAGAAATCTCCGACCGGGCCACCAGGAAGTATTCGGACCTGGTTCCAAAGGATTTCCCTGGGATGGTTTCATTGCACGTACC  
AGAAGGGGAAACAACATTCGCGTCTCAGAATTCGACAGAAGTTCGAAGAGTAGATGTGAATACTCAGGAACTATCACAGAGACAACCTGCAACAATC  
ATAGGCACCTAACGGTAACAACATGCAGATCTCCACCATCGGGACAGGACTGAGCTCCAGCCAAATCCTGAGTTCCTCACCGACCATGGCACCAGCC  
CTGAGACTCAGACCTCCACAACCTACACACCAAAACTACAGTGTGACCACCGAGGAATCAACAACACCACCGAGAACTCTCCTGGCTCAACAAC  
AGAAGCACCCACTCTCACCCCCAGAGAATATAACAACAGCGGTAAAACTGTTTTGCCACAAGAGTCCACAAGCAACGGTCTAATAACTTCAACA  
GTAACAGGGATTCTTGGGAGCCTTGGACTTCGAAAACGCAGCAGAAGACAAGTTAACACCAGGGCCACGGGTAATGCAATCCCACTTACACTACT  
GGACTGCACAAGAACAACATAATGCTGCTGGGATTGCCCTGGATCCCGTACTTTGGACCGGGTGCAGAAGGCATATACACTGAAGGCCTTATGCACAA  
CCAAAATGCCTTAGTCTGTGGACTCAGACAACCTGCAATGAAACAACCTCAAGCTCTGCAGCTTTTCTTAAAGGGCCACGACGGAGCTGGGCATAT  
ACCATACTCAATAGGAAGCCATAGATTTCTTCTGCGACGATGGGGCGGACATGTAGGATCCTGGGACCAGATTGTTGCATTGAGCCACATGATT  
GGACCAAAAAATCAGCTGATAAAAATCAACCAAATCATCCATGATTTTATCGACAAACCTTTACCCAATCAGGATAATGATGATAATTTGGTGGACGGG  
CTGGAGACAGTGGATCCCTGCAGGAATAGGCATTACTGGAATTATTATTGCAATCATTGCTCTTCTTTGCGTCTGCAAGCTGCTTTGTGTA

***Ebolavirus* | *Reston ebolavirus* | RESTV/Pennsylvania/USA/1989 | RESTV | AY769362 | 2034 |**

**Graham Simmons, Bloodsystems USA | C2.6**

ATGGGGTCAGGATATCAACTTCTCCAATTGCCTCGGGAACGTTTTTCGTA AAAACTTCGTTCTTAGTATGGGTAATCATCCTCTTCCAGCGAGCAATCT  
CCATGCCGCTTGGTATAGTGACAAAATAGCACTCTCAAAGCAACAGAAATGATCAATTTGGTTTGTTCGGGACAAAAGTGTATCAACAGCTCAGCTCAA  
GTCTGTGGGGCTGAATCTGGAAGGAAATGGAATTGCAACCGATGTCCCATCAGCAACAAAACGCTGGGGATTTCTGTTACAGTGTGCCCTCCAAGGTG  
GTCAGCTATGAAGCCGGAGAATGGGCAGAAAATTCGTACAATCTGGAGATCAAAAAGTCAAGCAGGAAAGTGAATGCCTCCCTCCTCCGACCGGTG  
TACGAGGATTCCTAGATGTCTGATGTCCACAAAAGTCAAGGAACAGGTCCTTGTCCCGGTGACTTAGCTTTCCATAAAAAATGGGGCTTTTCTTCT  
GTATGATAGATTGGCCTCACTGTCTATCTACCGAGGGACAACCTTTGCTGAAGGTGCTGCTAGCTTTTTTAATTCGTGACAGCCCAAGAAGCATTTT  
TGGAAGGCTACACCAGCTCATGAACCGGTGAACACAACAGATGATCCACAAGCTACTACATGACCTGACACTCAGTACGAGATGTCAAATTTG  
GGGGCAATGAAAGTAACACCTTTTTTAAGGTAGACAACCACACATATGTGCAACTAGATCGTCCACACACTCCGAGTTCCTTGTTCAGCTCAATGA  
AACACTTCGAAGAAAATATCGCCTTAGCAACAGTACAGGGAGATTGACTTGGACATTGGATCCTAAAAATGAACCAGATGTTGGTGAAGTGGGCTTCT  
TGGGAAACTAAAAAAAATTTTTCCCAACAACCTTCATGGAGAAAACCTGCAATTTCCAAATCTATCAACCCACACCAACAACCTCCTCAGATCAGAGCC  
CGGCGGAACTGTCCAAGGAAAAATTAGCTACCACCCACCGCAACAACCTCCGAGCTGGTTCCAACGGATTCCCTCCAGTGGTTTTCAGTGTCTCAC  
TGCAGGACGACAGAGGAAATGTGACCCAAAGGTCTAACCAACGGAGAGACAATCACAGGTTTACCGCGCAACCAATGACAACCACCATTGCCCA  
AGTCCAACCATGACAAGCGAGGTTGATAACAATGTACCAAGTGAACAACCGAACAACACAGCATCCATTGAAGACTCCCCCCTCAGGCAAGCAACG  
AGACAATTTACCACTCCGAGATGGATCCGATCCAAGGCTCGAACAACCTCCGCCAGAGCCACAGACCAAGACCACGCCAGCACCACAACATCCCC  
GATGACCCAGGACCCGAAGAGACGGCCAACAGCAGCAAACAGGAACAGCCAGGAAAGCGCAGCCGACCAAGTACAGCCCGGACTCACATAAAAT  
ACAGTAAGTAAGTAGCTGATTCAGTGTCCACCAGGAAACAAAGGCGATCGGTTGACAAAACACCGCTAATAAATGTAACCCAGATCTTTACT  
ATTGGACAGCTGTTGATGAGGGGGCAGCAGTAGGATTGGCATGGATTCCATATTTCCGACCTGCAGCAGAAGGCATCTACATTGAGGGTGTAAATGCA  
TAATCAGAATGGGCTTATTTGCGGGCTACGTGAGCTAGCCAATGAAACTACCCAGGCTCTTCAATTTATTTCTGCGGGCCACAACAGAACTGAGGACT  
TACTCACTTCTTAACAGAAAAGCTATTGATTTTCTTCTTCAACGATGGGGAGGTACCTGTGCAATCCTAGGACCATCTTGTTCATTGAGCCACATG  
ATTGGACAAAAATATTACTGATGAAATTAACCAAATTAACATGACTTTATTGACAATCCCTTACCAGACCACGGAGATGATCTTAATCTATGGAC  
AGGTTGGAGACAAATGGATCCCGGCTGGAATTTGGGATTATTGGAGTTATAATTTGCTATAATAGCCCTACTTTGTATATGTAAGATTTTGTGT

**Cuevavirus | *Lloviu cuevavirus* | LLOV/ESP/2003 | LLOV | JF828358 | 2154 | Ayato Takada | -**

ATGGTGCCACCTACCCGTACAGCAGCCTATTAGATTGGAGACCACCACCAAACCCCTACCATGGATCCTCAACCTTGTGGTCTTTTATACCATAG  
CCTGGCTGCCGGGGGAGTCTCAGGAATCCACTCGGTTTGTGGGAAACAACAGCATCACCCAACTGTCTGGACAATGTAGTGTGCAAGGAAACA  
CCTTGCCACAACAGATCAGCTACAGGCTATTGGATTGGGACTAGAGGGGCTTGGTGAACATGCTGACCTCCCGACTGCCACCAAGCGATGGGGTTTT  
CGATCTGATGTCATCCAAAAATCGTGGGATACACCGCTGGGAAATGGGTGAAAACTGCTACAATCTTGAATCACCAGAAAGATGGTCATCCTT  
GCCTCCCCAGCCGCCAACTGGCTTACTTGGCTATCCCCGATGCCCTATGTCCACAGAGCCAAAGGAGCAGGCCCTTGCCAGGTGGGAATGCTTT  
CCACAAACATGGTTCTTTCTTCTGTACCACGGTATGGCTTCTACAGTAATTTATCATGGTGTAACTTTACGGAAGGCACAATGCTTTCTTAATT  
GTCCCGAAGGATGCACCCCGTCTCAAGGCAGGGCTTGGAACAGGATTGATCATCAAGCAGAGAACCAAAACCCAAACAACCAATTTGCAACAACAA  
CTTTAGATTATGATGTAATGAGTCCCTGGATGGACAATGCTACCTTCTTCTTTCGAGCGAGGGAAGACACATCAATGCTAATCCAAACAAGGTACCC  
TCCAGCAAATCTAGAGCTTGTTCAGAAAGATTGGCTAATCTTACCGGAGATCAAGCTGATCCATCAAAGATGGAAGAGATTGTCGCTGAGGTTTTG  
ACATTGGAGCTCGGTGATTGGTCCGGTTGGACAATAAAAAAACCGCAGTACAAACCATACGGCTAAGAAACCTTACCAGCATCTGGTTCAACC  
AAGGACAAGACTGGCCAGAAGCCCATGACGGATCATCAGGATTCATCTCCAACCTCATTCTGCTGTTGGACAACCTGCTCTGGAACATCTTC  
GAACTCCGGGGCGGAACCTGCACGAAGGCACCGGGGGAACACCACCAACAATGTCATCACTGCTGCTCTGGGTGAGGATACAAGCCGTACAT  
CCAGGCAATACCTCTGGTGAATTTGATGCCATTGGGAGGGTCTCGGCATGTGTGTCGTCGATACCCCTCCTGGGTTCAGTGAGCAACAATAGTT  
CAATACAGGAGCTTGAGACTTCATCTAAAAGTGCAACAGAATTGACAACCTCCCATCAATCACTCCCAATCACTACAGCTCGCATCCGTACAAAACAC  
CCCCACACCGACAACACAGTCCAAGTCTTGGACAGTTGACTACAACAACAACCGCAACCAATGGATCCCAACAACAATACTGACGACACCCGACACC  
GCAACCATTCCCCCTAACAACATCATCTGATCACAACGCCACAACAACAAGCAAAACAAGAGCAAGGAGACAGGTCAACCCAGTGCCCCAACGATCA  
CCCAACAACCTTACAAGCATCAATACCTCCCACCACCCCAATATGACAACACAGTTAGCAAGACATCCGAGTGTGCAAAACAGGATGCAAAACCC  
CAGCTGTAATCCCAACCTTAGATACTGGACAAGCCGGGAGATGAGTAATGCTGGGGGGCTTGCATGGATTCCATGGATTGGACCAGGGATTGAGGGA  
GGGATCACAGACGGGATAATGGAGCATCAGAACAATTTGTCTGTCAGTTACGGGAGCTCGCGAACACCCTACTAAAGCCCTACAGCTTTTCTCTCC  
GGGTACCCTGAGCTCCGAACCTACTCTATCTCAACCGCCATGCGATTGACTTTCTACTACAGCGTTGGGGTGGTACCTGCAGAATCTTGGCCC  
AAACTGCTGTATCGAACCTCATGATTGGTCTGCCAACATTACGGCTGAGATAAATCATATTAGAGAAGATATCTGAACCATCATGAGATCCAACCT  
TCTCAAGACCCCTCCTTTTGGACTGGATGGCAACAGTGGATCCCAACAGGAGCCAGTGTCTCGGAATCATCTGGCAATATTAGCCTTGATTTGTC  
TGTGCAGAATAACACGATGA

**Marburgvirus | *Marburg marburgvirus* | RAVV/KEN/1987/KitumCave | RAVV | DQ447649 |  
2046 | Graham Simmons, Bloodsystems USA | -**

ATGAAGACCATATATTTTCTGATTAGTCTCATTTTAATCCAAAGTATAAAAACTCTCCCTGTTTTAGAAATGCTAGTAACAGCCAACTCAAGATG  
TAGATTAGTGTGCTCCGGAACCTCCAAAAGACAGAAGATGTCATCTGATGGGATTACTAGTGGGCAAAAAGTTGCTGATTCCCCTTTGGA  
AGCATCTAAACGATGGGCTTTCAGGACAGGTGTTCTCCCAAGAAGCTTGGATACGGAAGGAGAAGAAGCCAAAACATGTTACAATATAAGTGTA  
ACAGACCCCTTCTGAAAAATCCTTGCTGCTGGATCCTCCAGTAATATCCGCGATTACCTAAATGTAAGTAACTGTTTCATCATATTCAAGGTCAAAACC  
CTCATGCACAGGGATTGCCCTCCATTTTGGGGGGCATTTTTCTGTATGATCGCGTTGCCCTTACAACAATGTACCGAGGCAAGGTCTTCACTGA  
AGGAAATATAGCAGCTATGATTGTTAATAAGACAGTTACAGAATGATTTTTCTAGGCAAGGACAAGGTATCGTCACATGAACCTGACCTCCACC  
AATAAATATTGGACAAGCAGCAATGAAACGCAGAGAAATGATACGGGATTTTTGGCATCCTCCAAGAATACAACCTCCACAACAATCAACATGCC  
CTCCATCTCTAAACCTCCATCCCTGCCACAGTAACCCGAGCATTACTCTACAAATACTCAAATTAATACTGCTAAATCTGGAACATGAAACCC  
AAGTAGCCAGCATGAGGACCTTATGATTTCCGGCTCAGGATCTGGAGAACAGGGGCCCCACACAACCTTAAATGATGACTGAAACGAAACAATCG  
TCAACAATATGTCCACTCCTTCACTACATCCAAGCACCTCACACAATGAGCAAAACAGTACGAATCCTTCCCGACATGCTGTAACCTGAGCACAATG  
GAACCGACCCACAACAACCAACAGCAACGCTCCTCAACAATACTAATAACAACCTCCACCTATAACACTCTCAAGTACAACCTCAGTACTCCTTCCCC  
TCCAACCCGCAACATCACCAATAATGATACACAACGTGAAC TAGCAGAAAGCGAACAACCAATGCTCAGTTGAACACAACCTTAGATCCAACAGAA  
AATCCACCACAGGACAAGACACCAACAGCACACCAACATCATCATGACGACATCAGATATAAACAAGCAAAACCCCCACAATTTCTTCTCCGGATT  
CTAGTCCGACAACCCGCCCTCTATATACTTTAGAAAGAAACGAAGCATTCTTCTGGAAAGAAGGTGATATATCCCGTTTTTATAGATGGGTTAATAAAA  
TACTGAAATGATTTTGTATCCAAATCCCAACACAGAAACAATCTTTGATGAATCTCCAGCTTTAATACTTCAACTAATGAGGAACAACACACTCCC  
CCGAATATCAGTTTAACTTTCTTATTTTCTGATAAAAAATGGAGATACTGCCTACTCTGGGAAAACGAGAATGATTGTGATGCAGAGTTGAGGA  
TTTGGAGTGTGCAGGAGGACGATTTGGCGCAGGGCTTAGCTGGATAACATTTTTTGGCCCTGGAATCGAAGGACTCTATATGCGGGTTAATCAA  
AAATCAGAACAATTTAGTTTGTAGTTGAGGCGCTTAGCTAATCAAACCTGCTAAATCCTTGGAGCTCTGTTAAGGGTCAACAACCGAGGAAAGGACA  
TTTTCTTAAATCAATAGGCATGCAATGACTTTTTGCTTACGAGGTGGGGCGAACAATGCAAGGTGCTAGGACCTGATTGTTGCATAGGAATAGAAG  
ATCTATCTAAAAATATCTCAGAACAATCGACAAAATCAGAAAGGATGAACAAAAGGAGGAAACTGGCTGGGGTCTAGTGGCAAAATGGTGGACATC  
TGACTGGGGTGTCTCACAATTTGGGCATCCTGCTACTATTATCTATAGCTGTTCTGATTGCTCTGTCTGTATCTGTCTGATCTTCACTAAATAC  
ATTGGATGA

***Influenzavirus A* | *Influenza A virus* | A/Vietnam/1194/2004(H5N1) haemagglutinin | HA |**

**ABP51976 | 1707 | Nigel Temperton, University of Kent | -**

ATGGAGAAAAAGTGTCTCTTTTGGCAATAGTCAGTCTTGTTAAAAGTGATCAGATTTGCATTGGTTACCATGCAAACAACTCGACAGAGCAGGTTG  
ACACAATAATGAAAAGAACGTTACTGTTACACATGCCAAGACATACTGGAAAAAGACACACAATGGGAAGCTCTGCGATCTAGATGGAGTGAAGCC  
TCTAATTTTGAGAGATTGTAGTGTAGCTGGATGGCTCCTCGGAAACCCAAATGTGTGACGAATTCATCAATGTGCCGGAATGGTCTTACATAGTGGAG  
AAGGCCAATCCAGTCAATGACCTCTGTTACCCAGGGGATTTCAATGACTATGAAGAATTGAAACACCTATTGAGCAGAATAAACCATTTTGAGAAAA  
TTCAGATCATCCCCAAAAGTTCTTGGTCCAGTCAATGAAGCCATTTGGGGGTGAGCTCAGCATGTCCATACCAGGGAAAGTCTCTCTTTTCAGAAA  
TGTGGTATGGCTTATCAAAAAGAACAGTACATACCCAACAATAAAGAGGAGCTACAATAATACCAACCAAGAAGATCTTTTGGTACTGTGGGGGATT  
CACCATCCTAATGATGCGGCAGAGCAGACAAAGTCTATCAAAACCAACCACCTATATTTCCGGTTGGGACATCTACACTAAACCAGAGATTGGTAC  
CAAGAATAGCTACTAGATCCAAAGTAAACGGGCAAAGTGAAGGATGGAGTTCTTCTGGACAATTTTAAAACCGAATGATGCAATCAACTTCGAGAG  
TAATGGAAATTTCAATTGCTCCAGAATATGCATACAAAATTGTCAGAAAAGGGGACTCAACAATTATGAAAAGTGAATTGGAATATGGTAACGCAAC  
ACCAAGTGTCAAACCTCAATGGGGCGATAAACTCTAGCATGCCATTCCACAATATACACCCTCACCATCGGGGAATGCCCAATATGTGAAAT  
CAAACAGATTAGTCTTGGCACTGGGCTCAGAAATAGCCCTCAAAGAGAGAGAAGAAGAAAAAGAGAGGATTATTTGGAGCTATAGCAGGTTTTAT  
AGAGGGAGGATGGCAGGGAATGGTAGATGGTGGTATGGGTACCACCATAGCAACGAGCAGGGGAGTGGGTACGCTGCAGACAAAGAATCCACTCAA  
AAGGCAATAGATGGAGTCAACAATAAGGTCAACTCGATTATTGACAAAATGAACACTCAGTTTGAGGCCGTTGGAAGGGAATTTAACAACTTAGAAA  
GGAGAATAGAGAATTTAAACAAGAAGATGGAAGACGGGTTCCATAGATGTCTGGACTTATAATGCTGAACTTCTAGTTCTCATGGAAAAACGAGAGAAC  
TCTAGACTTTTATGACTCAAATGTCAAGAACCTTTACGACAAGGTCGACTACAGCTTAGGATAATGCAAAGGAGCTGGGTAAACGGTTGTTTCGAG  
TTCTATCATAAATGTGATAATGAATGTATGAAAAGTGAAGAAACGGAACGTATGACTACCCGCAGTATTGAGAAGAAGCAAGACTAAAAAGAGAGG  
AAATAAGTGGAGTAAATTTGGAATCAATAGGAATTTACCAATATGTCAATTTATTCTACAGTGGCGAGCTCCCTAGCACTGGCAATCATGGTAGC  
TGGTCTATCTTATGGATGTGCTCCAATGGGTCGTTACAATGCAGAAATTTGCATTTAA

***Lentivirus* | *Human Immunodeficiency Virus 1* | HXB2 gp160 | HIV | K03455 | 2571 | Greg**

**Towers, UCL | -**

ATGAGAGTGAAGGAGAAATATCAGCACTTGTGGAGATGGGGTGGAGATGGGGCACCATGCTCCTTGGGATGTTGATGATCTGTAGTGTACAGAAA  
AATTGTGGGTACAGTCTATTATGGGGTACCTGTGTGGAAGGAAGCAACCACCCTCTATTTGTGCATCAGATGCTAAAGCATATGATACAGAGGT  
ACATAATGTTTGGGCCACACATGCCTGTGTACCCACAGACCCCAACCCACAAGAAGTAGTATTGGTAAATGTGACAGAAAATTTAACATGTGGAAA  
AATGCATGGTAGAACAGATGCATGAGGATAAATCAGTTTATGGGATCAAAGCCTAAAGCCATGTGTAATAAATTAACCCACCTGTGTAGTTTAA  
AGTGCAGTATTGGAAGATGATACTAATACCAATAGTAGTAGCGGGGAGAATGATAATGGAGAAAGGAGAGATAAAAACTGCTCTTTCAATATCAG  
CACAAGCATAAGAGGTAAAGTGCAGAAAAGAAATATGCATTTTTTATAAACCCTGATATAATACCAATAGATAATGATACTACCAGCTATAAGTTGACA  
AGTTGTAACACCTCAGTCATTACACAGGCCGTGTCCAAAGGTATCCTTTGAGCCAAATCCCATACATATTGTGCCCCGGCTGGTTTTGCGATTCTAA  
AATGTAATAATAAGACGTTCAATGGAACAGGACCATGTACAAATGTGACACAGTACAATGTACACATGGAATTAGGCCAGTAGTATCAACTCAACT  
GCTGTTAAATGGCAGTCTAGCAGAAGAAGAGGTAGTAATTAGATCTGTCAATTTACACGACCAATGCTAAAACCAATAATAGTACAGCTGAACACATCT  
GTAGAAATTAATGTACAGACCCCAACAATAACAAGAAAAGAATCCGTATCCAGAGAGGACCAGGGAGAGCATTTGTTACAATAGGAAAAATAG  
GAAATATGAGACAAGCATTGTAACATTAGTAGAGCAAAAATGGAATAACACTTTAAAACAGATAGCTAGCAAATTAAGAGAACAAATTTGGAATAA  
TAAAACAATAATCTTAAAGCAATCCTCAGGAGGGGACCCAGAAATGTAACGCACAGTTTAAATGTGAGGGGAAATTTTCTACTGTAATTAACA  
CAACTGTTTAAATAGTACTTGGTTTAAATAGTACTTGGAGTACTGAAGGGTCAAATAACACTGAAGGAAGTACACAATCACCCCTCCATGCAGAATAA  
AACAAATTAACAATGTGGCAGAAAGTAGGAAAAGCAATGTATGCCCTCCCATCAGTGGACAAATTAGATGTTTATCAATATTAACAGGGCTGCT  
ATTAACAAGAGATGGTGGTAATAGCAACAATGAGTCCGAGATCTTACAGCCTGGAGGAGGAGATATGAGGGACAATGGAGAAGTGAATTAATAAAA  
TATAAAGTAGTAAAAATGAACCATTAGGAGTAGCACCCACCAAGGCAAAGAGAGAGTGGTGCAGAGAGAAAAAGAGCAGTGGGAATAGGAGCTT  
TGTTCTTGGGTTCTTGGGAGCAGCAGGAAGCACTATGGGCGCAGCCTCAATGACGCTGACGCTACAGGCCAGACAATATTGTCTGGTATAGTGA  
GCAGCAGAACAAATTTGCTGAGGGCTATTGAGGCGCAACAGCATCTGTGCAACTCACAGTCTGGGCATCAAGCAGCTCCAGGCAAGAATCCTGGCT  
GTGGAAGATACCTAAAGGATCAACAGCTCCTGGGGATTTGGGGTGTCTTGAAAACCTCATTGCAACTGCTGTGCCTTGGAAATGCTAGTTGGA  
GTAATAAATCTCTGGAACAGATTGGAATCACACGACCTGGATGGAGTGGGACAGAGAAAATTAACAATTACACAAGCTTAATACACTCTTAATGGA  
AGAATCGAAAACAGCAAGAAAAGAATGAACAAGAATTATGGAATTAGATAAATGGGCAAGTTTGTGGAATTTGGTTAACATAACAAATTTGGCTG  
TGGTATATAAAATTTATCATAATGATAGTAGGAGGCTTGGTAGGTTAAGAATAGTTTTTGTGTACTTTCTATAGTGAATAGAGTTAGGACGGGAT  
ATTCACCATTTATCGTTTCAGACCCACCTCCCAACCCCGAGGGGACCCGACAGGCCCAAGGAATAGAAGAAGAGGTGGAGAGAGAGACAGAGACAG  
ATCCATTTCGATTAGTGAACGGATCCTTGGCACTTATCTGGGACGATCTGCGGAGCCTGTGCCTTTCAGCTACCACCGCTTGGAGACTTACTCTTG  
ATTGTAACAGGATTGTGGAATCTTGGGACGCAGGGGGTGGGAAGCCCTCAAATATTGGTGGAAATCTCCTACAGTATTGGAGTCAAGAACTAAAGA  
ATAGTGTCTTTAGCTTGCTCAATGCCACAGCCATAGCAGTAGCTGAGGGGACAGATAGGGTTATAGAAGTAGTACAAGGAGCTTGTAGAGCTATTTCG  
CCACATACCTAGAAGAATAAGACAGGGCTTGGAAAGGATTTTGTCTATAA

## I.2. Reporter Protein Sequences

### Reporter Gene | Length (bp) | Accession Number | Plasmid Source (Supplier) | Construct ID<sup>1</sup>

<sup>1</sup>Refers to amplification primers detailed in Chapter 2 (Table 2.5 – 2.6)

#### Cypridina Luciferase | 1662 | - | pCMV-CLuc 2 (New England BioLabs) | C3.1

```
ATGAAGACCTTAATTCTTGCCGTTGCATTAGTCTACTGCGCCACTGTTTCATTGCCAGGACTGTCCTTACGAACTGATCCACCAAAACACAGTTCCAA
CTTCTGTGAAGCTAAAGAAGGAGAATGTATTGATAGCAGCTGTGGCACCTGCACGAGAGACATACTATCAGATGGACTGTGTGAAAATAAACAGG
AAAAACATGTTGCCGAATGTGTCACTATGTAATTGAATGCAGAGTAGAGGCCGAGGATGGTTTAGAACATTCTATGGAAAGAGATTCCAGTTCAG
GAACCTGGTACATACGTGTTGGGTCAAGGAACCAAGGGCGGCGACTGGAAGGTGTCCATCACCTGGAGAACCTGGATGGAACCAAGGGGGCTGTGC
TGACCAAGACAAGACTGGAAGTGGCTGGAGACATCATTGACATCGCTCAAGCTACTGAGAATCCCATCACTGTAAACGGTGGAGCTGACCCATCAT
CGCCAACCCGTACACCATCGGCGAGGTACCCATCGCTGTTGTTGAGATGCCAGGCTTCAACATCACCGTCATTGAGTTCTCAAACGTGATCGTGATC
GACATCCTCGGAGGAAGATCTGTAAGAATCGCCCCAGACACAGCAAACAAAGGAATGATCTCTGGCCTCTGTGGAGATCTAAAATGATGGAAGATA
CAGACTTCACTTCAGATCCAGAACAACCTCGCTATTGAGCCTAAGATCAACCAGGAGTTTGACGGTTGTCCACTCTATGGAAATCCTGATGACGTTGC
ATACTGCAAAGGTCTTCTGGAGCCGTACAAGGACAGCTGCCGCAACCCCATCAACTTCTACTACTACACCATCTCCTGCGCCTTCGCCCCGTGTATG
GGTGGAGACGAGCGAGCCTCACACGTGCTGCTTACTACAGGAGACGTGCGCTGCTCCCGAAACTAGAGGAACCTGCGTTTTGTCTGGACATACTT
TCTACGATACATTTGACAAAGCAAGATACCAATTCCAGGGTCCCTGCAAGGAGATTCTTATGGCCCGGACTGTTTCTGGAACACTTGGGATGTGAA
GGTTTACACAGGAATGTTGACTCTTACACTGAAGTAGAGAAAGTACGAATCAGGAAACAATCGACTGTAGTAGAACTCATTGTTGATGGAACACAG
ATTCTGGTTGGAGGAGAAGCCGTGTCCTGCCGTACAGCTCTCAGAACACTTCCATCTACTGGCAAGATGGTGACATACTGACTACACCCATCCTAC
CTGAAGCTCTGGTGGTCAAGTTCAACTTCAAGCAACTGCTCGTCGTACATATTAGAGATCCATTCGATGGTAAGACTTGGCGTATTTGCGGTAACATA
CAACCAGGATTTCACTGATGATTTCTTTGATGCTGAAGGAGCCTGTGATCTGACCCCAACCCACCGGGATGCACCGAAGAACAGAAACCTGAAGCT
GAACGACTCTGCAATAGTCTCTTCGCCGGTCAAAGTGATCTTGATCAGAAATGTAACGTGTGCCACAAGCCTGACCGTGTGCAACGATGCATGTACG
AGTATTGCCTGAGGGGACAACAGGGTTTCTGTGACCACGCATGGGAGTTCAAGAAAGAATGCTACATAAAGCATGGAGACACCTAGAAGTACCAGA
TGAATGCAAATAG
```

#### NanoLuc Luciferase | 516 | JQ437370 | pNL1.1[Nluc] (Promega) | C3.2

```
ATGGTCTTCACACTCGAAGATTTTCGTTGGGGACTGGCGACAGACAGCCGGCTACAACCTGGACCAAGTCCCTGAAACAGGGAGGTGTGTCCAGTTTGT
TTCAGAAATCTCGGGGTGTCGGTAACTCCGATCCAAAGGATTGTCTGAGCGGTGAAAATGGGCTGAAGATCGACATCCATGTCATCATCCCGTATGA
AGGTCTGAGCGGGACCAAAATGGGCCAGATCGAAAAAATTTTAAAGTGGTGTACCCCTGTGGATGATCATCACTTTAAGGTGATCCTGCACTATGGC
ACACTGGTAATCGACGGGGTTACGCCGAACATGATCGACTATTTCCGACGGCCGTATGAAGGCATCGCCGTGTTTCGACGGCAAAAAGATCACTGTAA
CAGGGACCTGTGGAACGGCAACAAAATTATCGACGAGCGCCTGATCAACCCCGACGGCTCCCTGCTGTTCCGAGTAACCATCAACGGAGTGACCCG
CTGGCGGCTGTGCGAACGCATTTCTGGCGTAA
```

### Secreted Alkaline Phosphatase (SEAP) | 1521 | U09660 | pSEAP-Basic (Clontech) | C3.3

ATGCTGCTGCTGCTGCTGCTGCTGGGCCTGAGGCTACAGCTCTCCCTGGGCATCATCCAGTTGAGGAGGAGAACCCGACTTCTGGAACCGCGAGG  
CAGCCGAGGCCCTGGGTGCCGCCAAGAAGCTGCAGCCTGCACAGACAGCCGCCAAGAACCTCATCATCTTCTGGGCGATGGGATGGGGGTGTCTAC  
GGTGACAGCTGCCAGAATCCTAAAAGGGCAGAAGAAGGACAAACTGGGGCTGAGATACCCCTGGCCATGGACCGCTTCCCATATGTGGCTCTGTCC  
AAGACATAACAATGTAGACAAACATGTGCCAGACAGTGGAGCCACAGCCACGGCCTACCTGTGCGGGTCAAGGGCAACTTCCAGACCATTGGCTTGA  
GTGCAGCCGCCGCTTTAACCAGTGAACACGACACGCGGCCAACGAGGTATCTCCGTGATGAATCGGGCCAAGAAAGCAGGGAAGTCAGTGGGAGT  
GGTAACCACCACACGAGTGCAGCACGCTCGCCAGCCGGCACCTACGCCACAGGTGAACCGCAACTGGTACTCGGACGCCGACGTGCCTGCCTCG  
GCCCCCAGGAGGGGTGCCAGGACATCGCTACGCAGCTCATCTCCAAATGGACATTGACGTGATCCTAGGTGGAGGCCGAAAGTACATGTTTCGCA  
TGGGAACCCAGACCCTGAGTACCCAGATGACTACAGCCAAGGTGGGACCAGGCTGGACGGGAAGAATCTGGTGCAGGAATGGCTGGCGAAGCGCCA  
GGGTGCCCGTATGTGTGGAACCGCACTGAGCTCATGCAGGTTCCCTGGACCCGTCTGTGACCCATCTCATGGGTCTCTTTGAGCCTGGAGACATG  
AAATACGAGATCCACCGAGACTCCACACTGGACCCCTCCCTGATGGAGATGACAGAGGCTGCCCTGCGCCTGCTGAGCAGGAACCCCGCGGCTTCT  
TCCTCTTCGTGGAGGGTGGTGCATCGACCATGGTTCATCATGAAAGCAGGGCTTACCGGGCACTGACTGAGACGATCATGTTTCGACGACGCCATTGA  
GAGGGCGGGCCAGCTCACCAGCGAGGAGGACAGCTGAGCCTCGTCACTGCCGACCCTCCACGCTTCTCCTTCGGAGGCTACCCCTGCGAGGG  
AGCTCCATCTTCGGGCTGGCCCTGGCAAGGCCCGGGACAGGAAGCCTACACGGTCTCTTATACGGAACCGTCCAGGCTATGTGCTCAAGGACG  
GCGCCCGCCGGATGTTACCAGAGCGAGAGCGGGAGCCCCGAGTATCGGCAGCAGTCAAGCAGTGCCTGGACGAAGAGACCCACGAGCGGAGGA  
CGTGGCGGTGTTTCGCGCGCGGCCCGCAGGCGCACCTGGTTCACGGCGTGCAGGAGCAGACCTTCATAGCGCACGTCATGGCCTTCGCGCCCTGCCTG  
GAGCCCTACACCGCTGCGACCTGGCGCCCCCGCGGCACCCACCGACGCGCGCACCCGGTTAA

### Secreted Alkaline Phosphatase (version 2) (SEAP2) | 1560 | U89937 | pSEAP2-Basic (Clontech) | C3.4

ATGCTGCTGCTGCTGCTGCTGCTGGGCCTGAGGCTACAGCTCTCCCTGGGCATCATCCAGTTGAGGAGGAGAACCCGACTTCTGGAACCGCGAGG  
CAGCCGAGGCCCTGGGTGCCGCCAAGAAGCTGCAGCCTGCACAGACAGCCGCCAAGAACCTCATCATCTTCTGGGCGATGGGATGGGGGTGTCTAC  
GGTGACAGCTGCCAGAATCCTAAAAGGGCAGAAGAAGGACAAACTGGGGCTGAGATACCCCTGGCCATGGACCGCTTCCCATATGTGGCTCTGTCC  
AAGACATAACAATGTAGACAAACATGTGCCAGACAGTGGAGCCACAGCCACGGCCTACCTGTGCGGGTCAAGGGCAACTTCCAGACCATTGGCTTGA  
GTGCAGCCGCCGCTTTAACCAGTGAACACGACACGCGGCCAACGAGGTATCTCCGTGATGAATCGGGCCAAGAAAGCAGGGAAGTCAGTGGGAGT  
GGTAACCACCACACGAGTGCAGCACGCTCGCCAGCCGGCACCTACGCCACAGGTGAACCGCAACTGGTACTCGGACGCCGACGTGCCTGCCTCG  
GCCCCCAGGAGGGGTGCCAGGACATCGCTACGCAGCTCATCTCCAAATGGACATTGACGTGATCCTAGGTGGAGGCCGAAAGTACATGTTTCGCA  
TGGGAACCCAGACCCTGAGTACCCAGATGACTACAGCCAAGGTGGGACCAGGCTGGACGGGAAGAATCTGGTGCAGGAATGGCTGGCGAAGCGCCA  
GGGTGCCCGTATGTGTGGAACCGCACTGAGCTCATGCAGGTTCCCTGGACCCGTCTGTGACCCATCTCATGGGTCTCTTTGAGCCTGGAGACATG  
AAATACGAGATCCACCGAGACTCCACACTGGACCCCTCCCTGATGGAGATGACAGAGGCTGCCCTGCGCCTGCTGAGCAGGAACCCCGCGGCTTCT  
TCCTCTTCGTGGAGGGTGGTGCATCGACCATGGTTCATCATGAAAGCAGGGCTTACCGGGCACTGACTGAGACGATCATGTTTCGACGACGCCATTGA  
GAGGGCGGGCCAGCTCACCAGCGAGGAGGACAGCTGAGCCTCGTCACTGCCGACCCTCCACGCTTCTCCTTCGGAGGCTACCCCTGCGAGGG  
AGCTCCATCTTCGGGCTGGCCCTGGCAAGGCCCGGGACAGGAAGCCTACACGGTCTCTTATACGGAACCGTCCAGGCTATGTGCTCAAGGACG  
GCGCCCGCCGGATGTTACCAGAGCGAGAGCGGGAGCCCCGAGTATCGGCAGCAGTCAAGCAGTGCCTGGACGAAGAGACCCACGAGCGGAGGA  
CGTGGCGGTGTTTCGCGCGCGGCCCGCAGGCGCACCTGGTTCACGGCGTGCAGGAGCAGACCTTCATAGCGCACGTCATGGCCTTCGCGCCCTGCCTG  
GAGCCCTACACCGCTGCGACCTGGCGCCCCCGCGGCACCCACCGACGCGCGCACCCGGTTACTCTAGAGTCGGGGCGGGCCGCTTCGAGC  
AGACATGA\*

\*39 nucleotide c-terminal extension in comparison to SEAP

**Dual-Nuclear Localised GFP (dNG) | 1503 | - | pCMS28-NLS-GFP-SAMHD1-CtD (Kate Bishop, Francis Crick Institute) | C3.5**

ATGCCCAAGAAAAAGCGGAAAGTGGGCGCGTGTCCAAGGGCGAGGAACGTTTACAGGCGTGGTGCCCATCCTGGTGAACGACGGGGATGTGA  
ACGGCCACAAGTTCAGCGTGTCCGGCGAGGGCGAAGGCGACGCCACATATGGCAAGCTGACCCTGAAGTTCATCTGCACCACCGCAAGCTGCCCGT  
GCCTTGCCCTACCCTCGTGACCACACTGACCTACGGCGTGCAGTGTTCAGCAGATACCCCGACCATATGAAGCAGCAGACTTCTTCAAGAGCGCC  
ATGCCCGAGGGCTACGTGCAGGAACGGACCATCTTCTTAAGGACGACGGCAACTACAAGACCAGGGCCGAAGTGAAGTTCGAGGGCGACACCCCTCG  
TGAACCGGATCGAGCTGAAGGCATCGACTTCAAAGAGGACGGCAACATCCTGGGCCACAAGCTGGAGTACAACACAACAGCCACAACGTTACAT  
CATGGCCGACAAGCAGAAAAACGGCATCAAAGTGAACCTCAAGATCCGGCACAACATCGAGGACGGCTCCGTGCAGCTGGCCGACCCTACCAGCAG  
AACACCCCATCGGAGATGGCCCCGTGCTGCTGCCGACAACCCTACCTGAGACACAGAGCGCCCTGAGCAAGGACCCCAACGAGAAGCGGGACC  
ACATGGTGTGCTGGAATTTGTGACCGCCGCTGGCATCACCTGGGCATGGACGAGCTGTACAAGTCCGGCATGCCAAAAAGAAAAGAAAAGTGGG  
GGGAGTGTCTAAAGGGGAAGAACTGTTACCGGGGTGGTGCCTATTCTGGTGAACGGATGGCGACGTGAACGGGCATAAGTTTTCCGTGTCTGGG  
GAGGGGAAGGGGATGCTACCTACGAAAGCTGACACTGAAGTTTATCTGTACAACAGGAAACTGCCTGTGCCCTGGCCACACTCGTGACAACCC  
TGACATATGGGGTGCAGTGTTCCTCCCGTACCCTGATCATATGAAGCAGCATGATTTTTTCAAATCCGCTATGCCCTGAGGGATATGTGCAGGAAAG  
AACATTTTTCTTCAAGGATGATGGGAATTACAAAACACGCGCTGAAGTGAATTTGAGGGGGATACACTCGTGAATCGCATTGAACTGAAGGGGATT  
GATTTCAAAGAGGACGGGAATTTCTGGGCGACAACCTGGAGTATAATTACAATTTCCACAATGTGTATATATGGCTGATAAGCAGAAAAATGGGA  
TCAAAGTGAATTTCAAATCAGACACAATATTGAGGATGGCAGTGTGCAGCTGGCTGATCATATCAGCAGAATACTCTATCGGCGACGGACCTGT  
GCTGTGCCTGATAATCACTATCTGTCCACCCAGTCCGCCCTGTCCAAGGACCCTAATGAGAAACGCGATCATATGGTGTGCTGGAATTTGTGACA  
GCTGCCGGAATTACACTGGGGATGGATGAACTGTATAAGAGCGGCTAA

**Dual-Nuclear Localised tdTomato (dNT) | 1542 | - | ptdTomato-Nuc (Colin Crump, University of Cambridge) | C3.6**

ATGGTGAAGGCGAGGAGGTCATCAAAGAGTTCATCGCGTTCAAAGTTCGCGATGGAGGGTCCATGAACGGCCACGAGTTCGAGATCGAGGGCG  
AGGGCGAGGGCCGCCCTACGAGGGCACCCAGACCGCAAGCTGAAGGTGACCAAGGGCGGCCCTGCCCTTCGCTGGGACATCCTGTCCCCCA  
GTTTATGTACGGCTCAAAGCGTACGTGAAGCACCCCGCCGACATCCCCGATTACAAGAAGCTGTCTTCCCGAGGGCTTCAAGTGGGAGCGGTG  
ATGAACCTCGAGGACGGCGGTCTGGTGACCGTGACCCAGGACTCCTCCCTGCAGGACGGCACGCTGATCTACAAGGTGAAGATGCGCGGCACCAACT  
TCCCCCGGACGGCCCGTAATGCAGAAGAAGACCATGGGCTGGGAGGCTCCACCGAGCGCTGTACCCCGGACGGCGTGTGAAGGGCGAGAT  
CCACCAGGCCCTGAAGCTGAAGGACGGCGGCCACTACCTGGTGGAGTTCAGACCATCTACATGGCCAAGAAGCCCGTGCAACTGCCCGGCTACTAC  
TACGTGGACACCAAGCTGGACATCACCTCCCACAACGAGGACTACACCATCGTGAACAGTACGAGCGCTCCGAGGGCCGCCACCACCTGTTCTGG  
GGCATGGCACCGGACCGGACCGGACGCTCCGGCACCGCCTCCTCCGAGGACAACAACATGGCCGTATCAAAGAGTTCATGCGCTTCAAGGT  
GCGCATGGAGGGTCCATGAACGGCCACGAGTTCGAGATCGAGGGCGAGGGCGAGGGCCGCCCTACGAGGGCACCCAGACCCCAAGCTGAAGGTG  
ACCAAGGGCGGCCCTGCCCTTCGCTGGGACATCCTGTCCCCAGTTCATGTACGGCTCCAAGGCGTACGTGAAGCACCCCGCCGACATCCCCG  
ATTACAAGAAGCTGTCTTCCCGAGGGCTTCAAGTGGGAGCGGTGATGAACCTCGAGGACGGCGGTCTGGTGACCGTGACCCAGGACTCCTCCCT  
GCAGGACGGCACGCTGATCTACAAGGTGAAGATGCGCGGCACCAACTTCCCCCGGACGGCCCGTAATGCAGAAGAAGACCATGGGCTGGGAGGCC  
TCCACCGAGCGCTGTACCCCGGACGGCGTGTGAAGGGCGAGATCCACCGGCCCTGAAGCTGAAGGACGGCGGCCACTACCTGGTGGAGTTCA  
AGACCATCTACATGGCCAAGAAGCCCGTGCAACTGCCCGGCTACTACTACGTGGACACCAAGCTGGACATCACCTCCCACAACGAGGACTACACCAT  
CGTGAACAGTACGAGCGCTCCGAGGGCCGCCACCCTGTTCTGTACGGCATGGACGAGCTGTACAAGTCCGGACTCAGATCTCGAGCTGATCCA  
AAAAAGAAGAAAAGGTAGATCCAAAAAGAAGAAAAGGTAGATCCAAAAAGAAGAAAAGGTAGGATCGACCGGATCAAGATAA

## LacZ | 3138 | - | pCSLZW (Edward Wright) | C4.1

ATGGCGCCAAAAAGAAGAGAAAGGTAGAAAGACCCCAAGGACTTTCCTTCAGAATTGCTAAGTTTTTTGAGTCCAAGCTTGGCACTGGCCGTCGTTTT  
TACAACGTCGTGACTGGGAAAACCCCTGGCGTTACCCAACTTAATCGCCTTGCAGCACATCCCCTTTCGCCAGCTGGCGTAATAGCGAAGAGGCCCG  
CACCGATCGCCCTTCCCAACAGTTGCGCAGCCTGAATGGCGAATGGCGCTTTCGCTGGTTCCGGCACCAGAAGCGGTGCCGAAAAGCTGGCTGGAG  
TGCGATCTTCTGAGGCCGATACTGTCGTCGTCGCCCTCAAACGGCAGATGCACGGTTACGATGCGCCCATCTACACCAACGTGACCTATCCCATTA  
CGGTCAATCCGCCGTTTTGTTCCACGGAGAATCCGACGGGTGTTACTCGCTCACATTTAATGTTGATGAAAGCTGGCTACAGGAAGGCCAGACGCG  
AATTATTTTTGATGGCGTTAACTCGCGTTTTCACTGTGGTGAACGGGCGCTGGGTGGTTACGGCCAGGACAGTCGTTTGCCGCTGAATTTGAC  
CTGAGCGCATTTTTACGCGCCGGAGAAAACCGCTCGCGGTGATGGTGTGCGCTGGAGTGACGGCAGTTATCTGGAAGATCAGGATATGTGGCGGA  
TGAGCGGCATTTTCCGTGACGCTCTGTTGCTGCATAAACCGACTACACAAATCAGCGATTTCCATGTTGCCACTCGCTTAAATGATGATTCAGCCG  
CGCTGTACTGGAGGCTGAAGTTCAGATGTGCGCGAGTTGCGTGACTACCTACGGGTAACAGTTTCTTTATGGCAGGGTGAAACGCAGGTGCCAGC  
GGCACCGCGCCTTTCGGCGGTGAAATATCGATGAGCGTGGTGGTTATGCCGATCGCGTCACACTACGCTGAAAGCTCGAAAACCCGAAACTGTGGA  
GCGCGAAATCCCGAATCTCTATCGTGGGTGGTTGAACTGCACACCGCCGACGGCACGCTGATTGAAGCAGAAGCCTGCCGATGTCGGTTTTCCGCGA  
GGTGGCGATTGAAAATGGTCTGCTGCTGCTGAACGGCAAGCCGTTGCTGATTCGAGGCGTTAACCGTCACGAGCATCATCTCTGCATGGTCAGGTC  
ATGGATGAGCAGACGATGGTGAGGATATCCTGCTGATGAAGCAGAACTTTAACGCCGTGCGCTGTTCCGATTTATCCGAACCATCCGCTGTGGT  
ACACGCTGTGCGACCGCTACGGCCTGTATGTGGTGGATGAAGCCAATATTGAAAACCCACGGCATGGTGCCAATGAATCGTCTGACCGATGATCCGCG  
CTGGTACCGGCGATGAGCGAACCGGTAACGCGAATGGTGCAGCGCATCGTAATCACCCGAGTGTGATCATCTGGTCGCTGGGGAATGAATCAGGC  
CACGGCGTAATCACGACGCGCTGTATCGCTGGATCAAATCTGTGATCTTCCCGCCCGGTGCAGTATGAAGCGCGGGAGCCGACACCACGGCCA  
CCGATATTATTTGCCCGATGTACGCGCGCTGGATGAAGACCAGCCCTTCCCGCTGTGCCGAAATGGTCCATCAAAAAATGGCTTTTCGCTACCTGG  
AGAGACGCGCCCGCTGATCCTTTGCGAATACGCCACCGCATGGGTAACAGTCTTGGCGGTTTCGCTAAATACTGGCAGGCGTTTCGTCAGTATCCC  
CGTTTACAGGGCGCTTCGCTCTGGACTGGGTGGATCAGTCGCTGATTAATATGATGAAAACGGCAACCCGTTGGTCGGCTTACGGCGGTGATTTG  
GCGATACGCCGAACGATCGCCAGTTCTGTATGAACGGTCTGGTCTTTGCCGACCGCACGCCGATCCAGCGCTGACGGAAGCAAAACACCAGCAGCA  
GTTTTTCCAGTTCGGTTTATCCGGGCAAACCATCGAAGTGACCAGCGAATACCTGTTCCGTCATAGCGATAACGAGCTCCTGCACTGGATGGTGGCG  
CTGGATGGTAAGCCGCTGGCAAGCGGTGAAGTGCCTCTGGATGTGCTCCACAAGGTAACAGTTGATTGAACTGCCTGAACTACCGCAGCCGGAGA  
GCGCCGGGCAACTCTGGCTCACAGTACGCGTAGTGCAACCGAACGCGACCGCATGGTTCAGAAAGCCGGGCACATCAGCGCCTGGCAGCAGTGGCGTCT  
GGCGGAAAACCTCAGTGTGACGCTCCCGCGCGTCCCACGCCATCCCGCATCTGACCACCAGCGAAATGGATTTTGCATCGAGCTGGGTAATAAG  
CGTTGGCAATTTAACCGCCAGTCAGGCTTCTTTTACAGATGTGGATTGGCGATAAAAAACAAGTGTGACGCCGCTGGCGCATCAGTTACCCGTCG  
CACCGCTGGATAACGACATTGGCGTAAGTGAAGCGACCCGCATTGACCCTAACGCTGGGTGCAAGCTGGAAGCGCGGGCCATTACCAGGCCGA  
AGCAGCGTTGTTGCAGTGCACGGCAGATACACTTGTGATGCGGTGCTGATTACGACCGCTCACGCGTGGCAGCATCAGGGGAAAACCTTATTTATC  
AGCCGGAAAACCTACCGGATGTAGGTAGTGGTCAAATGGCGATTACCGTTGATGTTGAAGTGGCGAGCGATACCCGCATCCGGCGCGGATTGGCC  
TGAATGCCAGCTGGCGCAGGTAGCAGAGCGGGTAAACTGGCTCGGATTAGGGCCGCAAGAAAATATCCCGACCGCCTTACTGCCGCTGTTTTGA  
CCGCTGGGATCTGCCATTGTGACAGATGTATACCCCGTACGCTTCCCGAGCGAAAACGGTCTGCGCTGCGGGACGCGGCAATTGAATATGGCCCA  
CACAGTGGCGCGGCGACTTCCAGTTCAACATCAGCCGCTACAGTCAACGCAACTGATGGAACCAGCCATCGCCATCTGCTGCACGCGGAAGAAG  
GCACATGGCTGAATATCGACGGTTTTCCATATGGGGATTGGTGGCGACGACTCTGGAGCCCGTCAGTATCGGGCAATTCAGCTGAGCGCGGTCCG  
CTACCATTACCAGTTGGTCTGGTGTCAAAAATAA

## **Firefly Luciferase (FLuc) | 1653 | - | pCSFLW (Edward Wright) | C4.2**

ATGGAAGATGCCAAAACATTAAGAAGGGCCAGCGCCATTCTACCCACTCGAAGACGGGACCGCGGCGAGCAGCTGCACAAAAGCCATGAAGCGCT  
ACGCCCTGGTGCCCGGCACCATCGCCTTTACCGACGCACATATCGAGGTGGACATTACCTACGCCGAGTACTTCGAGATGAGCGTTCCGGTGGCAGA  
AGCTATGAAGCGCTATGGGCTGAATACAAACCATCGGATCGTGGTGTGCAGCGAGAATAGCTTGCAGTTCTTCATGCCCGTGTGGGTGCCCTGTTC  
ATCGGTGTGGCTGTGGCCCCAGCTAACGACATCTACAACGAGCGCGAGCTGTGAACAGCATGGGCATCAGCCAGCCACCCTCGTATTTCGTGAGCA  
AGAAAGGGCTGCAAAAAGATCCTCAACGTGCAAAAAGAAGCTACCGATCATACAAAAAGATCATCATCATGGATAGCAAGACCGACTACCAGGGCTTCCA  
AAGCATGTACACCTTCGTGACTTCCCATTTGCCACCCGGCTTCAACGAGTACGACTTCGTGCCCGAGAGCTTCGACCCGGGACAAAACCATCGCCCTG  
ATCATGAACAGTAGTGGCAGTACCGGATTGCCCAAGGGCGTAGCCCTACCGCACCCGACCCGCTTGTGTCCGATTTCAGTCATGCCCGGACCCCATCT  
TCGGCAACCAGATCATCCCCGACCCGCTATCCTCAGCGTGGTGCCATTTACCACCGCTTCGGCATGTTACCACGCTGGGCTACTTGATCTGCGG  
CTTTCCGGTTCGTGCTCATGTACCGCTTCGAGGAGGAGTATTCTTGCAGCTTGAAGACTATAAGATTCAATCTGCCCTGTGGTGGCCACACTA  
TTTAGCTTCTTCGCTAAGAGCACTCTCATCGACAAGTACGACCTAAGCAACTTGCACGAGATCGCCAGCGGGGGCGCCGCTCAGCAAGGAGGTAG  
GTGAGGCCGTGGCCAAACGCTTCCACCTACCAGGCATCCGCCAGGGCTACGGCCTGACAGAAACAACCAGCGCCATTTCGATCACCCCGAAGGGGA  
CGACAAGCCTGGCGCAGTAGGCAAGGTGGTGCCTTCTTCGAGGCTAAGTGGTGGACTTGGACACCGGTAAGACACTGGGTGTGAACCAGCGCGGC  
GAGCTGTGCGTCCGTGGCCCCATGATCATGAGCGGCTACGTTAACAACCCGAGGCTACAACCGCTCTCATCGACAAGGACGGCTGGCTGCACAGCG  
GCGACATCGCCTACTGGGACGAGGACGAGCACTTCTTTCATCGTGGACCGCTGAAGAGCCTGATCAATAACAAGGGTACCAGGTAGCCCCAGCCGA  
ACTGGAGAGCATCCTGTGCAACACCCCAACATCTTCGACGCGGGGTTCGCCGCTTCCCGACGACGATGCCGGCGAGCTGCCCGCCGAGTCGTC  
GTGCTGGAACACGGTAAACCATGACCGAGAAGGAGATCGTGGACTATGTGGCCAGCCAGGTTACAACCGCCAAGAAGTGCAGCGTGGTGTGTGT  
TCGTGGACAGGTTGCCAAAGACTGACCGGCAAGTTGGACGCCCAAGATCCGCGAGATTCTCATTAAAGGCCAAGAAGGGCGGCAAGATCGCCGT  
GTAA

## **Green Fluorescent Protein (GFP) | 720 | - | pCSFLW (Edward Wright) | C4.2**

ATGGTGAGCAAGGGCGAGGAGCTGTTACCGGGTGGTGCCCATCTGGTCGAGCTGGACGGCGACGTAACCGGCCACAAGTTCAGCGTGTCCGGCG  
AGGGCGAGGGCGATGCCACCTACGGCAAGCTGACCCCTGAAGTTCTATCTGCACCACCGCAAGCTGCCCGTCCCTGGCCACCCCTCGTGACCACCT  
GACCTACGGCGTGCAGTGCTTCAGCCGCTACCCCGACCACATGAAGCAGCAGCACTTCTTCAAGTCCGCCATGCCCGAAGGCTACGTCCAGGAGCGC  
ACCATCTTCTTCAAGGACGACGGCAACTACAAGACCCGCGCCGAGGTGAAGTTGAGGGCGACACCCTGGTGAACCGCATCGAGCTGAAGGGCATCG  
ACTTCAAGGAGGACGGCAACATCTGGGGCACAAGCTGGAGTACAACAGCCACAACGCTCTATATCATGGCCGACAAGCAGAAGAAGCCGAT  
CAAGGTGAAGTTCAAGATCCGCCACAACATCGAGGACGGCAGCGTGCAGCTCGCCGACCACTACCAGCAGAACACCCCATCGGGCAGCGCCCGTG  
CTGCTGCCCGACAACCACTACCTGAGCACCCAGTCCGCCCTGAGCAAAGACCCCAACGAGAAGCGCGATCACATGGTCTGCTGGAGTTCGTGACCG  
CGCCCGGATCACTCTCGGCATGGACGAGCTGTACAAGTAA

### I.3. Plasmid Maps

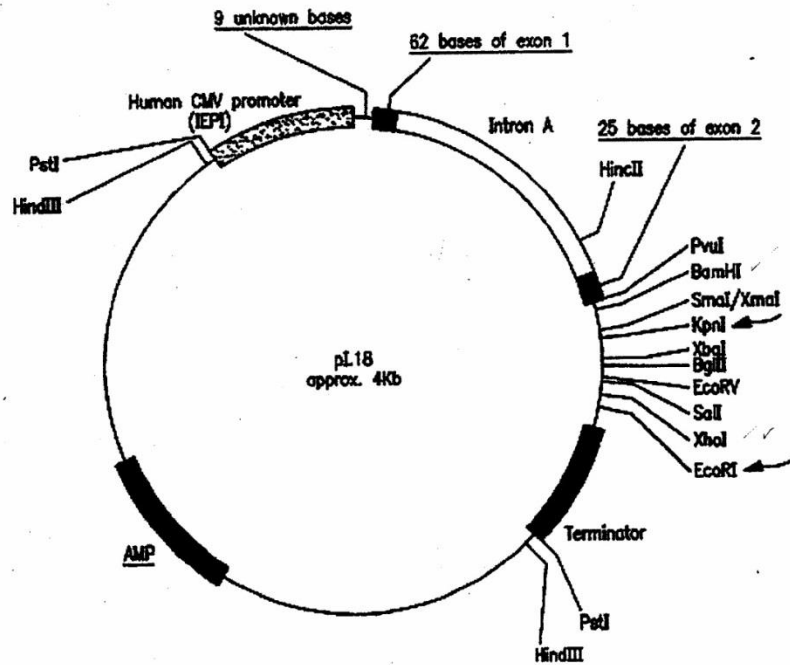
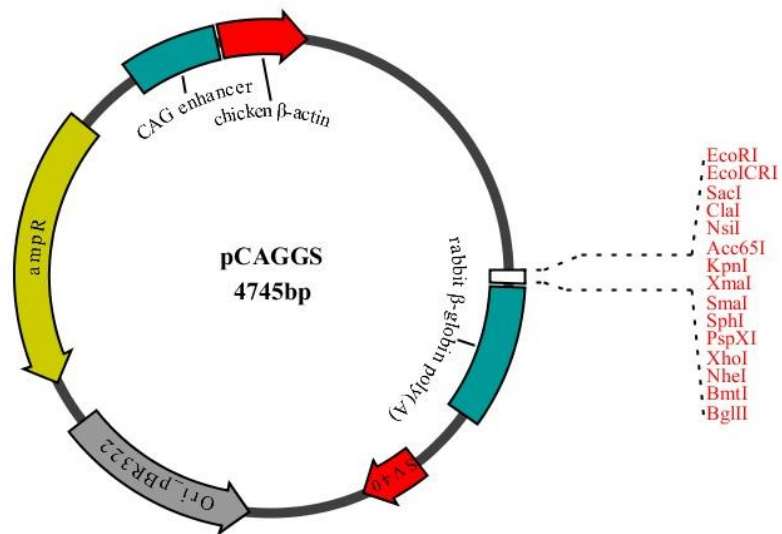


**Figure XVI** pI.18 Expression Plasmid

The pI.18 plasmid comprises a human cytomegalovirus (CMV) early immediate promoter, truncated enhancer region, intron A gene and terminator sequence. The multiple cloning site is shown. It contains an ampicillin resistance gene (AMP) as a selectable marker under a bacterial origin of replication (not shown).

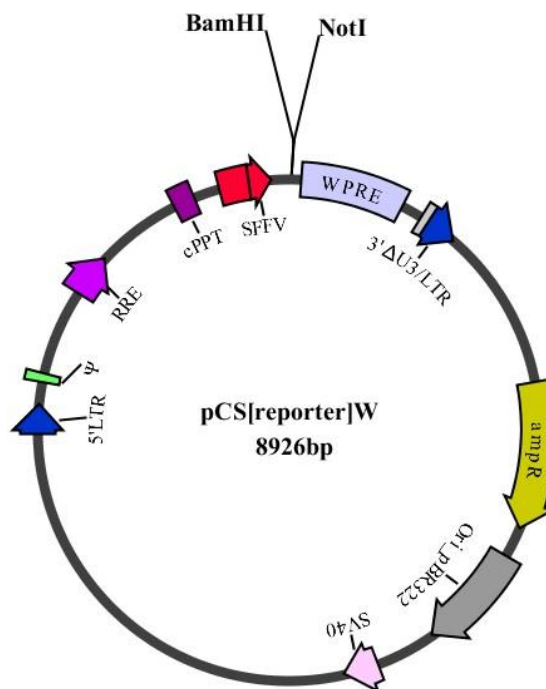


DNADynamo Vector Report

CAG enhancer	83-371
chicken $\beta$ -actin	383-662
MCS	1719-1766
rabbit $\beta$ -globin poly(A)	1772-2202
SV40	2420-2622
Ori_pBR322	2980-3599
ampR	3754-4614

### Figure XVII pCAGGS Expression Plasmid

The pCAGGS plasmid comprises a full chicken  $\beta$ -actin promoter and an efficient poly(A) signal from a rabbit  $\beta$ -globin gene. The multiple cloning site (MCS) is shown. It contains an ampicillin resistance gene (ampR) as a selectable marker under a bacterial origin of replication (pBR322). Map drawn using DNADynamo software.



DNADynamo Vector Report

WPRE	320-912
3'ΔU3/LTR	1019-1252
ampR	2188-3048
Ori_pBR322	3203-3822
SV40	4186-4388
5'LTR	6911-7091
Ψ	7202-7246
RRE	7756-7989
cPPT	8502-8620
SFFV	8772-126

### Figure XVIII pCS[reporter]W Expression Plasmid

The pCS[reporter]W plasmid comprises a HIV 5'LTR, packaging signal ( $\Psi$ ) and rev-response element (RRE) upstream of the reporter gene (cloned within the *Bam*HI and *Not*I restriction sites) which are required for reverse transcription and integration. The strong spleen focus forming virus (SFFV) promoter to drives gene expression and a 3'LTR with a deletion in the U3 region makes the system self-inactivating (SIN). The central polypurine tract (cPPT) and woodchuck hepatitis virus post-transcriptional regulatory element (WPRE), lacking the oncogenic X protein, act to enhance transduction efficiency and expression. The plasmid contains an ampicillin resistance gene (ampR) as a selectable marker under a bacterial origin of replication (pBR322). Map drawn using DNADynamo software.

## Appendix II

### II.1. Arctic-like Rabies Virus Phylogeny

A phylogenetic tree was constructed by Dr Daniel Horton (University of Surrey) to demonstrate the relatedness of the Arctic-like rabies virus isolates used in this study (Figure IV). Construction involved the analysis of 96 RABV glycoprotein sequences (1575 nucleotides) inferred using MEGA6, with a GTR substitution model, gamma distribution of rate variation sites as a proportion of invariant sites (GTR+G+I). Established lineages were illustrated and all except the Arctic-related viruses collapsed for clarity. Bootstrap values (100 replicates) were illustrated at key nodes.

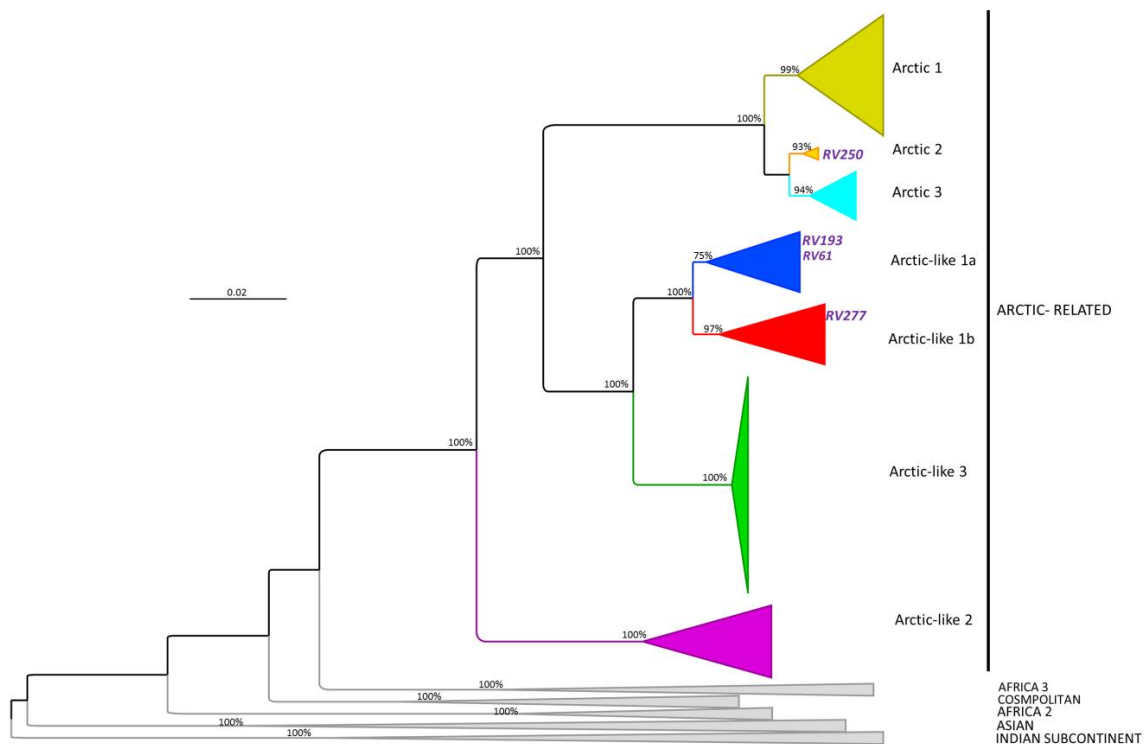


**Figure XIX Maximum Likelihood Phylogenetic Tree of 96 RABV Glycoprotein Coding Sequences**

Branches are labelled with bootstrap values at key nodes. Established clade, sub-clade and lineages are illustrated as previously defined (Pant *et al.*, 2013) and all except the Arctic-related viruses are collapsed for clarity. Positions of the viruses used in this study (RV61, RV193, RV250 and RV277) are indicated. Constructed by Dr Daniel Horton (University of Surrey)

## II.2. Serum Samples from Rabies Virus Vaccinated Humans and Domestic Animals

Details are provided on the FAVN titre of serum samples from human (Table I) and domestic animal (Table II) vaccinees. Samples were provided by Dr Edward Wright and had been obtained as part of a previous study (Wright *et al.*, 2008).

**Table III FAVN Titre Assigned to Vaccinated Human Serum Samples**

Samples from humans vaccinated with a Rabipur, Novartis vaccine and titres assigned by the fluorescent antibody virus neutralisation (FAVN) test

Sample ID	FAVN titre (IU/mL)
H1	0.03
H5	0.10
H6	0.10
H7	0.03
H61	0.38
H66	0.50
H67	17.77
H76	2.60
H77	2.60
H90	3.42

**Table IV FAVN Titre Assigned to Vaccinated Domestic Animal Serum Samples**

Samples from vaccinated domestic dogs and cats enrolled on the UK pet travel scheme (PETS), with titres assigned by the fluorescent antibody virus neutralisation (FAVN) test

Sample ID	FAVN titre (IU/mL)	Vaccine	Animal
PET-5531	0.38	Nobivac, Intervet	Dog
PET-5545	0.22	Rabisin, Merial	Dog
PET-5734	0.38	Rabisin, Merial	Dog
PET-5896	0.07	Quantum, Schering Plough	Dog
PET-7649	4.50	Rabvac, Fort Dodge	Cat
PET-7653	40.50	Rabvac, Fort Dodge	Cat
PET-8418	23.38	Rabvac, Fort Dodge	Cat
PET-8742	479.71	Nobivac, Intervet	Dog
PET-9240	7.79	Nobivac, Intervet	Dog
PET-1323	159.90	Quantum, Schering Plough	Dog

## Appendix III

### III.1. Assessment of Expression Plasmid for *Ebolavirus* Envelope Protein

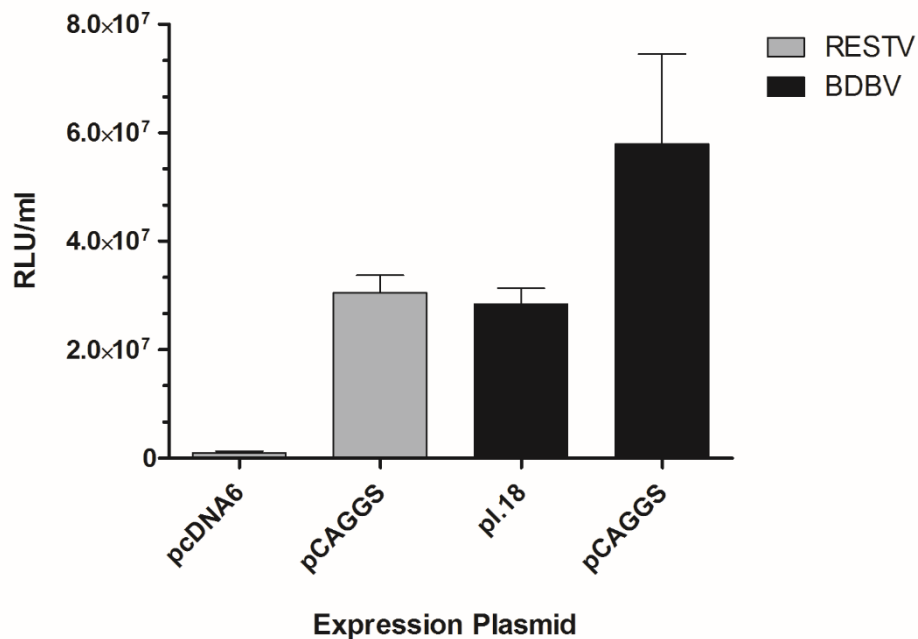


**Figure XX Comparison of Ebolavirus PV Titres using Different Envelope GP Expression Plasmids**

Lentiviral PV with a firefly luciferase reporter gene was produced by a standard three plasmid transfection, supplying the envelope GP of *Reston* or *Bundibugyo ebolavirus* within different expression plasmids for production comparison. Titres of PV were measured by a luciferase assay following infection of HEK 293T/17 cells, reported in relative light units per ml (RLU/mL). Error bars show SD (n = 4). Data produced by Edward Wright

### III.2. Morphology of *Zaire ebolavirus* Pseudotyped Virus

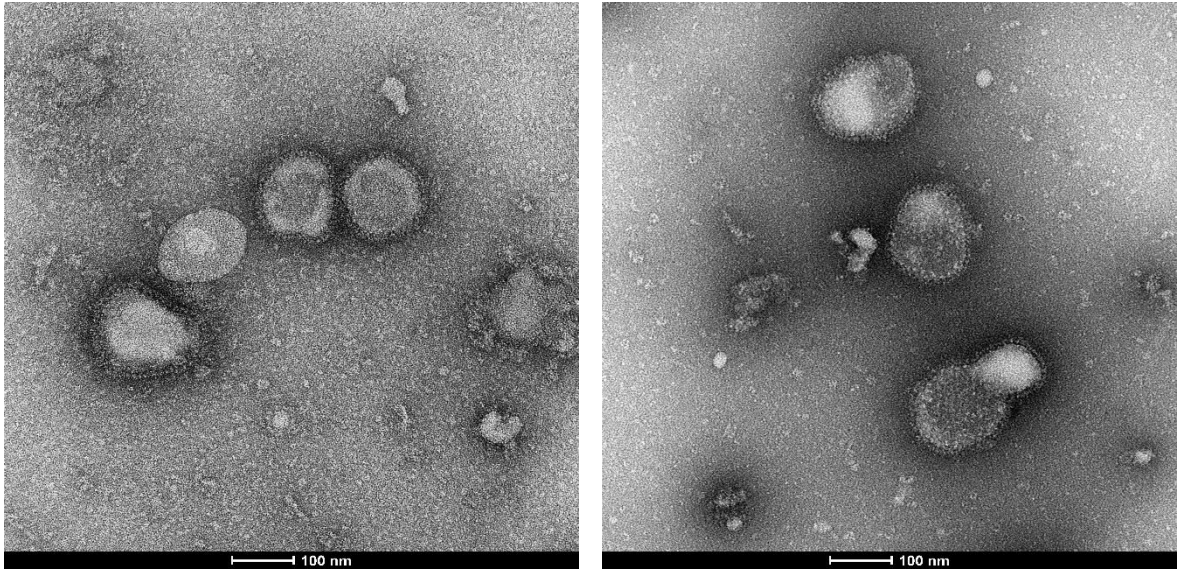


**Figure XXI** Electron Microscopy of *Zaire ebolavirus* PV

Samples of lentiviral PV produced with a *Zaire ebolavirus* GP (isolate: EBOV/Mayinga/COD/1976) were analysed via electron microscopy using a 4% ammonium molybdate pH6.0 with 1% trehalose composition at the Wellcome Trust Sanger Institute (credit: Rachael Wash, Špela Binter, Mathias Friedrich, David Goulding and Paul Kellam).

## Appendix IV

### IV.1. Quantification of PV genome copies via RT-qPCR

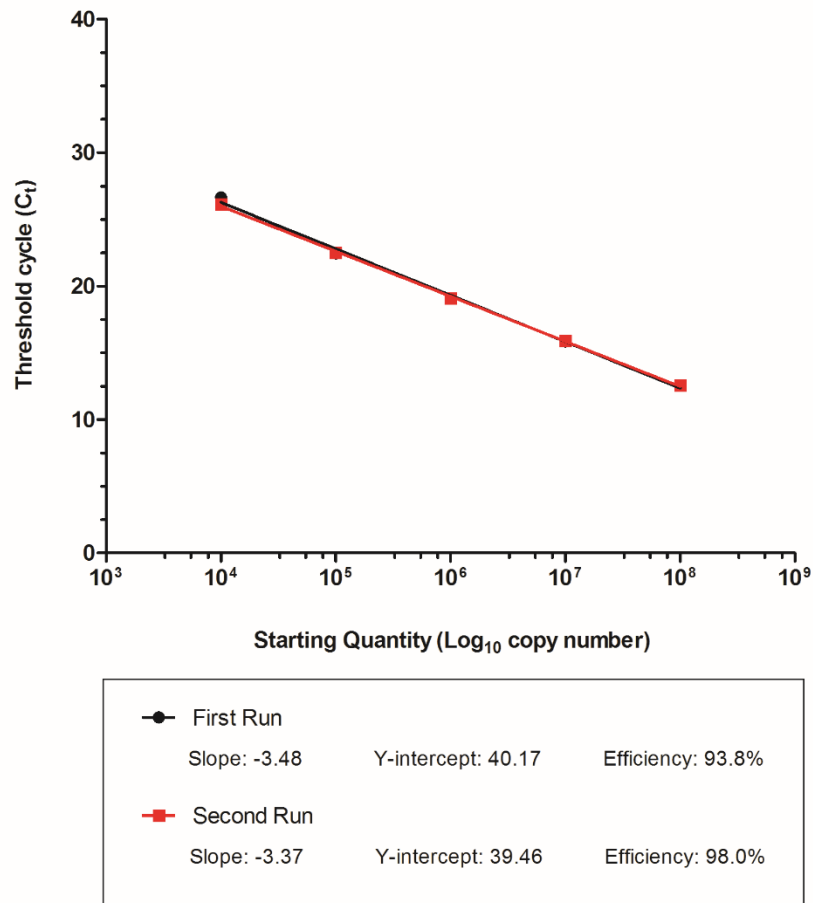


**Figure XXII Standard Curve for RT-qPCR Genome Quantification of PV**

Standard curve composed of a 10-fold dilution series of the pCSFLW plasmid, between  $1 \times 10^1 - 1 \times 10^8$  copies for the two independent runs ( $n = 2$ ). A  $C_t$  value was not assigned to quantities between  $1 \times 10^1 - 1 \times 10^3$ . The slope, y-intercept and efficiency of the reactions are displayed, calculated from the equation of the line in GraphPad Prism v.5.02.

#### IV.2. Quantification of PV core RT activity via SG-PERT Assay

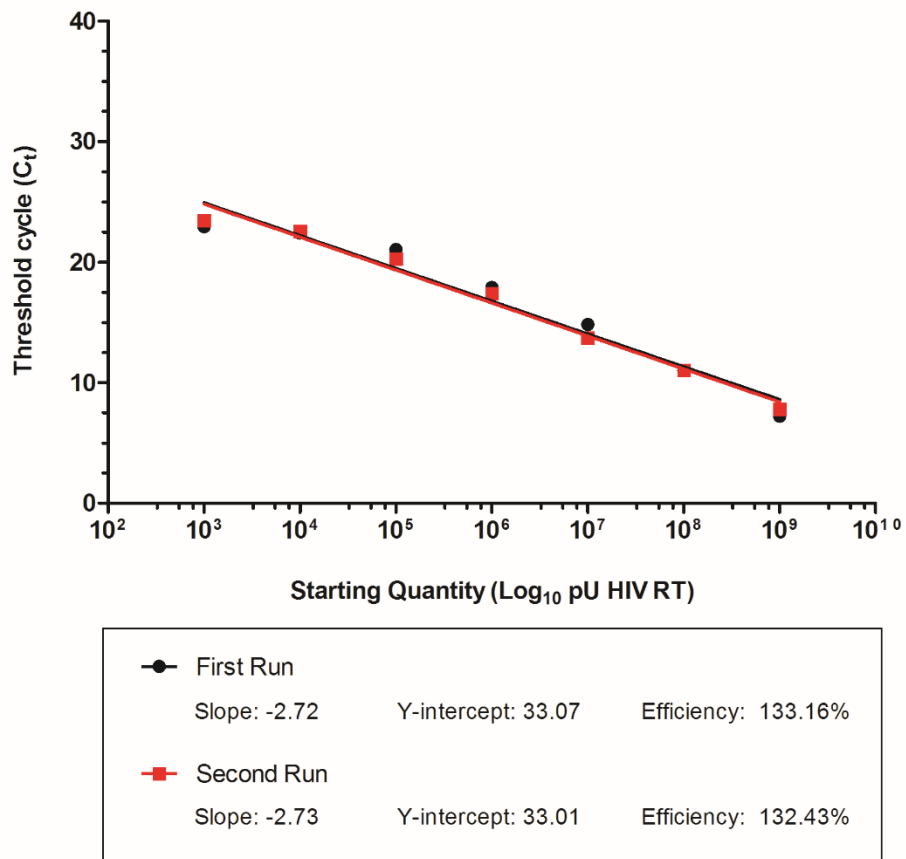


**Figure XXIII Standard Curve for SG-PERT Assay Core RT Activity Quantification of PV**

Standard curve composed of a 10-fold dilution series of the HIV RT standard between  $1 \times 10^3 - 1 \times 10^9$  pU for the two independent runs ( $n = 3$ ). The slope, y-intercept and efficiency of the reactions are displayed, calculated from the equation of the line in GraphPad Prism v.5.02.

## References

- Alam, J. & Cook, J. L. (2003).** Reporter genes for monitoring gene expression in mammalian cells. In *Gene Transf Expr Mamm Cells*, pp. 291–308. Edited by S. C. Makrides. Elsevier B.V.
- An, G., Hidaka, K. & Siminovitch, L. (1982).** Expression of bacterial beta-galactosidase in animal cells. *Mol Cell Biol* **2**, 1628–1632.
- Anderson, L. J. & Baric, R. S. (2012).** Emerging Human Coronaviruses - Disease Potential and Preparedness. *N Engl J Med* **367**, 1848–50.
- Anthony, S., Epstein, J., Murray, K., Navarrete-Macias, I., Zambrana-Torrel, C., Solovyov, A., Ojeda-Flores, R., Arrigo, N., Islam, A. & other authors. (2013).** A Strategy To Estimate Unknown Viral Diversity in Mammals. *MBio* **4**, e00598-13.
- Anthony, S. J., Gilardi, K., Menachery, V. D., Goldstein, T., Ssebide, B., Mbabazi, R., Navarrete-Macias, I., Liang, E., Wells, H. & other authors. (2017).** Further evidence for bats as the evolutionary source of middle east respiratory syndrome coronavirus. *MBio* **8**, 1–13.
- Arguin, P. M., Murray-Lillibridge, K., Miranda, M. E. G., Smith, J. S., Calaor, A. B. & Rupprecht, C. E. (2002).** Serologic evidence of Lyssavirus infections among bats, the Philippines. *Emerg Infect Dis* **8**, 258–262.
- Badrane, H., Bahloul, C., Perrin, P., Lyssavirus, L. & Pasteur, I. (2001).** Evidence of Two Lyssavirus Phylogroups with Distinct Pathogenicity and Immunogenicity. *J Virol* **75**, 3268–3276.
- Baize, S. (2015).** Ebola virus in West Africa: new conquered territories and new risks—or how I learned to stop worrying and (not) love Ebola virus. *Curr Opin Virol* **10**, 70–76. Elsevier B.V.
- Baize, S., Pannetier, D., Oestereich, L., Rieger, T., Koivogui, L., Magassouba, N., Soropogui, B., Sow, M. S., Keita, S. & other authors. (2014).** Emergence of Zaire Ebola Virus Disease in Guinea - Preliminary Report. *N Engl J Med* **371**, 1418–25.
- Bakker, A. B. H., Python, C., Kissling, C. J., Pandya, P., Marissen, W. E., Brink, M. F., Lagerwerf, F., Worst, S., van Corven, E. & other authors. (2008).** First administration to humans of a monoclonal antibody cocktail against rabies virus: Safety, tolerability, and neutralizing activity. *Vaccine* **26**, 5922–5927.
- Bakker, A. B. H., Marissen, W. E., Arjen, R., Rice, A. B., Weldon, W. C., Niezgoda, M., Hanlon, C. a, Thijsse, S., Backus, H. H. J. & other authors. (2005).** Novel Human Monoclonal Antibody Combination Effectively Neutralizing Natural Rabies Virus Variants and Individual In Vitro Escape Mutants Novel Human Monoclonal Antibody Combination Effectively Neutralizing Natural Rabies Virus Variants and Individual In. *J Virol* **79**, 9062–9068.

- Baldi, L., Hacker, D. L., Adam, M. & Wurm, F. M. (2007).** Recombinant protein production by large-scale transient gene expression in mammalian cells: State of the art and future perspectives. *Biotechnol Lett* **29**, 677–684.
- Bale, S., Dias, J. M., Fusco, M. L., Hashiguchi, T., Wong, A. C., Liu, T., Keuhne, A. I., Li, S., Woods, V. L. & other authors. (2012).** Structural Basis for differential neutralization of ebolaviruses. *Viruses* **4**, 447–470.
- Banyard, A. C., Horton, D. L., Freuling, C., Müller, T. & Fooks, A. R. (2013).** Control and prevention of canine rabies: the need for building laboratory-based surveillance capacity. *Antiviral Res* **98**, 357–64. Elsevier B.V.
- Banyard, A. C. & Fooks, A. R. (2017).** The impact of novel lyssavirus discovery. *Microbiol Aust* **38**, 17–21.
- Barrette, R. W., Metwally, S. A., Rowland, J. M., Xu, L., Zaki, S. R., Nichol, S. T., Rollin, P. E., Towner, J. S., Shieh, W. & other authors. (2009).** Discovery of Swine as a host for the Reston ebolavirus. *Science (80- )* **325**, 204–206.
- Bartosch, B., Bukh, J., Meunier, J.-C., Granier, C., Engle, R. E., Blackwelder, W. C., Emerson, S. U., Cosset, F.-L. & Purcell, R. H. (2003a).** In vitro assay for neutralizing antibody to hepatitis C virus: Evidence for broadly conserved neutralization epitopes. *Proc Natl Acad Sci* **100**, 14199–14204.
- Bartosch, B., Dubuisson, J. & Cosset, F.-L. (2003b).** Infectious hepatitis C virus pseudo-particles containing functional E1-E2 envelope protein complexes. *J Exp Med* **197**, 633–42.
- Baud, D., Gubler, D. J., Schaub, B., Lanteri, M. C. & Musso, D. (2017).** An update on Zika virus infection. *Lancet*. Elsevier Ltd.
- Baum, S. E., Machalaba, C., Daszak, P., Salerno, R. H. & Karesh, W. B. (2017).** Evaluating one health: Are we demonstrating effectiveness? *One Heal* **3**, 5–10. The Authors.
- Becquart, P., Wauquier, N., Mahlaköiv, T., Nkoghe, D., Padilla, C., Souris, M., Ollomo, B., Gonzalez, J. P., De Lamballerie, X. & other authors. (2010).** High prevalence of both humoral and cellular immunity to Zaire ebolavirus among rural populations in Gabon. *PLoS One* **5**, e9126.
- Beeck, A. Op De, Bartosch, B., Ciczora, Y., Cocquerel, L., Keck, Z., Fong, S. & Dubuisson, J. (2004).** Characterization of Functional Hepatitis C Virus Envelope Glycoproteins. *J Virol* **78**, 2994–3002.
- Beer, M., Conraths, F. J. & van der Poel, W. H. M. (2013).** ‘Schmallenberg virus’--a novel orthobunyavirus emerging in Europe. *Epidemiol Infect* **141**, 1–8.
- De Benedictis, P., Minola, A., Nodari, E. R., Aiello, R., Zecchin, B., Salomoni, A., Foglierini, M., Agatic, G., Vanzetta, F. & other authors. (2016).** Development of broad-spectrum human monoclonal antibodies for rabies post-exposure prophylaxis. *EMBO Mol Med* **8**, 407–421.

- Benfield, C. T. O., Smith, S. E., Wright, E., Wash, R. S., Ferrara, F., Temperton, N. J. & Kellam, P. (2015).** Bat and pig IFN-induced transmembrane protein 3 restrict cell entry by influenza virus and lyssaviruses. *J Gen Virol* **96**, 991–1005.
- Benmansour, A., Leblois, H., Coulon, P., Tuffereau, C., Gaudin, Y., Flamand, A. & Lafay, F. (1991).** Antigenicity of rabies virus glycoprotein. *J Virol* **65**, 4198–4203.
- Bentley, E. M., Mather, S. T. & Temperton, N. J. (2015).** The use of pseudotypes to study viruses, virus sero-epidemiology and vaccination. *Vaccine* **33**, 2955–2962.
- Berger, J., Hauber, J., Hauber, R., Geiger, R. & Cullen, B. R. (1988).** Secreted placental alkaline phosphatase: a powerful new quantitative indicator of gene expression in eukaryotic cells. *Gene* **66**, 1–10.
- Bermejo, M., Rodriguez-Teijeiro, J. D., Illera, G., Barroso, A., Vila, C. & Walsh, P. D. (2006).** Ebola Outbreak Killed 5000 Gorillas. *Science (80- )* **314**, 1564–1564.
- Bogoch, I. I., Creatore, M. I., Cetron, M. S., Brownstein, J. S., Pesik, N., Miniota, J., Tam, T., Hu, W., Nicolucci, A. & other authors. (2015).** Assessment of the potential for international dissemination of Ebola virus via commercial air travel during the 2014 west African outbreak. *Lancet* **385**, 29–35. Bogoch et al. Open Access article distributed under the terms of CC BY.
- Both, L., Banyard, A. C., Dolleweerd, C. Van, Wright, E., Ma, J. K. & Fooks, A. R. (2013a).** Monoclonal antibodies for prophylactic and therapeutic use against viral infections. *Vaccine* **31**, 1553–1559. Elsevier Ltd.
- Both, L., Dolleweerd, C. Van, Wright, E., Banyard, A. C., Bulmer-thomas, B., Selden, D., Altmann, F., Fooks, A. R. & Ma, J. K. (2013b).** Production, characterization, and antigen specificity of recombinant 62-71-3, a candidate monoclonal antibody for rabies prophylaxis in humans. *FASEB J* **27**, 2055–2065.
- Boulger, L. R. & Porterfield, J. S. (1958).** Isolation of a virus from Nigerian fruit bats. *Trans R Soc Trop Med Hyg* **52**, 421–424.
- Broadhurst, M. J., Brooks, T. J. G. & Pollock, R. (2016).** Diagnosis of Ebola Virus Disease: Past, Present , and Future. *Clin Microbiol Rev* **29**, 773–793.
- Brogan, J., Li, F., Li, W., He, Z., Huang, Q. & Li, C.-Y. (2012).** Imaging molecular pathways: reporter genes. *Radiat Res* **177**, 508–13.
- Brookes, S. M., Parsons, G., Johnson, N., McElhinney, L. M. & Fooks, a R. (2005).** Rabies human diploid cell vaccine elicits cross-neutralising and cross-protecting immune responses against European and Australian bat lyssaviruses. *Vaccine* **23**, 4101–9.
- Buthelezi, S. G., Dirr, H. W., Chakauya, E., Chikwamba, R., Martens, L., Tsekoa, T. L., Stoychev, S. H. & Vandermarliere, E. (2016).** The Lyssavirus glycoprotein: A key to cross-immunity. *Virology* **498**, 250–256.
- Byun, H. M., Suh, D., Jeong, Y., Hyung, S. W., Jung, M. K., Kim, W. K., Jung, J. K., Kim, J. S., Yong, B. L. & Oh, Y. K. (2005).** Plasmid vectors harboring cellular promoters can induce

- prolonged gene expression in hematopoietic and mesenchymal progenitor cells. *Biochem Biophys Res Commun* **332**, 518–523.
- Caglioti, C., Lalle, E., Castilletti, C., Carletti, F., Capobianchi, M. R. & Bordi, L. (2013).** Chikungunya virus infection: an overview. *New Microbiol* **36**, 211–27.
- Carnell, G. W., Ferrara, F., Grehan, K., Thompson, C. P. & Temperton, N. J. (2015).** Pseudotype-based neutralization assays for influenza : a systematic analysis. *Front Immunol* **6**.
- Carpentier, D. C. J., Vevis, K., Trabalza, A., Georgiadis, C., Ellison, S. M., Asfahani, R. I. & Mazarakis, N. D. (2011).** Enhanced pseudotyping efficiency of HIV-1 lentiviral vectors by a rabies/vesicular stomatitis virus chimeric envelope glycoprotein. *Gene Ther* **19**, 761–74. Nature Publishing Group.
- Chalfie, M., Tu, Y., Euskirchen, G., Ward, W. & Prasher, D. (1994).** Green fluorescent protein as a marker for gene expression. *Science (80- )* **263**, 802–805.
- Chan, J., To, K., Tse, H., Jin, D. & Yuen, K. (2013).** Interspecies transmission and emergence of novel viruses: lessons from bats and birds. *Trends Microbiol* **21**, 544–55. Elsevier Ltd.
- Chan, S. Y., Speck, R. F., Ma, M. C. & Goldsmith, M. a. (2000).** Distinct mechanisms of entry by envelope glycoproteins of Marburg and Ebola (Zaire) viruses. *J Virol* **74**, 4933–7.
- Cheng, V. C. C., Lau, S. K. P., Woo, P. C. Y. & Yuen, K. Y. (2007).** Severe acute respiratory syndrome coronavirus as an agent of emerging and reemerging infection. *Clin Microbiol Rev* **20**, 660–94.
- Clements, M. O., Ph, D., Godfrey, A., Crossley, J., Wilson, S. A. M. J., Takeuchi, Y., Boshoff, C. & Mbch, B. (2006).** Lentiviral Manipulation of Gene Expression in Human Adult and Embryonic Stem Cells. *Tissue Eng* **12**, 1741–1751.
- Cleverley, D. Z. & Lenard, J. (1998).** The transmembrane domain in viral fusion: essential role for a conserved glycine residue in vesicular stomatitis virus G protein. *Proc Natl Acad Sci U S A* **95**, 3425–3430.
- Cliquet, F., Aubert, M. & Sagné, L. (1998).** Development of a fluorescent antibody virus neutralisation test (FAVN test) for the quantitation of rabies-neutralising antibody. *J Immunol Methods* **212**, 79–87.
- Condit, R. C. (2001).** Principles of Virology. In *Fields Virol*, 4th edn., pp. 19–51. Edited by D. M. Knipe & P. M. Howley. Philadelphia: Lippincott Williams & Wilkins.
- Corti, D., Misasi, J., Mulangu, S., Stanley, D. A., Kanekiyo, M., Wollen, S., Ploquin, A., Doria-Rose, N. A., Staupe, R. P. & other authors. (2016).** Protective monotherapy against lethal Ebola virus infection by a potently neutralizing antibody. *Science (80- )* **351**, 1339–1342.
- Cosset, F.-L. & Lavillette, D. (2011).** Cell entry of enveloped viruses. In *Adv Genet*, pp. 121–83.
- Cosson, P. (1996).** Direct interaction between the envelope and matrix proteins of HIV-1. *EMBO J*

- 1, 5783–5788.
- Côté, M., Misasi, J., Ren, T., Bruchez, A., Lee, K., Filone, C. M., Hensley, L., Li, Q., Ory, D. & other authors. (2011).** Small molecule inhibitors reveal Niemann-Pick C1 is essential for Ebola virus infection. *Nature* **477**, 344–348.
- Coulon, P., Ternaux, J. P., Flamand, A. & Tuffereau, C. (1998).** An avirulent mutant of rabies virus is unable to infect motoneurons in vivo and in vitro. *J Virol* **72**, 273–8.
- Cox, R. J., Mykkeltvedt, E., Robertson, J. & Haaheim, L. R. (2002).** Non-lethal viral challenge of influenza haemagglutinin and nucleoprotein DNA vaccinated mice results in reduced viral replication. *Scand J Immunol* **55**, 14–23.
- Cubitt, A. B., Woollenweber, L. a & Heim, R. (1998).** Understanding Structure-Function Relationships in the Aequorea victoria Green Fluorescent Protein. *Methods Cell Biol* **58**, 19–30.
- Cullen, B. R. & Malim, M. H. (1992).** Secreted Placental Alkaline Phosphatase as a Eukaryotic Reporter Gene. *Methods Enzymol* **216**, 362–368.
- Daszak, P., Cunningham, A. A. & Hyatt, A. D. (2000).** Emerging Infectious Diseases of Wildlife — Threats to Biodiversity and Human Health. *Science (80- )* **287**, 443–449.
- Daugherty, M. D. & Malik, H. S. (2012).** Rules of engagement: molecular insights from host-virus arms races. *Annu Rev Genet* **46**, 677–700.
- Davis, J., Witt, R., Gross, P., Hokanson, C., Jungles, S., Cohen, L., Danos, O., Spratt, S. & Al, D. (1997).** Retroviral Particles Produced from Packaging a Stable Human-Derived Packaging Cell Line Transduce Target Cells Very High Efficiencies. *Hum Gene Ther* **8**, 1459–1467.
- Demaison, C., Parsley, K., Brouns, G., Scherr, M., Battmer, K., Kinnon, C., Grez, M. & Thrasher, A. J. (2002).** High-level transduction and gene expression in hematopoietic repopulating cells using a human immunodeficiency virus type 1-based lentiviral vector containing an internal spleen focus forming virus promoter. *Hum Gene Ther* **13**, 803–813.
- Dietzgen, R. G., Calisher, C. H., Kurath, G., Kuzmin, I. V., Rodriguez, L. L., Stone, D. M., Tesh, R. B., Tordo, N., Walker, P. J. & other authors. (2011).** Rhabdoviridae. In *Virus Taxon Ninth Rep Int Comm Taxon Viruses*. Edited by M. J. A. Andrew, M. Q. King, E. B. Carstens & E. J. Lefkowitz. Oxford, UK: Elsevier.
- Donnelly, M. L. L., Hughes, L. E., Luke, G., Mendoza, H., ten Dam, E., Gani, D. & Ryan, M. D. (2001).** The ‘cleavage’ activities of foot-and-mouth disease virus 2A site-directed mutants and naturally occurring ‘2A-like’ sequences. *J Gen Virol* **82**, 1027–1041.
- Le Doux, J. M., Morgan, J. R., Snow, R. G. & Yarmush, M. L. (1996).** Proteoglycans secreted by packaging cell lines inhibit retrovirus infection. *J Virol* **70**, 6468–73.
- Dull, T., Zufferey, R., Kelly, M., Mandel, R. J., Nguyen, M., Trono, D. & Naldini, L. (1998).** A third-generation lentivirus vector with a conditional packaging system. *J Virol* **72**, 8463–71.
- Elbers, A. R. W., Loeffen, W. L. A., Quak, S., de Boer-Luijtz, E., van der Spek, A. N.,**

- Bouwstra, R., Maas, R., Spierenburg, M. A. H., de Kluijver, E. P. & other authors. (2012).** Seroprevalence of Schmallenberg virus antibodies among dairy cattle, the Netherlands, winter 2011-2012. *Emerg Infect Dis* **18**, 1065–1071.
- Escors, D., Lopes, L., Lin, R., Hiscott, J., Akira, S., Davis, R. J., Mary, K. & Collins, M. K. (2008).** Targeting dendritic cell signaling to regulate the response to immunization. *Blood* **111**, 3050–3061.
- Evans, J. Wright, E. Easton, A. Fooks, A. Banyard, A. (2013).** Investigating the functionality and antigenicity of chimeric lyssavirus glycoproteins and their neutralisation profiles. In *Pseudotype Viruses Appl Troubl*. London.
- Evans, J. S., Horton, D. L., Easton, A. J., Fooks, A. R. & Banyard, A. C. (2012).** Rabies virus vaccines: is there a need for a pan-lyssavirus vaccine? *Vaccine* **30**, 7447–54. Elsevier Ltd.
- Ewer, K., Rampling, T., Venkatraman, N., Bowyer, G., Wright, D., Lambe, T., Imoukhuede, E. B., Payne, R., Fehling, S. K. & other authors. (2016).** A Monovalent Chimpanzee Adenovirus Ebola Vaccine Boosted with MVA. *N Engl J Med* **374**, 1635–1646.
- Fahrion, A. S., Taylor, L. H., Torres, G., Müller, T., Dürr, S., Knopf, L., de Balogh, K., Nel, L. H., Gordoncillo, M. J. & Abela-Ridder, B. (2017).** The Road to Dog Rabies Control and Elimination—What Keeps Us from Moving Faster? *Front Public Heal* **5**, 1–8.
- Fasina, F. O., Shittu, A., Lazarus, D., Tomori, O., Simonsen, L., Viboud, C. & Chowell, G. (2014).** Transmission dynamics and control of Ebola virus disease outbreak in Nigeria , July to September 2014. *Euro Surveill* **19**, 1–8.
- Feldmann, H., Volchkov, V. E., Volchkova, V. A., Ströher, U. & Klenk, H. D. (2001).** Biosynthesis and role of filoviral glycoproteins. *J Gen Virol* **82**, 2839–2848.
- Feldmann, H., Jones, S., Klenk, H. & Schnittler, H. (2003).** Ebola Virus: from discovery to vaccine. *Nat Rev* **3**, 677–685.
- Ferrara, F., Molesti, E., Böttcher-Friebertshäuser, E., Cattoli, G., Corti, D., Scott, S. D. & Temperton, N. J. (2012).** The human Transmembrane Protease Serine 2 is necessary for the production of Group 2 influenza A virus pseudotypes. *J Mol Genet Med* **7**, 309–14.
- Field, H., Young, P., Yob, J. M., Mills, J., Hall, L. & Mackenzie, J. (2001).** The natural history of Hendra and Nipah viruses. *Microbes Infect* **3**, 307–14.
- Filipe, V., Hawe, A. & Jiskoot, W. (2010).** Critical evaluation of nanoparticle tracking analysis (NTA) by NanoSight for the measurement of nanoparticles and protein aggregates. *Pharm Res* **27**, 796–810.
- Foley, H. D., McGettigan, J. P., Siler, C. a, Dietzschold, B. & Schnell, M. J. (2000).** A recombinant rabies virus expressing vesicular stomatitis virus glycoprotein fails to protect against rabies virus infection. *Proc Natl Acad Sci U S A* **97**, 14680–14685.
- Fooks, A. (2004).** The challenge of new and emerging lyssaviruses. *Expert Rev Vaccines* **3**, 333–6.
- Fooks, A. R., Johnson, N., Freuling, C. M., Wakeley, P. R., Banyard, A. C., McElhinney, L.**

- M., Marston, D. a, Dastjerdi, A., Wright, E. & other authors. (2009).** Emerging technologies for the detection of rabies virus: challenges and hopes in the 21st century. *PLoS Negl Trop Dis* **3**, e530.
- Fooks, A. R., Banyard, A. C., Horton, D. L., Johnson, N., McElhinney, L. M. & Jackson, A. C. (2014).** Current status of rabies and prospects for elimination. *Lancet* **6736**, 1–11. Elsevier Ltd.
- Fouchier, R. A. M. & Smith, D. J. (2010).** Use of Antigenic Cartography in Vaccine Seed Strain Selection. *Avian Dis* **54**, 220–223.
- Frecha, C., Costa, C., Nègre, D., Gauthier, E., Russell, S. J., Cosset, F.-L. & Verhoeven, E. (2008).** Stable transduction of quiescent T cells without induction of cycle progression by a novel lentiviral vector pseudotyped with measles virus glycoproteins. *Blood* **112**, 4843–52.
- Freed, E. O. (1998).** HIV-1 gag proteins: diverse functions in the virus life cycle. *Virology* **251**, 1–15.
- Freed, E. O. & Martin, M. A. (1995).** Virion incorporation of envelope glycoproteins with long but not short cytoplasmic tails is blocked by specific, single amino acid substitutions in the human immunodeficiency virus type 1 matrix. *J Virol* **69**, 1984–1989.
- Freuling, C. M., Hampson, K., Selhorst, T., Schroder, R., Meslin, F. X., Mettenleiter, T. C. & Muller, T. (2013).** The elimination of fox rabies from Europe: determinants of success and lessons for the future. *Philos Trans R Soc B Biol Sci* **368**, 20120142–20120142.
- Geraerts, M., Willems, S., Baekelandt, V., Debyser, Z. & Gijssbers, R. (2006).** Comparison of lentiviral vector titration methods. *BMC Biotechnol* **6**, 34.
- Ghim, C. M., Lee, S. K., Takayama, S. & Mitchell, R. J. (2010).** The art of reporter proteins in science: Past, present and future applications. *BMB Rep* **43**, 451–460.
- Gierer, S., Hofmann-Winkler, H., Albuali, W. H., Bertram, S., Al-Rubaish, A. M., Yousef, A. A., Al-Nafaie, A. N., Al-Ali, A. K., Obeid, O. E. & other authors. (2013).** Lack of MERS coronavirus neutralizing antibodies in humans, Eastern Province, Saudi Arabia. *Emerg Infect Dis* **19**, 2034–2036.
- Gilbert, A. T., Fooks, A. R., Hayman, D. T. S., Horton, D. L., Muller, T., Plowright, R. K., Peel, A. J., Bowen, R., Wood, J. L. N. & other authors. (2013).** Deciphering serology to understand the ecology of infectious diseases in wildlife. *Ecohealth* **10**, 298–313.
- Gilbert, S. C. (2015).** Adenovirus-vectored Ebola vaccines. *Expert Rev Vaccines* **14**, 1347–1357.
- Glynn, J. R., Bower, H., Johnson, S., Houlihan, C. F., Montesano, C., Scott, J. T., Semple, M. G., Bangura, M. S., Kamara, A. J. & other authors. (2017).** Asymptomatic infection and unrecognised Ebola virus disease in Ebola-affected households in Sierra Leone: a cross-sectional study using a new non-invasive assay for antibodies to Ebola virus. *Lancet Infect Dis* **17**, 645–653. The Author(s). Published by Elsevier Ltd. This is an Open Access article under the CC BY license.

- Gortazar, C., Reperant, L. a, Kuiken, T., de la Fuente, J., Boadella, M., Martínez-Lopez, B., Ruiz-Fons, F., Estrada-Peña, A., Drosten, C. & other authors. (2014).** Crossing the interspecies barrier: opening the door to zoonotic pathogens. *PLoS Pathog* **10**, e1004129.
- Le Guenno, B., Formenty, P., Wyers, M., Gounon, P., Walker, F. & Boesch, C. (1995).** Isolation and partial characterisation of a new strain of Ebola virus. *Lancet* **345**, 1271–4.
- Hacein-Bey-Abina, S., von Kalle, C., Schmidt, M., Le Deist, F., Wulfraat, N., McIntyre, E., Radford, I., Villeval, J.-L., Fraser, C. C. & other authors. (2003).** A Serious Adverse Event after Successful Gene Therapy for X-Linked Severe Combined Immunodeficiency. *N Engl J Med* **348**, 255–256.
- Hall, M. P., Unch, J., Binkowski, B. F., Valley, M. P., Butler, B. L., Wood, M. G., Otto, P., Zimmerman, K., Vidugiris, G. & other authors. (2012).** Engineered luciferase reporter from a deep sea shrimp utilizing a novel imidazopyrazinone substrate. *ACS Chem Biol* **7**, 1848–57.
- Hampson, K., Dobson, A., Kaare, M., Dushoff, J., Magoto, M., Sindoya, E. & Cleaveland, S. (2008).** Rabies exposures, post-exposure prophylaxis and deaths in a region of endemic canine rabies. *PLoS Negl Trop Dis* **2**, e339.
- Hampson, K., Coudeville, L., Lembo, T., Sambo, M., Kieffer, A., Attlan, M., Barrat, J., Blanton, J. D., Briggs, D. J. & other authors. (2015).** Estimating the Global Burden of Endemic Canine Rabies. *PLoS Negl Trop Dis* **9**, e0003709.
- Hanlon, C. A., Kuzmin, I. V., Blanton, J. D., Weldon, W. C., Manangan, J. S. & Rupprecht, C. E. (2005).** Efficacy of rabies biologics against new lyssaviruses from Eurasia. *Virus Res* **111**, 44–54.
- Harrison, S. (2013).** Principles of Virus Structure. In *Fields Virol*, Sixth., pp. 52–86. Edited by D. Knipe & P. Howley. Philadelphia: Lippincott Williams & Wilkins.
- Harrison, S. C. (2008).** Viral membrane fusion. *Natl Struct Mol Biol* **15**, 690–698.
- Heckman, K. L. & Pease, L. R. (2007).** Gene splicing and mutagenesis by PCR-driven overlap extension. *Nat Protoc* **2**, 924–32.
- Heider, S. & Metzner, C. (2014).** Quantitative real-time single particle analysis of virions. *Virology* **462–463**, 199–206. Elsevier.
- Hemida, M. G., Perera, R. A., Wang, P., Alhammadi, M. A., Siu, L. Y., Li, M., Poon, L. L., Saif, L., Alnaeem, A. & Peiris, M. (2013).** Middle east respiratory syndrome (MERS) coronavirus seroprevalence in domestic livestock in Saudi Arabia, 2010 to 2013. *Eurosurveillance* **18**, 1–7.
- Higashikawa, F. & Chang, L.-J. (2001).** Kinetic Analyses of Stability of Simple and Complex Retroviral Vectors. *Virology* **280**, 124–131.
- Horton, D. L., McElhinney, L. M., Marston, D. A., Wood, J. L. N., Russell, C. A., Lewis, N., Kuzmin, I. V., Fouchier, R., Osterhaus, A. D. & other authors. (2010).** Quantifying

- antigenic relationships among the lyssaviruses. *J Virol* **84**, 11841–8.
- Horton, D. L., Banyard, A., Marston, D. a, Wise, E., Selden, D., Nunez, A., Hicks, D., Lembo, T., Cleaveland, S. & other authors. (2014).** Antigenic and genetic characterisation of a divergent African virus, Ikoma lyssavirus. *J Gen Virol* 1–23.
- Ibrahimi, A., Vande Velde, G., Reumers, V., Toelen, J., Thiry, I., Vandeputte, C., Vets, S., Deroose, C., Bormans, G. & other authors. (2009).** Highly efficient multicistronic lentiviral vectors with peptide 2A sequences. *Hum Gene Ther* **20**, 845–860.
- Ikeda, Y., Collins, M. K. L., Radcliffe, P. a, Mitrophanous, K. a & Takeuchi, Y. (2002).** Gene transduction efficiency in cells of different species by HIV and EIAV vectors. *Gene Ther* **9**, 932–938.
- Ito, H., Watanabe, S. & Takada, A. (2001).** Ebola Virus Glycoprotein: Proteolytic Processing , Acylation , Cell Tropism , and Detection of Neutralizing Antibodies. *J Virol* **75**, 1576–1580.
- Jallet, C., Jacob, Y., Bahloul, C., Drings, a, Desmezieres, E., Tordo, N. & Perrin, P. (1999).** Chimeric lyssavirus glycoproteins with increased immunological potential. *J Virol* **73**, 225–233.
- Johnson, N., Cunningham, A. F. & Fooks, A. R. (2010a).** The immune response to rabies virus infection and vaccination. *Vaccine* **28**, 3896–3901. Elsevier Ltd.
- Johnson, N., Vos, A., Freuling, C., Tordo, N., Fooks, A. R. & Müller, T. (2010b).** Human rabies due to lyssavirus infection of bat origin. *Vet Microbiol* **142**, 151–159.
- Johnson, N. P. A. S. & Mueller, J. (2002).** Updating the accounts: global mortality of the 1918–1920 ‘Spanish’ Influenza Pandemic. *Bull Hist Med* **76**, 105–115.
- Jones, K. E., Patel, N. G., Levy, M. a, Storeygard, A., Balk, D., Gittleman, J. L. & Daszak, P. (2008).** Global trends in emerging infectious diseases. *Nature* **451**, 990–3.
- Kaku, Y., Noguchi, A., Marsh, G. A., Barr, J. A., Okutani, A., Hotta, K., Bazartseren, B., Fukushi, S., Broder, C. C. & other authors. (2012).** Second generation of pseudotype-based serum neutralization assay for Nipah virus antibodies: Sensitive and high-throughput analysis utilizing secreted alkaline phosphatase. *J Virol Methods* **179**, 226–232. Elsevier B.V.
- Kaskova, Z. M., Tsarkova, A. S. & Yampolsky, I. V. (2016).** 1001 Lights: Luciferins, Luciferases, Their Mechanisms of Action and Applications in Chemical Analysis, Biology and Medicine. *Chem Soc Rev* **45**, 6048–6077. Royal Society of Chemistry.
- Kato, S., Kobayashi, K., Inoue, K., Kuramochi, M., Okada, T., Yaginuma, H., Morimoto, K., Shimada, T., Takada, M. & Kobayashi, K. (2011).** A Lentiviral Strategy for Highly Efficient Retrograde Gene Transfer by Pseudotyping with Fusion Envelope Glycoprotein. *Hum Gene Ther* **22**, 197–206.
- Kelly, T. R., Karesh, W. B., Johnson, C. K., Gilardi, K. V. K., Anthony, S. J., Goldstein, T., Olson, S. H., Machalaba, C. & Mazet, J. A. K. (2017).** One Health proof of concept: Bringing a transdisciplinary approach to surveillance for zoonotic viruses at the human-wild

- animal interface. *Prev Vet Med* **137**, 112–118.
- Khan, S. U., Gurley, E. S., Hossain, M. J., Nahar, N., Sharker, M. A. Y. & Luby, S. P. (2012).** A randomized controlled trial of interventions to impede date palm sap contamination by bats to prevent Nipah virus transmission in Bangladesh. *PLoS One* **7**, 1–7.
- King, B., Temperton, N. J., Grehan, K., Scott, S. D., Wright, E., Tarr, A. W. & Daly, J. M. (2016).** Technical considerations for the generation of novel pseudotyped viruses. *Future Virol* **11**, 47–59.
- Kirkwood, T. B. & Bangham, C. R. (1994).** Cycles, chaos, and evolution in virus cultures: a model of defective interfering particles. *Proc Natl Acad Sci* **91**, 8685–8689.
- Klasse, P. J. (2014).** Neutralization of Virus Infectivity by Antibodies: Old Problems in New Perspectives. *Adv Biol* **2014**, 1–24.
- Kumar, S., Stecher, G. & Tamura, K. (2016).** MEGA7: Molecular Evolutionary Genetics Analysis version 7.0 for bigger datasets. *Mol Biol Evol* **33**, 1870–1874.
- Kuroda, M., Fujikura, D., Nanbo, A., Marzi, A., Noyori, O., Kajihara, M., Maruyama, J., Matsuno, K., Miyamoto, H. & other authors. (2015).** Interaction between TIM-1 and NPC1 Is Important for Cellular Entry of Ebola Virus. *J Virol* **89**, 6481–93.
- Kuzmin, I. V., Bozick, B., Guagliardo, S. A., Kunkel, R., Shak, J. R., Tong, S. & Rupprecht, C. E. (2011).** Bats, Emerging Infectious Diseases, and the Rabies Paradigm Revisited. *Emerg Health Threats J* **4**, 7159.
- Kuzmin, I. V., Hughes, G. J., Botvinkin, a D., Gribencha, S. G. & Rupprecht, C. E. (2008).** Arctic and Arctic-like rabies viruses: distribution, phylogeny and evolutionary history. *Epidemiol Infect* **136**, 509–19.
- Kuzmin, I. V., Hughes, G. J., Botvinkin, A. D., Orciari, L. a & Rupprecht, C. E. (2005).** Phylogenetic relationships of Irkut and West Caucasian bat viruses within the Lyssavirus genus and suggested quantitative criteria based on the N gene sequence for lyssavirus genotype definition. *Virus Res* **111**, 28–43.
- Kuzmin, I. V., Niezgod, M., Carroll, D. S., Keeler, N., Hossain, M. J., Breiman, R. F., Ksiazek, T. G. & Rupprecht, C. E. (2006).** Lyssavirus surveillance in bats, Bangladesh. *Emerg Infect Dis* **12**, 486–488.
- Kuzmina, N., Kuzmin, I. V., Ellison, J. A. & Rupprecht, C. E. (2013).** Conservation of Binding Epitopes for Monoclonal Antibodies on the Rabies Virus Glycoprotein. *J Antivir Antiretrovir* **5**, 37–43.
- Lafon, M., Wiktor, T. & Macfarlan, R. (1983).** Antigenic Sites on the CVS Rabies Virus Glycoprotein : Analysis with Monoclonal Antibodies. *J Gen Virol* **64**, 843–851.
- Lam, S. K. & Chua, K. B. (2002).** Nipah virus encephalitis outbreak in Malaysia. *Clin Infect Dis* **34**, S48–S51.
- Lambe, T., Bowyer, G. & Ewer, K. (2017).** A review of Phase I trials of Ebolavirus vaccines:

- What can we learn from the race to develop novel vaccines? *Philos Trans R Soc B* **372**, 20160295.
- Lau, L., Gray, E. E., Brunette, R. L. & Stetson, D. B. (2015).** DNA tumor virus oncogenes antagonize the cGAS-STING DNA-sensing pathway. *Science* (80- ) **350**, 568–571.
- Lee, J. E., Kuehne, A., Abelson, D. M., Fusco, M. L., Hart, M. K. & Saphire, E. O. (2008a).** Complex of a protective antibody with its Ebola virus GP peptide epitope: unusual features of a  $V_{\lambda x}$ -light chain. *J Mol Biol* **375**, 202–216.
- Lee, J. E., Fusco, M. L., Hessel, A. J., Oswald, W. B. & Burton, D. R. (2008b).** Structure of the Ebola virus glycoprotein bound to a human survivor antibody. *Nature* **454**, 177–182.
- Leroy, E. M., Gonzalez, J.-P. & Baize, S. (2011).** Ebola and Marburg haemorrhagic fever viruses: major scientific advances, but a relatively minor public health threat for Africa. *Clin Microbiol Infect* **17**, 964–76.
- Leroy, E. M., Kumulungui, B., Pourrut, X., Rouquet, P., Hassanin, A., Yaba, P., Délicat, A., Paweska, J. T., Gonzalez, J.-P. & Swanepoel, R. (2005).** Fruit bats as reservoirs of Ebola virus. *Nature* **438**, 575–576.
- Leroy, E. M., Epelboin, A., Mondonge, V., Pourrut, X., Gonzalez, J.-P., Muyembe-Tamfum, J.-J. & Formenty, P. (2009).** Human Ebola Outbreak Resulting from Direct Exposure to Fruit Bats in Luebo, Democratic Republic of Congo, 2007. *Vector-Borne Zoonotic Dis* **9**, 723–728.
- Liu, Y., Liu, J., Du, S., Shan, C., Nie, K., Zhang, R., Li, X.-F., Zhang, R., Wang, T. & other authors. (2017).** Evolutionary enhancement of Zika virus infectivity in *Aedes aegypti* mosquitoes. *Nature* **545**, 482–486. Nature Publishing Group.
- Lizée, G., Aerts, J. L., Gonzales, M. I., Chinnasamy, N., Morgan, R. A. & Topalian, S. L. (2003).** Real-time quantitative reverse transcriptase-polymerase chain reaction as a method for determining lentiviral vector titers and measuring transgene expression. *Hum Gene Ther* **14**, 497–507.
- Logan, A. C., Nightingale, S. J., Haas, D. L., Cho, G. J., Pepper, K. a & Kohn, D. B. (2004).** Factors influencing the titer and infectivity of lentiviral vectors. *Hum Gene Ther* **15**, 976–988.
- Long, J., Wright, E., Molesti, E., Temperton, N. & Barclay, W. (2015).** Antiviral therapies against Ebola and other emerging viral diseases using existing medicines that block virus entry. *F1000Research* **4**, 1–11.
- Lorenz, W. W., Cormier, M. J., Kane, D. J., Hua, D., Escher, A. A. & Szalay, A. A. (1996).** Expression of the *Renilla reniformis* luciferase gene in mammalian cells. *J Biolumin Chemilumin* **11**, 31–37.
- Luo, T. R., Minamoto, N., Ito, H., Goto, H., Hiraga, S., Ito, N., Sugiyama, M. & Kinjo, T. (1997).** A virus-neutralizing epitope on the glycoprotein of rabies virus that contains Trp251 is a linear epitope. *Virus Res* **51**, 35–41.

- Machalaba, C. & Karesh, W. B. (2015).** Envisioning a World Without Emerging Disease Outbreaks. *Solutions* **6**, 63–71.
- Madrid, P. B., Chopra, S., Manger, I. D., Gilfillan, L., Keepers, T. R., Shurtleff, A. C., Green, C. E., Iyer, L. V., Dilks, H. H. & other authors. (2013).** A Systematic Screen of FDA-Approved Drugs for Inhibitors of Biological Threat Agents. *PLoS One* **8**, e60579.
- Maetzig, T., Galla, M., Baum, C. & Schambach, A. (2011).** Gammaretroviral vectors: Biology, technology and application. *Viruses* **3**, 677–713.
- Magre, S., Takeuchi, Y., Langford, G., Richards, A., Patience, C. & Weiss, R. (2004).** Reduced sensitivity to human serum inactivation of enveloped viruses produced by pig cells transgenic for human CD55 or deficient for the galactosyl-alpha(1-3) galactosyl epitope. *J Virol* **78**, 5812–5819.
- Marissen, W. E., Kramer, R. A., Rice, A., Weldon, W. C., Niezgod, M., Faber, M., Slotstra, J. W., Meloen, R. H., Clijsters-van der Horst, M. & other authors. (2005).** Novel rabies virus-neutralizing epitope recognized by human monoclonal antibody: fine mapping and escape mutant analysis. *J Virol* **79**, 4672–4678.
- Martin-Rendon, E., White, L. J., Olsen, A., Mitrophanous, K. A. & Mazarakis, N. D. (2002).** New Methods to Titrate EIAV-Based Lentiviral Vectors. *Mol Ther* **5**, 566–570.
- Mather, S., Scott, S., Temperton, N., Wright, E., King, B. & Daly, J. (2013).** Current progress with serological assays for exotic emerging/re-emerging viruses. *Future Virol* **8**, 745–755.
- Mather, S., Wright, E., Scott, S. & Temperton, N. (2014).** Lyophilisation of influenza, rabies and Marburg lentiviral pseudotype viruses for the development and distribution of a neutralisation-assay-based diagnostic kit. *J Virol Methods* **210**, 51–58.
- Matrosovich, M., Matrosovich, T., Carr, J., Roberts, N. a & Klenk, H.-D. (2003).** Overexpression of the alpha-2,6-sialyltransferase in MDCK cells increases influenza virus sensitivity to neuraminidase inhibitors. *J Virol* **77**, 8418–8425.
- Matsumoto, T., Ahmed, K., Karunanayake, D., Wimalaratne, O., Nanayakkara, S., Perera, D., Kobayashi, Y. & Nishizono, A. (2013).** Molecular epidemiology of human rabies viruses in Sri Lanka. *Infect Genet Evol* **18**, 160–7. Elsevier B.V.
- Mattiuazzo, G., Ashall, J., Doris, K. S., MacLellan-Gibson, K., Nicolson, C., Wilkinson, D. E., Harvey, R., Almond, N., Anderson, R. & other authors. (2015).** Development of Lentivirus-Based Reference Materials for Ebola Virus Nucleic Acid Amplification Technology-Based Assays. *PLoS One* **10**, e0142751.
- McCloskey, B. & Endericks, T. (2017).** The rise of Zika infection and microcephaly: what can we learn from a public health emergency? *Public Health* **150**, 87–92. Elsevier Ltd.
- Meckes, D. G. & Raab-Traub, N. (2011).** Microvesicles and Viral Infection. *J Virol* **85**, 12844–12854.
- Memish, Z. A., Mishra, N., Olival, K. J., Fagbo, S. F., Kapoor, V., Epstein, J. H., AlHakeem,**

- R., Al Asmari, M., Islam, A. & other authors. (2013).** Middle East respiratory syndrome coronavirus in Bats, Saudi Arabia. *Emerg Infect Dis* **19**, 1819–1823.
- Meslin, F., Stöhr, K. & Heymann, D. (2000).** Public health implications of emerging zoonoses morbidity and mortality of new, large outbreaks: the tip of the iceberg. *Rev Sci Tech L'office Int des Epizoot* **19**, 310–317.
- Miller, A. D. (1990).** Retrovirus Packaging Cells. *Hum Gene Ther* **1**, 5–14.
- Miller, E. H., Obernosterer, G., Raaben, M., Herbert, A. S., Deffieu, M. S., Krishnan, A., Ndungo, E., Sandesara, R. G., Carette, J. E. & other authors. (2012).** Ebola virus entry requires the host-programmed recognition of an intracellular receptor. *EMBO J* **31**, 1947–60. Nature Publishing Group.
- Miranda, M. E., Ksiazek, T. G., Retuya, T. J., Khan, A. S., Sanchez, A., Fulhorst, C. F., Rollin, P. E., Calaor, A. B., Manalo, D. L. & other authors. (1999).** Epidemiology of Ebola (subtype Reston) Virus in the Philippines, 1996. *J Infect Dis* **179**, S115–S119.
- Mittler, E., Kolesnikova, L., Hartlieb, B., Davey, R. & Becker, S. (2011).** The cytoplasmic domain of Marburg virus GP modulates early steps of viral infection. *J Virol* **85**, 8188–96.
- Mittler, E., Kolesnikova, L., Herwig, A., Dolnik, O. & Becker, S. (2013).** Assembly of the Marburg virus envelope. *Cell Microbiol* **15**, 270–84.
- Modjarrad, K., Moorthy, V. S., Embarek, P. Ben, Kerkhove, M. Van, Kim, J. & Kieny, M. (2016).** A roadmap for MERS-CoV research and product development : report from a World Health Organization consultation. *Nat Publ Gr* **22**, 701–705. Nature Publishing Group.
- Moeschler, S., Locher, S., Conzelmann, K. K., Kramer, B. & Zimmer, G. (2016).** Quantification of Lyssavirus-neutralizing antibodies using vesicular stomatitis virus pseudotype particles. *Viruses* **8**.
- Mohan, G. S., Ye, L., Li, W., Monteiro, A., Lin, X., Sapkota, B., Pollack, B. P., Compans, R. W. & Yang, C. (2015).** Less is More: Ebola Surface Glycoprotein Expression Levels Regulate Virus Production and Infectivity. *J Virol* **89**, 1205–1217.
- Mohan, G. S., Li, W., Ye, L., Compans, R. W. & Yang, C. (2012).** Antigenic Subversion: A Novel Mechanism of Host Immune Evasion by Ebola Virus. *PLoS Pathog* **8**.
- Molesti, E., Milani, A., Terregino, C., Cattoli, G. & Temperton, N. J. (2013).** Comparative serological assays for the study of h5 and h7 avian influenza viruses. *Influenza Res Treat* **2013**, 286158.
- Molesti, E., Terregino, C., Rahman, R., Cattoli, G. & Wright, E. (2014a).** Multiplex evaluation of influenza neutralizing antibodies with potential applicability to in-field serological studies. *J Immunol Res* **44**.
- Molesti, E., Wright, E., Terregino, C., Rahman, R., Cattoli, G. & Temperton, N. J. (2014b).** Multiplex Evaluation of Influenza Neutralizing Antibodies with Potential Applicability to In-Field Serological Studies. *J Immunol Res* **2014**.

- Moller-Tank, S. & Maury, W. (2015).** Ebola Virus Entry: A Curious and Complex Series of Events. *PLOS Pathog* **11**, e1004731.
- Morse, S. S. (1995).** Factors in the emergence of infectious diseases. *Emerg Infect Dis* **1**, 7–15.
- Morse, S. S., Mazet, J. a K., Woolhouse, M., Parrish, C. R., Carroll, D., Karesh, W. B., Zambrana-torrel, C., Lipkin, W. I. & Daszak, P. (2012).** Prediction and prevention of the next pandemic zoonosis. *Lancet* **380**, 1956–1965.
- Muller, T., Moynagh, J., Cliquet, F., Fooks, A. R., Conraths, F. J., Mettenleiter, T. C. & Freuling, C. M. (2012).** Rabies Elimination in Europe - A Success Story. In *Rabies Control - Toward Sustain Prev Source Compend OIE Globabl Conf Rabies Control*, pp. 31–43. Incheon-Seoul, Republic of Korea.
- Murin, C. D., Fusco, M. L., Bornholdt, Z. a, Qiu, X., Olinger, G. G. & Zeitlin, L. (2014).** Structures of protective antibodies reveal sites of vulnerability on Ebola virus. *PNAS* **111**, 17182–7.
- Nadin-Davis, S. a, Turner, G., Paul, J. P. V, Madhusudana, S. N. & Wandeler, A. I. (2007).** Emergence of Arctic-like rabies lineage in India. *Emerg Infect Dis* **13**, 111–6.
- Nagarajan, T., Marissen, W. E. & Rupprecht, C. E. (2014).** Monoclonal antibodies for the prevention of rabies : theory and clinical practice. *Antib Technol J* **4**, 1–12.
- Nakajima, Y., Kobayashi, K., Yamagishi, K., Enomoto, T. & Ohmiya, Y. (2004).** cDNA Cloning and Characterization of a Secreted Luciferase from the Luminous Japanese Ostracod, *Cypridina noctiluca*. *Biosci Biotechnol Biochem* **68**, 565–570.
- Naldini, L. (1998).** Lentiviruses as gene transfer agents for delivery to non-dividing cells. *Curr Opin Biotechnol* **9**, 457–463.
- Naldini, L., Blömer, U., Gallay, P., Ory, D., Mulligan, R., Gage, F. H., Verma, I. M. & Trono, D. (1996).** In vivo gene delivery and stable transduction of nondividing cells by a lentiviral vector. *Science* **272**, 263–7.
- Nanbo, A., Imai, M., Watanabe, S., Noda, T., Takahashi, K., Neumann, G., Halfmann, P. & Kawaoka, Y. (2010).** Ebolavirus is internalized into host cells via macropinocytosis in a viral glycoprotein-dependent manner. *PLoS Pathog* **6**, e1001121.
- Nash, K. L. & Lever, A. M. L. (2004).** Green fluorescent protein: green cells do not always indicate gene expression. *Gene Ther* **11**, 882–883.
- National Acadamey of Medicine. (2016).** *The Neglected Dimension of Global Security: A Framework to Counter Infectious Disease Crises*. Washington D.C.: National Academies Press.
- Negredo, A., Palacios, G., Vázquez-Morón, S., González, F., Dopazo, H., Molero, F., Juste, J., Quetglas, J., Savji, N. & other authors. (2011).** Discovery of an ebolavirus-like filovirus in europe. *PLoS Pathog* **7**, 1–8.
- Neumann, G., Feldmann, H., Watanabe, S. & Lukashevich, I. (2002).** Reverse Genetics

- Demonstrates that Proteolytic Processing of the Ebola Virus Glycoprotein Is Not Essential for Replication in Cell Culture Reverse Genetics Demonstrates that Proteolytic Processing of the Ebola Virus Glycoprotein Is Not Essential for Repli. *J Virol* **76**, 406–410.
- Neumann, G., Geisbert, T. W., Ebihara, H., Geisbert, J. B., Daddario-DiCaprio, K. M., Feldmann, H. & Kawaoka, Y. (2007).** Proteolytic processing of the Ebola virus glycoprotein is not critical for Ebola virus replication in nonhuman primates. *J Virol* **81**, 2995–8.
- Nichol, S. T., Arikawa, J. & Kawaoka, Y. (2000).** Emerging Viral Diseases. *Proc Natl Acad Sci* **97**, 12411–12412.
- Niwa, H., Yamamura, K. & Miyazaki, J. (1991).** Efficient selection for high-expression transfectants with a novel eukaryotic vector. *Gene* **108**, 193–199.
- O’Hearn, A. E., Voorhees, M. A., Fetterer, D. P., Wauquier, N., Coomber, M. R., Bangura, J., Fair, J. N., Gonzalez, J.-P. & Schoepp, R. J. (2016).** Serosurveillance of viral pathogens circulating in West Africa. *Virol J* **13**, 163. Virology Journal.
- O’Keefe, L., Bentley, E., Kinsley, R. & Wright, E. (2017).** Pseudotyping Efficiency Of (Re-)Emerging Virus Envelope Proteins Using Alternative Cores. In *Microbiol Soc Annu Conf*. Edinburgh.
- O’Shea, T. J., Cryan, P. M., Cunningham, A. a, Fooks, A. R., Hayman, D. T. S., Luis, A. D., Peel, A. J., Plowright, R. K. & Wood, J. L. N. (2014).** Bat flight and zoonotic viruses. *Emerg Infect Dis* **20**, 741–5.
- Olival, K. J. & Hayman, D. T. S. (2014).** Filoviruses in bats: Current knowledge and future directions. *Viruses* **6**, 1759–1788.
- Olival, K. J., Islam, A., Yu, M., Anthony, S. J., Epstein, J. H., Khan, S. A., Khan, S. U., Crameri, G., Wang, L. F. & other authors. (2013).** Ebola virus antibodies in fruit bats, bangladesh. *Emerg Infect Dis* **19**, 270–273.
- Pan, Y., Zhang, W., Cui, L., Hua, X., Wang, M. & Zeng, Q. (2014).** Reston virus in domestic pigs in China. *Arch Virol* **159**, 1129–1132.
- Pant, G. R., Lavenir, R., Wong, F. Y. K., Certoma, A., Larrous, F., Bhatta, D. R., Bourhy, H., Stevens, V. & Dacheux, L. (2013).** Recent emergence and spread of an Arctic-related phylogenetic lineage of rabies virus in Nepal. *PLoS Negl Trop Dis* **7**, e2560.
- Pastrana, D. V., Buck, C. B., Pang, Y. Y. S., Thompson, C. D., Castle, P. E., FitzGerald, P. C., Kjaer, S. K., Lowy, D. R. & Schiller, J. T. (2004).** Reactivity of human sera in a sensitive, high-throughput pseudovirus-based papillomavirus neutralization assay for HPV16 and HPV18. *Virology* **321**, 205–216.
- Pear, W. S., Nolan, G. P., Scott, M. L. & Baltimore, D. (1993).** Production of high-titer helper-free retroviruses by transient transfection (retroviral packaging cells/gene therapy). *Cell Biol* **90**, 8392–8396.
- Peel, A. J., Baker, K. S., Crameri, G., Barr, J. A., Hayman, D. T. S., Fooks, A. R., Wang, L.,**

- Broder, C. C., Cunningham, A. A. & Wood, J. L. N. (2012).** Henipavirus Neutralising Antibodies in an Isolated Island Population of African Fruit Bats. *PLoS One* **7**, 1–9.
- Peiris, J. S., Poon, L. L. & Guan, Y. (2012).** Public health. Surveillance of animal influenza for pandemic preparedness. *Science (80- )* **335**, 1173–1174.
- Perera, R. A., Wang, P., Gomaa, M. R., El-Shesheny, R., Kandeil, A., Bagato, O., Siu, L. Y., Shehata, M. M., Kayed, A. S. & other authors. (2013).** Seroprevalence for MERS coronavirus using microneutralisation and pseudoparticle virus neutralisation assays reveal a high prevalence of antibody in dromedary camels in Egypt, June 2013. *Eurosurveillance* **18**, 1–7.
- Pigott, D. M., Golding, N., Mylne, A., Huang, Z., Henry, A. J., Weiss, D. J., Brady, O. J., Kraemer, M. U. G., Smith, D. L. & other authors. (2014).** Mapping the zoonotic niche of Ebola virus disease in Africa. *Elife* **3**, e04395.
- Pizzato, M., Marlow, S. A. & Blair, E. D. (1999).** Initial Binding of Murine Leukemia Virus Particles to Cells Does Not Require Specific Env-Receptor Interaction. *J Virol* **73**, 8599–8611.
- Pizzato, M., Erlwein, O., Bonsall, D., Kaye, S., Muir, D. & McClure, M. O. (2009).** A one-step SYBR Green I-based product-enhanced reverse transcriptase assay for the quantitation of retroviruses in cell culture supernatants. *J Virol Methods* **156**, 1–7.
- Pöhlmann, S. (2013).** *Viral Entry into Host Cells*. Advances in Experimental Medicine and Biology (S. Pöhlmann & G. Simmons, Eds.). New York, NY: Springer New York.
- Powell, T. J., Silk, J. D., Sharps, J., Fodor, E. & Townsend, A. R. M. (2012).** Pseudotyped influenza A virus as a vaccine for the induction of heterotypic immunity. *J Virol* **86**, 13397–406.
- PREDICT. (2017).** *2017 SEMI-ANNUAL REPORT*.
- Prehaud, C., Coulon, P., LaFay, F., Thiers, C. & Flamand, A. (1988).** Antigenic site II of the rabies virus glycoprotein: structure and role in viral virulence. *J Virol* **62**, 1–7.
- Pybus, O. G., Tatem, A. J. & Lemey, P. (2015).** Virus evolution and transmission in an ever more connected world. *Proc R Soc B* **282**.
- Ramnial, V., Kosmider, R., Aylan, O., Freuling, C., Müller, T. & Fooks, A. R. (2010).** Quantitative risk assessment to compare the risk of rabies entering the UK from Turkey via quarantine, the Pet Travel Scheme and the EU Pet Movement Policy. *Epidemiol Infect* **138**, 1114–1125.
- Raposo, G. & Stoorvogel, W. (2013).** Extracellular vesicles: Exosomes, microvesicles, and friends. *J Cell Biol* **200**, 373–383.
- Reed, L. & Muench, H. (1938).** A simple method of estimating fifty per cent endpoints. *Am J Hyg* **27**, 493–497.
- Reperant, L. A. & Osterhaus, A. D. M. E. (2017).** AIDS, Avian flu, SARS, MERS, Ebola,

- Zika... what next? *Vaccine* **16**, 4470–74.
- Roche, S., Bressanelli, S., Rey, F. & Gaudin, Y. (2006).** Crystal Structure of the Low-pH Form of the Vesicular Stomatitis Virus Glycoprotein G. *Science* **313**, 187–192.
- Rose, J. K., Welch, W. J., Sefton, B. M., Esch, F. S. & Ling, N. C. (1980).** Vesicular stomatitis virus glycoprotein is anchored in the viral membrane by a hydrophobic domain near the COOH terminus. *Proc Natl Acad Sci U S A* **77**, 3884–8.
- Ross, R. S., Wolters, B., Hoffmann, B., Geue, L., Viazov, S., Grüner, N., Roggendorf, M. & Müller, T. (2015).** Instructive even after a decade: Complete results of initial virological diagnostics and re-evaluation of molecular data in the German rabies virus ‘outbreak’ caused by transplantations. *Int J Med Microbiol* **305**, 636–643. Elsevier GmbH.
- Ryan, M. D., King, A. M. Q. & Thomas, G. P. (1991).** Cleavage of foot-and-mouth disease virus polyprotein is mediated by residues located within a 19 amino acid sequence. *J Gen Virol* **72**, 2727–2732.
- Saeed, M. F., Kolokoltsov, A. A., Albrecht, T. & Davey, R. A. (2010).** Cellular entry of ebola virus involves uptake by a macropinocytosis-like mechanism and subsequent trafficking through early and late endosomes. *PLoS Pathog* **6**, e1001110.
- Sakuma, T., Barry, M. A. & Ikeda, Y. (2012).** Lentiviral vectors: basic to translational. *Biochem J* **443**, 603–618.
- Sanchez, A., Trappier, S. G., Mahy, B. W., Peters, C. J. & Nichol, S. T. (1996).** The virion glycoproteins of Ebola viruses are encoded in two reading frames and are expressed through transcriptional editing. *Proc Natl Acad Sci U S A* **93**, 3602–7.
- Sandrin, V. & Cosset, F.-L. (2006).** Intracellular versus cell surface assembly of retroviral pseudotypes is determined by the cellular localization of the viral glycoprotein, its capacity to interact with Gag, and the expression of the Nef protein. *J Biol Chem* **281**, 528–42.
- Sandrin, V., Muriaux, D., Darlix, J. & Inserm, U. (2004).** Intracellular Trafficking of Gag and Env Proteins and Their Interactions Modulate Pseudotyping of Retroviruses. *J Virol* **78**, 7153–7164.
- Sastry, L., Johnson, T., Hobson, M. J., Smucker, B. & Cornetta, K. (2002).** Titering lentiviral vectors: comparison of DNA, RNA and marker expression methods. *Gene Ther* **9**, 1155–1162.
- Schatz, J., Freuling, C. M., Auer, E., Goharriz, H., Harbusch, C., Johnson, N., Kaipf, I., Mettenleiter, T. C., Mühldorfer, K. & other authors. (2014).** Enhanced passive bat rabies surveillance in indigenous bat species from Germany - a retrospective study. *PLoS Negl Trop Dis* **8**, e2835.
- Scherr, M., Battmer, K., Blömer, U., Ganser, A. & Grez, M. (2001).** Quantitative determination of lentiviral vector particle numbers by real-time PCR. *Biotechniques* **31**, 520–526.
- Schornberg, K., Matsuyama, S., Kabsch, K., Delos, S., Bouton, A. & White, J. (2006).** Role of

- Endosomal Cathepsins in Entry Mediated by the Ebola Virus Glycoprotein Role of Endosomal Cathepsins in Entry Mediated by the Ebola Virus Glycoprotein. *J Virol* **80**, 4174–4178.
- Schultz, A., Koch, S., Fuss, M., Mazzotta, A. S., Sarzotti-Kelsoe, M., Ozaki, D. A., Montefiori, D. C., von Briesen, H., Zimmermann, H. & Meyerhans, A. (2012).** An Automated HIV-1 Env-Pseudotyped Virus Production for Global HIV Vaccine Trials. *PLoS One* **7**, e51715.
- Schwefel, D., Groom, H. C. T., Boucherit, V. C., Christodoulou, E., Walker, P. A., Stoye, J. P., Bishop, K. N. & Taylor, I. A. (2014).** Structural basis of lentiviral subversion of a cellular protein degradation pathway. *Nature* **505**, 234–8.
- Scolari, S., Imkeller, K., Jolmes, F., Veit, M., Herrmann, A. & Schwarzer, R. (2016).** Modulation of cell surface transport and lipid raft localization by the cytoplasmic tail of the influenza virus hemagglutinin. *Cell Microbiol* **18**, 125–136.
- Shaner, N. C., Campbell, R. E., Steinbach, P. A., Giepmans, B. N. G., Palmer, A. E. & Tsien, R. Y. (2004).** Improved monomeric red, orange and yellow fluorescent proteins derived from *Discosoma* sp. red fluorescent protein. *Nat Biotechnol* **22**, 1567–1572.
- Shaner, N. C., Steinbach, P. A. & Tsien, R. Y. (2005).** A guide to choosing fluorescent proteins. *Nat Methods* **2**, 905–909.
- Sharma, S., Miyahara, A. & Friedmann, T. (2000).** Separable mechanisms of attachment and cell uptake during retrovirus infection. *J Virol* **74**, 10790–5.
- Shtanko, O., Nikitina, R. A., Altuntas, C. Z., Chepurinov, A. A. & Davey, R. A. (2014).** Crimean-Congo Hemorrhagic Fever Virus Entry into Host Cells Occurs through the Multivesicular Body and Requires ESCRT Regulators. *PLoS Pathog* **10**, e1004390.
- Simmons, G., Rennekamp, A. J., Chai, N., Vandenberghe, L. H., Riley, J. L. & Bates, P. (2003a).** Folate receptor alpha and caveolae are not required for Ebola virus glycoprotein-mediated viral infection. *J Virol* **77**, 13433–13438.
- Simmons, G., Reeves, J. D., Grogan, C. C., Vandenberghe, L. H., Baribaud, F., Whitbeck, J. C., Burke, E., Buchmeier, M. J., Soilleux, E. J. & other authors. (2003b).** DC-SIGN and DC-SIGNR bind ebola glycoproteins and enhance infection of macrophages and endothelial cells. *Virology* **305**, 115–123.
- Sims, L. D. & Peiris, M. (2013).** One Health: The Hong Kong Experience with Avian Influenza. *Curr Top Microbiol Immunol* **365**, 281–298.
- Smith, C. E. G., Simpson, D. I. H., Bowen, E. T. W. & Zlotnik, I. (1967).** Fatal human disease from vervet monkeys. *Lancet* **2**, 1119–1121.
- Smith, D. J., Lapedes, A. S., de Jong, J. C., Bestebroer, T. M., Rimmelzwaan, G. F., Osterhaus, A. D. & Fouchier, R. A. (2004).** Mapping the Antigenic and Genetic Evolution of Influenza Virus. *Science (80- )* **305**, 371–376.
- Smith, J. S., Yager, P. A. & Baer, G. M. (1973).** A rapid reproducible test for determining rabies

- neutralizing antibody. *Bull World Health Organ* **48**, 535–541.
- Smith, K. F., Goldberg, M., Rosenthal, S., Carlson, L., Chen, J., Chen, C. & Ramachandran, S. (2014).** Global rise in human infectious disease outbreaks. *J R Soc Interface* **11**, 1–6.
- Smith, K. M., Machalaba, C. M., Jones, H., Cáceres, P., Popovic, M., Olival, K. J., Ben Jebara, K. & Karesh, W. B. (2017).** Wildlife hosts for OIE-Listed diseases: considerations regarding global wildlife trade and host-pathogen relationships. *Vet Med Sci* **3**, 71–81.
- Smith, S. E., Gibson, M. S., Wash, R. S., Ferrara, F., Wright, E., Temperton, N., Kellam, P. & Fife, M. (2013).** Chicken Interferon-Inducible Transmembrane Protein 3 Restricts Influenza Viruses and Lyssaviruses In Vitro. *J Virol* **87**, 12957–12966.
- Soneoka, Y., Cannon, P. M., Ramsdale, E. E., Griffiths, J. C., Romano, G., Kingsman, S. M. & Kingsman, A. J. (1995).** A transient three-plasmid expression system for the production of high titer retroviral vectors. *Nucleic Acids Res* **23**, 628–33.
- Spellberg, B. & Taylor-Blake, B. (2013).** On the exoneration of Dr. William H. Stewart: debunking an urban legend. *Infect Dis Poverty* **2**.
- Steffen, I. & Simmons, G. (2016).** Pseudotyping Viral Vectors With Emerging Virus Envelope Proteins. *Curr Gene Ther* **16**, 47–55.
- Storch, G. & Wang, D. (2013).** Diagnostic Virology. In *Fields Virol*, Sixth Edit., pp. 414–452. Edited by D. Knipe & P. Howley. Philadelphia: Lippincott Williams & Wilkins.
- Stremlau, M., Owens, C. M., Perron, M. J., Kiessling, M., Autissier, P. & Sodroski, J. (2004).** The cytoplasmic body component TRIM5 $\alpha$  restricts HIV-1 infection in Old World monkeys. *Nature* **427**, 848–853.
- Su, C. Y., Wang, S. Y., Shie, J. J., Jeng, K. S., Temperton, N. J., Fang, J. M., Wong, C. H. & Cheng, Y. S. E. (2008).** In vitro evaluation of neuraminidase inhibitors using the neuraminidase-dependent release assay of hemagglutinin-pseudotyped viruses. *Antiviral Res* **79**, 199–205.
- Su, S., Wong, G., Liu, Y., Gao, G. F., Li, S. & Bi, Y. (2015).** MERS in South Korea and China: a potential outbreak threat? *Lancet* **385**, 2349–2350. Elsevier Ltd.
- Sudarshan, M. K., Madhusudana, S. N., Mahendra, B. J., Rao, N. S. N., Ashwath Narayana, D. H., Abdul Rahman, S., Meslin, F.-X., Lobo, D., Ravikumar, K. & Gangaboraiah. (2007).** Assessing the burden of human rabies in India: results of a national multi-center epidemiological survey. *Int J Infect Dis* **11**, 29–35.
- Szécsi, J., Boson, B., Johnsson, P., Dupeyrot-Lacas, P., Matrosovich, M., Klenk, H.-D., Klatzmann, D., Volchkov, V. & Cosset, F.-L. (2006).** Induction of neutralising antibodies by virus-like particles harbouring surface proteins from highly pathogenic H5N1 and H7N1 influenza viruses. *Virology* **3**, 70.
- Szymczak-Workman, A. L., Vignali, K. M. & Vignali, D. A. A. (2012).** Design and construction of 2A peptide-linked multicistronic vectors. *Cold Spring Harb Protoc* **7**, 199–204.

- Szymczak, A. L. & Vignali, D. a a. (2005).** Development of 2A peptide-based strategies in the design of multicistronic vectors. *Expert Opin Biol Ther* **5**, 627–38.
- Szymczak, A. L., Workman, C. J., Wang, Y., Vignali, K. M., Dilioglou, S., Vanin, E. F. & Vignali, D. A. A. (2004).** Correction of multi-gene deficiency in vivo using a single ‘self-cleaving’ 2A peptide-based retroviral vector. *Nat Biotechnol* **22**, 589–594.
- Takada, A. (2012).** Filovirus tropism: Cellular molecules for viral entry. *Front Microbiol* **3**, 1–9.
- Takeuchi, Y., Porter, C. D., Strahan, K. M., Preece, A. F., Gustafsson, K., Cosset, F. L., Weiss, R. A. & Collins, M. K. (1996).** Sensitization of cells and retroviruses to human serum by (alpha 1-3) galactosyltransferase. *Nature* **379**, 85–8.
- Tamura, K., Stecher, G., Peterson, D., Filipinski, A. & Kumar, S. (2013).** MEGA6: Molecular evolutionary genetics analysis version 6.0. *Mol Biol Evol* **30**, 2725–2729.
- Taniguchi, S., Watanabe, S., Masangkay, J. S., Omatsu, T., Ikegami, T., Alviola, P., Ueda, N., Iha, K., Fujii, H. & other authors. (2011).** Reston Ebolavirus antibodies in bats, the Philippines. *Emerg Infect Dis* **17**, 1559–60.
- Tarlinton, R., Daly, J., Dunham, S. & Kydd, J. (2012).** The challenge of Schmallenberg virus emergence in Europe. *Vet J* **194**, 10–18. Elsevier Ltd.
- Tarr, A. W., Owsianka, A. M., Szwejk, A., Ball, J. K. & Patel, A. H. (2007).** Cloning, expression, and functional analysis of patient-derived hepatitis C virus glycoproteins. *Methods Mol Biol* **379**, 177–97.
- Taylor, L. H., Latham, S. M. & Woolhouse, M. E. (2001).** Risk factors for human disease emergence. *Philos Trans R Soc Lond B Biol Sci* **356**, 983–9.
- Temperton, N. J. & Page, M. (2015).** Ebolavirus: pseudotypes, libraries and standards. *Futur Virol* **10**, 1187–1189.
- Temperton, N. J., Chan, P. K., Simmons, G., Zambon, M. C., Tedder, R. S., Takeuchi, Y. & Weiss, R. a. (2005).** Longitudinally profiling neutralizing antibody response to SARS coronavirus with pseudotypes. *Emerg Infect Dis* **11**, 411–6.
- Temperton, N. J., Hoschler, K., Major, D., Nicolson, C., Manvell, R., Hien, V. M., Ha, D. Q., de Jong, M., Zambon, M. & other authors. (2007).** A sensitive retroviral pseudotype assay for influenza H5N1-neutralizing antibodies. *Influenza Other Respi Viruses* **1**, 105–12.
- Temperton, N. J., Wright, E. & Scott, S. D. (2015a).** Retroviral Pseudotypes – from scientific tools to clinical utility. In *Encycl Life Sci*, pp. 1–21. John Wiley & Sons.
- Temperton, N. J., Wright, E. & Scott, S. D. (2015b).** Retroviral Pseudotypes – from scientific tools to clinical utility. *Encycl Life Sci* 1–21.
- The World Bank. (2012).** *The Economics of One Health. People, Pathog Our Planet.*
- Thomas, P. & Smart, T. G. (2005).** HEK293 cell line: A vehicle for the expression of recombinant proteins. *J Pharmacol Toxicol Methods* **51**, 187–200.
- To, K. K. W., Chan, J. F. W., Tsang, A. K. L., Cheng, V. C. C. & Yuen, K.-Y. (2015).** Ebola

- virus disease: a highly fatal infectious disease reemerging in West Africa. *Microbes Infect* **17**, 84–97. Elsevier Masson SAS.
- Towers, G., Bock, M., Martin, S., Takeuchi, Y., Stoye, J. P. & Danos, O. (2000).** A conserved mechanism of retrovirus restriction in mammals. *Proc Natl Acad Sci* **97**, 12295–12299.
- Towner, J. S., Pourrut, X., Albariño, C. G., Nkogue, C. N., Bird, B. H., Grard, G., Ksiazek, T. G., Gonzalez, J. P., Nichol, S. T. & Leroy, E. M. (2007).** Marburg virus infection detected in a common African bat. *PLoS One* **2**, e764.
- Towner, J. S., Sealy, T. K., Khristova, M. L., Albariño, C. G., Conlan, S., Reeder, S. A., Quan, P. L., Lipkin, W. I., Downing, R. & other authors. (2008).** Newly discovered Ebola virus associated with hemorrhagic fever outbreak in Uganda. *PLoS Pathog* **4**, 3–8.
- Towner, J. S., Amman, B. R., Sealy, T. K., Reeder Carroll, S. A., Comer, J. A., Kemp, A., Swanepoel, R., Paddock, C. D., Balinandi, S. & other authors. (2009).** Isolation of genetically diverse Marburg viruses from Egyptian fruit bats. *PLoS Pathog* **5**, e1000536.
- Troupin, C., Dacheux, L., Tanguy, M., Sabeta, C., Holmes, E. C., Bouchier, C., Vignuzzi, M., Duchene, S., Holmes, E. & Bourhy, H. (2016).** Large-Scale Phylogenomic Analysis Reveals the Complex Evolutionary History of Rabies Virus in Multiple Carnivore Hosts. *PLoS Pathog* **12**, e1006041.
- Tssetsarkin, K. A. & Weaver, S. C. (2011).** Sequential adaptive mutations enhance efficient vector switching by Chikungunya virus and its epidemic emergence. *PLoS Pathog* **7**, e1002412.
- Tssetsarkin, K. A., Vanlandingham, D. L., McGee, C. E. & Higgs, S. (2007).** A single mutation in chikungunya virus affects vector specificity and epidemic potential. *PLoS Pathog* **3**, e201.
- Urbanowicz, R. A., McClure, C. P., Brown, R. J. P., Tsoleridis, T., Persson, M. A. A., Krey, T., Irving, W. L., Ball, J. K. & Tarr, A. W. (2016a).** A Diverse Panel of Hepatitis C Virus Glycoproteins for Use in Vaccine Research Reveals Extremes of Monoclonal Antibody Neutralization Resistance. *J Virol* **90**, 3288–3301.
- Urbanowicz, R. A., McClure, C. P., Sakuntabhai, A., Sall, A. A., Kobinger, G., Müller, M. A., Holmes, E. C., Rey, F. A., Simon-Loriere, E. & Ball, J. K. (2016b).** Human Adaptation of Ebola Virus during the West African Outbreak. *Cell* **167**, 1079–1087.e5.
- Uttenthal, A., Parida, S., Rasmussen, T. B., Paton, D. J., Haas, B. & Dundon, W. G. (2010).** Strategies for differentiating infection in vaccinated animals (DIVA) for foot-and-mouth disease, classical swine fever and avian influenza. *Expert Rev Vaccines* **9**, 73–87.
- Venkatraman, N., Silman, D., Folegatti, P. M. & Hill, A. V. S. (2017).** Vaccines against Ebola virus. *Vaccine*.
- Vermeire, J., Naessens, E., Vanderstraeten, H., Landi, A., Iannucci, V., Van Nuffel, A., Taghon, T., Pizzato, M. & Verhasselt, B. (2012).** Quantification of Reverse Transcriptase Activity by Real-Time PCR as a Fast and Accurate Method for Titration of HIV, Lenti- and Retroviral Vectors. *PLoS One* **7**, e50859.

- Vigant, F., Santos, N. C. & Lee, B. (2015).** Broad-spectrum antivirals against viral fusion. *Nat Rev Microbiol* **13**, 426–437. Nature Publishing Group.
- Vigilato, M. A. N., Cosivi, O., Knobl, T., Clavijo, A. & Silva, H. M. T. (2013).** Rabies update for Latin America and the Caribbean. *Emerg Infect Dis* **19**, 678–679.
- Voelkel, C., Galla, M., Dannhauser, P. N., Maetzig, T., Sodeik, B., Schambach, A. & Baum, C. (2012).** Pseudotype-Independent Nonspecific Uptake of Gammaretroviral and Lentiviral Particles in Human Cells. *Hum Gene Ther* **23**, 274–286.
- Volchkov, V. E. (2001).** Recovery of Infectious Ebola Virus from Complementary DNA: RNA Editing of the GP Gene and Viral Cytotoxicity. *Science (80- )* **291**, 1965–1969.
- Volchkov, V. E., Becker, S., Volchkova, V. A., Ternovoj, V. A., Kotov, A. N., Netesov, S. V. & Klenk, H. (1995).** GP mRNA of Ebola Virus Is Edited by the Ebola Virus Polymerase and by T7 and Vaccinia Virus Polymerases I. *Virology* **214**, 421–430.
- Walsh, P. D., Abernethy, K. A., Bermejo, M., Beyers, R., De Wachter, P., Akou, M. E., Huijbregts, B., Mambounga, D. I., Toham, A. K. & other authors. (2003).** Catastrophic ape decline in western equatorial Africa. *Nature* **422**, 611–614.
- Wang, J., Cheng, H., Ratia, K., Varhegyi, E., Hendrickson, W. G., Li, J. & Rong, L. (2014).** A Comparative High-Throughput Screening Protocol to Identify Entry Inhibitors of Enveloped Viruses. *J Biomol Screen* **19**, 100–7.
- Wang, L.-F., Walker, P. J. & Poon, L. L. M. (2011).** Mass extinctions, biodiversity and mitochondrial function: are bats ‘special’ as reservoirs for emerging viruses? *Curr Opin Virol* **1**, 649–57. Elsevier B.V.
- Wang, Y., Li, J., Hu, Y., Liang, Q., Wei, M. & Zhu, F. (2017).** Ebola vaccines in clinical trial: The promising candidates. *Hum Vaccines Immunother* **13**, 153–168.
- Warrell, M. J. (2012).** Current rabies vaccines and prophylaxis schedules: Preventing rabies before and after exposure. *Travel Med Infect Dis* **10**, 1–15. Elsevier Ltd.
- Webby, R. J. & Webster, R. G. (2001).** Emergence of influenza A viruses. *Philos Trans R Soc B Biol Sci* **356**, 1817–1828.
- Weiss, R. A. & McMichael, A. J. (2004).** Social and environmental risk factors in the emergence of infectious diseases. *Nat Med* **10**, S70–6.
- Welfare, W. & Wright, E. (2016).** Planning for the unexpected: Ebola virus, Zika virus, what’s next? *Br J Hosp Med* **77**, 704–707.
- De Wet, J. R., Wood, K. V., Deluca, M., Helinski, D. R. & Subramani, S. (1987).** Firefly luciferase gene: structure and expression in mammalian cells. *Mol Cell Biol* **7**, 725–737.
- White, J. M., Delos, S. E., Brecher, M. & Schornberg, K. (2008).** Structures and Mechanisms of Viral Membrane Fusion Proteins. *Crit Rev Biochem Mol Biol* **43**, 189–219.
- Whitt, M. A. (2010).** Generation of VSV pseudotypes using recombinant G-VSV for studies on virus entry, identification of entry inhibitors, and immune responses to vaccines. *J Virol*

- Methods* **169**, 365–374. Elsevier B.V.
- WHO. (1978a).** Ebola Haemorrhagic Fever in Sudan, 1976. *Bull World Health Organ* **56**, 247–270.
- WHO. (1978b).** Ebola Haemorrhagic Fever in Zaire, 1976. *Bull World Health Organ* **56**, 271–293.
- WHO. (2013).** *WHO Expert Consultation on Rabies - Second Report*. Geneva.
- WHO. (2014).** *Ebola virus disease, West Africa – update 8 August 2014*.
- WHO. (2016).** *WHO Situation Report: Ebola Virus Disease, 10 June 2016*.
- WHO. (2017).** List of Blueprint Priority Diseases.
- WHO & OIE. (2015).** Global Elimination of Dog-Mediated Human Rabies: The Time is Now! In *Rabies Glob Conf*, p. 27. Geneva, Switzerland.
- Wilkinson, D. E., Page, M., Mattiuzzo, G., Hassall, M., Dougall, T., Rigsby, P., Stone, L. & Minor, P. (2017).** Comparison of platform technologies for assaying antibody to Ebola virus. *Vaccine* **35**, 1347–1352. The Author(s).
- de Wit, E., van Doremalen, N., Falzarano, D. & Munster, V. J. (2016).** SARS and MERS: recent insights into emerging coronaviruses. *Nat Rev Microbiol* **14**, 523–534. Nature Publishing Group.
- Wool-Lewis, R. J. & Bates, P. (1998).** Characterization of Ebola virus entry by using pseudotyped viruses: identification of receptor-deficient cell lines. *J Virol* **72**, 3155–60.
- Wright, E., Temperton, N. J., Marston, D. A., McElhinney, L. M., Fooks, A. R. & Weiss, R. A. (2008).** Investigating antibody neutralization of lyssaviruses using lentiviral pseudotypes: a cross-species comparison. *J Gen Virol* **89**, 2204–13.
- Wright, E., McNabb, S., Goddard, T., Horton, D. L., Lembo, T., Nel, L. H., Weiss, R. a, Cleaveland, S. & Fooks, A. R. (2009).** A robust lentiviral pseudotype neutralisation assay for in-field serosurveillance of rabies and lyssaviruses in Africa. *Vaccine* **27**, 7178–86.
- Wright, E., Hayman, D. T. S., Vaughan, A., Temperton, N. J., Wood, J. L. N., Cunningham, A. A., Suu-Ire, R., Weiss, R. A. & Fooks, A. R. (2010).** Virus neutralising activity of African fruit bat (*Eidolon helvum*) sera against emerging lyssaviruses. *Virology* **408**, 183–9. Elsevier Inc.
- Wu, B., Piatkevich, K., Lionnet, T., Robert, S. & Verkhusha, V. (2011).** Modern fluorescent proteins and imaging technologies to study gene expression, nuclear localization, and dynamics. *Curr Opin Cell Biol* **23**, 310–317.
- Yang, J., Li, W., Long, Y., Song, S., Liu, J., Zhang, X., Wang, X., Jiang, S. & Liao, G. (2014).** Reliability of pseudotyped influenza viral particles in neutralizing antibody detection. *PLoS One* **9**, e113629.
- Yang, T. T., Sinai, P., Kitts, P. a & Kain, S. R. (1997).** Quantification of gene expression with a secreted alkaline phosphatase reporter system. *Biotechniques* **23**, 1110–4.
- Ye, L. & Yang, C. (2015).** Development of vaccines for prevention of Ebola virus infection.

- Microbes Infect* **17**, 98–108. Elsevier Masson SAS.
- Young, C. C. W. & Olival, K. J. (2016).** Optimizing viral discovery in bats. *PLoS One* **11**, 1–18.
- Yu, X., Yuan, X., Matsuda, Z., Lee, T. H. & Essex, M. (1992).** The matrix protein of human immunodeficiency virus type 1 is required for incorporation of viral envelope protein into mature virions. *J Virol* **66**, 4966–4971.
- Yuan, J., Zhang, Y., Li, J., Zhang, Y., Wang, L.-F. & Shi, Z. (2012).** Serological evidence of ebolavirus infection in bats, China. *Virol J* **9**, 236.
- Zhang, G., Gurtu, V. & Kain, S. R. (1996).** An enhanced green fluorescent protein allows sensitive detection of gene transfer in mammalian cells. *Biochem Biophys Res Commun* **227**, 707–711.
- Zhang, G., Cowled, C., Shi, Z., Huang, Z., Bishop-Lilly, K. A., Fang, X., Wynne, J. W., Xiong, Z., Baker, M. L. & other authors. (2013).** Comparative analysis of bat genomes provides insight into the evolution of flight and immunity. *Science* **339**, 456–60.
- Zhou, Y. & Simmons, G. (2012).** Development of novel entry inhibitors targeting emerging viruses. *Expert Rev Anti Infect Ther* **10**, 1129–38.
- Zhou, Y., Agudelo, J., Lu, K., Goetz, D. H., Hansell, E., Chen, Y. T., Roush, W. R., McKerrow, J., Craik, C. S. & other authors. (2011).** Inhibitors of SARS-CoV entry--identification using an internally-controlled dual envelope pseudovirion assay. *Antiviral Res* **92**, 187–94.
- Zinsstag, J., Schelling, E., Roth, F., Bonfoh, B., De Savigny, D. & Tanner, M. (2007).** Human benefits of animal interventions for zoonosis control. *Emerg Infect Dis* **13**, 527–531.
- Zufferey, R., Nagy, D., Mandel, R. J., Naldini, L. & Trono, D. (1997).** Multiply attenuated lentiviral vector achieves efficient gene delivery in vivo. *Nat Biotechnol* **15**, 871–875.
- Zufferey, R., Dull, T., Mandel, R. J., Bukovsky, A., Quiroz, D., Naldini, L. & Trono, D. (1998).** Self-inactivating lentivirus vector for safe and efficient in vivo gene delivery. *J Virol* **72**, 9873–9880.
- Zufferey, R., Donello, J. E., Trono, D. & Hope, T. J. (1999).** Woodchuck hepatitis virus posttranscriptional regulatory element enhances expression of transgenes delivered by retroviral vectors. *J Virol* **73**, 2886–2892.